Brain–Specific Proteins in Multiple Sclerosis

Thesis submitted for the degree of
Doctor of Philosophy
in the
Faculty of Medicine
University London
By
Axel Petzold, M.D.

Friday the 13th of December 2002
Institute of Neurology
University London

To the Goulden and Ward families

Contents

List of Figures

List of Tables

Abstract

Brain–specific proteins (BSP) are each relatively specific for particular cell–types within the nervous system. The BSP studied were glial fibrillary acidic protein (GFAP) and S100B for the astrocyte, ferritin for microglia and neurofilaments (Nf) for the axon. BSP are released into the extracellular fluid (ECF) following cellular destruction and during phases of high cellular activity such as astrocytic or microglial activation. ECF BSP equilibrate with those in the cerebrospinal fluid (CSF). This allows us to quantify BSP from the CSF and estimate the overall average of axonal damage (CSF Nf), astrocytic and microglia activation (respectively CSF S100B, CSF ferritin) and astrogliosis (CSF GFAP).

New enzyme linked immunoabsorbant assays (ELISA) have been developed for measuring Nf and GFAP in the CSF. Previously established ELISAs have been used to measure S100B and ferritin.

It has been shown that spinal cord atrophy in a mouse model of autoimmune encephalomyelitis (EAE) was paralleled by a decrease of Nf indicating loss of axons, and an increase in GFAP indicating astrogliosis. These findings have been confirmed and extended in a human post–mortem study where BSP levels were quantified in multiple sclerosis (MS) lesions of different age and activity. S100B and Nf were associated with acute lesions, ferritin was elevated in all lesion types, while GFAP was increased in both acute and chronic lesions.

CSF BSP levels were then quantified in a cross–sectional study of MS patients with the aim of distinguishing clinical subgroups, such as relapsing remitting (RR), primary progressive (PP) and secondary progressive (SP) disease. In addition an attempt was made to relate CSF BSP levels to grades of disability using clinical scales including Kurtzke's EDSS, an ambulation index (AI) and the 9–hole PEG test (9HPT). It was shown that CSF S100B was higher in RR MS while CSF ferritin was elevated in PP MS patients. The S100B:ferritin ratio emphasised the distinction between the MS subtypes. CSF GFAP was higher in poorly ambulating (AI) and severely disabled (EDSS) patients. CSF GFAP correlated with the EDSS in SP MS patients. This suggests that gliosis is an important feature in SP MS.

CSF Nf levels were quantified in a longitudinal study at baseline and at 3–year follow–up. It was shown that more SP/PP than RR MS patients experienced an increase in CSF Nf levels over this time, suggesting cumulative axonal damage in this subgroup. RR MS patients who had elevated CSF Nf levels at baseline had a worse clinical course, suggesting that initial high CSF Nf levels in RR MS patients are a poor prognostic sign. CSF Nf levels at follow–up correlated with the EDSS, AI and 9HPT suggesting that axonal pathology in MS is a dynamic process possibly balancing features of de- and regenerative activities.

Acknowledgement

I am grateful to my supervisors Ed Thompson and Louise Cuzner who with invaluable academic experience guided my thirst for knowledge. I am deeply indebted to Gordon Plant who with great care nourished my clinical skills. I feel humble towards the knowledge and personal skills of Geoff Keir.

I thank all those who have to whatever degree enriched the discussions, challenged and exchanged hypotheses and contributed to the work.

Glossary

2

2,5-HD 2,5-hexandione: a neurotoxic substance which induces dying back neuropathy.

9

9HPT Nine–hole PEG test: a clinical scale which measures upper limb function.

A

ABI Acute brain injury.

AD Alzheimer's disease.

ADEM Acute demyelinating encephalomyelitis.

AI Ambulation index.

AL Acute lesion.

Alb Albumin.

ANOVA Analysis of variance.

APC Antigen presenting cell.

APP amyloid precursor protein.

B

BIH Benign intracranial hypertension.

BSA Bovine serum albumin.

BSP Brain–specific proteins.

C

C2 Complement factor 2.

C3 Complement factor 3.

C9 Complement factor 9.

C9neo Activated terminal complement component.

CANTAB Cambridge Neuropsychological Test Automated Battery.

CD Cluster differentiation. The abbreviation CD is used to categorise the proteins on cell surfaces. These proteins are numbered.

CD3 A set of cell surface antigens which are regarded as a pan T–cell marker. They are part of the TCR complex and are necessary for signal transduction from the cell membrane to the cytoplasm once an antigen occupies the antigen–binding site of the TCR.

CD4 A cell surface protein present on a subset of T–cells. The CD4 protein binds to class II MHC proteins.

CD8 A cell surface protein present on a subset of T–cells which are usually cytotoxic. CD8 interacts with class I MHC proteins.

CI Confidence interval.

CJD Creutzfeldt–Jakob disease.

CMH The Mantel–Haenzel trend analysis.

CNS Central nervous system.

CRP C–reactive protein.

CTRL Control group.

CV Coefficient of variation.

D

DEM Dementia.

DM Demyelinating disease.

DNA Deoxyribonucleic acid.

E

ECF Extracellular fluid.

ECM Extracellular matrix.

EDSS Extended disability status scale: a clinical scale developed by Kurtzke which measures disability.

ELISA Enzyme–linked immuno–assay.

F

FTH Ferritin heavy chain. Predominantly expressed in heart tissue.

FTL Ferritin light chain. Predominantly expressed in liver.

G

GBS Guillain–Barré Syndrome.

G-CSF a colony stimulating factor (CSF) which acts upon granulocytes.

Gd Gadolinium: an element of the periodic table (No. 64) which belongs to the group of lanthanoids and has a molecular mass of 298 K. Because of its paramagnetic properties Gd is used as a contrast medium in MRI.

GDC granular disintegration of the cytoskeleton. A stage of Wallerian degeneration.

GFAP Glial fibrillary acidic protein. A structural protein of the cytoskeleton of the astrocyte. The soluble form has a molecular mass of about 41 kDa.

GLM General linear model. A two–way unbalanced ANOVA.

GM-CSF a colony stimulating factor (CSF) which acts upon granulocytes and macrophages.

H

HAD The National Hospital anxiety and depression scale.

HD Headache.

I

IFN Interferon.

Ig Immunoglobulin.

IgG Immunoglobulin G.

IL Interleukin.

index The ratio of quotients.

iNOS Inducible NO synthetase.

IQ Intelligence quotient.

K

KSP Repeats of the aminoacid sequence: Lys-Ser-Pro. KSP repeats are particularly abundant in Nf and determine the phosphorylation sites of the protein.

M

M Molar.

MAG Myelin associated glycoprotein.

MAP microtubules associated protein.

MBP Myelin basic protein.

M-CSF a colony stimulating factor (CSF) which acts upon macrophages.

MDEM Multiphasic disseminated encephalomyelitis.

E

EAE Experimental autoimmune encephalomyelitis.

M

M-H χ^2 see CMH.

MHC major histocompatibility complex.

Monoclonal A single band in the gamma region of the electrophoresis pattern indicating the secretion of a homogeneous protein.

MRC Medical Research Council.

MRI Magnetic resonance imaging.

MRS Magnetic resonance spectroscopy.

MSFC Multiple Sclerosis Functional Composite.

MSGM MS grey matter.

MSWM MS white matter.

N

N/A Not applicable.

NAGM Normal appearing grey matter.

NART National Adult Reading Test.

NAWM Normal appearing white matter.

N.D. Not determined.

Nf Neurofilament protein: an obligate heteropolymer of the intermediate filament group. The normal human Nf consists of 3 subunits (NfL, NfM, NfH). Intermediate filaments have a diameter of about 8–10 nm, which is between the large diameter of the myosin filaments of the muscle cell and the small diameter of actin filaments (microfilaments).

NfH Neurofilament heavy chain. The 190-210 kDa Nf subunit.

NfL Neurofilament light chain. The 68 kDa Nf subunit.

NfM Neurofilament medium chain. The 150 kDa Nf subunit.

nm nanometer: meter * 10^{-9}.

NO Nitric oxide.

NO_2 Nitrate.

NO_3 Nitrite.

NSE Neuron specific enolase.

O

OCB Oligoclonal bands.

OD Optical density.

Oligoclonal A limited number of bands in the gamma region of the electrophoresis pattern indicating the secretion of a few proteins suggestive of a yet restricted antigen response.

ON Optic neuritis.

OPD O–phenylenediamine.

P

p The significance of a statistical test is indicated by the p–value.

PAGE Polyacrylamide gel electrophoresis.

PASAT Paced auditory serial addition test.

PBS Phosphate buffered saline.

P.M. Post mortem.

PNS peripheral nervous system.

Polyclonal Many bands in the gamma region of the electrophoresis pattern indicating the secretion of a heterogeneous population of proteins.

PPMS Primary progressive multiple sclerosis.

PPWM Periplaque white matter.

Q

Quotient A calculation between different fluid compartments on the same substance, of the form: $\frac{\text{substanceA}_{\text{CSF}}}{\text{substanceB}_{\text{serum}}}$.

R

R The strength of a correlation is indicated by the R–value.

Ratio A calculation within the same fluid compartment of the form: $\frac{\text{substanceA}_{\text{CSF}}}{\text{substanceB}_{\text{CSF}}}$.

RRMS Relapsing remitting multiple sclerosis.

RT Room temperature.

S

S100B The S100B protein. A member of a multigenic family of calcium-modulated S100 proteins of the EF-hand type with intracellular and extracellular functional roles.

SAH Subarachnoid haemorrhage.

SAL Subacute lesion.

SAS A statistical package provided by the SAS Institute Inc., Cary, NC, USA.

SD Standard deviation.

SDS Sodium dodecyl sulfate.

SMI Sternberger Monoclonal Incorporated. A company providing the monoclonal antibodies. Due to the extensive work of Nancy and Ludwig Sternberger the label 'SMI' became an acronym for many antibodies used in immunocytochemistry. In this thesis the name of the clone for a particular antibody has been chosen to describe the antigen recognised by this SMI clone. Hence the terminology NfH-SMI32, which describes the neurofilament heavy chain which is recognised by Sternberger's monoclonal clone No. 32.
The terminology Sternberger refers to in his publications is different to the label of the commercially available antibodies (SMI). SMI32 was 02–135, SMI33 was 02–40, SMI34 was 07–5, SMI35 was 03–44, SMI 37 was 06–32, SMI38 was 10–1, SMI310 was 04–7.

SO Space occupying lesion.

SPMS Secondary progressive multiple sclerosis.

T

TCR T–cell antigen receptor.

Th-1 (T cytotoxic cells): a population of T cells which can be stimulated to secrete cytokines such as IL-2, IFγ or TNFβ. Th1 cells are involved in many delayed–type hypersensitivity reactions. Th1 cells have an important role in the pathogenesis of autoimmune diseases such as MS and EAE.

Th-2 (T helper cells): a population of T cells which can be stimulated to secrete cytokines such as IL-2, IL-4, IL-5, etc. Th2 cells

support the differentiation of B cells and thereby modulate the specific humoral immuneresponse. Most cytokines secreted by Th2-cells have antagonistic properties to Th1–cell cytokines.

TNF Tumor necrosis factor.

TNFα Tumor necrosis factor α.

TNFR2 The tumor necrosis factor receptor 2 (TNFR2) is expressed on specific progenitor cells and promotes the differentiation into mature and functional oligodendrocytes.

TWT The timed walk test.

U

UK United Kingdom.

W

WHO World Health Organisation.

w/v weight per volume.

Y

yrs Years.

Part I

Introduction

Chapter 1

Multiple sclerosis

Although multiple sclerosis (MS) has been recognised for over 160 years[58,61,76,325] its aetiology remains unknown.[298] There is epidemiological evidence that infectious or nutritional factors can contribute.[207,210,440] Additional disease susceptibility factors have been considered on the basis of genetic studies and twin studies,[89,90,326] with the strongest link to the Human Leukocyte Antigen system. This is all consistent with the notion that disease progression is predominantly driven by autoimmunity.

The pathological hallmarks of MS are inflammation, demyelination, gliosis and to a lesser extent, axonal loss.[258,315] The classical MS plaque has a clear demarcation line, is hypocellular, has axons which are relatively well preserved and has a histological picture dominated by an astrogliotic scar–tissue.[101] The formation of such a lesion is thought to be triggered by inflammation and is expressed clinically as a relapse. The symptoms to the patient depend on the anatomical site of the lesion.

The diagnosis of MS remains clinical, despite ever–increasing experimen-

tal knowledge. The clinical diagnosis is based on established international consensus criteria which require that lesions of the central nervous system are separated by time and space.[257,311] The introduction of the McDonald criteria increased the sensitivity of diagnosis of MS.[79] The number of patients diagnosed with early MS can therefore be expected to increase in the coming years. These patients are an important target for emerging treatment strategies.

The treatment of MS is based on (1) diet and lifestyle, (2) pharmacological and/ or (3) interventional procedures.[38,298] There are currently no established measures other then magnetic resonance imaging markers which allow for either good prognostic estimates or monitoring of disease progression on a subclinical level. Surrogate markers are therefore needed in order to refine future strategies for the treatment of MS.

1.1 Disease heterogeneity

Multiple sclerosis is a heterogeneous disease. This includes the clinical picture,[213] the pathological appearance[238] and the magnetic resonance imaging findings.[50,217] This has implications for the selection of treatment strategies.[39]

Clinical heterogeneity The dynamics of clinical symptoms in MS are used to determine the clinical subtypes.[236] The classical patterns for development of disability are outlined in Figure 1.1. These are:

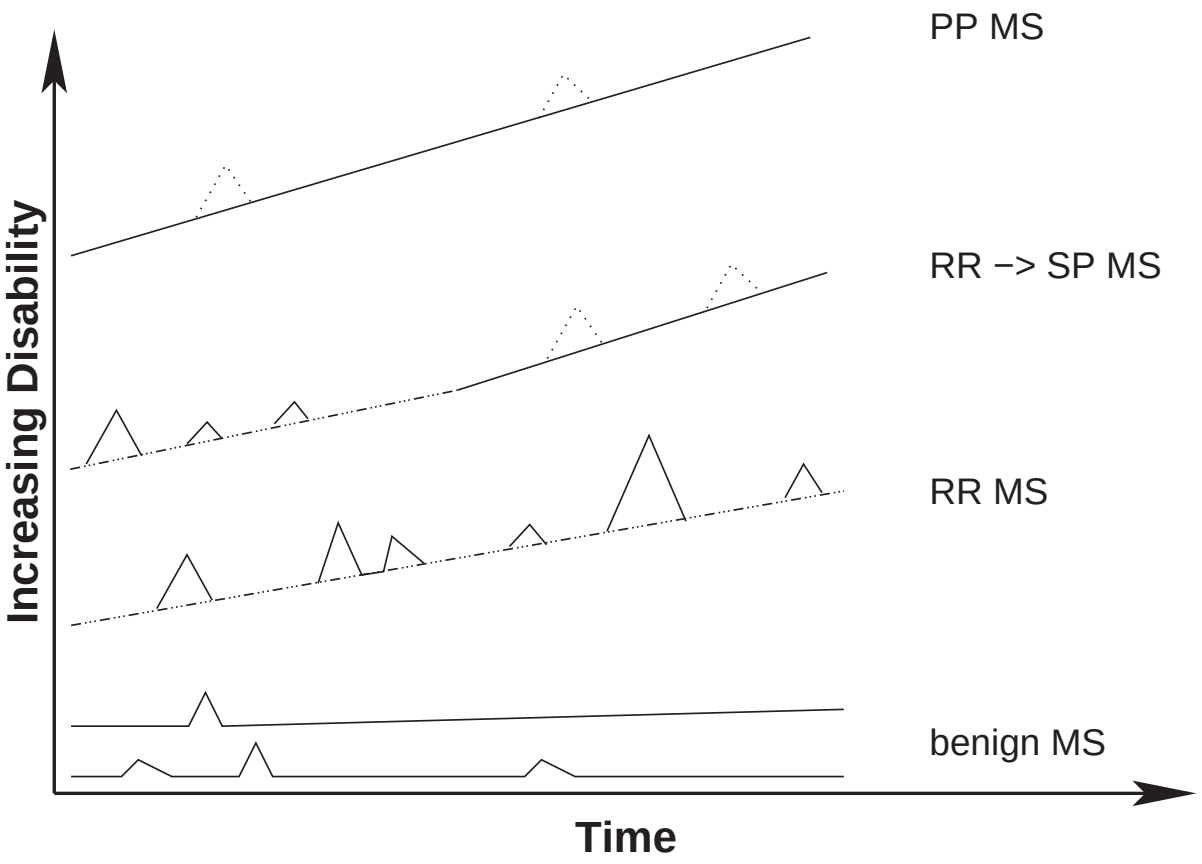

Figure 1.1: *Disease progression in multiple sclerosis. The dynamics of disability over time are shown for benign MS, relapsing–remitting MS (RR MS), the conversion from relapsing–remitting to secondary progressive MS (RR→SP MS) and primary progressive MS. A relapse is indicated by a triangle and disease progression by the slope of the curve (dashed for RR and closed for SP/PP MS). Adapted from Lublin*[236] et al. *(1996).*

1. Relapsing–remitting MS (RR MS). This pattern shows the most remarkable changes of disability over time. The triangular peaks in Figure 1.1 describe what is clinically observed as a relapse. The onset of functional loss is acute and recovers within 2-4 months. As indicated by the dotted line there is however increasing evidence that the irreversible deficit increases over time.

2. Secondary progressive MS (SP MS). This pattern frequently starts in similar fashion to that observed in RR MS. A crucial moment is reached when RR MS converts to SP MS. From this point on the progression of the disease is clinically irreversible. The occurrence of relapses during this phase is possible but not necessary for the classification.[70,190]

3. Primary progressive MS (PP MS). This pattern has a subacute onset, but loss of function seems to be irreversible and progressive.

4. A heterogeneous group of acute–onset demyelinating diseases are characterised by their clinical picture:

   - Optic neuritis (ON): localised demyelination of the optic nerve .[330,342,344]
   - Transverse myelitis: localised demyelination of the spinal cord.[12]
   - Neuromyelitis optica or Devic's syndrome [84]: the strict definition includes only patients with monophasic ON and complete

transverse myelitis, frequently found after infections.[427] The case reported by Devic was a 45 year old woman who suffered from gastrointestinal problems and a disturbed sleep pattern, and subsequently developed headaches. She was diagnosed having neurasthenia, but continued to develop ON with a severely swollen disc and retinal hemorrhages. Subsequently she became paraplegic and died within 35 days. The autopsy confirmed bilateral ON and acute demyelination of the lumbar spinal cord.[84]

- Balo's disease[30]: autopsy[30,444] and MRI findings[184] demonstrate concentric lamellae of demyelination affecting the cerebral hemispheres. Presentation acute and mortality is high. Balo reported a 23 year old patient who suffered from acute onset right hemiparesis, aphasia and papilloedema. The patient died within 8 months *. Autopsy showed concentric lamellae of demyelination and partially myelinated axons.[30]

- Acute disseminated encephalomyelitis (ADEM): a monophasic inflammatory/ demyelinating disease, more frequently seen in children than in adults.[78,187] In cases with relapses, the term "multiphasic disseminated encephalomyelitis" (MDEM) is used.[78,310]

*This case is frequently cited as an example for the high mortality of Balo's disease. However, the patient of Balo died from an autopsy confirmed subdural haematoma after exploratory neurosurgery. Neurosurgery was done because a brain tumor was suspected as primary aetiology for the clinical presentation. This could not be confirmed, the wound was closed and the patient died on the following day.

- Marburg's variant [247]: a rapidly progressive, non–remitting disease with very high mortality, involving the cerebral hemispheres, brainstem and optic nerve.[427] The case reported by Marburg was a 30–year old woman in a confusional state with headaches, vomiting and unsteady gait. She developed a left hemiparesis and died within 26 days. The autopsy confirmed white matter demyelination.[247]

5. Benign MS. The patient remains fully functional in all neurological systems 15 years after disease onset.[236]

Given the clinical heterogeneity it is worthwhile remembering that the definition of categories (1) to (3) was not unanimously accepted by the members of the committee responsible for this task:

> "Informal discussions among clinicians and clinical researchers and consensus developed among investigators attending a 1994 MS clinical trials design workshop[13] revealed that there was no unanimous agreement on definitions for the various clinical subtypes of MS [236, p.907, 3rd paragraph, 1st line]."

It was suggested that this could possibly be overcome if the additional information derived by biological markers was used in order to distinguish subtypes of MS .[236] Such markers will be discussed in section 1.3 (page 40). Furthermore the definition of these categories was based on a survey with

an initial population of 215 patients but with a drop out of 42%, so that only 125 questionnaires were available for analysis.

Pathological heterogeneity The classical MS plaque, as already described in the 19th century,[58,59,76,325] is characterised by selective destruction of myelin with relative preservation of axons.[215]

Lesions which are actively demyelinating in contrast show many different structural and immunological features. The activation of glia and macrophages,[48,52,225,372,407] the presence of free radicals,[25,374] cytokines[154,352] and the interaction of specific antibodies with activated complement have been studied in detail.[112,116,312,382] The systematic analysis of demyelination in active lesions revealed a high degree of inter–individual heterogeneity.[237,238] On the basis of this finding a classification of demyelination into 2 main categories was proposed: (1) those with close similarity to autoimmune encephalomyelitis (EAE), i.e. *inflammation* and (2) those with predominantly *oligodendrocyte dystrophy*. Each category features 2 typical immunohistological patterns adding up to 4 patterns altogether[237] (Table 1.1).

Table 1.1: *Pathological heterogeneity in MS. Patterns of demyelination according to the dominant associated pathology. The values represent cells per mm^2. AL = active lesion, PPWM = periplaque white matter. Adapted from Lucchinetti*[237] et al. *(2000).*

	Inflammation		***Degeneration***	
Feature	Pattern I	Pattern II	Pattern III	Pattern IV
Inflammation				
CD3 T cells	197±68	133±18	145±23	134±71
Plasma cells	5.9±1.9	9.3±2.1	5.4±1.6	3.8±
Macrophages	1158±105	931±71	842±91	1650±30
C9neo	—	++	—	—
Oligodendrocytes				
DNA fragmentation	±	±	++ in AL	++ in PPWM
Apoptosis	—	—	14–37%	—
Myelin protein loss	Even	Even	MAG≫others	Even

The first 2 patterns dominate in acute lesions (pattern 1) or RR MS (pattern 2). These 2 patterns are characterised by large demyelinated plaques, have a high number of CD3 T–cells, plasma cells and macrophages. Remyelination as demonstrated by shadow plaques is present and the number of oligodendrocytes in the plaque is about 5 times higher compared to patterns 3 and 4, which in turn showed no signs of remyelination. Pattern 2 can be distinguished from pattern 1 by the high concentration of the activated terminal complement component, C9neo.[382] The presence of C9neo suggests that antibodies are likely to play an important pathological role.[112,312,382] In pattern 1 these antibodies were present to a much lesser degree suggesting that other pathological features such as tumor necrosis factor–α (TNF-α) [154,352,355] and cytokines [154,352] contribute to the destructive process. Pattern 1 and 2 resemble the structural hallmarks of MS lesions as described by Charcot ,[59] Rindfleisch[325] and Dawson.[81] They are consistent with a delayed–type hypersensitivity reaction[215] which is T–cell mediated. These

2 patterns are consistent with the notion that MS is mainly a Th-1 T–cell–driven disease.[155,156]

Pattern 3 dominates in patients with monophasic disease or who died from acute disease within 1 year.[237] This pattern showed an ill–defined lesion edge, a high rate of DNA fragmentation and apoptosis of oligodendrocytes. There is a marked decrease of myelin–associated glycoprotein compared to the three other patterns.

Pattern 4 had the highest content of macrophages and lowest content of plasma cells. Pattern 4 was only observed in lesions from 3 MS patients having a primary progressive course. In these patients cerebellar, brainstem and cognitive symptoms dominated.[237]

Taking these findings together it appears that pathological heterogeneity is a feature particularly of early MS. Different pathological mechanisms are likely to account for demyelination in subgroups of MS patients. How the histopathological differences relate to the phenotype, the genotype or differences in the disease–inducing trigger remains to be clarified.[215,216]

Although axonal pathology is not the most striking feature in MS brain tissue it is possibly the one with the highest impact for the patient.[43,256,398,400,424,438] Historically axonal loss in MS has been been associated with the "burnt–out" phase of the disease .[130,313] Using immunohistology Ferguson *et al.* (1997) were able to demonstrate axonal pathology in *active* MS lesions .[106] Extensive staining for amyloid precursor protein (APP) was observed and

the APP positive structures resembled terminal ends of transected axons. A three dimensional reconstruction of these axonal ovoids using confocal microscopy confirmed the presence of transected axons in acute MS lesions.[398] An accumulation of neurofilament protein was observed in these end–bulbs. An additional relationship between the frequency of axonal transections and active inflammation was described.[398]

The concept of axonal loss in MS is not new,[20,58,59,76,80,106,252,255,261,286,325,398] but the important new insight is that a high number of transected axons is already present in acute lesions[106,398] and in patients with a short clinical course.[398] This finding might have important prognostic implications for individual MS patients. Secondly the concept of axonal loss provides a testable hypothesis which could explain the conversion of RR MS to SP MS[255,261] (Figure 1.1). However axonal injury is a dynamic process and quantification of axonal loss in histological material is complicated by tissue oedema, the presence of inflammatory cells and the problem of establishing a relationship with the number of healthy axons.[399]

Morphology and dynamics of axonal injury The first systematic description of axonal injury in humans was done 1850 by Waller,[415] hence the eponym "Wallerian degeneration".

Wallerian degeneration is a complex process which describes the degeneration of the *distal* axonal stump after axonal transection from the neuron.

Wallerian degeneration begins with the enzymatic proteolysis of the axonal cytoskeleton ,[117] but proceeds outside the axon causing changes in the ensheathing glial cells, alterations in the adjacent blood–tissue barriers and responses of cells of macrophage lineage. In mammalian nerves Wallerian degeneration becomes macroscopically visible 24-36 hours post injury .[66,235] The dynamics of Wallerian degeneration are, however, broad and rapid Wallerian degeneration has been distinguished from slow Wallerian degeneration which can last for up to 3 weeks.[66] It was hypothesised that one function of Wallerian degeneration is to prepare a pathway for potential axonal regeneration. The cellular events of Wallerian degeneration following axonotomy are considered to be sequential and a classification into 5 stages has been proposed[131] (Figure 1.2 A - E):

(A) Survival of the disconnected distal stump: the distal segment adjacent to transection progressively accumulates neurofilaments (Nf) and intra–axonal organelles,[423,445] histologically observed as "axonal bulbs".[398] This phenomenon originates from the continuity of retrograde axonal transport .[317]

(B) Granular disintegration of the axoplasm and axonal breakdown: Granular disintegration of the cytoskeleton (GDC) is defined as the abrupt conversion of the axoplasm into fine particulate and amorphous debris. This is considered to be an extremely rapid process of disintegration of the axonal cytoskeleton along the entire length of the axon.[118,239]

GDC correlates with the cleavage of Nf into lower molecular weight products[347,348] recognised by anti–Nf antibodies.[401]

(C) Early responses of non-neuronal cells involve the blood–tissue barrier and glial cells. Local breakdown of the blood–tissue barrier occurs 24 to 48 hours after axonal injury and leads to early endoneurial oedema.[47] The glial cell reaction is divided into (1) astrocytic activation , (2) microglial and macrophage activation and (3) oligodendrocyte response .[24,199] The relative timing of these cellular events differs considerably between the central nervous system (CNS) and peripheral nervous system (PNS) .[24,131] In general terms the CNS response is much slower and most macrophages are recruited by differentiation of microglia, rather recruitment from the circulation.[117,380,381]

(D) Mature glial and macrophage lineage cell responses: These represent a continuum from the previous stage and describe the clearance of cellular debris. Again the time scale of events in the CNS is prolonged when compared to the PNS.[380,381]

(E) Late changes: oligodendrocytes progressively disappear,[426] endoneurial fibroblasts remain prominent, endoneurial collagen content increases and the former nerve tissue is replaced by a fibrillary glial scar [61,118]

Wallerian degeneration has to be distinguished from *dying back* neuropathy, defined as the slow *proximal* spread of nerve fibre breakdown and

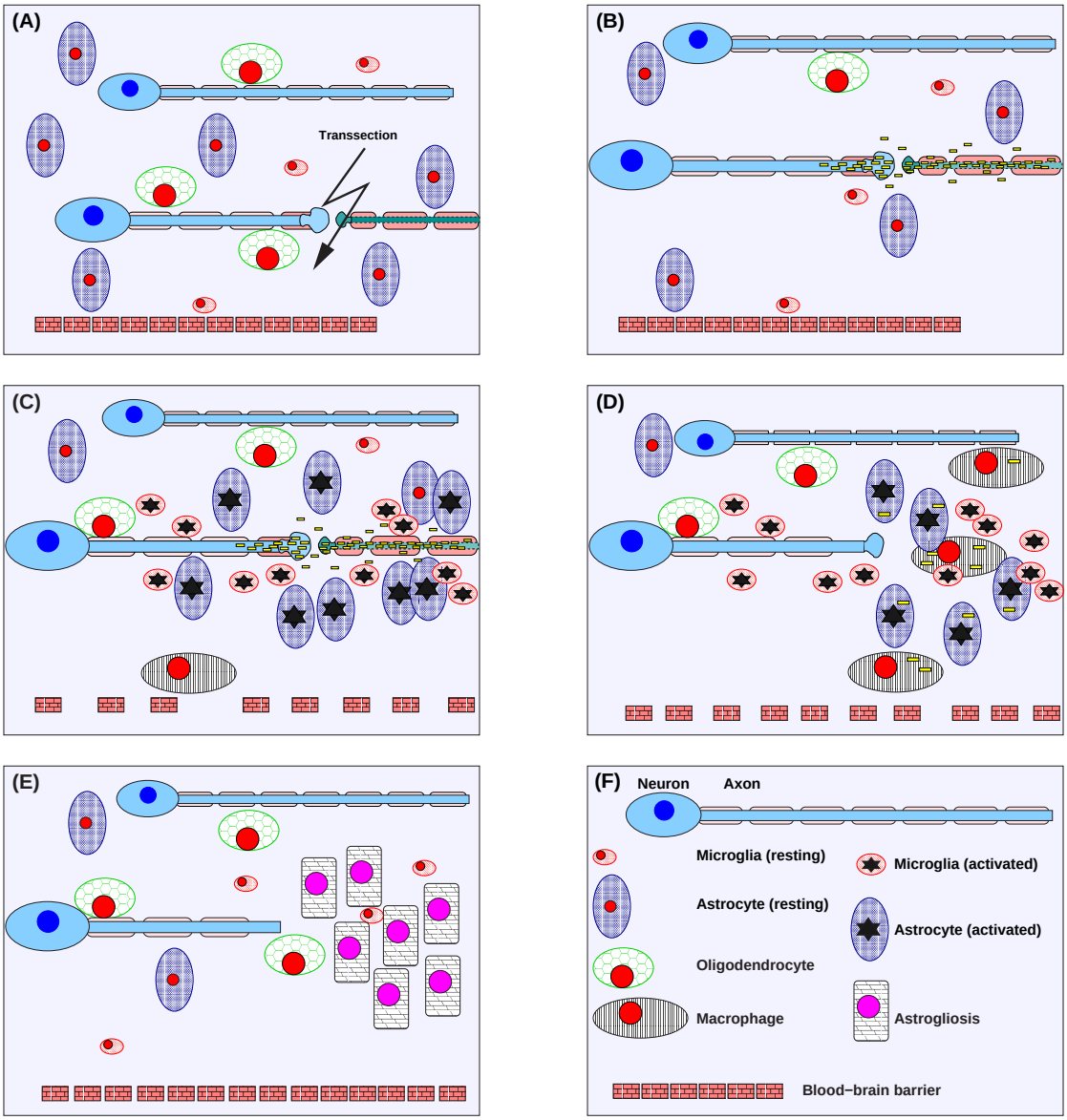

Figure 1.2: *Wallerian degeneration. (A) Transection and transient survival of the distal stump, (B) granular disintegration, (C) early responses of non–neuronal cells, (D) mature glial and macrophage lineage response, (E) late changes, (F) legend.*

ultimate apoptosis of the neuron .[371] The term *dying back* was introduced to describe the spatio–temporal pattern of central and peripheral nerve fibre pathology in degenerative diseases. Particular experiments with 2,5-hexanedione (2,5-HD) and acrylamid showed that the initial changes in the ultrastructure of the axon consisted of Nf accumulation which was accompanied by clearly visible focal fibre swelling.[309,346] Focal Nf accumulation started proximal to the Ranvier nodes with subsequent impairment of axonal transport.[412]

1.2 Disability

The terms *impairment* (i.e. "loss or abnormality... of structure of function), *disability* (i.e. "a restriction or lack... of ability to perform an activity in the manner of within the range considered normal for a human being") and *handicap* (i.e. "the disadvantage for an individual... that prevents or limits the performance of a role that is normal... for that individual") are used according to the recommendations of the system adopted by the World Health Organisation (WHO).[300] Handicap represents the effects of impairments or disabilities in a wide social context and may be heavily influenced by culture. It will therefore not be used for any type of classification in this thesis.

Clinical scales Impairment or loss of function[300] is quantified by clinical scales. The paradox between clinical examination and each clinical scale is that normal functioning is tested, but loss of function is quantified. Because

of the potential of CNS regeneration and plasticity the clinical appearance of disability is a dynamic process. This has been illustrated in Figure 1.1 and forms the basis on which MS patients are classified.

A range of validated clinical scales is now in use. For MS the most widely applied scale is the extended disability status scale (EDSS) for multiple sclerosis developed by Kurtzke in 1983.[206] The EDSS combines a disability status scale[203] with functional systems.[204,205,208,209] A simple assessment of lower limb function is provided by the ambulation index (AI) or the timed walk test.[177] Motor function of the upper limbs is quantified by the 9 hole peg test (9HPT) .[177]

Psychometry is tested by the paced auditory serial addition test (PASAT) .[133] The National Adult Reading Test (NART) is used to give an estimate of the premorbid IQ .[287] Current intellectual function is assessed by the Advance Progressive Matrices, Set 1 (Ravens). Memory is assessed by recognition of words and faces.[419] The paired associated learning test estimates learning abilities. Attention is quantified by the speed of letter counting.[437] Tests of executive function include the Wisconsin Card sorting test (Nelson) and the Cambridge Neuropsychological Test Automated Battery (CANTAB) .[287,343] Fatigue is commonly estimated by Krupp's Fatigue Rating Scale .[200] Anxiety and depression have been measured using the National Hospital anxiety and depression scale (HAD) .[449] There is an emerging range of scales measuring quality of life and measures for outcome

of neuro–rehabilitation.[393]

Recently the timed walk test (TWT), 9 hole peg test (9HPT) and Paced Auditory Serial Addition Test (PASAT) have been combined mathematically to give the Multiple Sclerosis Functional Composite (MSFC) .[77,158] The MSFC has the potential to provide a more reliable measure of changes of function in MS than the EDSS, which is non–linear and biased towards locomotion.[31]

It has been argued that the rate of progression of sustained disability is relapse–independent.[68–70] This hypothesis is based on the epidemiological evidence that the rate of progression remains "linear" during pregnancy despite a significant reduction in the relapse rate[68] (Figure 1.3 A). Additional evidence comes from an epidemiological study on a cohort of 1844 MS patients. The progression of sustained disability from an EDSS of 4 to a score of 6 or 7 was unaffected by the number of relapses prior to the progressive phase[70] (Figure 1.3 B).

Is MS a two–phase disease? The epidemiological findings raise the question whether the pathological process which drives disease progression in MS falls into one of two phases[375]: (1) "inflammatory" and (2) "degenerative" [69,367,400] (Figure 1.4 A). On the basis of clinical and pathological disease heterogeneity, particularly in the early or acute phase of the disease one could speculate that heterogeneity decreases while disability accumu-

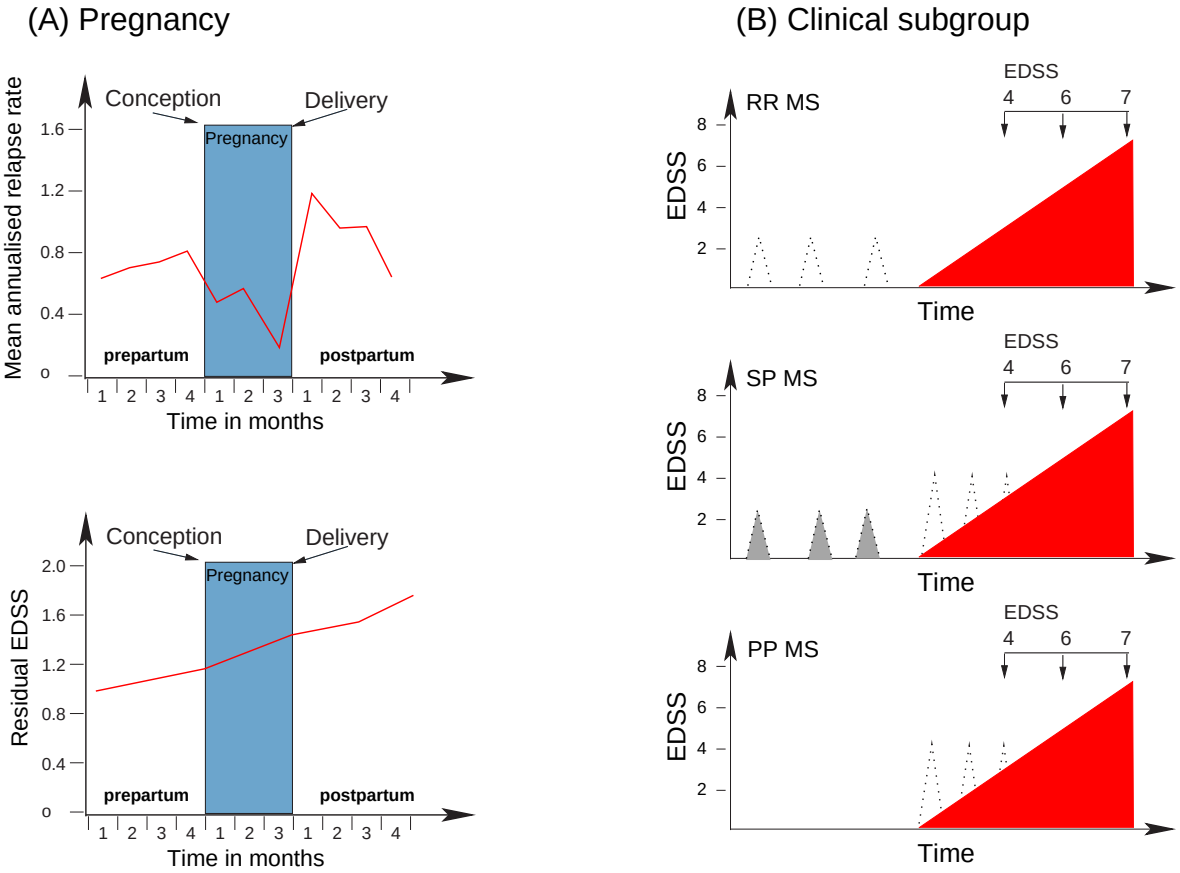

Figure 1.3: *Progression of sustained disability in MS is relapse–independent. (A) During pregnancy the relapse rate decreases significantly, but this does not halt progression of irreversible deficit. (B) The rate of progression of EDSS from 4 to 6 and from 6 to 7 is not affected by the presence or absence of relapses during the relapsing–remitting phase. This also holds true for the presence or absence of relapses superimposed on the progressive phase of either PP or SP MS. Modified from Confavreux*[68,70] et al. *(1998, 2000).*

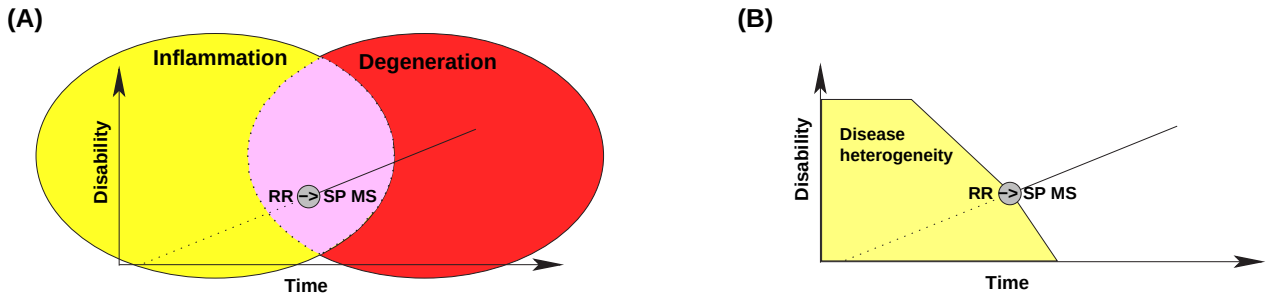

Figure 1.4: *MS as a two–phase disease. (A) the earlier "inflammatory" phase progresses into a "degenerative" phase with accumulation of impairment. A critical threshold (circle) describes the conversion from RR to SP MS. (B) Disease heterogeneity is high during the early "inflammatory" phase of the disease and decreases with emerging degeneration.*

lates (Figure 1.4 B).

The clinical heterogeneity in the early phase of MS is likely to be triggered by a range of factors, further complicating the formulation of a single unifying hypothesis of the aetiology of MS. Simplification is also hampered by the notion that inflammation, particularly the innate arm of the immune response, has beneficial/ neuroprotective roles .[291,324] Macrophages are required for effective remyelination,[196] astrocytes and immune cells potentially provide neurotrophic factors[186,291] and autoimmune T–cells protect neurons from secondary degeneration after experimental trauma .[277] TNF–

α contributes to the apoptosis of immune cells[244] and binds to TNFR2 on the surface of specific progenitor cells to promote their differentiation into mature and functional oligodendrocytes .[291] The wide range of inter–individual heterogeneity during the "inflammatory" phase of the disease is thus not surprising. It is therefore interesting that the heterogeneous group of MS subtypes (item 4 on page 24) have all been linked to inflammation and acute onset.[12,30,78,84,187,247,330,342,344,427,444]

The "degenerative" phase of the disease seems to be characterised by an inexorable loss of function (Figure 1.4). The pathological mechanisms accounting for this are few: conduction block, demyelination and axonal loss.[105,182,259,320,365,366,398] Among these only axonal loss is irreversible. Plasticity of the CNS might transiently overcome the reduced operational abilities of many functional systems. However some systems such as the optic nerve, tract and radiation have no capacity for plasticity whatsoever.[178–181] In these cases only partial recovery is possible by adaptive changes of higher cortical centres following the reduced input.[167]

Once a critical threshold is reached, the inexorable loss of axons and neurons integrated into the functional CNS network will surpass the potential for plasticity. This phase is possibly reflected by the epidemiological finding that once an EDSS of about 4 is reached, the disease continues to progress inexorably.[70]

1.3 Surrogate markers

A surrogate is a substitute or deputy. With regard to MS a surrogate marker is a substitute for the clinical observation. As yet there are no biological markers available which allow for either a clear–cut distinction between the various subgroups of MS or a correlation with disability.[236, 399, 431]

Biomarkers can be attributed to 3 categories with regard to specificity and sensitivity.

- Metabolic biomarkers
- Inflammatory/immunological biomarkers
- Cell–type specific biomarkers

Metabolic biomarkers The main advantage of using metabolic biomarkers is based on the analytical experience. Very small samples can be analysed and results can be obtained within minutes to hours. Because the basic metabolic pathways are shared by all cell types, the specificity is low. The main problem is that the analysis of serum or urine does not permit the differentiation between the CNS and the systemic compartments. Metabolic biomarkers are therefore unlikely to gain widespread acceptance as surrogate markers in MS.

Inflammatory biomarker Monitoring the CNS inflammatory response is of particular interest because pathology in MS is triggered by inflam-

mation and is largely autoimmune driven. However, the balance between detrimental and beneficial factors remains to be elucidated.[291,324]

Some inflammatory biomarkers have gained particular interest for MS:

- Acute phase proteins. In inflammation a marked increase is observed for C–reactive protein (CRP) and a mannose–binding protein which fixes complement and opsonises, the transport protein α_1–acid glycoprotein and serum amyloid P component. Only moderately increased levels are observed for α_1–proteinase inhibitors, α_1–antichymotrypsin, C3, C9 , factor B, ceruloplasmin, fibrinogen, angiotensin, haptoglobin and fibronectin.[331] Of these, C–reactive protein has been associated with Gd–enhanced MRI activity in MS .[88,122]

- Cytokines describe a class of low molecular weight (15–25 kDa) protein mediators which include molecules known as lymphokines, monokines, interleukines and interferons (IFN).

  - Interleukins (IL–1 to IL–18). In MS raised levels of the IL-1,[32] IL-2,[64] IL-10,[64,176,384] IL-17[229] and IL-18[233] were observed compared to controls. IL-4 increased after intravenous prednisolone treatment in MS,[176] as did IL-12 after interferon beta treatment.[26,232] IL-6 levels were reported to be either increased[64,229,271] or decreased.[32] No difference between controls and MS patients was observed for IL-8.[67] Out of these IL-1, IL-2, IL-4 and IL-6

have been associated with acute relapses.

- Colony stimulating factors: GM–CSF, G–CSF, M–CSF and steel factor.[331] No differences between MS and neurological control patients were found for GM–CSF in the stable phase of the disease,[57,221] whilst GM–CSF levels were elevated in the active phase.[57] A treatment trial with G–CSF in MS patients increased disease activity and resulted in one fatality.[299]

- Tumor necrosis factors: TNFα was found to be increased in MS patients and to correlate with progression of disability [249,355,356] and disease activity as assessed by MRI .[53] This finding was not confirmed by another group who also measured TNFβ.[197] TNFα was also found to rise prior to clinical relapse .[35,323]

- The interferons, α, β and γ all exhibit anti–viral properties. Although the long–term effects remain unknown, IFNβ has been accepted as a treatment strategy in MS .[298]

- Chemokines exhibit strong chemotactic properties. The α–chemokine CXCL10 was increased in MS patients when compared to neurological controls.[245] CXCL10 levels could be associated with acute relapse.[245] The βchemokine MCP-1 was decreased[245,345,362] or increased[162,265,408] in MS patients when compared to neurological controls. Comparing active and stable MS patients lower MCP-1 levels were found in the active group,[109] but the speci-

ficity remains a matter of discussion.[192] RANTES was increased in MS patients.[362]

- Free radicals: the nitric oxide metabolites NO_2 and NO_3 have been found to be elevated in MS patients when compared to controls.[121]

In summary there is evidence that inflammatory markers have an important role as surrogate markers for the "inflammatory" arm of the disease. They may have additional value for monitoring anti-inflammatory effects of new immunomodulatory treatment strategies. However they have proved less reliable for measuring disease progression and disability.

Cell–type specific biomarker Each cell is characterised by its morphology and function, both of which are programmed genetically and materialised by the interaction of proteins, sugars and lipids. The process of post–translational modification leads to complex protein structures, which can be cell–type specific. The lipid membrane of the cell is not an absolute barrier and soluble proteins diffuse into the extracellular space .[104] Soluble glial and neuro–axonal proteins are regularly found in the cerebral extracellular space. The extracellular fluid (ECF) concentration is relatively high, because there is no lymphatic drainage from the brain and all proteins equilibrate with the cerebrospinal fluid (CSF) or diffuse into the blood. These "brain–specific proteins" (BSP) [395] can be measured in the CSF and other body fluids.

The quantification of cell–type specific markers allows us to draw relatively specific conclusions on the type of cell involved in a pathological process. Whether this involvement means cellular destruction and release of cell–type specific proteins into the ECF following disintegration of the cellular lipid membrane, or an increase which parallels upregulation of cellular metabolism is difficult if not impossible to distinguish by the measurement of a single marker.

The two main cellular populations of the brain are either of glial or neuronal origin. Specific glial markers are summarised in Table 1.2.

Table 1.2: *Glial biomarkers in the cerebrospinal fluid. All values are given as mean±SD unless indicated otherwise. GFAP = glial fibrillary acidic protein.*

Surrogate	***CTRL***	***MS***	***Heterogeneity***	***Disability***
S100B[278]	0.33±0.09 ng/mL (n=18)	Acute 1.1 (n=1) stationary 0.36, 0.52 (n=2)	(+)	N/A
S100B[129]	0.2±0.08 ng/mL (n=13)	0.18±0.09 ng/mL (n>20)	N/A	N/A
S100B[363]	N/A	Not detectable in MS (n=5)	N/A	N/A
S100B[212]	Extrapyramidal disorder: 82 (median) μg/L (n=26)	MS all: 92 μg/L (n=87) progressive: 93 μg/L (n=41) relapsing: 93 μg/L (n=29)	—	N/A
S100B[172]	0.7–2.0 μg/L	RR (n=18) 1.5 μg/L SP (n=16) 1.2 μg/L	— *	N/A
S100B[270]	< 6 ng/mL detection limit	acute phase: > 6 ng/mL in 14/17 stationary: > 6 ng/mL in 4/9	(+) †	N/A
S100B[251]	< 5 ng/mL detection limit	Time from relapse: numbers with "high" values 1–7 days: 6/7 8–14 days: 5/5 15–21 days: 7/7 2–28 days: 4/6 29–35 days: 1/4	+ ‡	N/A
GFAP [5]	4.3±0.7 ng/ml	Acute (n=25): <10 ng/mL progressive (n=7): <10 ng/mL	—	N/A
GFAP [336]	142±26 pg/ml	386±169 pg/ml	N/A	+

The glial marker S100B was detectable in the CSF of patients with MS

*No single marker can be used to distinguish RR from SP MS. The authors use a "composite score" combining the measurements of $\frac{CSF}{serum}$albumin ratio, mononuclear cell count, CD4+, CD8+, B1+ subsets, CD4+:CD8+ ratio, IgG, IgG index, IgM, IgM index, complement components C3 and C4, C3 and C4 indices, myelin basic protein, neuron specific enolase, S100 and lactate in order to distinguish between RR and SP MS patients.

†The following post–hoc categorical analysis can be done on the presented data, using the 100% cumulative frequency of the stationary MS patients (≈8 ng/mL) as cut–off for defining "high" S100B levels, 0% (0/9) of the stationary and 65% (11/17) of the acute phase MS patients have "high" S100B levels (p=0.002, Fisher's exact test). Using the assay sensitivity (6.0 ng/mL) as cut–off does not separate the 2 groups (numbers as given in the table, p=0.06).

‡The same assay as for[270] is used. In Figure 1 in[251] a cut–off of 8 ng/mL (100% cumulative frequency of MS patients 29–35 days after relapse) seems more reasonable than using the assay sensitivity. The 100% cumulative frequency for CSF S100B of the stationary MS patients was 8 ng/mL in 1980,[270] which equals the top value found 29–35 days after relapse in the present study. Taking 8 ng/mL as cut–off, the numbers of patients with high CSF S100B values are on day 1–7: 6/7 (86%), day 8–14: 4/5 (80%), day 15–21: 5/7 (71%), day 22–28: 1/6 (17%) and day 29–35: 0/4 (0%). Using these numbers the hypothesis that there is a trend for decreasing CSF S100B levels with time from relapse can be tested. This is highly significant for a cut–off of 8 ng/mL (M-Hχ^2=10.8, p<0.001), and also significant for a cut–off of 6 ng/mL (M-Hχ^2=5.37, p=0.02). For description of trend-analysis using the Mantel-Haenzel χ^2 test, see paragraph 7.2 on page 155

in some[129,172,212,251,270,278] but not all[363] studies. There is evidence that CSF S100B is higher in patients with MS when compared to control patients.[251,270,278] None of the studies performed a statistical analysis to determine whether CSF S100B could be used to separate RR from SP or PP MS patients. The data given in two studies from the same group[251,270] were sufficient detailed to perform a post–hoc analyses (see footnotes to Table 1.2). These post–hoc analysis showed (1) that CSF S100B is significantly elevated in acute disease ($p=0.002$) and (2) that there is a significant linear trend for decreasing CSF S100B levels following a relapse ($p<0.001$). None of the studies investigated the relation of CSF S100B to disability.

The glial marker GFAP was detectable in the CSF of MS patients in two studies.[5,336] There was evidence that CSF GFAP might relate to disability in one study,[336] but not to disease heterogeneity.[5]

The neuronal marker, NSE was detectable in the CSF of MS patients in three studies, but no conclusions could be drawn regarding either disease heterogeneity or disability (Table 1.3).[172,212,278]

The axonal marker, neurofilament (Nf) was detectable in two studies and Nf was related to disability in both (Table 1.3).[242,353] The data in the study by Semra *et al.* (2002) was presented in sufficient detail for a post–hoc analysis regarding disease heterogeneity which was not significant for either RR, SP or PP MS patients.[353] The data presented by Lycke *et al.* (1998) does not allow for post–hoc analysis, but the mean CSF Nf levels in the first

two months after relapse are 4–5 times greater compared to levels measured after four months.

Table 1.3: *Neuro–axonal biomarkers in the cerebrospinal fluid. All values are given as mean±SD if not indicated otherwise. NSE = neuron specific enolase, Nf = neurofilament.*

Surrogate	***CTRL***	***MS***	***Heterogeneity***	***Disability***
NSE[278]	4.5±1.2 ng/mL (n=18)	acute phase: 3.3 ng/ml (n=1) stable phase: 3.8, 4.5 (n=2)	N/A	N/A
NSE[172]	2.0–10.0 μg/L	RR (n=17) 6.2 μg/L SP (n=16) 4.9 μg/L	—	N/A
NSE[212]	Extrapyramidal disorder: 94 μg/L (n=26) median value	MS all: 90 μg/L (n=91) progressive: 88 μg/L (n=41) relapsing: 94 μg/L (n=29)	—	N/A
Nf[242]	<125 ng/mL	days after relapse: day 0–49: 1000±250 (n=16) * days 50–99: 780±150 (n=24) days 100-149: 350±50 (n=16) days 150–199: 400±70 (n=15) days 200–299: 200±30 (n=12) days 300-499: 220±50 (n=13) > 500 days: 200±30 (n=14)	+	+
Nf [353]	≈100 (60–125) above cut–off: 0/8 †	RR: ≈170 (70–280) above cut–off: 10/16 SP/PP: ≈200 (65–380) above cut–off: 14/19	—	+

Myelin basic protein is possibly the best characterised human autoantigen.[266] There is clear evidence from a range of studies that CSF MBP, particular the carboxy end of peptide 45-89, is related to acute disease and disability (Table 1.4).[137,394] It was however not possible to distinguish SP from RR MS using either CSF MBP[212] or urinary MBP–like material.[432]

*The SEM is given. Values read from [242, Figure 1].

†Values read from [353, Figure 4]. The cut–off was determined as the mean+2SD of the control group.

Table 1.4: *Myelin basic protein as a marker for axonal damage. All values are given as mean±SD if not indicated otherwise. MBP = myelin specific protein, MBP_{45_89} = MBP peptide as detected by a monoclonal antibody against the 45_89 carboxy fragment, MBP_{69_89} = MBP peptide as detected by a monoclonal antibody against the 69_89 carboxy fragment*

Surrogate	***CTRL***	***MS***	***Heterogeneity***	***Disability***
MBP [430]	MBP_{45_89} cut–off: 0.50 ng/mL above cut–off: 0/6 MBP_{69_89} cut–off: 0.04 ng/mL above cut–off: 0/6	*acute MS:* # above cut–off * MBP_{45_89}: 6/0 MBP_{69_89}: 6/0 *chronic progressive MS:* MBP_{45_89}: 14/15 MBP_{69_89}: 10/15 *stable MS:* MBP_{45_89}: 6/0 MBP_{69_89}: 1/6	+ †	N/A
MBP[394]	above cut–off: 11/85 cut–off = assay sensitivity (2 ng/mL)	Time from relapse: 0-2 weeks: 23/26 2-4 weeks: 16/21 4-6 weeks: 7/8 remission: 15/44	+ ‡	+ §
MBP[137]	above cut–off: 13/67 ¶	Time from relapse: <4 weeks: 8/11 >4 weeks: 8/16 Time or EDSS: <4wk or EDSS>5: 11/14 >4wk or EDSS<5: 5/13	+	+
MBP[172]	0.2–1.2 μg/L	RR (n=11) 0.6 μg/L SP (n=16) 0.5 μg/L	—	N/A
MBP[212]	Extrapyramidal disorder: 94 μg/L (n=25) ‖	MS all: 215 μg/L (n=91) progressive: 159 μg/L (n=41) relapsing: 263 μg/L (n=29)	+ **	N/A

*The cut–off value was determined as the 100% cumulative frequency of the control group. Significantly more numbers of *acute* MS patients have high CSF MBP levels if compared to controls for both MBP peptides in the post–hoc analysis (p=0.001). Significantly more numbers of *chronic progressive* MS patients have high CSF MBP levels if compared to controls for both MBP peptides in the post–hoc analysis (MBP_{45_89} p<0.001; MBP_{69_89}, p<0.01). Significantly more numbers of *stable* MS patients have high CSF MBP levels if compared to controls only for MBP_{45_89} in the post–hoc analysis (MBP_{45_89} p=0.001; MBP_{69_89}, N.S.)

†In the post-hoc analysis MBP_{69_89} distinguishes significantly between acute and stable MS (p<0.01).

‡In the post–hoc analysis significantly more MS patients with acute relapse have levels above cut–off when compared to MS patients in remission (p<0.001). Taking the numbers of patients with high CSF MBP values at the 4 time–points one can confirm the hypothesis that there is a trend for decreasing CSF MBP levels with time from relapse. This is highly significant for a cut–off of 8 ng/mL (M-Hχ^2=22.13, p<0.001)

§There was a correlation between CSF MBP levels and Millars relapse score.[272]

¶The cut–off for MBP_{45_89} assay was set to 68 pmol/mL.

‖median value. A critical point regarding this paper is that the authors mention the control group, but do not show the raw data.

**The following post–hoc analysis is possible on basis of the presented data: 27% (11/41) of the chronic progressive and 53% (17/32) of the relapsing remitting MS patients had MBP values above the 95%ile of the control group. This is significant using two-sided Fisher's exact test, p=0.02.

A range of commercial assays are available for the measurement of MBP, NSE and S100B. NSE did not prove to be relevant in any of the previous studies. No commercial assays are currently available for GFAP and Nf. GFAP and Nf are promising candidates as surrogate markers for disability. S100B and Nf are also likely candidates to help distinguish between MS subtypes.

An attempt to describe these brain–specific proteins into greater detail and to relate them to a broader clinical context will be made in the next chapter.

Chapter 2

Brain–specific proteins

Proteins are called brain–specific if they are predominantly expressed in CNS cells. Measuring brain–specific proteins (BSP) allows us to draw certain conclusions regarding their role in normal function and pathophysiology in specific cell types. A list of BSP currently used for diagnostic purposes was summarised in Tables 1.2 to 1.4.

This study focuses primarily on two astrocytic proteins (GFAP, S100B) and a family of neuro–axonal proteins (neurofilaments). The microglial–derived protein ferritin was of some interest during the clinical studies since it reflected the other cell which played an additional role in the inflammatory response.

2.1 Neurofilament proteins

2.1.1 Background

The dominant proteins of the axonal cytoskeleton are neurofilaments (Nf). Nf are obligate heteropolymers composed of 3 subunits and belong to the class IV–intermediate filaments (IF).[110]

The Nf light chain (NfL) is coded on chromosome 8p21 and consists of 543 amino acids. The molecular mass corresponds to 61 kDa, but due to phosphorylation and glycosylation, migration in sodium dodecyl sulfate (SDS) polyacrylamide gels (PAGE) is slow, and most authors refer to a molecular mass of 68 kDa as determined in SDS–PAGE. The Nf medium chain (NfM) is also coded on chromosome 8p21 and consists of 916 amino acids. The molecular mass is calculated as 102.5 kDa, and runs at 150 kDa in SDS gels. The Nf heavy chain (NfH) is coded on chromosome 22q12.2[219] and consists of 1020 amino acids. The molecular mass of the amino acids corresponds to 111 kDa. Most authors however refer to the molecular mass derived by SDS gels which is also influenced by the charge/weight of bound phosphate and therefore ranges from 190 to 210 kDa for the various phosphoforms (Figure 2.1 A). Each Nf subunit is composed of a highly conserved α–helical region of approximately 310 amino acids. The core region forms double–stranded coiled coils flanked by the head (N–terminus) and the hypervariable tail (C–terminus) domains.[114]

The formation of the typical IF of 10 nm diameter is determined by the correct assembly of the NfL, NfM and NfH subunits. The assembly of the three Nf subunits is dependent on the N–terminal head region.[120,150,283,359] NfL is known to polymerise on its own, while NfM and NfH cannot. However, both NfM and NfH can co–assemble with NfL in vitro.[115]

Cross–linking and interaction of the assembled heteropolymers with other

cytoskeletal proteins depends upon the C–terminal NfH tail domain (Figure 2.1 B). This may also play a role in the control of axonal transport.[295] Phosphorylation of the C–terminal tail domain is thought to occur at the side arms protruding from the assembled filaments. The C–terminal tail domain consists of over 40 KSP (Lys-Ser-Pro) repeats in humans as determined by mass–spectroscopy.[36,273,385] Phosphate is coupled with high affinity to the aminoacid serine within the KSP repeats.[36,385] Neurofilaments belong to the most extensively phosphorylated proteins of the human brain. Phosphorylation and dephosphorylation of the neurofilament proteins is a complex process which is predominately regulated within the axonal compartment.[85,293] Optimal performance of the neuronal network depends upon the normal functioning of these processes. The N–terminal domain is phosphorylated by glycogen synthetase kinase-3,[135,136] extracellular signal-regulated kinases[328,329] and cyclin-dependent kinase-5.[224,293,358] Phosphorylation of the C–terminal domain is regulated by a range of protein kinases.[359–361]

About 80% of axonal Nf are highly phosphorylated and integrated by cross–linking in the axoskeleton, thus constituting the "static pool".[214] Because phosphorylation alters the charge on the side–arms, it seems likely that one function of phosphorylation is to increase the charge–based repulsion of neighbouring filaments, thereby increasing interfilament spacing and consequently increasing axonal calibre.[131] However radial axonal growth does not

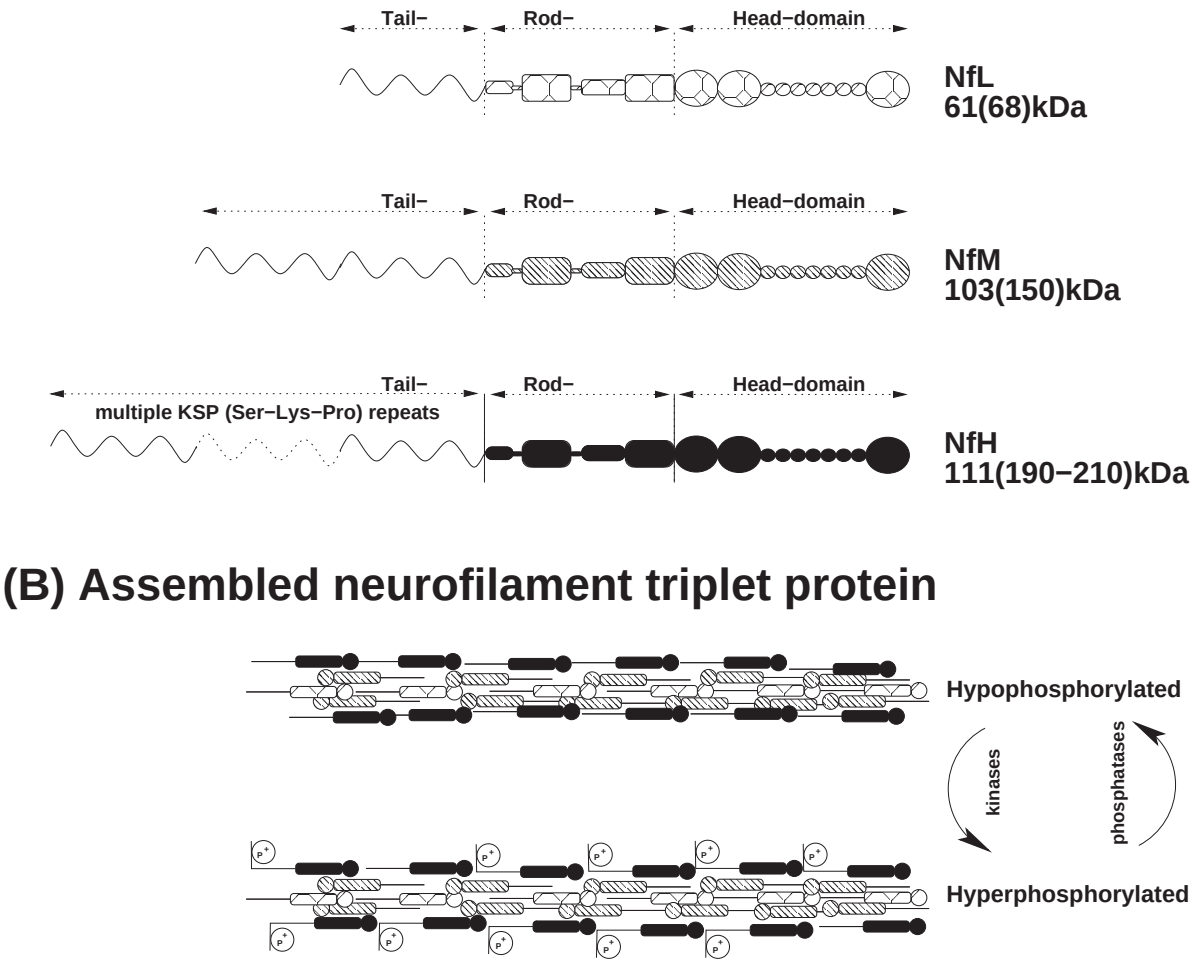

Figure 2.1: *(A) The neurofilament protein subunits. The aminoterminal tail domain is of variable length whilst the central rod and carboxyterminal head domain remain constant. The calculated molecular weights and the molecular weights as determined by SDS gel electrophoresis (in brackets) are shown.*
(B) Functional properties of the neurofilament protein such as cross-linking and protein–protein interactions are controlled locally in the axon by phosphorylation and dephosphorylation of the tail domain.

depend only on mechanisms of NfH phosphorylation[318] but also on Nf stoichochemistry as demonstrated by knockout experiments.[74,93,168,173,293,436,447] The close relation of axonal diameter and conduction velocity [153,425] is of physiological relevance. Additionally phosphorylation of NfH changes functional intracellular properties such as mobility and protein-protein interactions.[19,175,403,404,435] The remaining 20% of less extensively phosphorylated Nf constitute the so called "dynamic pool" [214,294]and are involved in ante- and retrograde axonal transport .[340] Because of the high amount of hydrophobic sides this is likely to be raft–mediated on specific kinin/dynine motors.[124] Axonal transport of Nf is a complex and vulnerable process involving phases of rapid polymer movements interrupted by prolonged pauses.[1,442,443]

Neurofilaments are prone to protease digestion .[349,418] Under physiological conditions this is mediated by calmodulin, a Ca^{2+}–dependent protease.[253] Susceptibility of Nf to protease digestion decreases with increase of phosphorylation.[124,378] This has implications for NfH stability in protease–rich body fluids such as the CSF.

Neurofilament phosphoforms There is no consistent terminology for naming the different neurofilament phosphoforms. Reference is made commonly to non–phosphorylated or hypophosphorylated versus hyperphosphorylated or extensively phosphorylated, with phosphorylated being the as-

sumed normal phosphoform. The use of mass–spectroscopy permits us to identify the phosphorylation sides within the protein,[36,385] but given that there are over 40 phosphorylation sites, such an approach will be unsuitable for clinical laboratory practise. The more practical approach chosen has been to name the NfH phosphoform according to the monoclonal antibody used either in immunohistology or enzyme–linked immuno–assay (ELISA). Several monoclonal antibodies have been shown to bind to non–phosphorylated epitopes of the NfH subunit. If NfH was detected by the Sternberger monoclonal antibody *SMI32* this NfH phosphoform is labelled NfH^{SMI32}. Likewise when phosphorylated NfH, was detected by the binding to a phosphorylated epitope recognised by the Sternberger monoclonal antibody *SMI35*, this is labelled NfH^{SMI35}. Extensively phosphorylated NfH as recognised by the Sternberger monoclonal antibody *SMI34*, is labelled NfH^{SMI34}, and so forth. The advantage of using Sternberger monoclonal antibodies is that these antibodies have been studied extensively by immunohistology[376] and are used by most neuropathological laboratories. If antibodies from other sources are used the name of the clone and the source are given. This terminology facilitates comparisons with results from other studies.

2.1.2 Clinical relevance

General Axonal injury causes disintegration of the axonal membrane and axoskeletal proteins such as Nf are released into the extracellular space

(ECF). The ECF is continuous with the CSF. A 5–fold increase of the CSF NfL has been reported after relapse in MS .[241] This finding was confirmed by a different study.[353] The CSF NfL levels returned to baseline values within approximately 3 months[241] suggesting the role of NfL as a putative marker for acute axonal injury. Histological observations provided evidence for the increase of a different Nf subunit, NfH .[398] In injured axons an increase of the (NfH^{SMI32}) NfH phosphoform was observed. Staining for NfH^{SMI32} has therefore been used as a immunohistological marker for damaged axons.[398] In contrast to MS, an increase of phosphorylated NfH was observed in stroke proximal/ rostral to the lesion.[145] Different NfH phosphoforms could thus be of clinical relevance in describing axonal injury.

Functional implications of Nf alterations for axonal pathology Nf subunits are not only constituents of the axoskeleton, but are also actively involved in the pathogenesis of axonal dysfunctioning and degeneration. The accumulation of Nf proteins has been observed in amyotrophic lateral sclerosis (ALS) ,[339] spinal muscular atrophy[441] and in giant axonal neuropathy.[21] A frameshift, nonsense and missense mutation of Gigaxonin on chromosome 16q24.1 is now recognised to cause disorganisation of the cytoskeletal IFs.[46]

Mutation close to the NfL rod–domain causes an increase of neuronal NF-L due to impaired Nf assembly.[218] It has been suggested that axonal transport is “strangulated” .[174] In humans a mutation within the NfL rod

domain has now been associated with the development of the axonal variant of Charcot–Marie–Tooth disease type 2E .[82,240,267] Whether the problem is primarily due to increased axonal vulnerability, caused by impaired axonal transport[218] or to cytoskeletal instability needs to be clarified.

The role Nf subunits play in axonal pathology has been studied in knock-out mice models[93,168,436]:

1. NfL$^{-/-}$ mice: the cellular NfM and NfH cannot form heteropolymers without NfM resulting in perikaryal accumulation of Nf subunits.[436]

2. NfM$^{-/-}$ mice: a severe effect on the radial growth of axons was observed.[93,168] Unassembled NfL sequestered in the neuronal perikarya and axonal atrophy was observed.[168] It has therefore been suggested that NfM is needed for transport of NfL from the perikaryon into the axon.

3. NfH$^{-/-}$ mice: radial growth of axons was reduced to a lesser extend then in NfM knockout mice.[93,168] This was however an inconsistent finding, suggestive of a range of compensatory changes. Such changes could include NfL and NfM over expression and increased phosphorylation.[94,173,447]

The observation that Nf accumulates in ALS suggests that alterations of the expression pattern of Nf subunits could accelerate the degeneration of pre–damaged axons. This hypothesis led to the development of mice mu-

tants combining transgenic mice expressing mutants SOD1^{G93A}, SOD1^{G37R} or SOD1^{G85R} with either Nf subunit knockout or transgenic Nf subunit overexpression:

1. Double knockout: in SOD1^{G85R}/NfL$^{-/-}$ mice a slight accumulation of NfH and NfM subunits was observed in the neuronal perikaryon.[436] This confirms the hypothesis that NfL is essential for the neuro-axonal transport of Nf. Interestingly this did not contribute to accelerated disease progression. Surprisingly the life–span increased by about 15%.[436] This has been explained by the neuroprotective effects of the accumulated NfH subunit.[174, 293, 436]

2. Triple knockout: in SOD^{G37R} mice with NfL$^{+/-}$/ NfM$^{+/-}$/ NfH$^{+/-}$ a stoichochemical balanced reduction of all three Nf subunits by about 40% did not influence the life–span at all.[292]

3. Nf over-expression:

   - Human NfH: despite a substantial reduction of the axonal calibre the life–span of offspring from SOD1^{G37R} mutant mice mated with transgenic mice overexpressing human NfH increased by about 65%. Accumulation of all Nf subunits was observed in the neuronal perikaryon.[74]
   - Human NfL: the increase of NfL lead to a increase of the axonal calibre of about 50%, but the life–span of the mice was not

affected.[74]

- Mouse NfH: the increase of NfH lead to accumulation of Nf subunits in the neuronal perikaryon and a substantial reduction of the axonal calibre. The life–span of the mice increased by 15%.[193]

- Mouse NfL: a slight increase of Nf subunits was observed in the neuronal perikaryon and the axonal calibre increased. The life span of the mice increased by 15%.[193]

The surprise finding that either NfH overexpression or perikaryal Nf accumulation in SOD1 mutant mice increases the life–span led to the suggestion that Nf could act as a Ca^{2+}–chelator reducing oxidative damage.[173,174] Alternatively it could act as a "phosphorylation–sink" and thus prevent the phosphorylation–dependent activation of enzymes which finally lead to apoptosis .[293] The finding that NfH has protects from oxidative damage has been confirmed independently.[420]

2.2 Glial fibrillary acidic protein

2.2.1 Background

Glial fibrillary acid protein (GFAP) is a non–soluble acidic cytoskeletal protein. It is the principal intermediate filament of the human astrocyte. GFAP was first extracted by LF Eng in 1969 from MS plaque tissue[96,100] and belongs to the class–III intermediate filament proteins. GFAP is coded on

chromosome 17q21.1-q25 and consists of 432 amino acids.[321] The corresponding molecular mass is 49.8 kDa. Cytoskeletal GFAP is tightly packed into polymers. After break–up of the GFAP polymer a soluble fragment of GFAP of approximately 41 kDa is released to the adjacent fluid compartments.[97] The structure of GFAP has not yet been determined. A schematic outline of the intracellular organisation of GFAP is shown in Figure 2.2.

2.2.2 Clinical relevance

The astrocyte is a major regulator of brain homeostasis and controls the molecular and ionic contents of the extracellular space of the CNS. Activation of astrocytes is a consequence of any insult to the CNS. This includes in particular trauma, genetic disorders, chemical or immunological challenge and degeneration. Elevated levels of GFAP have been found in the CSF of various diseases including MS ,[336] dementia,[97] normal pressure hydrocephalus,[7] asphyxiated newborns,[44] head injury,[276] brain infarction[22,148] Lyme–borreliosis[87] and trypanosomiasis.[220] Astrocytic hypertrophy is observed rapidly after axonal injury[322] and increased levels of GFAP become significant 24 hours post–event in semi–quantitative immunoblotting analysis.[392] The motility and shape of astrocytes depends upon the rearrangement of GFAP, the major cytoskeletal protein.

The term *astrocytic activation* or *reactive astrocytosis* is used to describe the proliferation of astrocytes with hypertrophy of the cell body and the cytoplasmic processes. Immunohistochemistry at this stage shows ex-

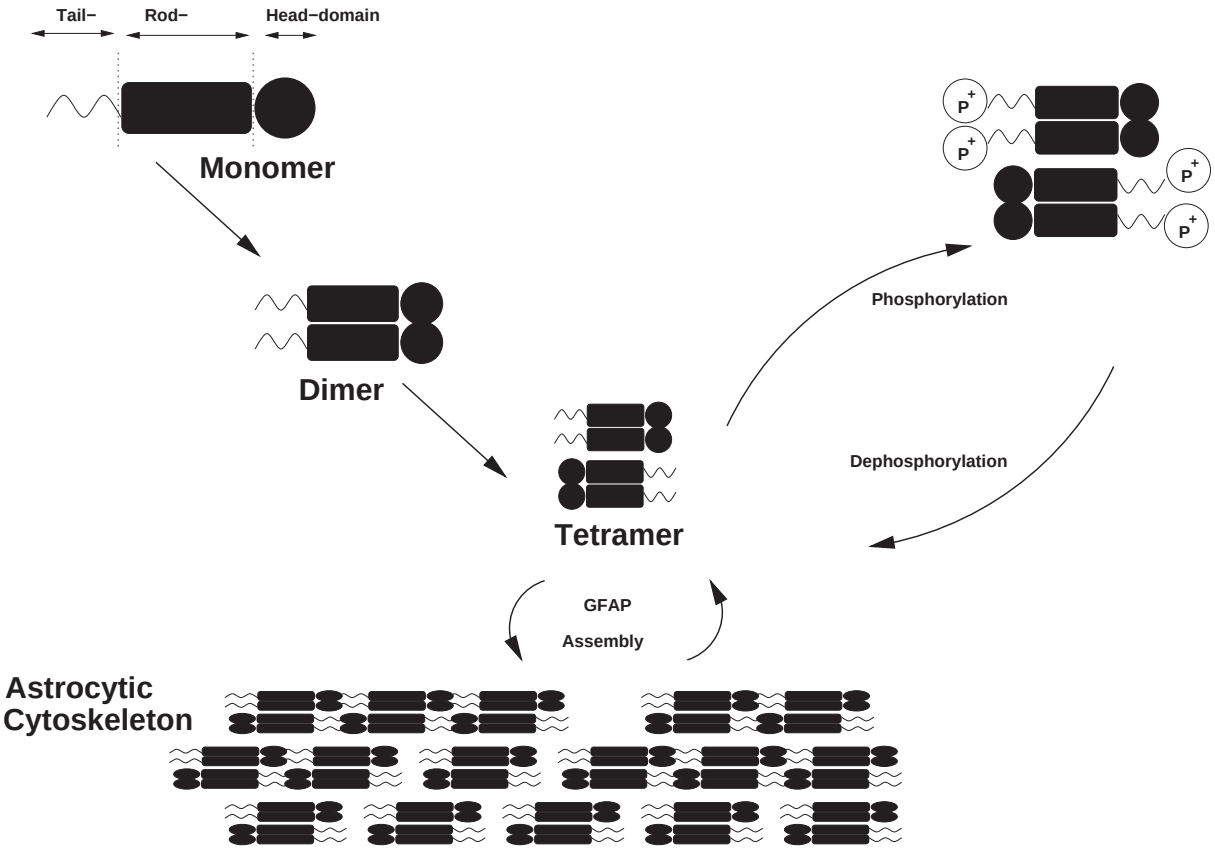

Figure 2.2: *Intracellular organisation of GFAP. The dynamics between the GFAP monomer and the functional relevant cytoskeletal 8-9 nm intermediate filament are shown.*

tensive staining for GFAP without increase of the total GFAP content. This is largely caused by rearrangement of the cytoskeletal GFAP polymer and unmasking of epitopes.[368] Electron microscopy of swollen astrocytes has demonstrated disrupted and loose bundles of glial filaments contrasting with the normally observed tight bundles.[95] Reactive astrocytosis has been shown to participate in removal of myelin and neuronal debris in areas where no activation of microglia was observed and macrophages were absent.[98]

The term *astrogliosis* is used to describe the gliotic scar formation after CNS insult. Astrogliosis walls off areas of the CNS exposed to potentially hazardous tissue/ substances. The barrier has, however, a pathological role in itself by preventing remyelination and inhibiting axonal regeneration.[97]

2.3 S100B protein

2.3.1 Background

Originally isolated from the bovine CNS by Moore in 1965[279] the protein was named S100 because of its solubility in 100% saturated ammonium sulphate at neutral pH. S100B is now known to belong to a large family of S100 proteins.[86] S100B is coded on chromosome 21q22.3[143] whereas the other 13 members of the family cluster around 1q21. S100B consists of 91 amino acids and its molecular weight corresponds to 10 kDa. S100B is a water–soluble, cytoplasmic protein and contains 2 EF–hand calcium–binding domains. The 3D structure of Ca^{2+}-free S100B is compact when compared to bound S100B (Figure 2.3). The resulting exposure of epitopes hidden by

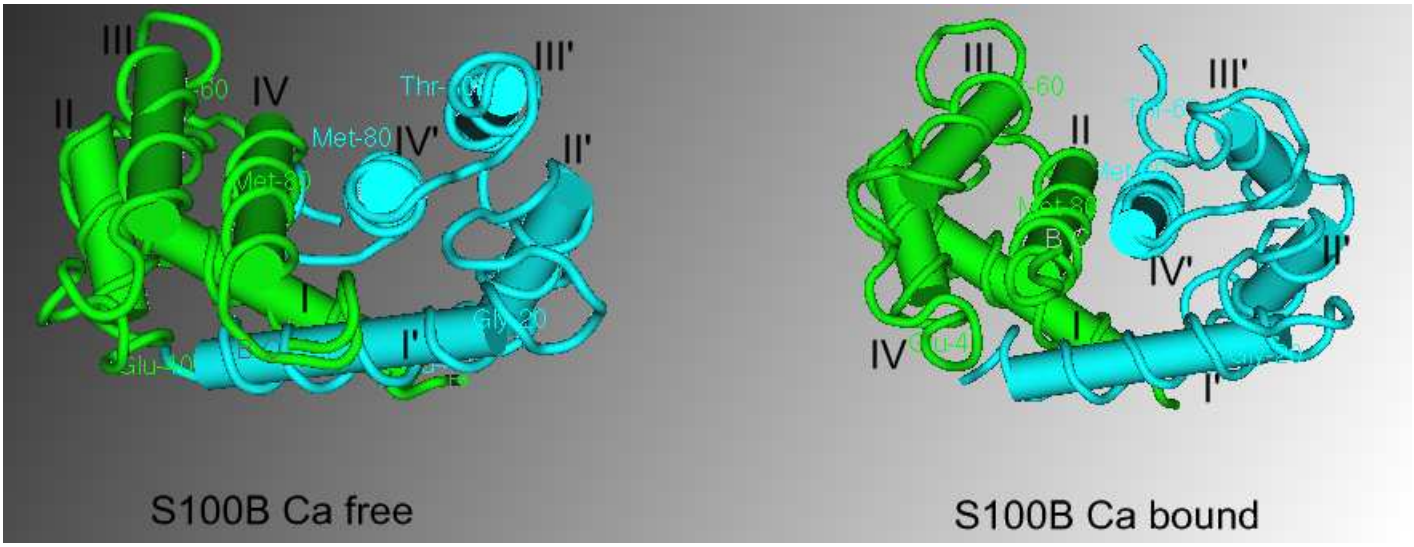

Figure 2.3: *Structure of the Ca^{2+}–free (left) and Ca^{2+}–loaded (right) S100B dimer. One S100B monomer is in blue and the other is in green. Helices are indicated by Roman numerals (I-IV) Binding of Ca^{2+} to S100B causes reorientation of helix III relative to all other helices. Note that the Ca^{2+}–loaded dimer is more extended than the Ca^{2+}–free dimer. The change of confirmation exposes otherwise hidden epitopes to the solvent*[†].

the Ca^{2+}–free isoform influences antibody recognition. This is of relevance when the protein is measured by immunological methods.[129,363]

The functions of S100B are both intra- and extracellular. Intracellularly the Ca^{2+} dependent conformational change of S100B triggers of the phosphorylation of enzymes by inhibition of e.g. PKC–mediated phosphorylation.[33,434] Extracellularly S100B protein is involved in neurite extension, astrocytosis, axonal proliferation and inhibition of microtubule assembly. This can partly be explained by the Ca^{2+} dependent interaction with cytoskeletal proteins such as the type III IF GFAP, vimentin and desmin.[254,370] For the interaction with GFAP it was demonstrated that binding of S100B

to the N–terminal tail domain hinders GFAP assembly.[448]

2.3.2 Clinical relevance

S100B has mostly been measured in the CSF and elevated levels were found in acute and chronic neurological conditions.

It appears from these studies that S100B is possibly of prognostic value in acute brain injury (ABI) .[147,314,338] There was also a suggestion that longer term outcome measures such as the Glasgow Outcome Score (GOS) or psychometry were related to S100B levels.[148,354] Of particular interest were two reports from the same group where S100B was shown to be elevated in patients with mild head injury (GCS 13–15).[37,163,421] S100B was therefore considered to be a very sensitive marker of diffuse brain injury. Consequently, it was included in prospective studies investigating cerebral injury due to cardiac surgery. It is a consistent finding that an increase of serum S100B levels during surgery is related to a higher rate of complications such as cerebrovascular accidents (CVA) .[10,11,15,45,165,188,202,228,319,327,417,428,429] Consequently the role of S100B in acute neurology is increasing, with particular reference to stroke.

Few studies have investigated S100B levels in subarachnoid hemorrhage (SAH) on a systematic basis,[278,304,391,433] but levels were generally elevated. This contrasts with the study by Sindic *et al.* who found elevated levels only in 47% (8/17), but did not distinguish between SAH and intracranial haematoma.[363] High CSF levels were associated with a poor Fisher grade[391]

or more severe impairment on the Hunt and Hess scale.[433]

Measurement of S100B increases the sensitivity and specificity of the differential diagnosis of dementia syndromes with particular reference to CJD and vCJD.[127]

On the premise that S100B levels are highly sensitive to changes of the CNS homeostasis this protein has been investigated as a marker for disease activity in MS. It appears from 5 studies[212,212,250,251,269] that S100B is increased in the CSF of patients with MS. In particular the longitudinal study by Michetti *et al.* (1979) demonstrated an increase of S100B after relapse with regression to the mean after 29–35 days[269] (Table 1.2 on page 45). The results of measuring S100B in MS have however been disappointing in one cross–sectional study.[363] This might have been due to the sensitivity of the assay using a Particle Counting ImmunoAssay (PACIA) based on latex agglutination. Importantly, these investigators determined that Ca^{2+} influenced the sensitivity of the assay, with a concentration of 5 mM being the optimum for their assay.[363]

There is also some evidence for elevated S100B levels in epilepsy [212,373] and amyotrophic lateral sclerosis, [278] however systematic investigations have not yet been performed.

2.4 Ferritin apoprotein complex

2.4.1 Background

Iron–free ferritin is a nearly spherical apoprotein complex of 450 kDa and approximately 480 kDa if iron–loaded. The apoprotein shell consist of 24 subunits containing a central cavity with binding capacity for approximately 4,500 iron atoms. There are 2 ferritin subunits: a heavy chain predominantly expressed in heart tissue (FTH) and a lighter chain expressed in liver (FTL). FTH is coded on chromosome 11q12-q13, and consists of 182 amino acid with a molecular mass of 21 kDa. FTH is associated with low iron storage and high iron utilisation due to its ferroxidase activity.[75] FTL is coded on chromosome 19q13.3-q13.4, consists of 174 amino acids with a molecular mass of 19.9 kDa.[146] FTL is associated with slow uptake and long–term storage.

CSF ferritin has been shown to be largely non–glycosylated[54] in contrast to serum ferritin. There is evidence for intrathecal ferritin synthesis.[185] The cellular origin of CSF ferritin derives from microglia and oligodendrocytes. Whereas oligodendrocytes express mainly FTH, microglia are capable of expressing FTL. Iron is required as a cofactor for cholesterol and lipid biosynthesis in order to produce myelin. Increased endocytotic ferritin uptake could be demonstrated in oligodendrocyte progenitor cells .[71,159] Using in–situ hybridisation and immunohistochemistry it could be demonstrated that cellular distribution of ferritin however changes during development

from predominant expression in microglia to oligodendrocytes. In pathological conditions however microglia seem to considerably upregulate ferritin expression. In adult rat brain tissue ferritin is mainly present in oligodendrocytes.[62] In MS the distribution of ferritin and transferrin binding-sites undergoes an inversion of the physiological state when compared to normal controls.[160] This suggests a possible role for oligodendroglial ferritin (FTH) in remyelination.

2.4.2 Clinical relevance

High CSF levels of ferritin have been associated with subarachnoid haemorrhage, intraparenchymal cerebrovascular events, miscellaneous central nervous system infections and vasculitis.[54,134,140,364]

The most characteristic feature of microglial cells is their rapid activation in response to even minor pathological changes in the CNS. Microglial activation is a key factor in the defence of the neural parenchyma against infectious diseases, inflammation, trauma, ischaemia, brain tumours and neurodegeneration.[141,199,262,263,383] Microglial activation occurs as a graded response in vivo.[227,383] The transformation of microglia into potentially cytotoxic cells is under strict control and occurs mainly in response to neuronal or terminal degeneration, or both.[9,305,306,350] Activated microglia are mainly scavenger cells but also perform various other functions in tissue repair and neural regeneration. They form a network of immune alert resident macrophages with a capacity for immune surveillance and control. Ac-

tivated microglia can destroy invading micro-organisms, remove potentially deleterious debris and promote tissue repair by secreting growth factors. An understanding of intercellular signalling pathways for microglial proliferation and activation could form a rational basis for targeted intervention to injuries in the CNS.[199]

Chapter 3

Hypothesis

Disease heterogeneity is a feature of early MS and suitable biomarkers might contribute to improving the subclassification of these patients .[236] This study first aims to test the hypothesis that BSP can help to distinguish different MS subtypes.

The assessment of the development of disability requires long observation periods when clinical scales are applied. In addition the inter–observer variation is high. This study addresses the second question as to whether BSP can be used as a surrogate for monitoring the development of disability.

Axonal damage is observed early in the disease and is responsible for irreversible loss of function. Thirdly this study investigates whether BSP can be used early on as a prognostic marker indicating those patients who suffer from a high level of axonal injury and thus will develop greater disability.

Taking these together the following hypotheses were formulated:

- Axonal damage is paralleled by release of neurofilament proteins into

the extracellular space, which equilibrates with the adjacent fluid compartment (e.g. CSF). Therefore the quantification of neurofilaments from body fluids should allow to estimate the amount of axonal damage. Because axonal damage is directly related to sustained disability, the neurofilament levels should be an indirect measure, a surrogate for disability.

- Astrocytic activation is a direct response to any challenge to brain–homeostasis. A relapse in MS is such a challenge and therefore S100B, a surrogate for early astrocytic activation, should be increased in body fluids. Because relapses are an indicator for disease activity and tend to be less frequent in progressive than in relapsing disease, the S100B levels should help to distinguish clinical subgroups of MS.

- Microglial activation, in an analogy to astrocytic activation should be a direct response to any challenge to brain homeostasis. Therefore the measurement of CSF ferritin should provide another indirect measure for disease activity.

- Astrogliosis describes the fibrotic scar tissue replacing any irreversibly damaged CNS parenchyma and represents therefore the "burnt–out" phase of the disease. Because these astrogliotic plaques are rich of GFAP, GFAP levels in body fluids should give a measure of the "total lesion load" (i.e. with chronic lesions) (CL) which should indirectly

relate to disability. Additionally GFAP should distinguish progressive from relapsing disease on the rationale that the total amount of chronic lesions is higher in the former.

- if the course of MS would be homogeneous then, in theory there should be a negative relation between GFAP with either S100B or ferritin with GFAP being higher in progressive/ "burnt–out" MS.

In order to address these questions it was necessary to develop quantitative methods for the assessment of Nf and GFAP. The hypothesis which claims that BSP are released from MS lesions was tested in animal and post–mortem studies prior to a cross–sectional and longitudinal approach in human CSF.

Part II

Methods

Chapter 4

Development of a neurofilament ELISA

4.1 Background

Neurofilaments (Nf) are possible candidates for estimating axonal damage in neurological disorders (Chapter 1.3) and the basic structure of Nf was reviewed in Chapter 2.1. There are currently no commercial ELISA kits available for quantification of any of the three Nf subunits. One group developed a sandwich ELISA technique for the detection of NfL, based on in–house antibodies. Confirmation of the results derived by this group is however hampered by the non–availability of the antibodies*. Another group tried to develop an ELISA based on commercially available substances but was not able to obtain satisfactory sensitivity and reproducibility (Dr Eli Silber, personal communication).

*In a personal communication Dr Rosengren argued that he preferred not to provide an external researcher with his antibody on the basis that previously there were problems with repeating the NfL assay which were related to the expertise of the researcher. Dr Rosengren was however positive towards a collaborative study where he would be provided with snap–frozen CSF and perform the NfL assay.

The aim of this part of the study was to develop an ELISA for the neurofilament subunits NfL and NfH.

4.2 Materials and methods

4.2.1 Antibodies

Capture (first) antibody

NfH Mouse monoclonal IgG1 anti–NfH antibodies (SMI) were purchased from Sternberger Monoclonals (Sternberger Monoclonals Incorporated, 10 Burwood Court, Utherville, MD 21093) and Sigma (NE14). The NfH phosphoforms were named as discussed (paragraph 2.1.1 on page 54). The purchased antibodies were all provided as ascites fluid and have the following characteristics [†]:

NfH^{SMI32} SMI32 (old notation[378]: 02–135) is a mouse monoclonal IgG1 which reacts with a non–phosphorylated epitope in NfH of most mammalian species. On Western immunoblots two bands (200 and 180 kDa) were seen for SMI32. On 2D immunoblots these bands merged into a single NfH line.[123,376] The reaction could be abolished on immunoblots and immunohistochemistry by phosphorylation. Dephosphorylation of NfH in contrast lead to increased staining. These findings suggest that the SMI32 binding–site can be masked and unmasked.[123,376,378] NfH^{SMI32} was present in neuronal cell bodies, dendrites and some

[†]The information on the antibodies is largely derived through personal communication with Dr Ludwig Sternberger and his own summary, which is available on: http://home.att.net/ sternbmonoc/SMIMonoclonalAntibodies.htm

thick axons of the central and peripheral nervous system. Thin axons were NfH^{SMI32} negative. There was no cross–reactivity with either tau or with other tissues.[18,55,56,152,303,378,422] Treatment with trypsin abolished the staining for NfH^{SMI32} ‡. However after incubating the trypsin–treated tissue with alkaline phosphatase, staining for NfH^{SMI32} reappeared. NfH^{SMI32} was now visible in cell bodies, dendrites , thick and thin axons. This pattern was indistinguishable from the one obtained with anti–phospho–neurofilaments such as NfH^{SMI35} .[378] The interpretation of these results implies that phosphorylation protects NfH from digestion and confirms the hypothesis that phosphorylation masked the NfH binding epitope for SMI32.

A subset of cortical neurons which are lost in pathological conditions such as Alzheimer's and Huntington's disease were NfH^{SMI32} positive.[18,56,152] In primary cell cultures of murine cortex a neuronal population with enhanced vulnerability to kainate toxicity was also NfH^{SMI32} positive. In this model toxicity was related to GABAergic and kainate–activated Ca^{2+} uptake.[126] In MS, demyelination of axons and the axon-terminal spheroids of transected axons contain abundant NfH^{SMI32} .[398] In Alzheimer's disease unmasking of the SMI32 epitope by dephosphorylation, revealed that swollen neurites contained a high concentration of NfH^{SMI32} suggestive of aberrant NfH phosphoryla-

‡Note that trypsin treatment did not affect the staining for NfH^{SMI34} .

tion.[379,446] Consequently it has been shown that dephosphorylation of brain tissue from patients with Alzheimer's disease had a high number of NfH^{SMI32} positive swollen neurites which extended outside the area positive for tau.[387] In a rat model early stages of Alzheimer's disease demonstrated axons positive for NfH^{SMI32} , whilst tau remained negative.[191] It was speculated that projection pathways positive for NfH^{SMI32} might be vulnerable[152] and that there was a retrograde toxic effect of the plaque as the primary lesion.[386]

NfH^{SMI33} SMI33 (old notation[378]: 02–04) is a mouse monoclonal IgM which binds to a non–phosphorylated epitope accessible in both, phosphorylated and non–phosphorylated NfH. Some cross–reactivity was observed with NfM. In contrast to other anti–non–phospho-neurofilaments, reaction with isolated neurofilaments was not intensified by phosphorylation with alkaline phosphatase. Immunocytochemically, SMI 33 visualises neuronal cell bodies, dendrites and some thick axons in the central and peripheral nervous system. SMI33 stained neuronal cell bodies and processes more abundantly than SMI32. There was some binding of SMI 33 to non-neuronal elements in peripheral, non-nervous system tissue, particularly to macrophages. In some pathological conditions, the neuronal cell body showed an increased NfH^{SMI33} content.

NfH^{SMI34} SMI34 (old notation[378]: 07-05) is a mouse monoclonal IgG1 which

binds to a phosphorylated epitope of extensively phosphorylated NfH in mammalian species and chicken. There was some cross–reactivity with NfM, but not with other cells and tissues. Treatment with alkaline phosphatase but not trypsin abolished the NfH^{SMI34} bands on Western–blots and NfH^{SMI34} positivity in immunohistology. In untreated tissue sections thick and thin axons and basket cell dendrites were NfH^{SMI34} positive. In some pathological conditions neuronal cell bodies became NfH^{SMI34} positive. Aberrant phosphorylation of NfH of the neuronal cell body could be demonstrated in cell cultures after exposure to agents which induce stress-activated protein kinase.[119] In Alzheimer's disease indexintraneuronal tangles intraneuronal tangles, but not extraneuronal (ghost) tangles were NfH^{SMI34} positive.[72,357,379,414,446]

NfH^{SMI35} SMI35 (old notation[378]: 03–44) is a mouse monoclonal IgG1 which reacts with high (200 kDa, pI 5.1) to low (170 kDa, pI 6.2) phosphorylated NfH phosphoforms.[123,376] The latter distinguishes SMI35 from SMI34 and SMI310. There was some cross–reactivity with NfM in Western–blots. No cross–reactivity with other tissue was observed.[55,72,123,377] In pathological conditions, SMI 35 frequently detected early changes in neuronal cell body staining. A Golgi-like image of pathological phosphorylation in neuronal perikarya and their dendritic arborizations for NfH^{SMI35} provided evidence for pre–chromatolytic, retrograde demonstration of neuronal connectivities .[145] In Alzheimer's disease intraneu-

ronal tangles were NfH^{SMI35} positive, a result which could be amplified by mild dephosphorylation.

NfH^{SMI37} SMI37 (old notation[378]: 06–32) is a mouse monoclonal IgM which binds to a non–phosphorylated epitope in NfH of most mammalian species. Immunocytochemically a subpopulation of neuronal cell bodies, dendrites and some thick axons in the central and peripheral nervous systems were NfH^{SMI37} positive. The pattern was however more restricted than for NfH^{SMI32} or NfH^{SMI38} .

NfH^{SMI38} SMI38 (old notation[378]: 10–01) is a mouse monoclonal IgG1 which binds to a non–phosphorylated epitope in NfH of most mammalian species. No cross–reactivity was observed towards other cells or tissues. Immunocytochemically neuronal cell bodies, dendrites and some thick axons in the central and peripheral nervous systems were NfH^{SMI38} positive.

NfH^{SMI310} SMI310 (old notation[378]: 04–07) is a mouse monoclonal IgG1 which binds to a phosphorylated epitope in extensively phosphorylated NfH in most mammals. Phosphorylation of this epitope is essential as phosphatase–treated tissue sections or Western–blots became NfH^{SMI310} negative. There was some cross–reactivity with NfM. Immunocytochemically only some axons, but no neurons or dendrites were NfH^{SMI310} positive. This contrasted with with the staining for all other anti–

phospho–neurofilaments, e.g. NfH^{SMI34} or NfH^{SMI35} .

In pathological conditions neuronal cell bodies became NfH^{SMI310} positive. In Alzheimer's diseased extraneuronal (ghost) neurofibrillary tangles but not intraneuronal tangles were strongly NfH^{SMI310} positive. It was therefore speculated that NfH^{SMI310} could represent an unusual and sparsely distributed form of phosphorylated NfH which might be increased in certain pathologic conditions.[414] Staining for NfH^{SMI310} distinguished sporadic inclusion–body myositis from hereditary inclusion–body myopathies .[275]

NfH^{SMI311} SMI311 is a cocktail of a number of monoclonal IgG1 and IgM antibodies to non-phosphorylated NfH. SMI 311 is a convenient marker for neurons in general and their differentiation from non–neuronal cells.[102] In specifically delineating cell bodies and dendrites, SMI311 has been used to trace the "inside-out gradient" of neuron production and differentiation.[405] Pathological conditions, such as under–nutrition, affected SMI311 visualised soma size and dendritic arborisation.[406]

NfH^{NE14} NE14 is derived from the hybridoma produced by the fusion of mouse myeloma cells and splenocytes from an immunised mouse. Neurofilaments purified from pig spinal cord were used as the immunogen. NE14 recognises a phosphorylated epitope on NfH.[125] NE14 was purchased from Sigma.

NfL Mouse monoclonal IgG1 anti–NfL antibodies (Clone NR4) were purchased from Sigma. This antibody was developed by Debus *et al.* and stained specifically for NfL.[83] NR4 detected NfL in mammalian and mouse tissue.[243]

Detector (second) antibody

Affinity–purified rabbit polyclonal anti–NfH was purchased from Affiniti Research Products, Exeter. Isoelectric focusing and immunoblotting demonstrated that this antibody reacted against NfH, with some cross–reactivity against NfL and NfM. Affinity purified rabbit polyclonal anti–NfL was purchased from Affiniti (batch Z01495).

Indicator (third) antibody

Horseradish peroxidase conjugated swine polyclonal anti–rabbit Ig was purchased from Dako (Copenhagen, Denmark). Isoelectric focusing and immunoblotting demonstrated that this antibody reacted primarily against rabbit IgG, with no reactivity against mouse IgG1.

Sodium barbitone, barbitone, ethylene diamine tetra acetic acid disodium salt (EDTA), calcium lactate, 30% hydrogen peroxide, bovine serum albumin (BSA) were of analytical grade (Sigma). TMB was purchased from DAKO (Copenhagen, Denmark). Hydrochloric acid was obtained from Merck (Darmstadt, Germany). Nunc Maxisorb Microtitre plates were obtained from Life Technologies (Paisley, Scotland).

4.2.2 Working reagents and buffers

Carbonate buffer The stock solution of 0.5 M carbonate buffer contained: Na_2CO_3 14.85 g, $NaHCO_3$ 26.1 g, add H_2O to 1 L $\Rightarrow$ 0.5 M. The working strength solution (0.05 M) was prepared directly prior to the experiment. The pH was 9.6. Carbonate buffer was used for coating the ELISA plates with the appropriate antibody.

Phosphate buffered saline (PBS) The 10–fold concentrated stock solution contained: NaCl 80.0 g, KCl 2 g, KH_2PO_4 2 g, Na_2HPO_4 11.5 g. The working–strength solution was prepared directly prior to the experiment. The pH was 7.4.

Barbitone buffer The working–strength solution contained 13.1 g sodium barbitone, 2.1 g barbitone in 1 L of purified water. The pH was 8.6.

Washing solution 1 g BSA (0.1%) was dissolved in 1 L of the appropriate buffer (PBS or barbitone) and 500 μL Tween 20 (0.5%) were added.

Block solution 1 g BSA (1%) was dissolved in 100 mL of the appropriate buffer (PBS or barbitone).

Antibody diluent 0.1 g BSA (0.1%) in 100 mL of the appropriate buffer (PBS or barbitone).

Sample diluent 0.1 g BSA (0.1%) in 100 mL of the appropriate buffer (PBS or barbitone).

4.2.3 Standards

NfH standards Bovine NfH (200/210 kDa) was obtained from Affiniti Research Products, Exeter. A range of standards from 0 to 2 ng/mL were prepared by diluting bovine NfH in barbitone buffer (pH 8.9) containing 0.1% bovine serum albumin, 6 mM EDTA and stored in 1 mL aliquots at -20°C.

NfL standards Bovine NfL (68 kDa) was obtained from Affiniti Research Products, Exeter. A range of standards from 0 to 1.5 ng/mL were prepared by diluting bovine NfL in barbitone buffer (pH 8.9) containing 0.1% bovine serum albumin and stored in 1 mL aliquots at -20°C.

4.2.4 CSF samples and reference population

NfH reference population CSF samples from 463 neurological patients undergoing a routine diagnostic lumbar puncture were obtained. The selection was randomised from the department's sample library in order to obtain a heterogeneous population. Clinical details were only obtained after analysis. The CSF samples were centrifuged on receipt and stored at 4°C. Analysis was performed within 1 week.

NfL reference population CSF samples from 127 neurological patients undergoing a routine diagnostic lumbar puncture were obtained. The selection was randomised from the department's sample library in order to obtain a heterogeneous population. Clinical details were obtained only after analysis. The CSF samples were centrifuged on receipt and stored at 4°C. Analysis was performed within 1 week.

4.2.5 Analytical procedure

The microtitre plates were coated overnight with capturing antibody (SMI) diluted 1:5000 in 0.05 M carbonate buffer, 100 μL, pH 9.5. The plate was washed with barbitone buffer containing 0.1% BSA and 0.05% Tween 20. Fifty μL of barbitone buffer, 6 mM EDTA. 0.1% BSA were added as sample diluent to each well. Fifty μL of standard, control or CSF sample were then added in duplicate to the plate. The plate was incubated at room temperature (RT) for 1 h. After washing, 100 μL of rabbit anti NfH diluted 1:1000 in barbitone buffer were added to each well and the plate was incubated for 1 h at RT. The microtitre plate was then washed with appropriate wash solution. HRP–labelled swine anti–rabbit antibody diluted 1:1000 was added and incubated for 1 h at RT. After a final wash, 100 μL of TMB substrate were added. The plate was incubated for 20 minutes at RT in the dark, the reaction was stopped by adding 50 μL 1 M HCl and the absorbance was read at 450 nm with 750 nm as the reference wavelength on a Wallac Victor2.

4.2.6 Statistical evaluation

Data were managed and analysed as described (Chapter 7, page 151).

4.3 Results

4.3.1 NfH phosphoforms

Standard curves All standard curves were run on the same plate to minimise the inter-assay variation. The concentration for the first antibody was 1:10000, for the second and third antibody 1:1000. The standard curves determined for the NfH capture antibodies were expressed as the percentage optical density (OD) for each calibrant.

This normalised procedure allows firstly direct comparison of the performance of the assay, which was e.g. linear for NfH^{SMI34} (Figure 4.1) versus quadratic for NfH^{SMI35} (Figure 4.2). Secondly, those capturing antibodies which might still be worth using for the further development for an ELISA specific for one NfH phosphoform can be seen (e.g. SMI34 but not SMI311). The standard curves for the antibodies binding to phosphorylated NfH (NfH^{SMI34} NfH^{SMI35} NfH^{SMI310} NfH^{NE14}) are shown in Figures 4.1 to 4.4. The standard curves for the antibodies binding to non–phosphorylated NfH (NfH^{SMI32} NfH^{SMI33} NfH^{SMI37} NfH^{SMI38} NfH^{SMI311}) are shown in Figures 4.5 to 4.9.

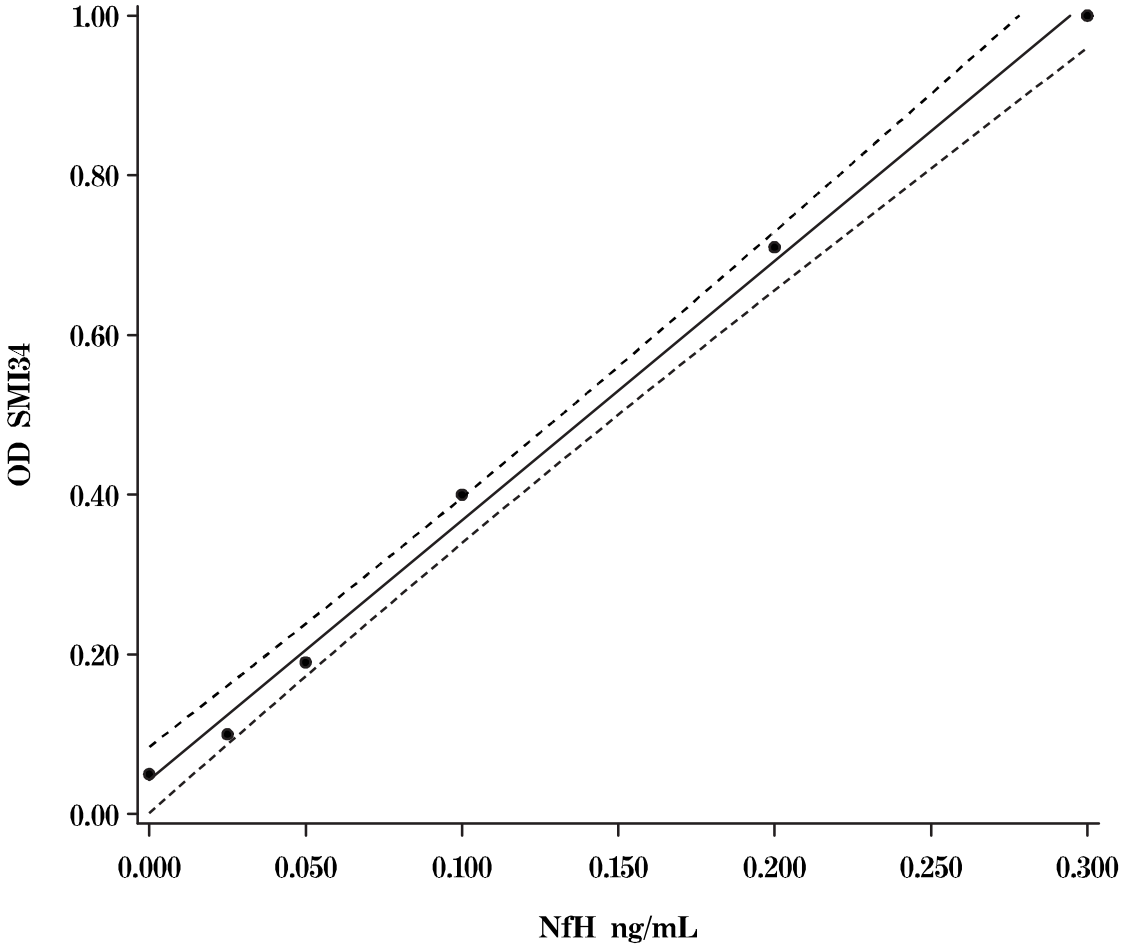

Figure 4.1: *Standard curve for NfH^{SMI34} . The regression line and 95% confidence interval curves are shown.*

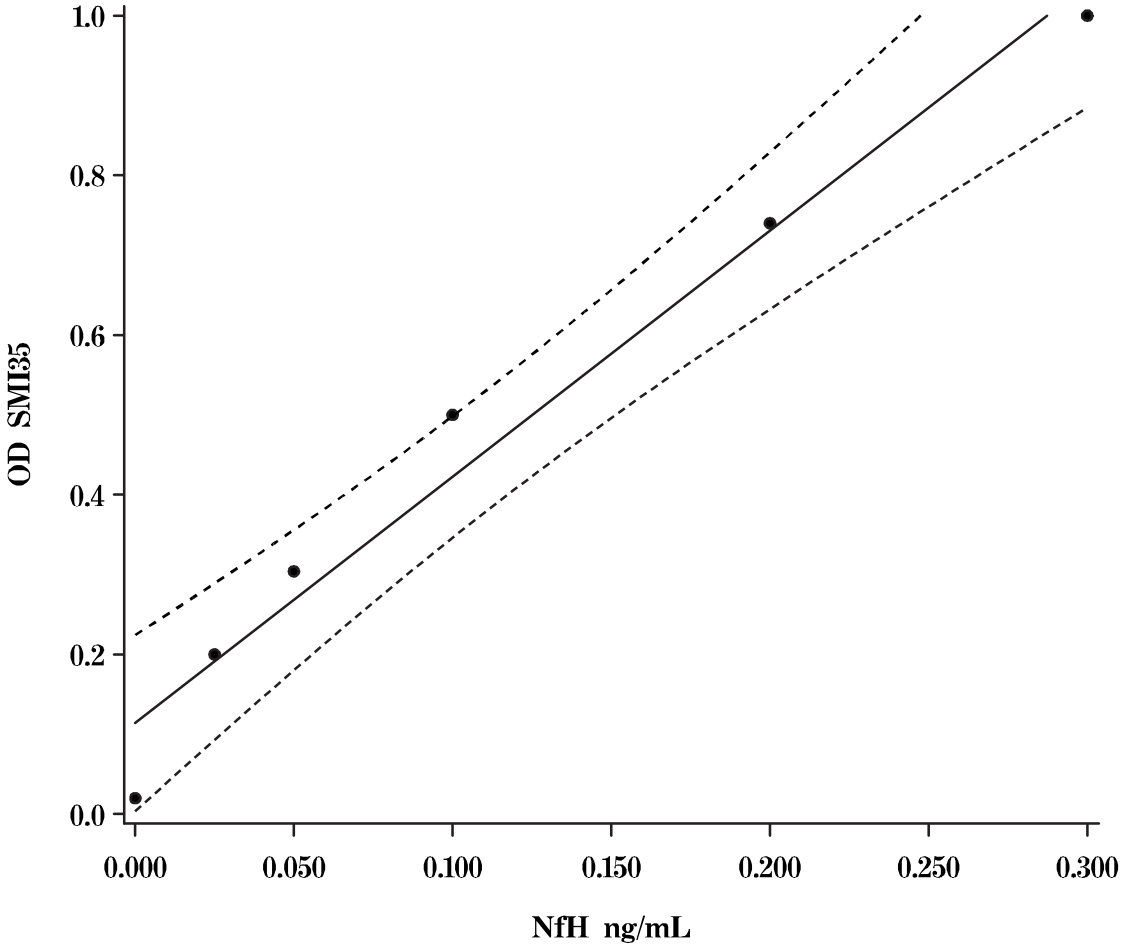

Figure 4.2: *Standard curve for NfH^{SMI35} . The regression line and 95% confidence interval curves are shown.*

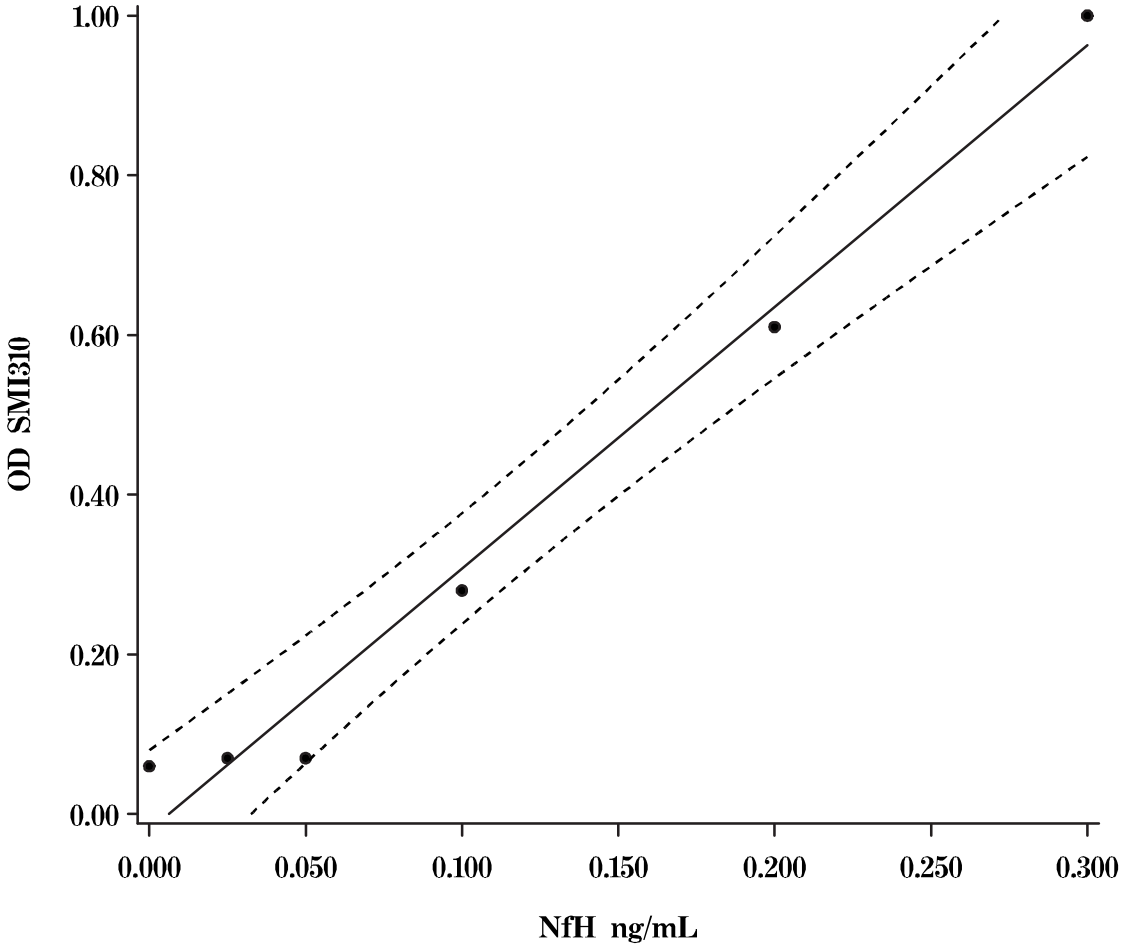

Figure 4.3: *Standard curve for NfH^{SMI310} . The regression line and 95% confidence interval curves are shown.*

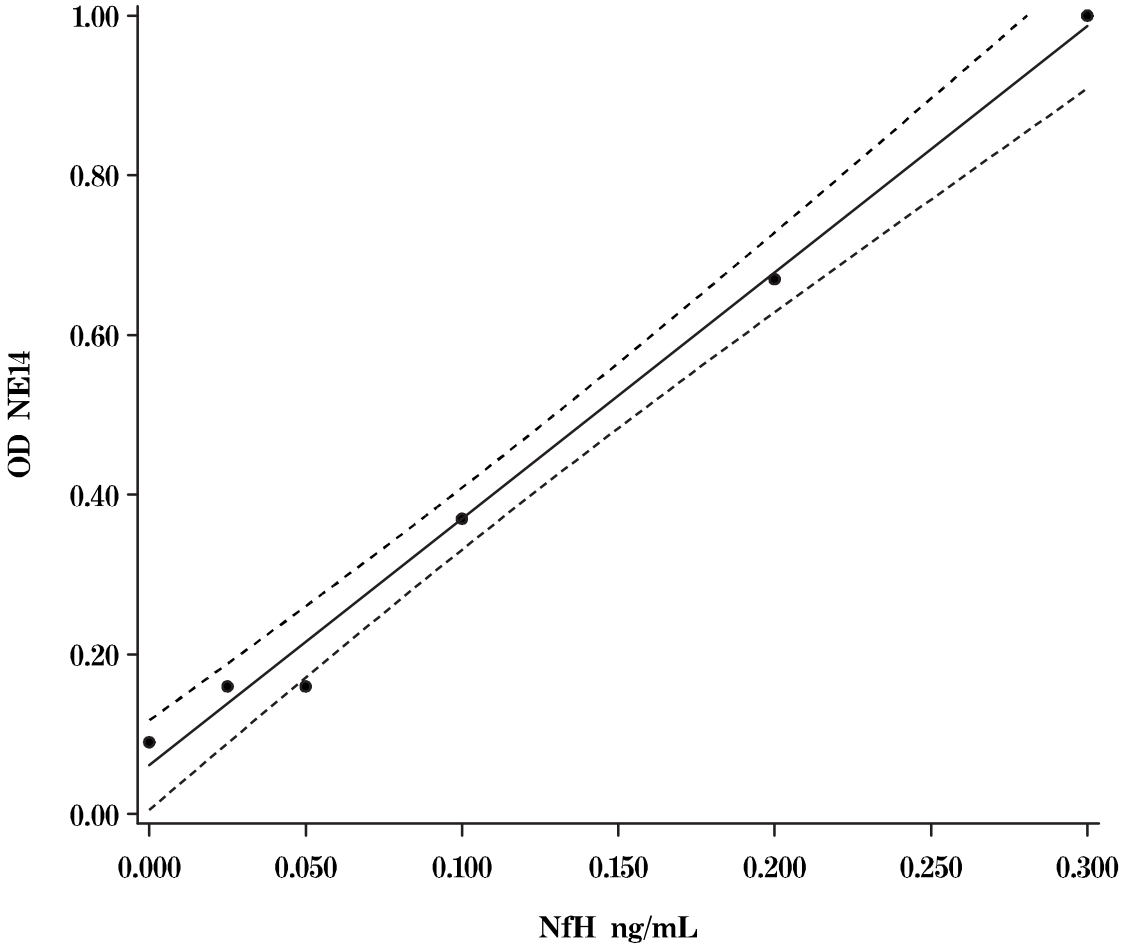

Figure 4.4: *Standard curve for NfH^{NE14} . The regression line and 95% confidence interval curves are shown.*

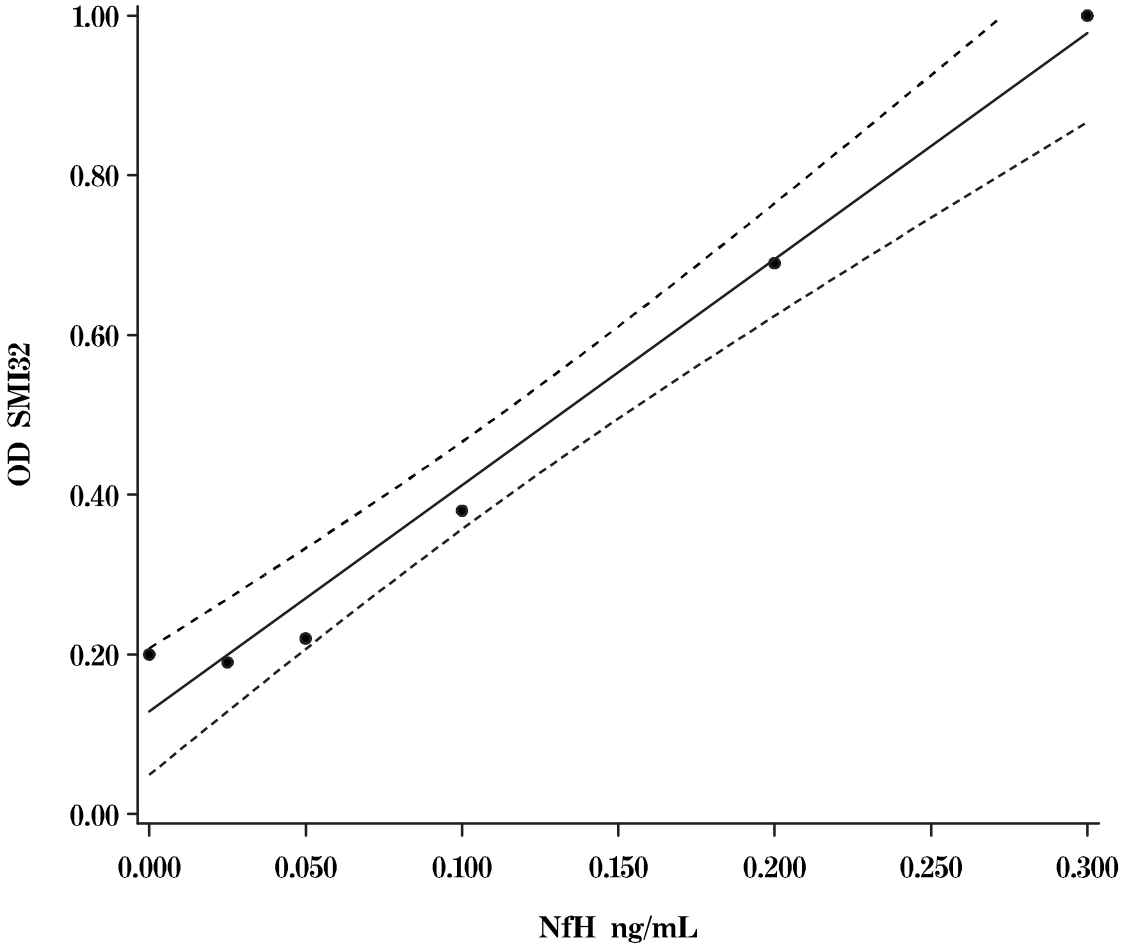

Figure 4.5: *Standard curve for NfH^{SMI32} . The regression line and 95% confidence interval curves are shown.*

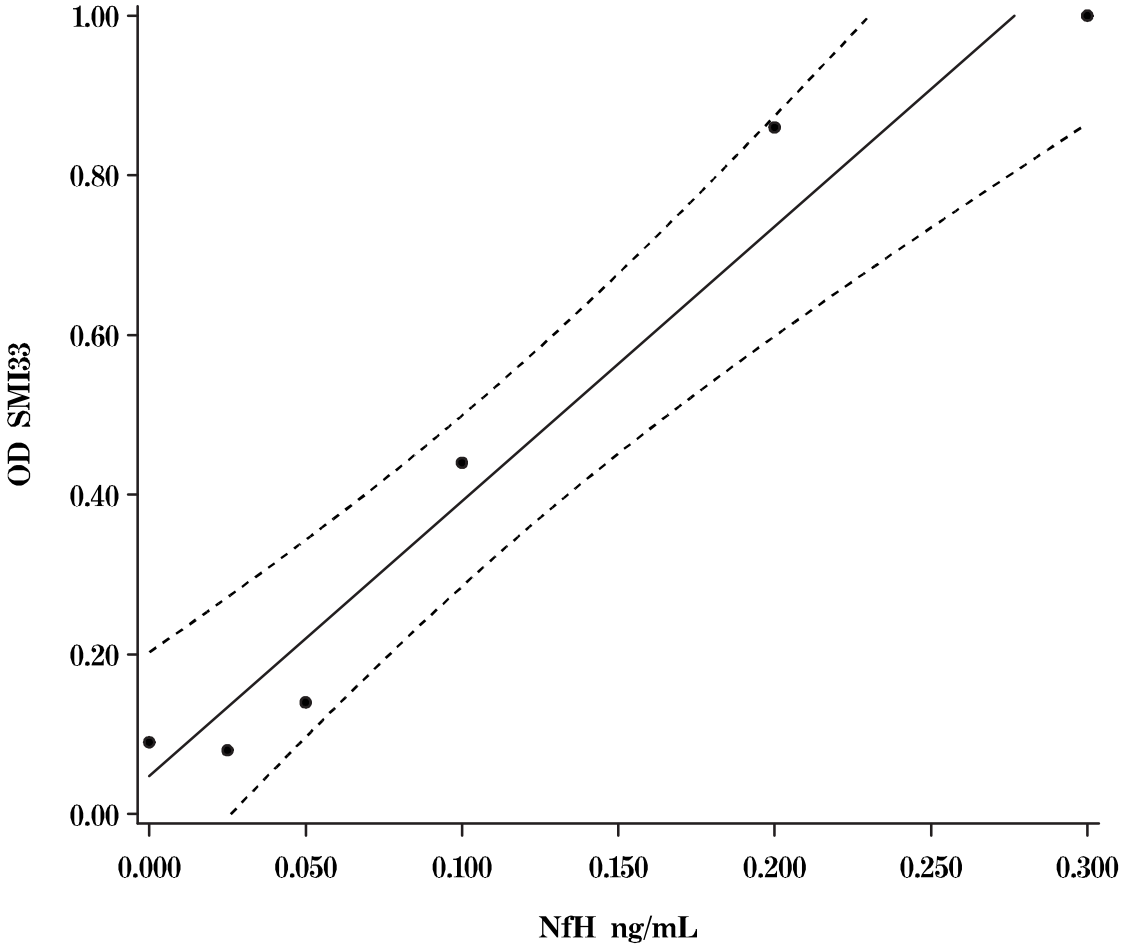

Figure 4.6: *Standard curve for NfH^{SMI33} . The regression line and 95% confidence interval curves are shown.*

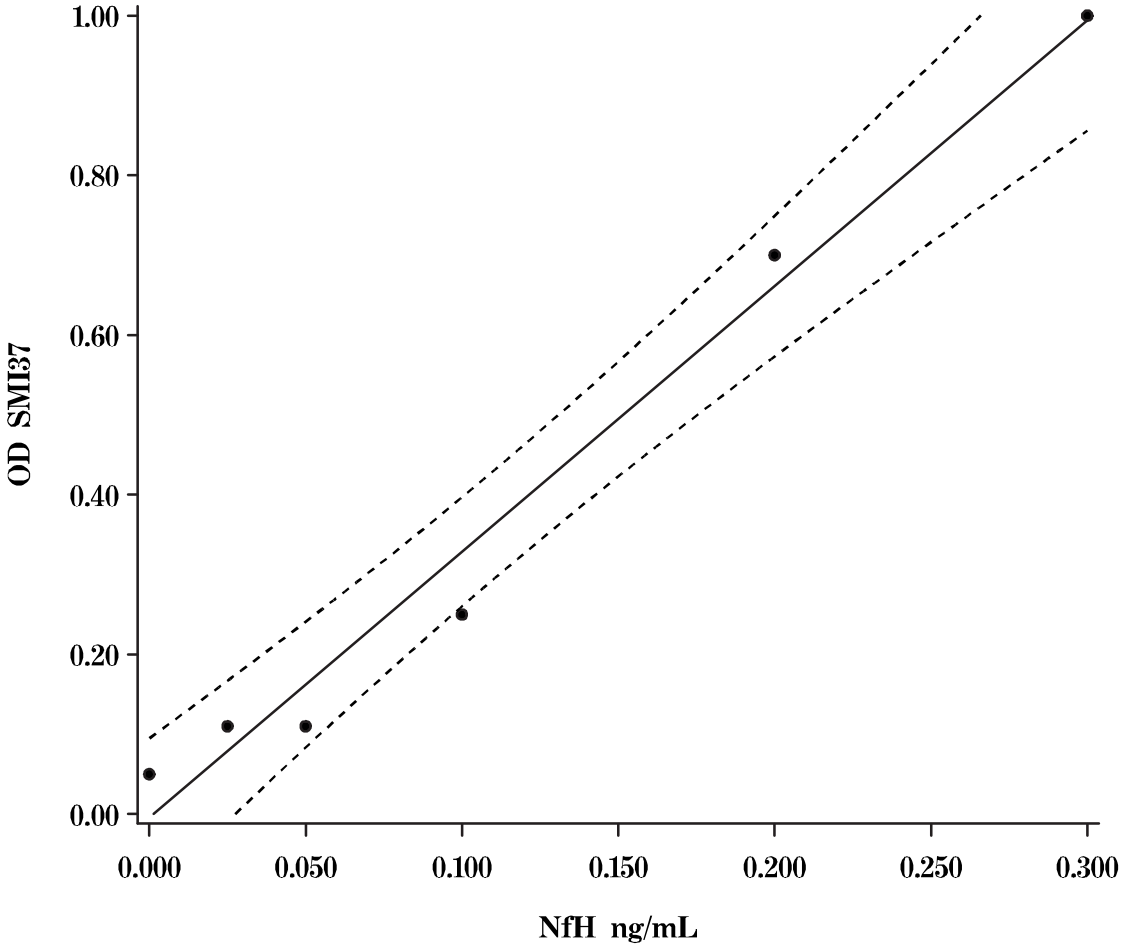

Figure 4.7: *Standard curve for NfH^{SMI37}. The regression line and 95% confidence interval curves are shown.*

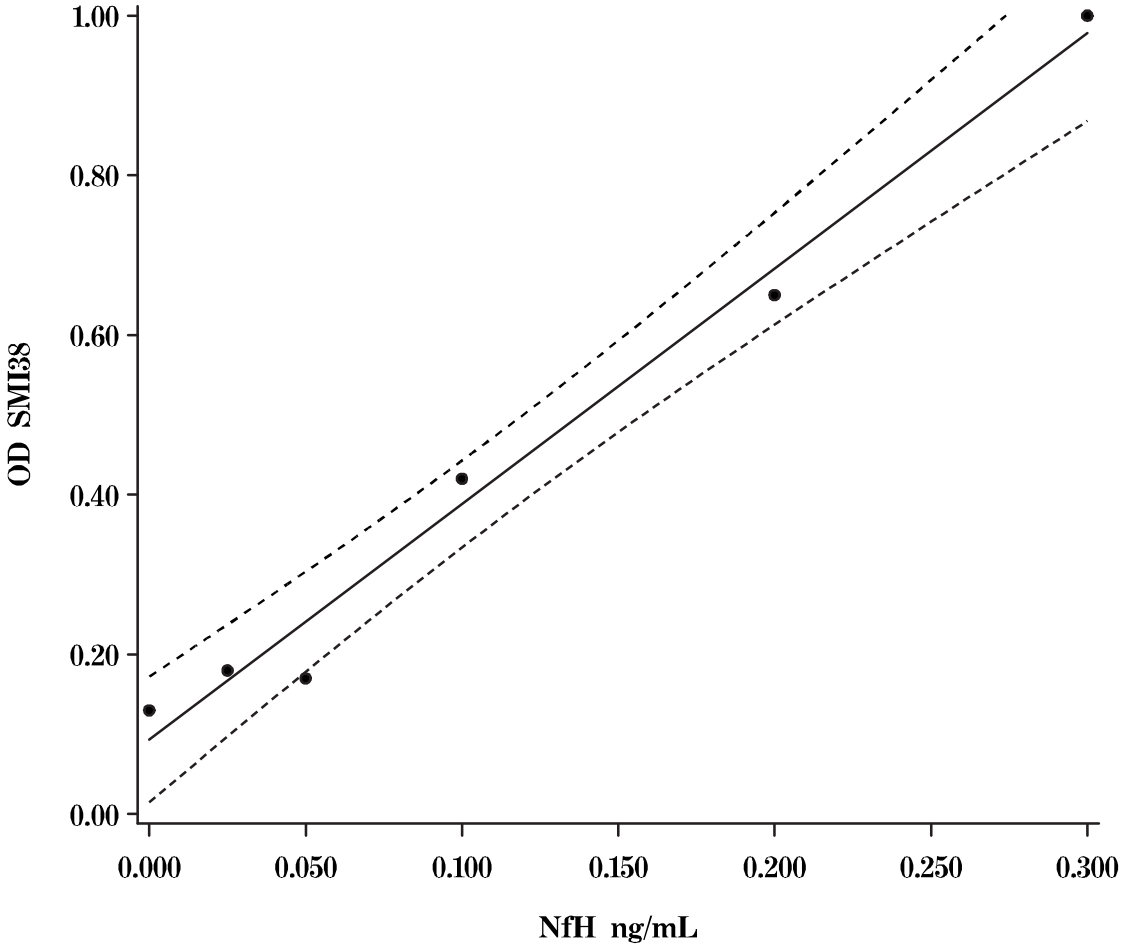

Figure 4.8: *Standard curve for NfH^{SMI38} . The regression line and 95% confidence interval curves are shown.*

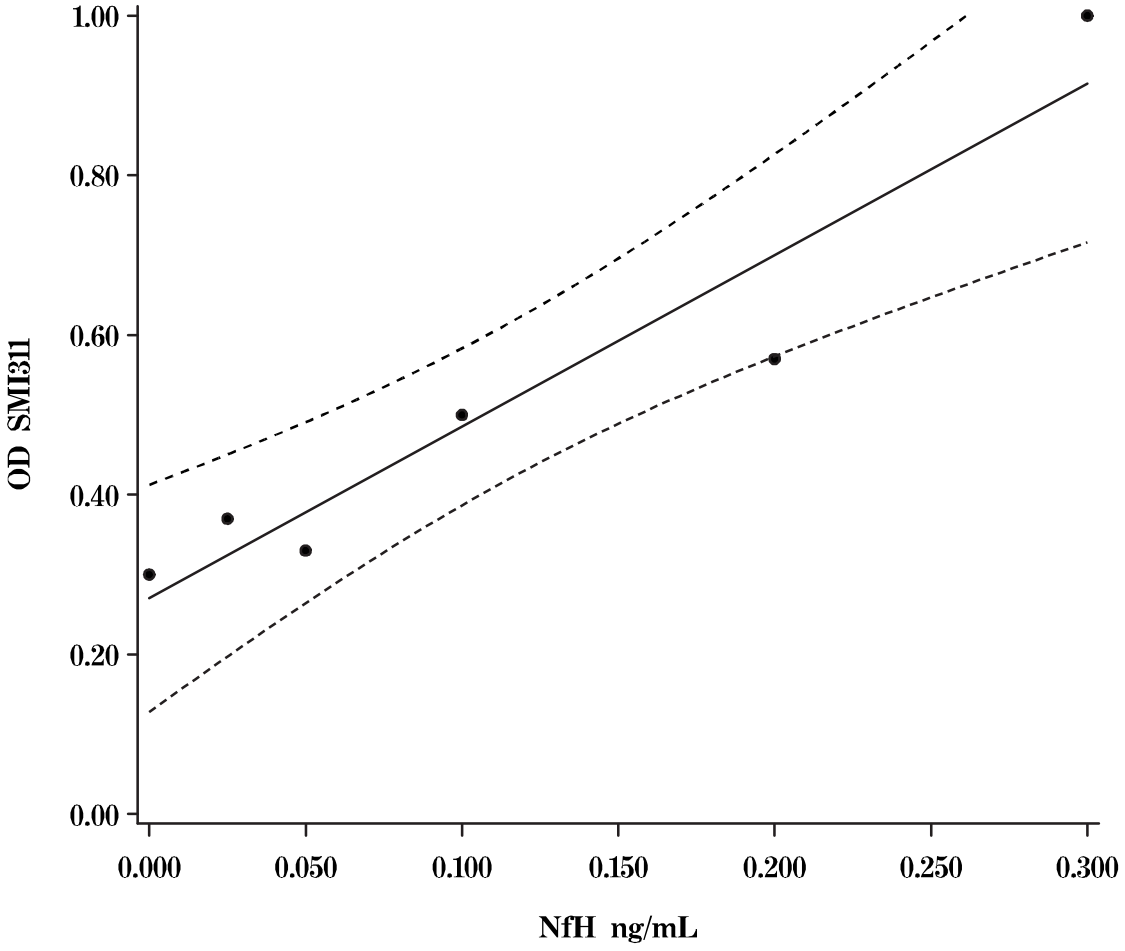

Figure 4.9: *Standard curve for NfH^{SMI311} . The regression line and 95% confidence interval curves are shown.*

Detection limit and analytical range The detection limit was determined by the signal–to–noise ratio of the lowest calibrant to the blank (background), Figure 4.10. An estimate for the analytical range for a particular antibody combination is the ratio of the highest calibrant to the noise (Figure 4.11). The signal–to–noise ratio for SMI35 was about 4- to 10–fold and the analytical range 2- to 10–fold higher than for the other antibody combinations. On the basis of these results SMI35 was selected as the capture antibody for the further development of the NfH ELISA.

Antibody concentration

NfH assay The first antibody was titrated against the second antibody. Dilutions used for the first antibody were $\frac{1}{1000}$, $\frac{1}{5000}$, $\frac{1}{10000}$ and $\frac{1}{100000}$. Dilutions used for the second antibody were $\frac{1}{500}$, $\frac{1}{1000}$ and $\frac{1}{5000}$. All standard curves were run in on the same plate. The results are summarised in Figures 4.12 to 4.15.

The signal–to–noise ratio and analytical range were calculated for each combination. The individual results for the detection limit are shown in Figure 4.17 and for the analytical range in Figure 4.17. The best result was received for the combination of SMI35 $\frac{1}{5000}$ with polyclonal rabbit anti–NfH $\frac{1}{10000}$ (signal–to–noise = 9.1; analytical range = 73) which was therefore chosen for the further development of the assay.

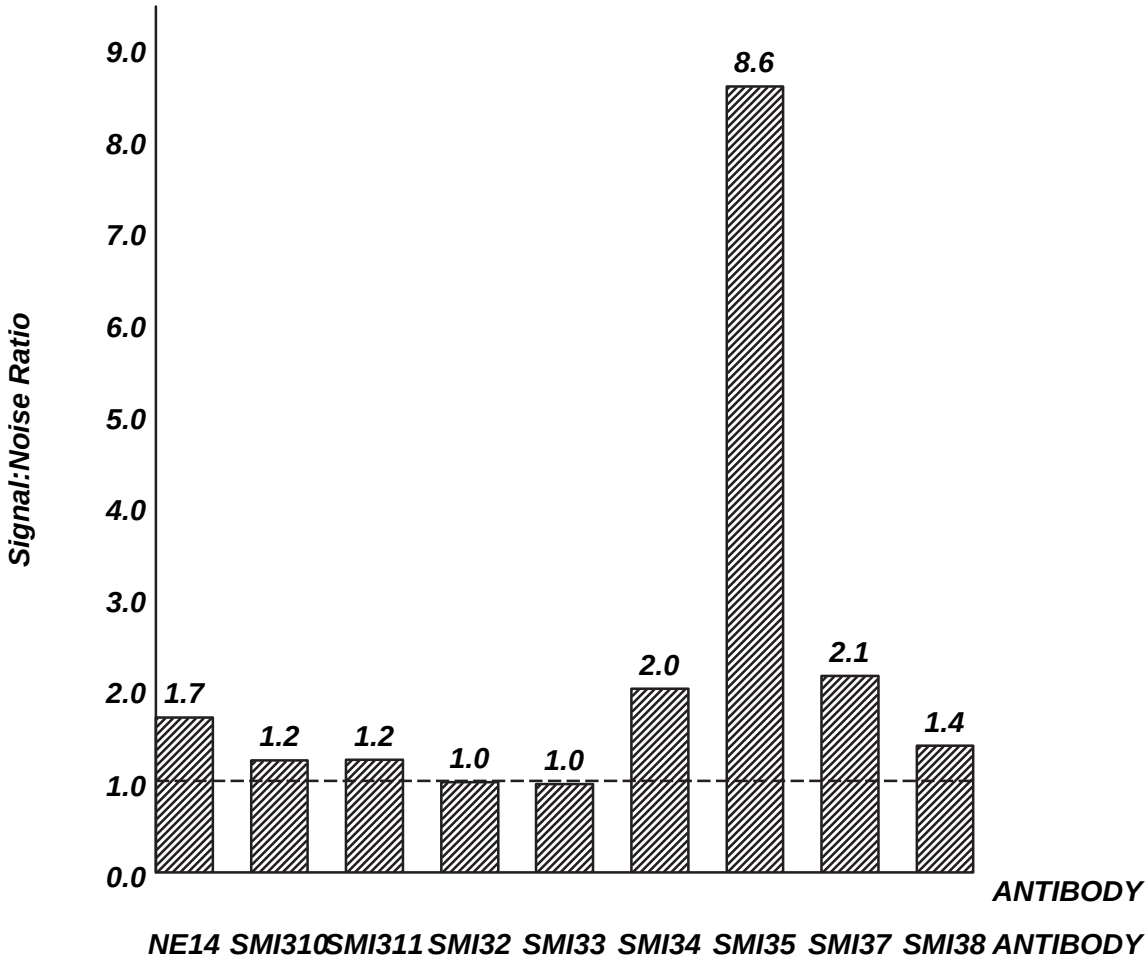

Figure 4.10: *The detection limit of the NfH assay as determined by the signal–to–noise ratio (OD of the lowest standard divided by the blank OD) for different capture antibodies. A signal–to–noise ratio of greater than 1 (reference line) is required in order to obtain a readable signal.*

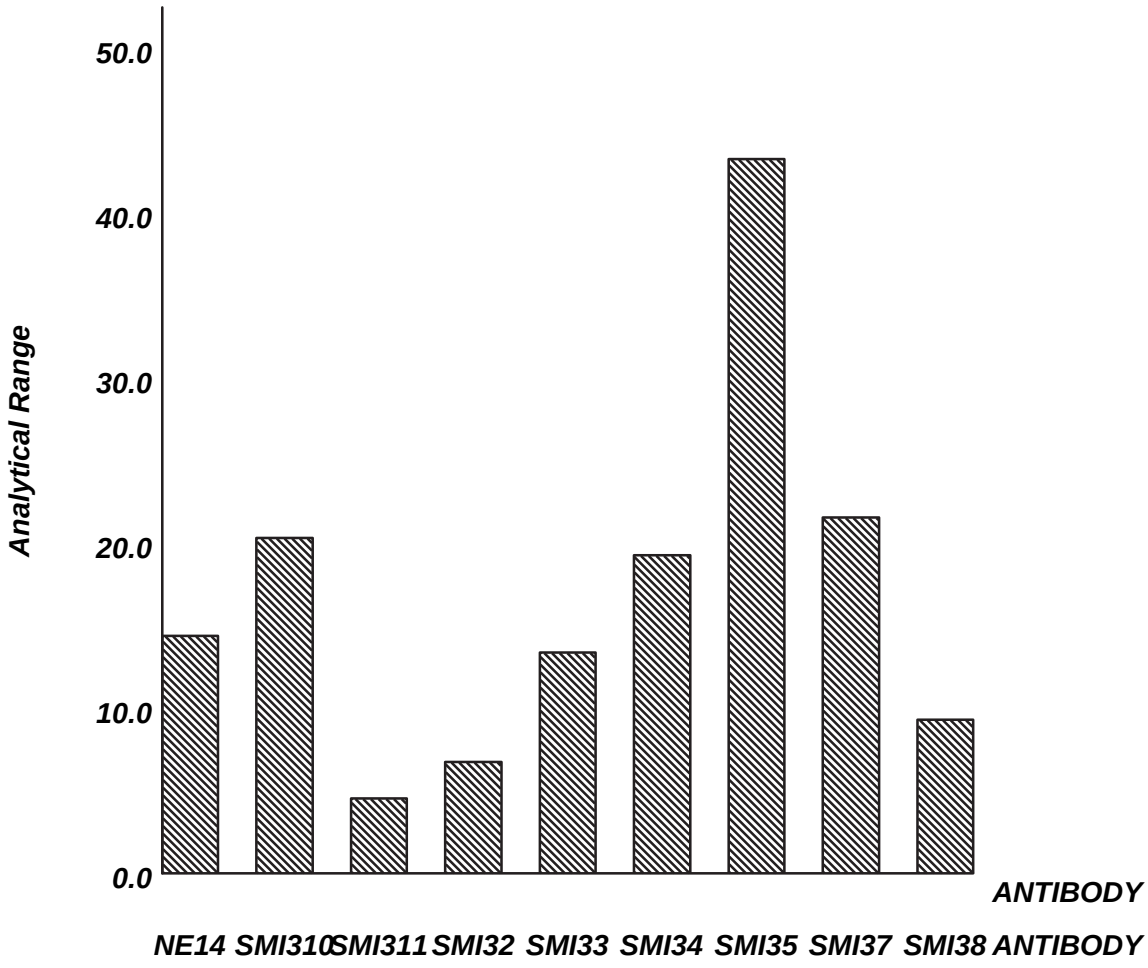

Figure 4.11: *The analytical range as determined by the signal–to–noise ratio for different capture antibodies for NfH.*

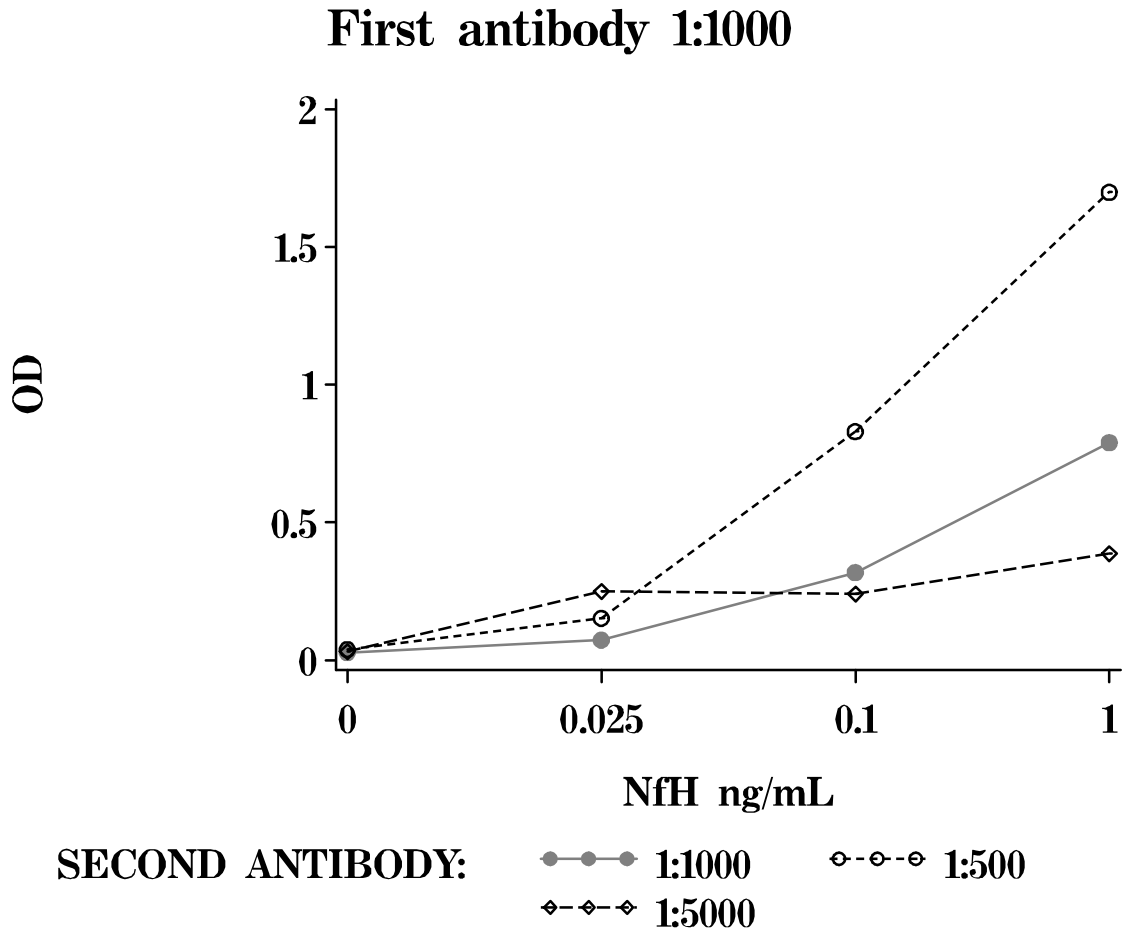

Figure 4.12: *Optical density (OD) for different antibody concentrations of the polyclonal rabbit anti NfH antibody (second antibody) with the first antibody (SMI35) diluted* $\frac{1}{1000}$.

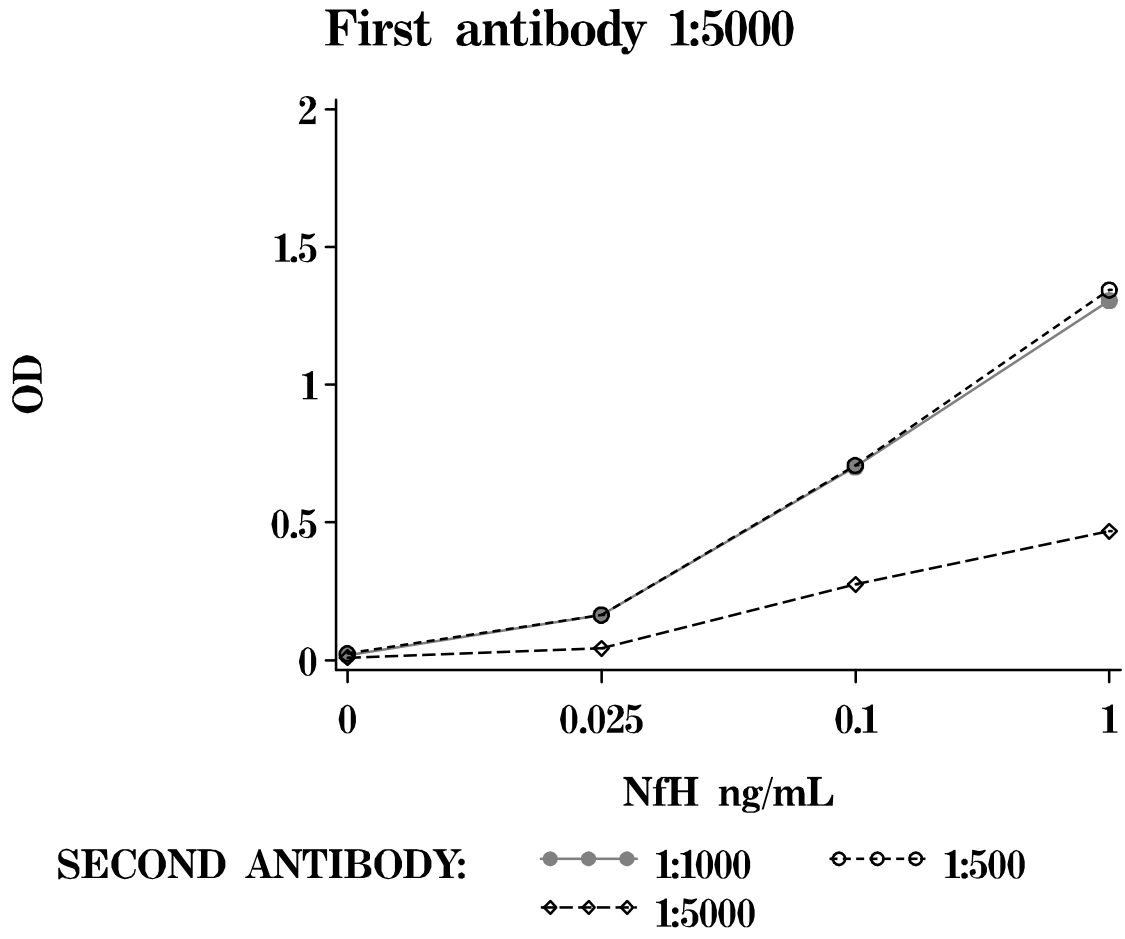

Figure 4.13: *Optical density (OD) for different antibody concentrations of the polyclonal rabbit anti NfH antibody (second antibody) with the first antibody (SMI35) diluted* $\frac{1}{5000}$.

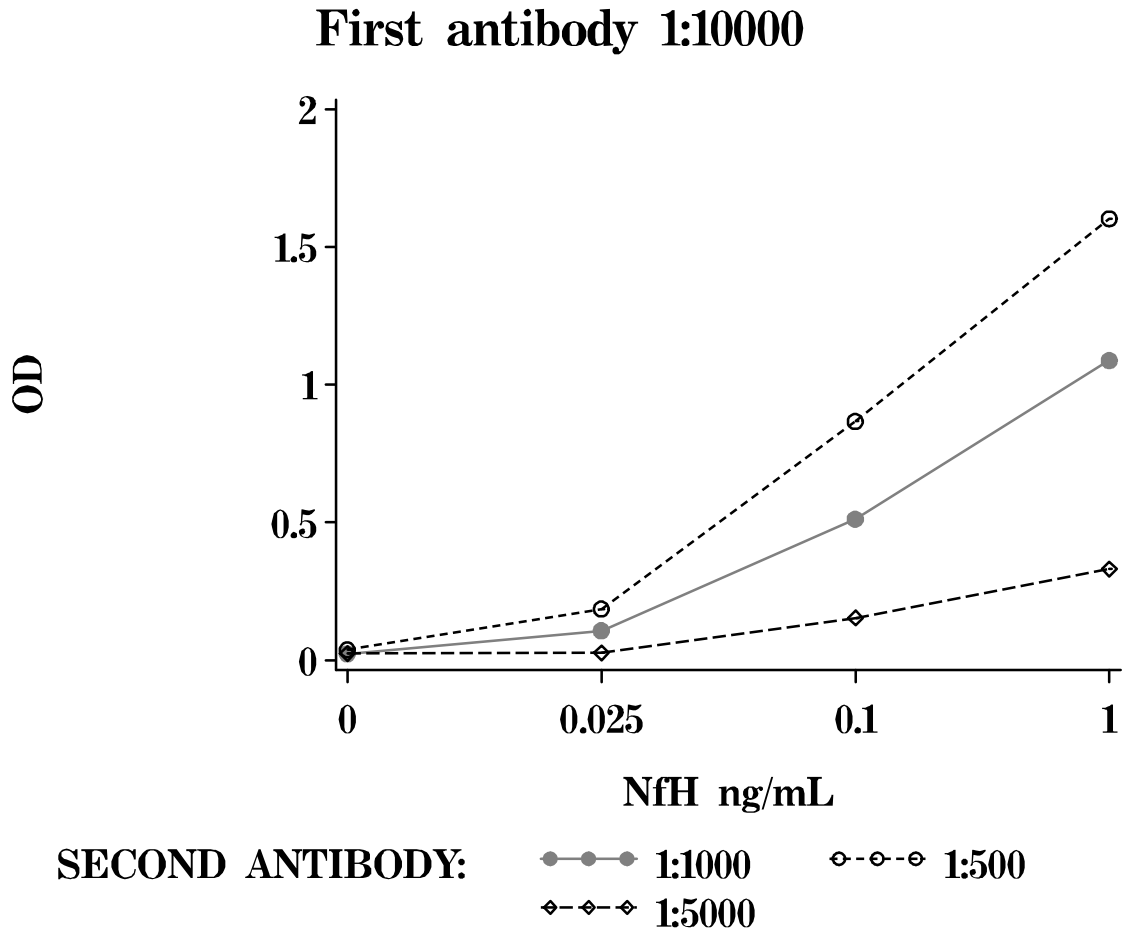

Figure 4.14: *Optical density (OD) for different antibody concentrations of the polyclonal rabbit anti NfH antibody (second antibody) with the first antibody (SMI35) diluted* $\frac{1}{10000}$.

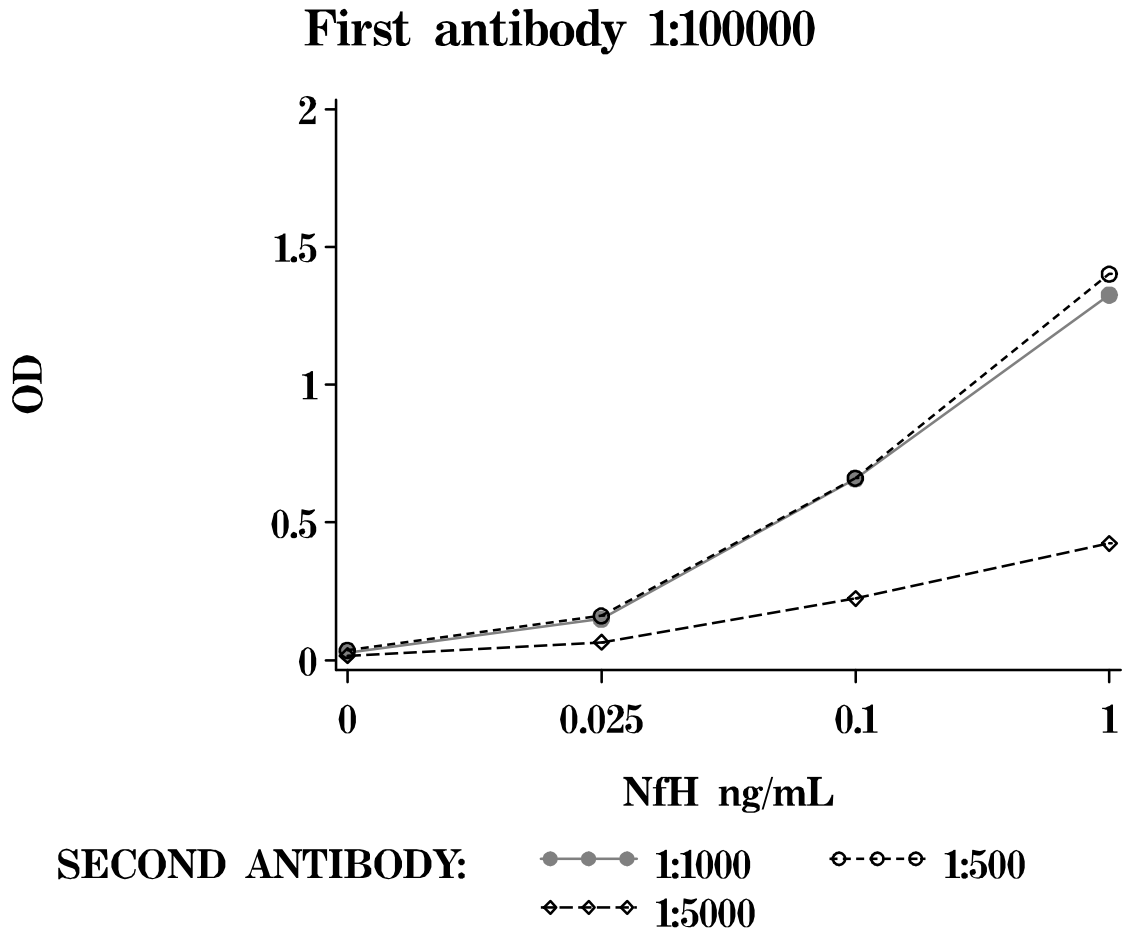

Figure 4.15: *Optical density (OD) for different antibody concentrations of the polyclonal rabbit anti NfH antibody (second antibody) with the first antibody (SMI35) diluted* $\frac{1}{100000}$.

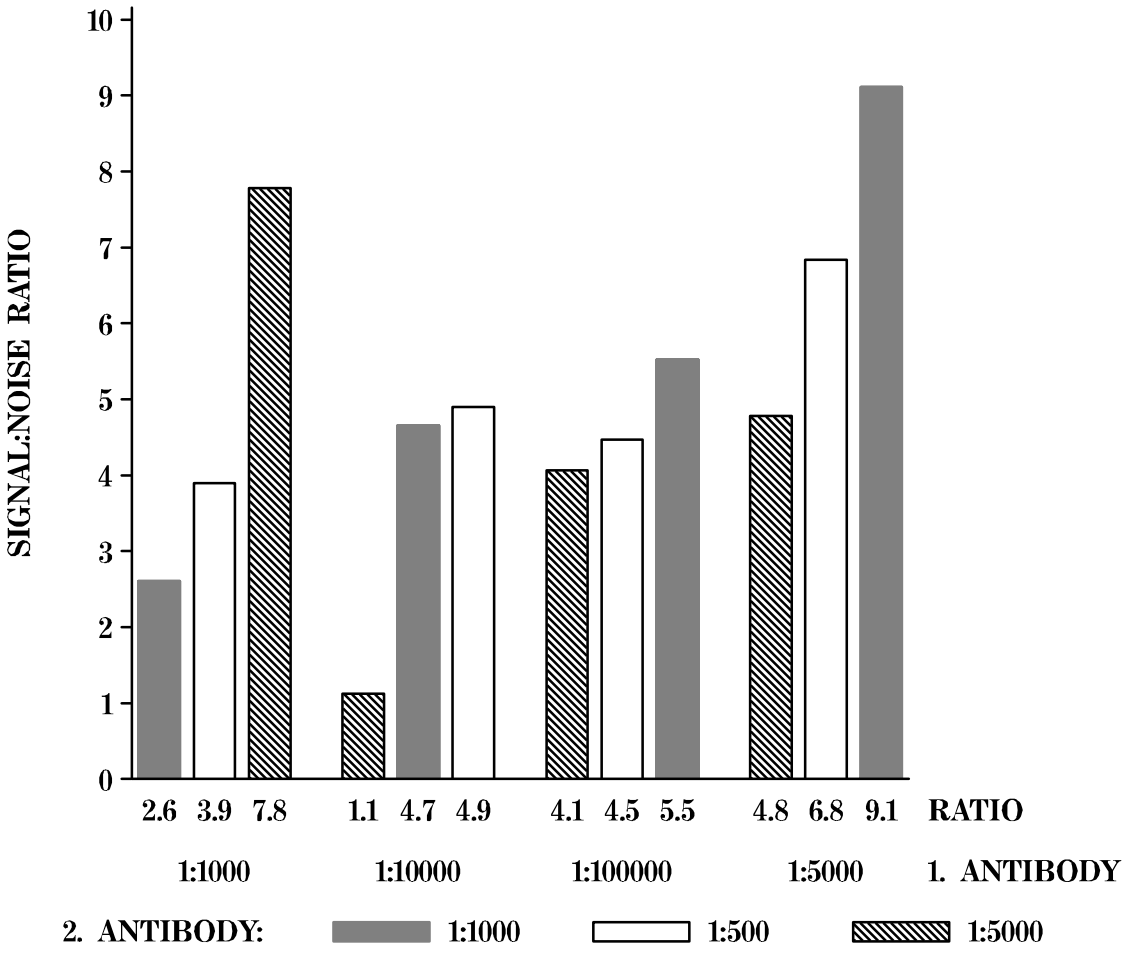

Figure 4.16: *Detection limit as determined by the signal–to–noise ratio for NfH 0.025 ng/mL. Columns are "colour"–coded (black, grey, white) according to the concentration of the second antibody as indicated in the legend. The absolute value of the signal–to–noise ratio is given for each antibody combination below the appropriate column.*

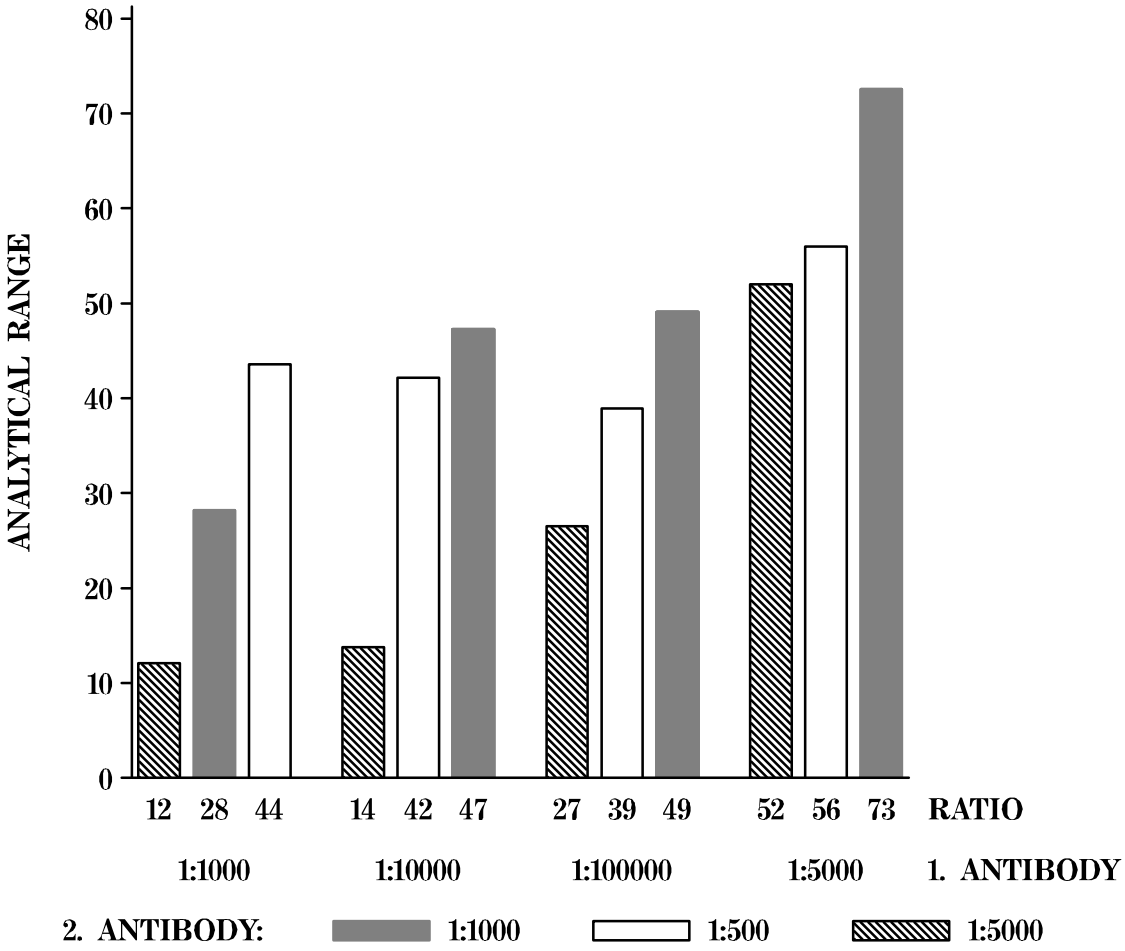

Figure 4.17: *Analytical range as determined by the signal–to–noise ratio for NfH 1 ng/mL. Columns are grouped according to the dilution for SMI35 as capture (first). Columns are "colour"–coded (black, grey, white) according to the concentration of the second antibody as indicated in the legend. The absolute value of the signal–to–noise ratio is given for each antibody combination below the appropriate column.*

NfL assay The antibody concentration for the NfL assay was determined in a similar way to the NfH assay (data not shown). The optimal combination was found to be $\frac{1}{5000}$ for NR4 and $\frac{1}{500}$ for the polyclonal rabbit anti–NfL.

4.3.2 Reproducibility of the standard curve

Reproducibility of the standard curve was determined by expressing the optical density (OD) obtained for each calibrant as a percentage of the optical density. Twenty consecutive standard curves were normalised and the results averaged. The resulting regression for NfL is shown in Figure 4.18 and forNfH^{SMI35} in Figure 4.19.

4.3.3 Precision

CSF samples (neat and spiked with either NfH or NfL) were used to calculate the within- and between-batch precision and recovery.

NfH Within–batch and between–batch precision was determined for high and low concentrations. The within–batch precision was 5.6% for 2 ng/mL, 6.6% for 0.4 ng/mL and 19.8% for 0.2 ng/mL. The between–batch precision was 15% for 1.3 ng/mL and 31% for 0.16 ng/mL. The detection limit was 0.1 ng/mL. The sensitivity was calculated as the mean + 3 standard deviations of the blank signal. The sensitivity was 0.2 ng/mL. The recovery of NfH in CSF was 121% for pool 1 and 116% for pool 2, averaging at 119%.

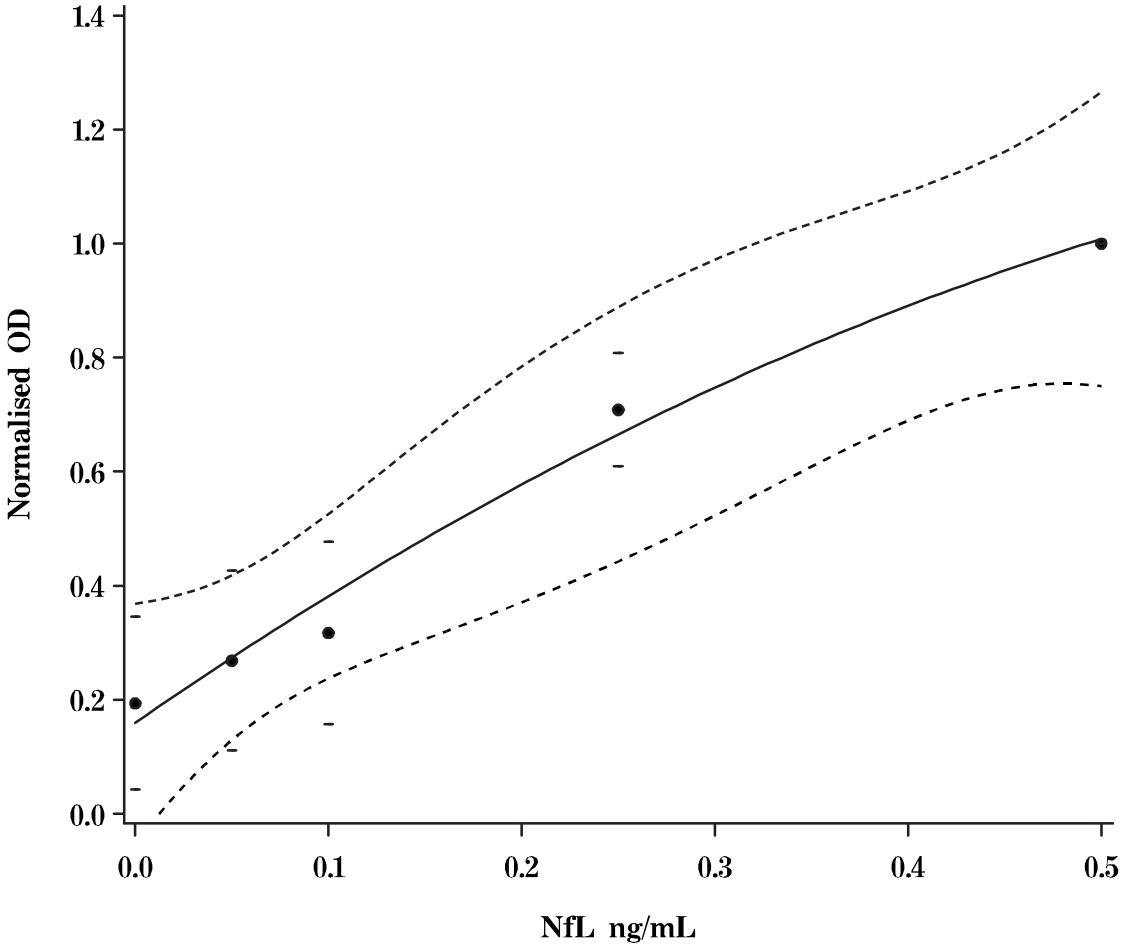

Figure 4.18: *Standard–curve for the NfL assay. Reproducibility of twenty consecutive normalised calibration lines. The graph shows the mean values (dots) ± standard deviation (bars), quadratic regression line, 5% and 95% confidence interval curves.*

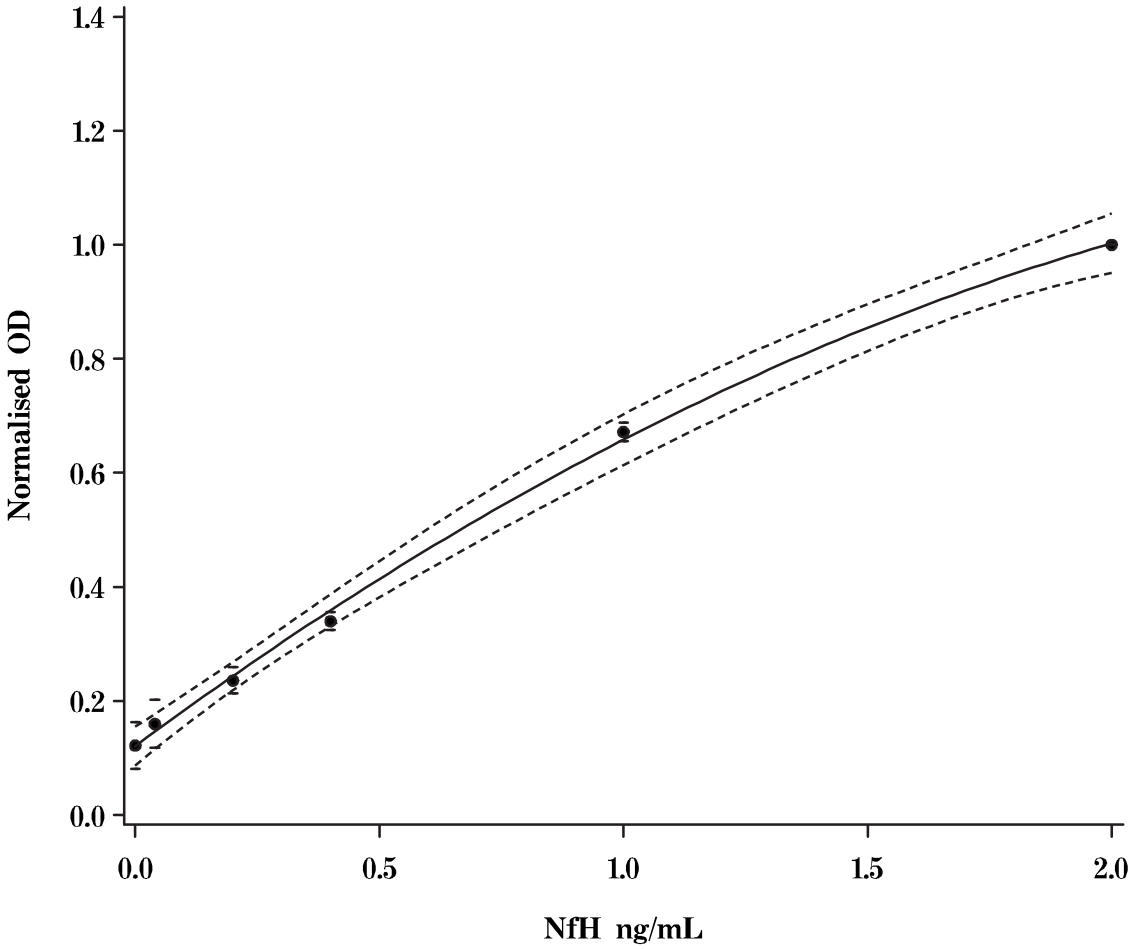

Figure 4.19: *Standard–curve for the NfH^{SMI35} assay. Reproducibility of twenty consecutive normalised calibration lines. The graph shows the mean values (dots) ± standard deviation (bars), quadratic regression line, 5% and 95% confidence interval curves.*

NfL The within–batch precision was 27% for 0.25 ng/mL. The between–batch precision was over 50%. The sensitivity was 0.25 ng/mL. The recovery of NfH in CSF was 60% for pool 1 and 66% for pool 2, averaging at 63%.

4.3.4 Parallelism

Parallelism between calibrant and CSF was studied by quantifying reciprocal dilutions of buffer spiked with NfH and CSF samples with known high NfH^{SMI35} concentrations. The obtained OD for each series of dilutions was normalised to the highest value within this series (100%). Because of the vertical displacement the top value is not shown. The parallel relationship was shown and suggested the absence of endogenous binding between CSF NfH^{SMI35} and other CSF substrates (Figure 4.20).

4.3.5 Stability of CSF samples

NfH^{SMI35} Stability was tested at room temperature (RT), 4°C and -70°C. CSF samples spiked with NfH were frozen in duplicate at -70°C, thawed on subsequent days and stored at 4°C and RT (Figure 4.21). Linear regression analysis of the 7–day observation period demonstrated no significant decrease in NfH^{SMI35} at -70°C and 4°C. At RT there was however a significant ($p<0.05$) decrease in the measured NfH^{SMI35} concentration.

NfL Stability was tested at room temperature (RT) and 4°C. CSF samples spiked with NfL were frozen in duplicate at -70°C, thawed on subsequent days and stored at 4°C and RT (Figure 4.22). Linear regression analysis of

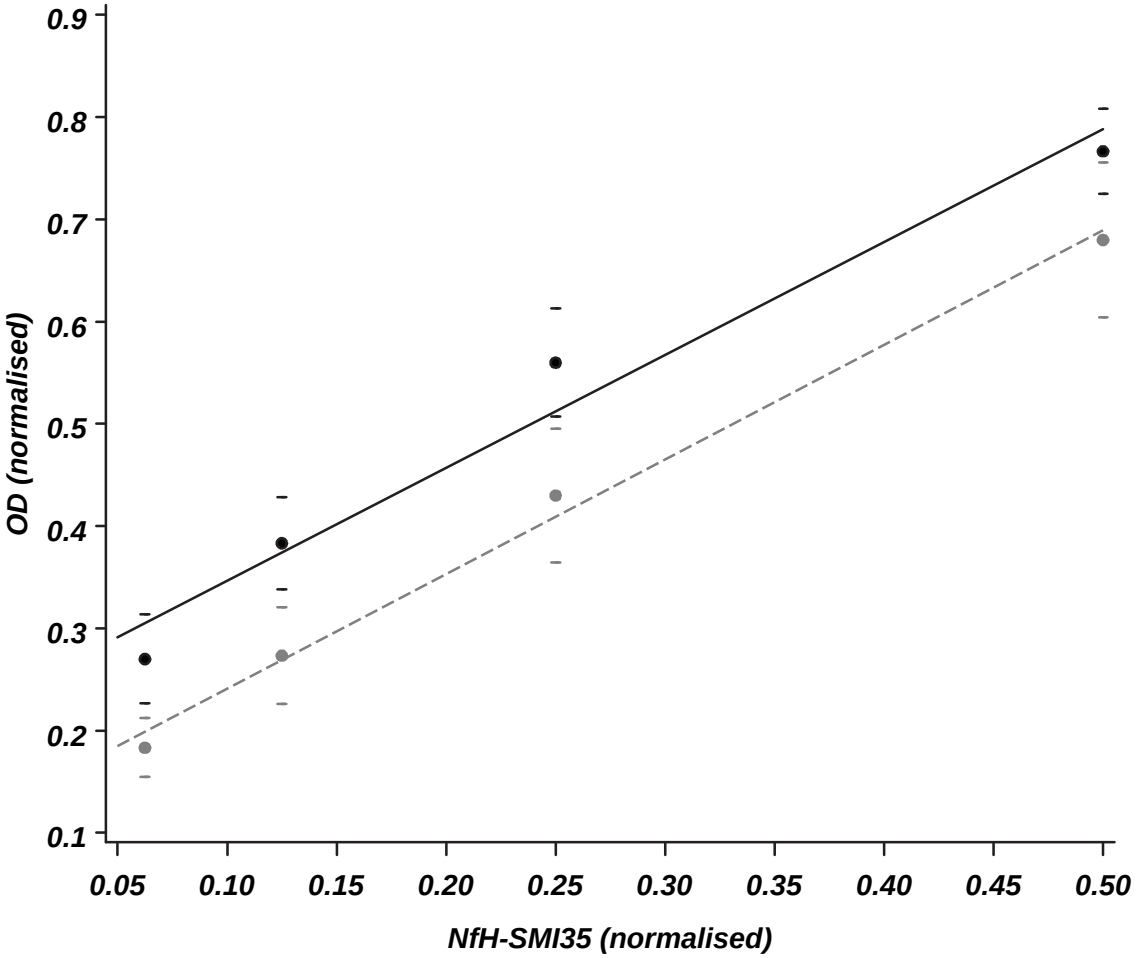

Figure 4.20: *Parallelism for NfH^{SMI35} between calibrant (open, grey circles) and CSF (closed, black circles). The linear regression, mean (circles) and standard deviation (horizontal bars) are shown.*

the 3–day observation period demonstrated significant decreases in NfL at 4°C and RT.

4.3.6 Stability of reagents

No problems were found with stability of antibodies. To minimise any problems with cumulative contamination, the antibodies were stored in 100 μL aliquots and used within 4 weeks. All buffers were stored at 4°C and used within 1 week.

4.3.7 Cell–type specificity

Abundant neurofilament levels were found in neuronal cell culture and isolated synaptosomes from rat brain tissue and human cerebral and spinal cord tissue homogenate. In cultures of primary astrocytes an average of 63 fg/mg protein were detected. No NfH was detected in primary microglial cultures.

4.3.8 Cross reactivity

Measuring double dilutions of a known amount of protein, the cross–reactivity with NfM was 7.8%, with NfL 6.5% and with GFAP 0.06%. There was no cross–reactivity with red–cells, white cells or haemolysed blood.

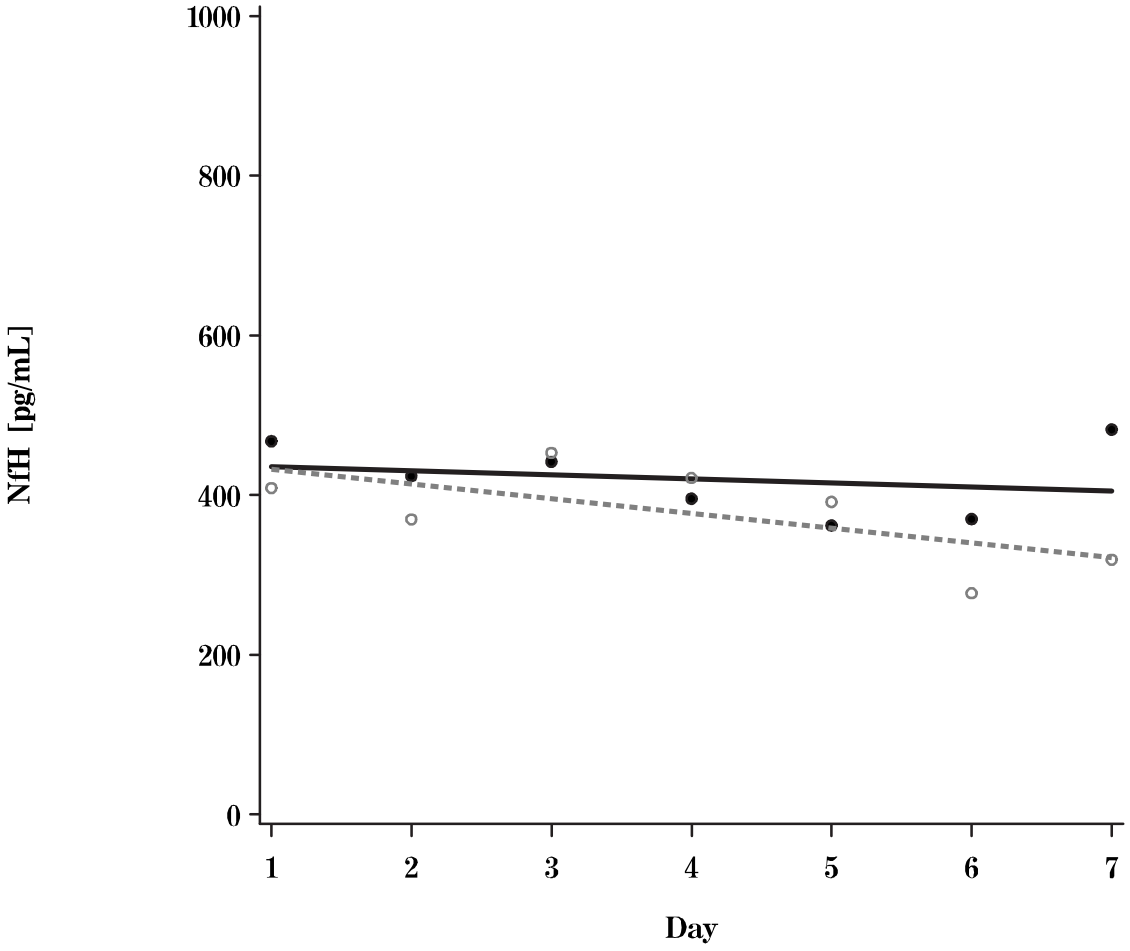

Figure 4.21: *Stability profile of NfH^{SMI35} in CSF at 4°C (continuous line) and at room temperature (dotted line) over 7 days.*

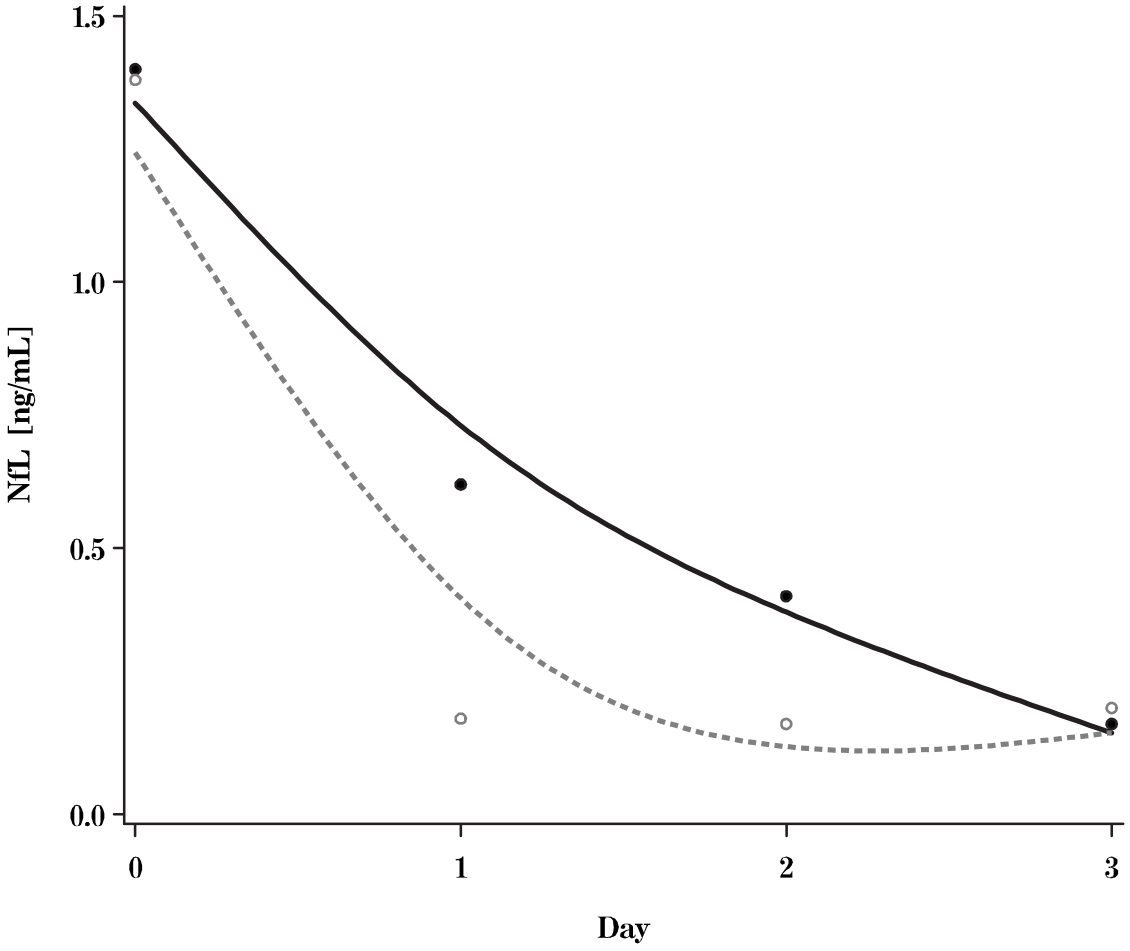

Figure 4.22: *Stability profile of NfL in CSF at 4°C (continuous line) and at room temperature (dotted line) over 4 days.*

4.3.9 Reference population

Out of 561 CSF samples 463 were assayed for NfH^{SMI35} and 127 for NfL. In 29 patients enough CSF was available to assay for NfH^{SMI35} and NfL^{NR4} .

NfH^{SMI35} The distribution of the NfH^{SMI35} CSF levels was non–Gaussian (Figure 4.23). In order to obtain a biological representative population the top 10% (NfH > 1.119 ng/mL) have been removed, leaving 416 patients. The mean age of the so determined reference population was 42.4±17.9 years, with a median of 41.9 (Range 3–80) years. There was no correlation between CSF NfH^{SMI35} and age (R=0.065, p=0.2). Fifty–eight percent (242/416) were female, 39.9% (166/416) male, and in 8 (1.9%) patients no gender information was available. There was no significant difference in CSF NfH^{SMI35} levels between the genders.

The relative frequency distribution of the reference–population was then subjected to non–parametric definition of the upper reference value of the 95 percentile.[369] The upper reference value corresponds to 0.73 ng/mL (Figure 4.23, reference line). The mean value of CSF NfH^{SMI35} was 0.25±0.23 ng/mL with a median of 0.21 ng/mL and an interquartile range of 0.07 to 0.35 ng/mL. The data were skewed towards zero by 1.33. The kurtosis was 2.15 indicating a high slim peak with more values in the tails than expected by the Gaussian type. This was due to 18% of samples with non detectable CSF NfH^{SMI35} levels.

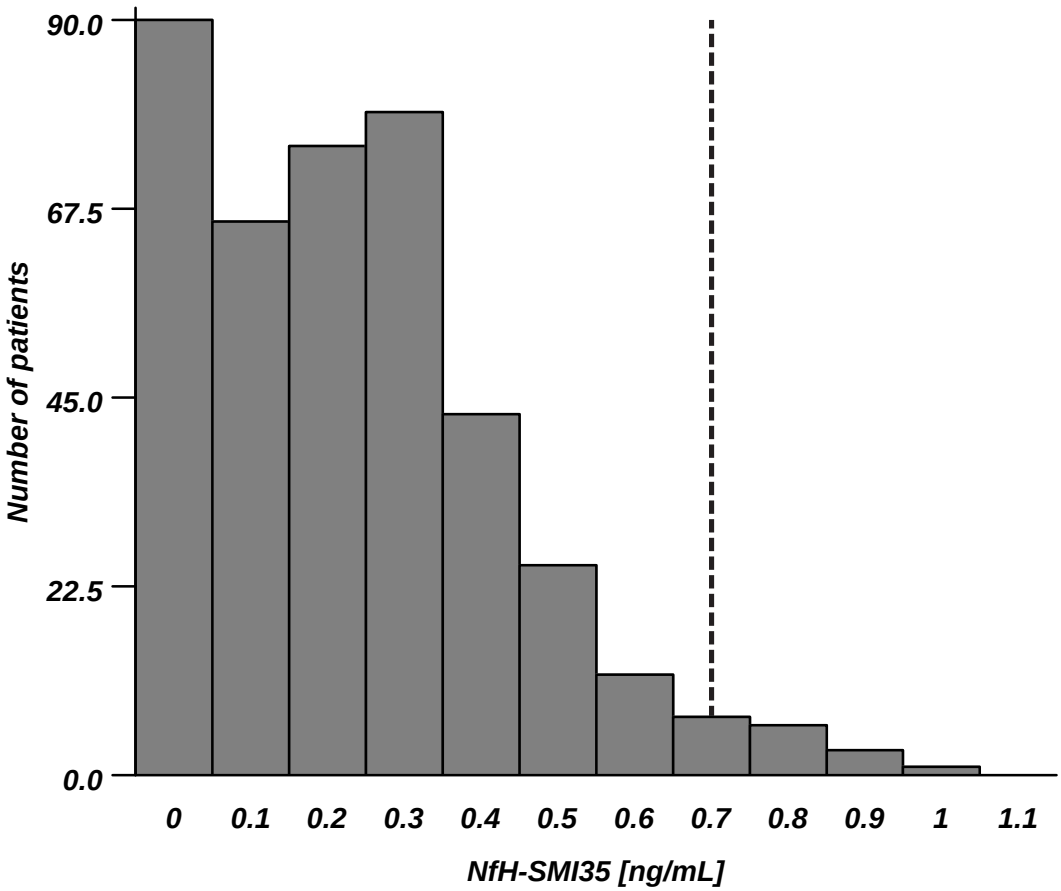

Figure 4.23: *Frequency histogram for the reference population for CSF NfH^{SMI35} (n=416). The upper reference value of 0.73 ng/mL is shown (dotted line).*

NfL The distribution of the CSF NfL^{NR4} levels was non–Gaussian (Figure 4.24). In order to obtain a biological representative population the top 10% (NfL^{NR4} > 0.24 ng/mL) have been removed, leaving 113 patients. The 95 percentile corresponds to 0.14 ng/mL (Figure 4.24, reference line). The mean value of CSF NfL^{NR4} was 0.024±0.06 ng/mL with a median of 0.00 ng/mL and an interquartile range of 0.00 to 0.013 ng/mL. The data were skewed towards zero by 2.9. The kurtosis was 7.4 indicating a high slim peak with more values in the tails than expected by the Gaussian type. This was due to 71% samples having no detectable NfL^{NR4} .

The mean age of the reference population was 46.3±18.2 years, with a median of 44.7 (Range 1–76) years. There was no correlation between CSF NfL and age (R=0.089, p=0.39). Fifty–two percent (59/113) were female and 42% (47/113) male, in 7 (6%) patients no gender information was available. There was no significant difference of CSF NfL levels between the genders.

There was no correlation between CSF NfL^{NR4} and CSF NfH^{SMI35} (R=-0.1, p=0.6) in those 29 samples were both proteins were measured.

4.3.10 Neurological disorders

After determination of the upper reference limit for the NfH^{SMI35} assay, a second population of patients was selected according to the clinical diagnosis: Nine patients had cluster headache (HD) with no other evidence of organic pathology in the central nervous system. Two had a space–occupying lesion

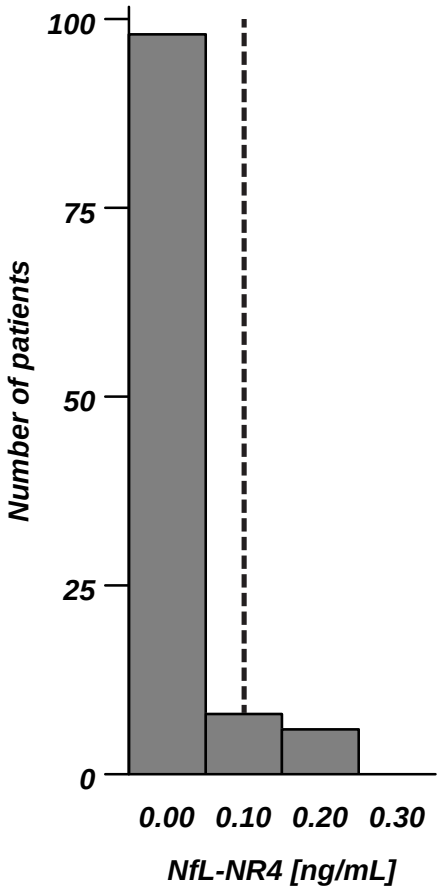

Figure 4.24: *Frequency histogram for the reference population for CSF NfL (n=113), the upper reference value of 0.14 ng/mL is shown (dotted line).*

(SO), one due to a cyst of the right lateral ventricle and one to a non Hodgkin lymphoma. Three had amyotrophic lateral sclerosis (ALS), 3 a lumbar disc prolapse (DP), 36 laboratory supported (isolated intrathecal IgG synthesis) evidence for demyelinating disease (DM), 14 had Guillain–Barré syndrome (GBS) and 5 had a subarachnoid haemorrhage (SAH). All CSF was taken by routine lumbar puncture, except for SAH where the CSF was taken for routine infectious screening 2 days after placement of an extra-ventricular drain. The values for the SAH therefore represent ventricular CSF.

Because of the small patient numbers statistical significance was checked on a categorical level by the Fisher's exact test comparing proportions of patients with CSF NfH^{SMI35} levels above the previously calculated upper reference value (cut–off) of 0.73 ng/mL. A significantly higher number of patients with SAH had CSF NfH^{SMI35} levels above cut–off when compared to HD ($p<0.001$) or DM ($p<0.001$). A significantly higher number of patients with SO had CSF NfH^{SMI35} levels above cut–off when compared to HD ($p<0.05$) or DM ($p<0.01$) and a significantly higher number of patients with ALS or DP had CSF NfH^{SMI35} levels above cut–off when compared to DM ($p<0.05$, $p<0.05$, respectively).

4.3.11 CSF oligoclonal bands

The detection of OCB was done on time–matched CSF and serum using standard isoelectric focusing[16] on all 402 patients of the reference population.

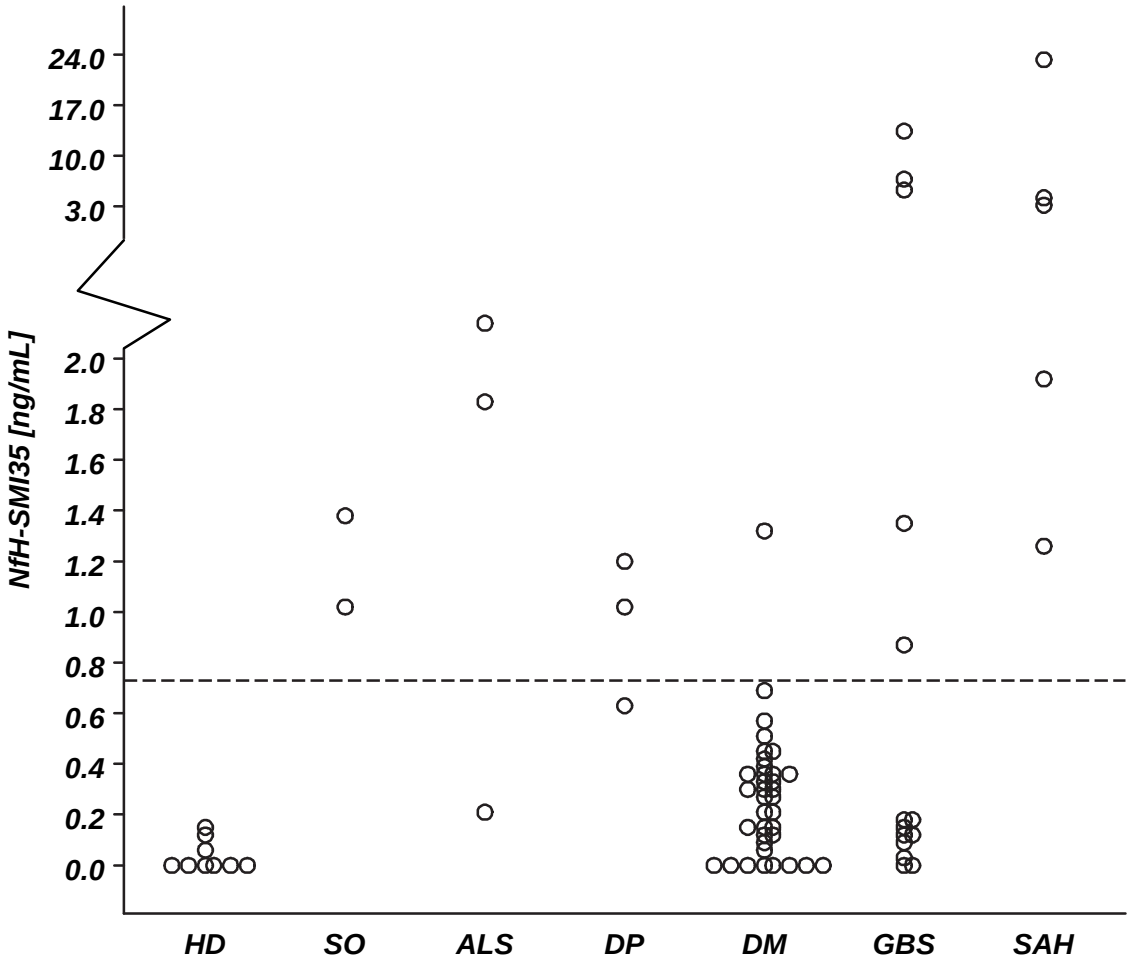

Figure 4.25: *Scatter plot of CSF NfH^{SMI35} levels in patients with cluster headache (HD), space–occupying lesions (SO), amyotrophic lateral sclerosis (ALS), disc prolapse (DP, demyelinating disease (DM), Guillain–Barré syndrome (GBS) and subarachnoid haemorrhage (SAH). The horizontal reference line (dotted) represents the cut–off (0.73 ng/mL) derived from the reference population, the y–axis is split at 2 ng/mL.*

Patients were classified according to their OCB pattern as described (Chapter 6.5, page 150).

Table 4.1: *Distribution of CSF NfH concentration according to the OCB pattern*

OCB	Number	Mean ± SD	Median	Range [ng/mL]
OCB -/-	214	0.21 ± 0.19	0.19	0 - 0.92
OCB +/+	46	0.22 ± 0.16	0.23	0 - 0.67
OCB +/-	68	0.21 ± 0.19	0.19	0 - 0.64
OCB ++/+	21	0.24 ± 0.18	0.19	0 - 0.62
OCB +++/+	14	0.26 ± 0.21	0.26	0 - 0.62
OCB m/-	9	0.2 ± 0.24	0.16	0 - 0.67
OCB m/m	4	0.08 ± 0.09	0.07	0 - 0.18

Table 4.2: *Distribution of CSF NfL concentration according to the OCB pattern.*

OCB	Number	Mean ± SD	Median	Range [ng/mL]
OCB -/-	55	0.044 ± 0.09	0.0	0.0 - 0.29
OCB +/+	21	0.04 ± 0.08	0.008	0.0 - 0.28
OCB +/-	23	0.1 ± 0.12	0.013	0.0 - 0.35
OCB ++/+	3	0.002 ± 0.003	0.0	0.0 - 0.007
OCB +++/+	3	0.019 ± 0.23	0.011	0.0 - 0.045
OCB m/-	1	0.008	0.008	
OCB m/m	1	0.0	0.0	

There was no significant difference in the NfH^{SMI35} concentration in patients separated according to the OCB pattern ($F(6,369)=0.58$, table 4.1). There was a trend for higher CSF NfL levels in OCB +/- patients ($F(6,100)=1.45$, $p=0.2$), with OCB +/- having significantly higher levels then OCB +/+ ($p<0.05$) *only* in the post–hoc analysis.

4.4 Discussion

The novel ELISA method presented here is straightforward and based entirely on commercially available antibodies. The NfH^{SMI35} protein was stable over a 1–week period if samples were stored at 4°C. For longer storage either freezing at or below -20°C or addition of a protease inhibitor cocktail is recommended. The detection limit of the NfH^{SMI35} ELISA was 0.01 ng/mL and the sensitivity 0.02 ng/mL with a reasonable precision profile (5.6% – 31%). In comparison the sensitivity of the NfL ELISA was 0.25 ng/mL with a relatively poor precision (CV>50%).

The upper reference value of 0.73 ng/mL NfH^{SMI35} has to be regarded as conservative. It applies to a hospital population of a tertiary referral centre biased towards neurological diseases. In a general hospital population a more suitable upper reference value would need to be established, which is likely to be lower.

Because this ELISA is the first one reported to measure NfH in human CSF, no cross–validation with any other method is possible. An ELISA for measuring NfH in brain homogenate has been reported, but the reproducibility was not rigorous.[142] An ELISA for quantifying the light chain (NfL) has already been developed.[335] A stability profile of NfL in CSF was not presented by Rosengren *et al.* (1996), but the authors mentioned the high susceptibility of NfL to proteolysis and refer to previous work.[349,418] The instability of NfL is confirmed by the present results. The strategy

chosen to overcome this difficulty was to snap–freeze samples directly after lumbar puncture and store at -70°C. Samples were only thawed directly prior to analysis.[335] No data on aggregate formation of NfL in CSF is available. Rosengren *et al.* (1996) report a cross–reactivity of their assay with NfH of 15%.[335] The amount of CSf–NfH contributing to the CSF–NfL levels in a series of studies[51,157,242,334,335] is not known, but could be significant if the in–vivo half–life of NfL is significantly shorter than that of NfH as suggested by the present results and others.[349,418]

In neurological diseases the highest levels of CSF NfH^{SMI35} were observed in the ventricular CSF of patients with SAH, followed by lumbar CSF from patients with amyotrophic lateral sclerosis, space–occupying lesions and disc prolapses. The comparison of ventricular with lumbar CSF has to be done with caution as nothing is known about the NfH concentration across the CSF compartment. Interestingly, the distribution for CSF NfH^{SMI35} was bimodal in GBS patients. This finding warrants further investigation.

There was no association between the pattern of OCB and either CSF NfH^{SMI35} or NfL levels. Although similar mean CSF NfH^{SMI35} levels were found for OCB -/- and OCB +/- patients a trend for higher CSF NfL levels was observed in OCB +/- patients.

Phosphorylation is responsible for modification of epitopes recognised by different antibodies on NfH. Because phosphorylation also modifies the function of the protein and contributes to Nf cross–linking and axonal di-

ameter, it is likely that the CSF contains a range of NfH phosphoforms. The rationale for choosing SMI35 antibody as the capture antibody was that it gave the best signal–to–noise ratio. In addition SMI35 recognises both phosphorylated and non–phosphorylated epitopes on the NfH protein. Importantly SMI35 stained for early neuro–axonal damage in histological studies.[124,377,378] This is relevant as the NfH^{SMI35} ELISA might be useful for detecting early axonal injury in neurological disorders.

Chapter 5

Development of a GFAP ELISA

5.1 Background

Glial fibrillary acidic protein (GFAP) is a cytoskeletal astrocytic protein which has been found to be elevated in neurological disorders (Chapter 2.2). In addition CSF GFAP levels have been associated with disability in MS (Chapter 1.3). Currently there is no commercial ELISA available for the measurement of GFAP. All previously developed assays used antibodies produced in–house[6,7,99,297,332] or resource–demanding technology.[276] Although the in–house developed antibodies are supposed to be of high specificity and high avidity, confirmation of the results by independent groups is difficult. This part of the study was aimed at developing a sensitive ELISA for the detection of GFAP in the CSF based on commercially available antisera.

5.2 Materials and methods

5.2.1 Antibodies

Capture (first) antibody

Mouse monoclonal IgG1 anti–GFAP antibodies (SMI) were purchased from Sternberger Monoclonals (Sternberger Monoclonals Incorporated, 10 Burwood Court, Utherville, MD 21093).

GFAP^{SMI21} SMI21 is a mouse monoclonal IgG_1 raised against human brain microvessels. No cross–reactivity with other intermediate filaments or tissues was observed. Astrocytes, Bergmann glia in human, monkeys and dogs were GFAP^{SMI21} positive. In contrast rat, rabbit and mouse GFAP was not recognised by SMI21.

GFAP^{SMI22} SMI22 is the mouse monoclonal cocktail of all three Bigner–Eng clones (Mab1B4, MAb2E1 and Mab4A11) GFAP IgG_{2b}. SMI22 reacted with astrocytes and Bergmann glia in human, monkey and dog. The Bigner–Eng clones are specific for astrocytes, astrocytic processes and Bergmann glia in human, sheep, cow, dog, pig, rat, guinea pig, rat, mouse and chicken. There was no cross–reactivity with other intermediate filaments on tissue sections or Western blots.

GFAP^{SMI24} SMI24 is a mouse monoclonal IgG_{2b} derived from the original Bigner–Eng clone MAb2E1.[264,302,413] SMI24 stains only for some human astrocytes, but the significance of this pattern has not yet been related

to a specific pathology.

GFAP^{SMI26} SMI26 is a cocktail of SMI21 IgG_1 and SMI24 IgG_{2b}. SMI26 provided the most abundant and intensive staining for astrocytes in human brain tissue sections.

Detecting (second) antibody

Horseradish peroxidase conjugated swine polyclonal anti–rabbit Ig was purchased from Dako (Copenhagen, Denmark). SDS–PAGE and immunoblotting demonstrated that this antibody reacted primarily against rabbit IgG, with no reactivity against mouse Ig_1 or IgG_{2b} (SMI 26).

5.2.2 Working reagents and buffers

All working reagents and buffers were purchased, prepared and stored as outlined for the neurofilament ELISA (section 4.2.2 on page 81).

5.2.3 Standards

Bovine GFAP (41 kDa), was obtained from Affiniti Research Products, Exeter. SDS–PAGE and immunoblotting showed six equidistant bands between 39 and 50 kDa. A range of standards from 0 to 200 pg/mL were prepared by diluting human GFAP in barbitone buffer containing 0.1% serum albumin, 6 mM EDTA and stored in aliquots at -20°C.

Recovery and precision

Pooled CSF samples spiked with GFAP were used to calculate the within- and between-batch precision and recovery. The within–batch precision is

expressed as CV %, and was calculated from the mean and SD of at least 20 replicate analyses of pooled CSF spiked with GFAP, performed on a single microtitre plate.

The between–batch precision, expressed as CV % was calculated from the mean and SD from at least 20 replicates of pooled CSF spiked with GFAP.

The recovery of GFAP was obtained by measuring GFAP in pooled CSF before and after the addition of a known amount of GFAP. At least 20 replicates of unspiked and spiked pooled CSF were measured.

5.2.4 CSF samples and reference population

CSF samples from 348 neurological patients undergoing a routine diagnostic lumbar puncture were obtained in order to define the upper reference limit. The selection was randomised from the department's sample library in order to obtain a heterogeneous population. The CSF samples were centrifuged on receipt and stored at 4°C. Analysis was performed within 1 week.

After determination of the upper reference limit five well–defined patient cohorts were studied: 68 patients with dementia (DEM), 11 patients with traumatic brain injury (TBI), 5 patients with subarachnoid hemorrhage (SAH), 11 children with hydrocephalus (HC) and 29 patients with miscellaneous disorders of the peripheral nervous system (PNS). CSF samples from these groups were stored at -20°C until analysis.

5.2.5 Analytical procedure

The microtitre plates were coated overnight with the capturing antibody diluted 1:1000 in 0.05 M carbonate buffer, 100 μL, pH 9.5. The plate was washed with barbitone buffer containing 0.1% BSA and 0.05% Tween 20. Fifty μL of barbitone buffer, 6 mM EDTA and 0.1% BSA were added as sample diluent to each well. Fifty μL of standard, control or CSF sample were then added in duplicates to the plate. The plate was incubated at room temperature (RT) for 1 h. After washing, 100 μL of HRP labelled cow anti GFAP diluted 1:1000 in barbitone buffer were added to each well and the plate was incubated for 1 h at RT. After a final wash 100 μL of TMB substrate was added. The plate was incubated for 30 to 40 minutes at RT in the dark, the reaction was stopped by adding 50 μL 1 M HCl and the absorbance was read at 450 nm with 750 nm as the reference wavelength on a Wallac Victor 2.

5.2.6 Statistical evaluation

Data were managed and analysed as described (Chapter 7, page 151).

5.3 Results

5.3.1 GFAP epitopes

Standard curves The standard curves determined for the GFAP capturing antibodies were expressed as the percentage optical density (OD) for each calibrant. This normalised procedure corrects for differences arising

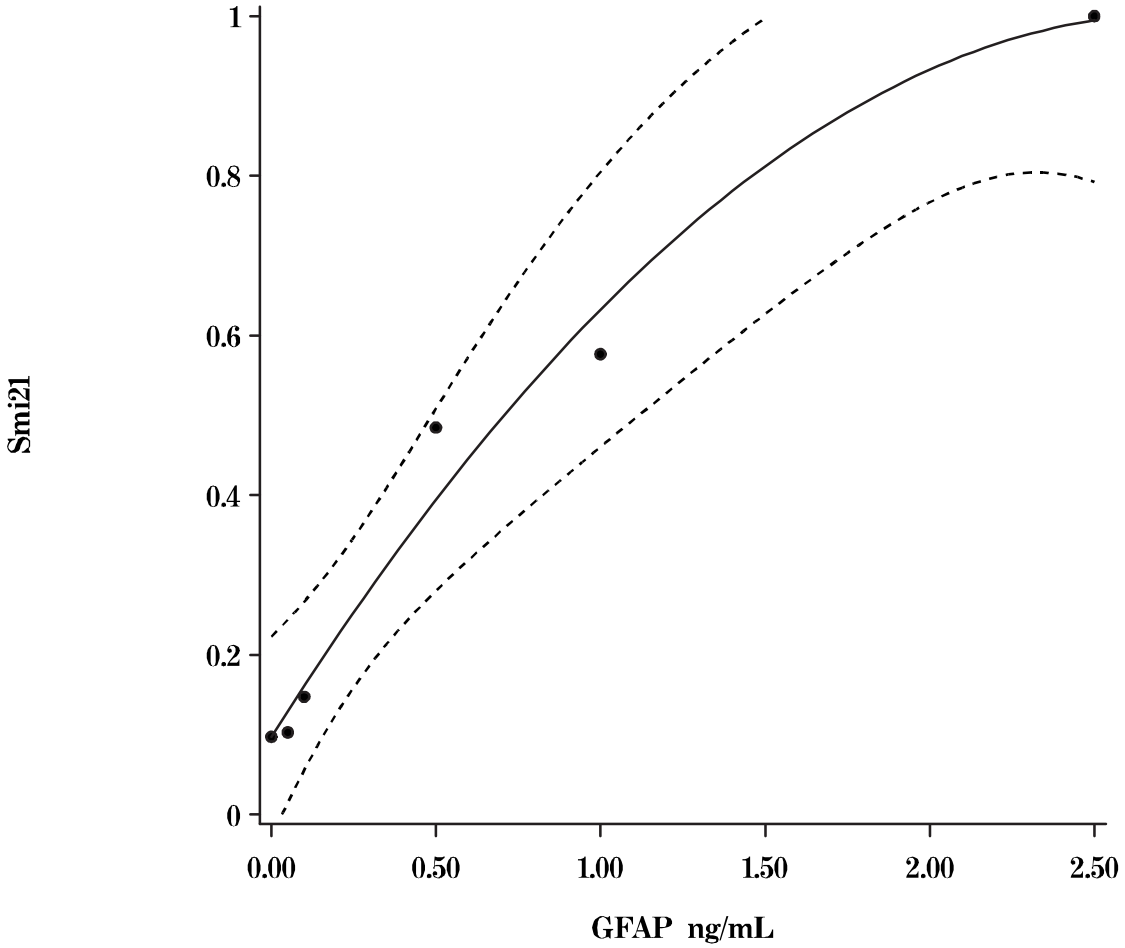

Figure 5.1: *Standard curve for (A) GFAP^{SMI21} , the quadratic regression and the 95% confidence interval curves are shown.*

from variations in incubation times, temperature and colour reagent. All standard curves were run on the same plate to minimise the inter-assay variation. The concentration for all antibodies was 1:1000, including the second and third antibody. The standard curves for the antibodies binding to different epitopes on GFAP (GFAP^{SMI21} , GFAP^{SMI22} , GFAP^{SMI24} , GFAP^{SMI26}) are shown in Figure 5.2 to 5.4.

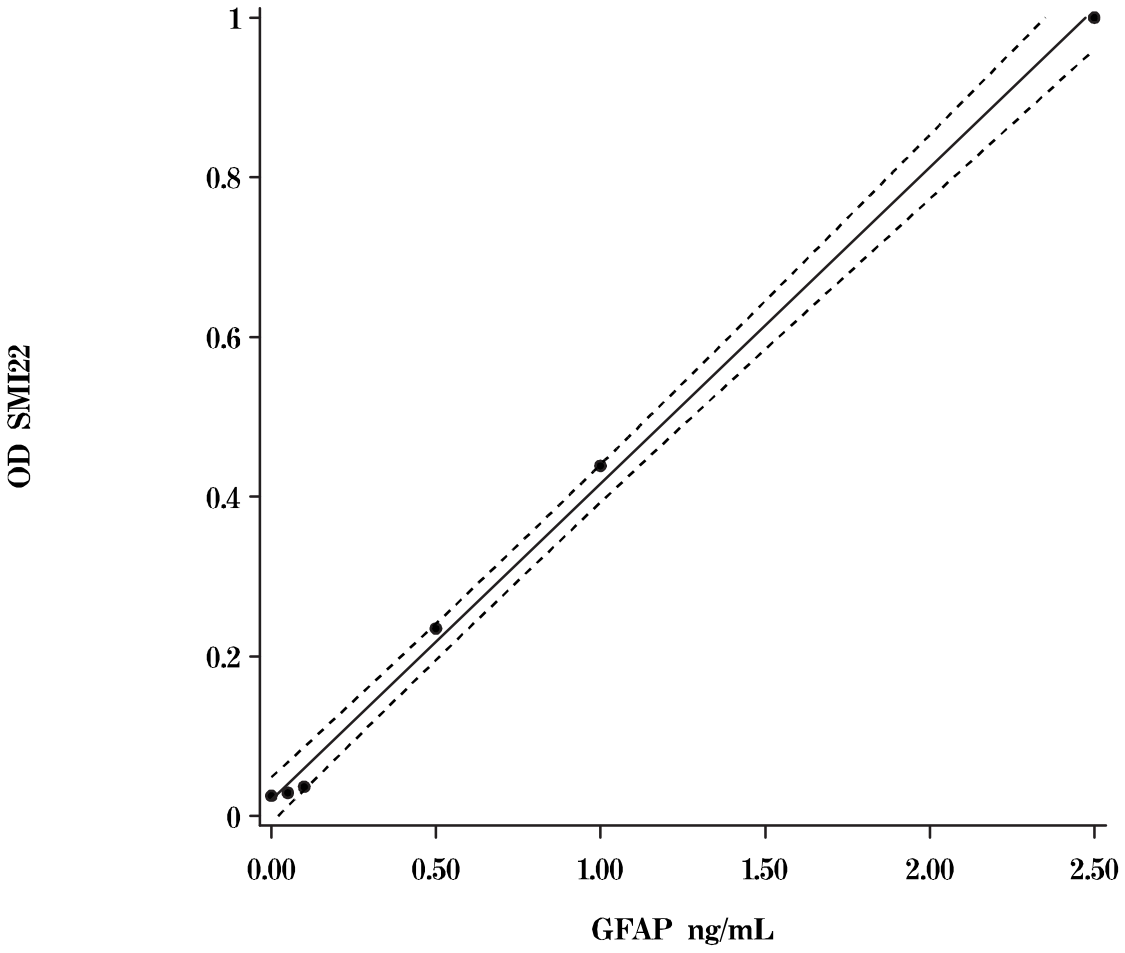

Figure 5.2: *Standard curve for GFAP^{SMI22} . The regression line and 95% confidence interval curves are shown.*

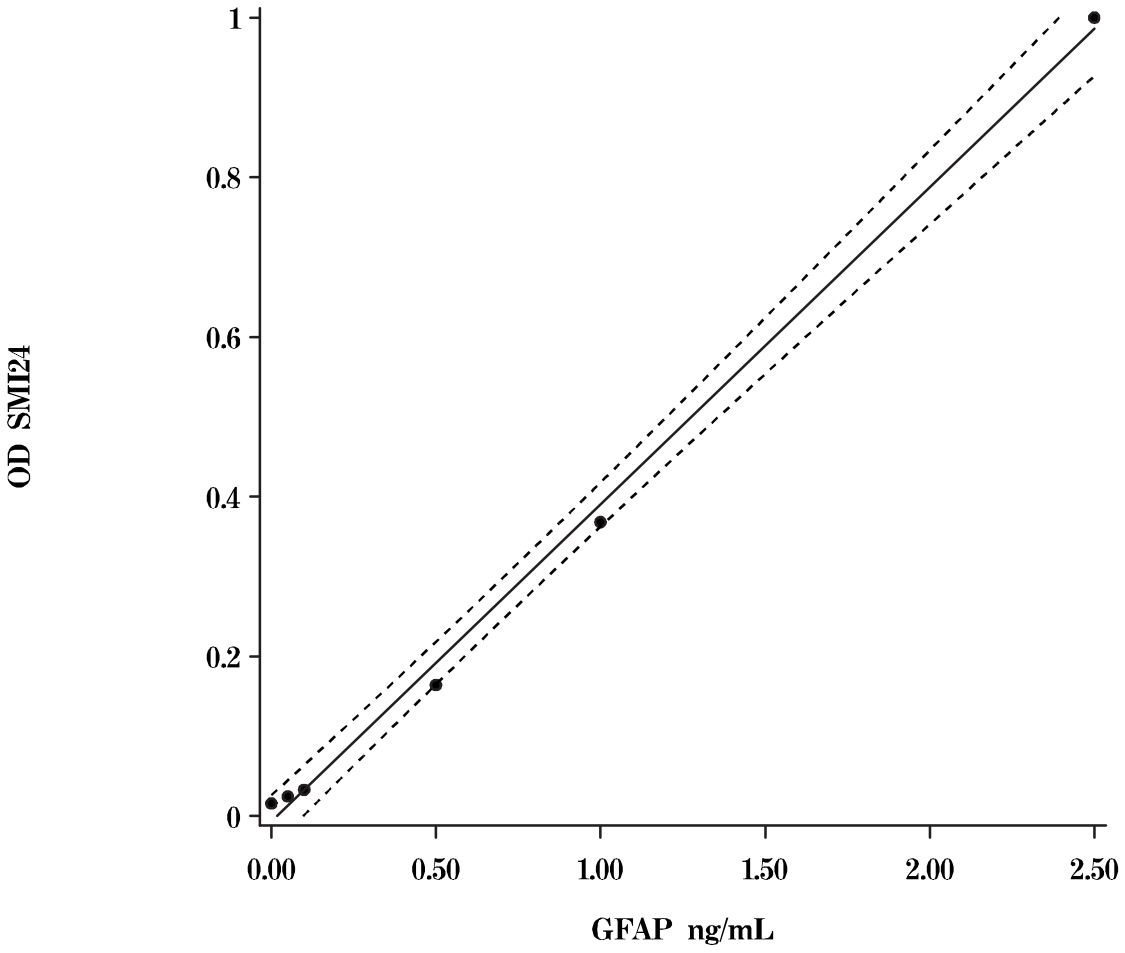

Figure 5.3: *Standard curve for GFAP^{SMI24} . The regression line and 95% confidence interval curves are shown.*

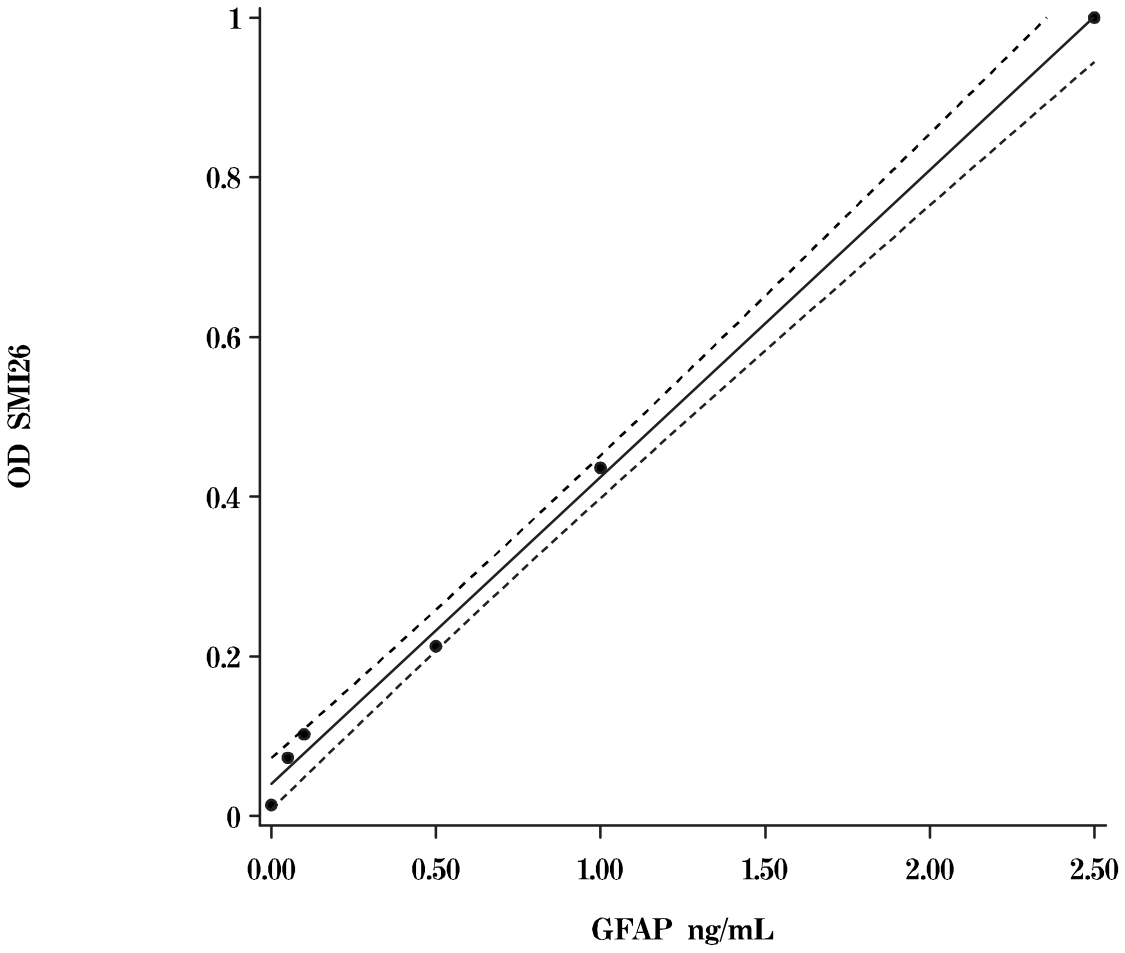

Figure 5.4: *Standard curve for GFAP^{SMI26} . The regression line and 95% confidence interval curves are shown.*

Detection limit and analytical range The detection limit was determined by the signal–to–noise–ratio of the lowest calibrant to the blank (Figure 5.5). An estimate for the analytical range for a particular antibody combination is the ratio of the highest calibrant to the noise (Figure 5.6). The signal–to–noise–ratio for SMI26 was about 3–fold and the analytical range 1.2 to 50–fold higher than for the other antibody combinations. On the basis of these results SMI26 was selected as the capture antibody for the GFAP ELISA.

5.3.2 Reproducibility of the standard curve

Reproducibility of the standard curve was determined by expressing the optical density (OD) obtained for each calibrant as a percentage of the optical density of the top standard. This normalised procedure corrects for differences arising from variations in incubation times, temperature and colour reagent. Eight consecutive standard curves were normalised and the results averaged. The resulting linear regression is shown in Figure 5.7.

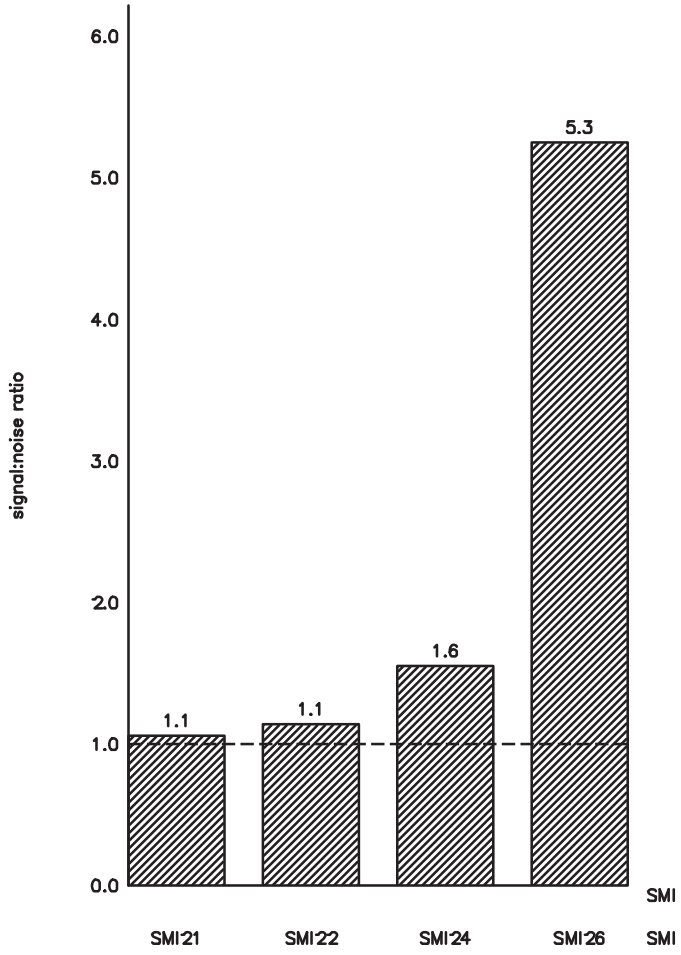

Figure 5.5: *The detection limit of the GFAP assay as determined by the signal–to–noise ratio (OD of the lowest standard divided by the blank OD) for different capture antibodies. A signal–to–noise ratio of greater than 1 (reference line) is required in order to obtain a readable signal.*

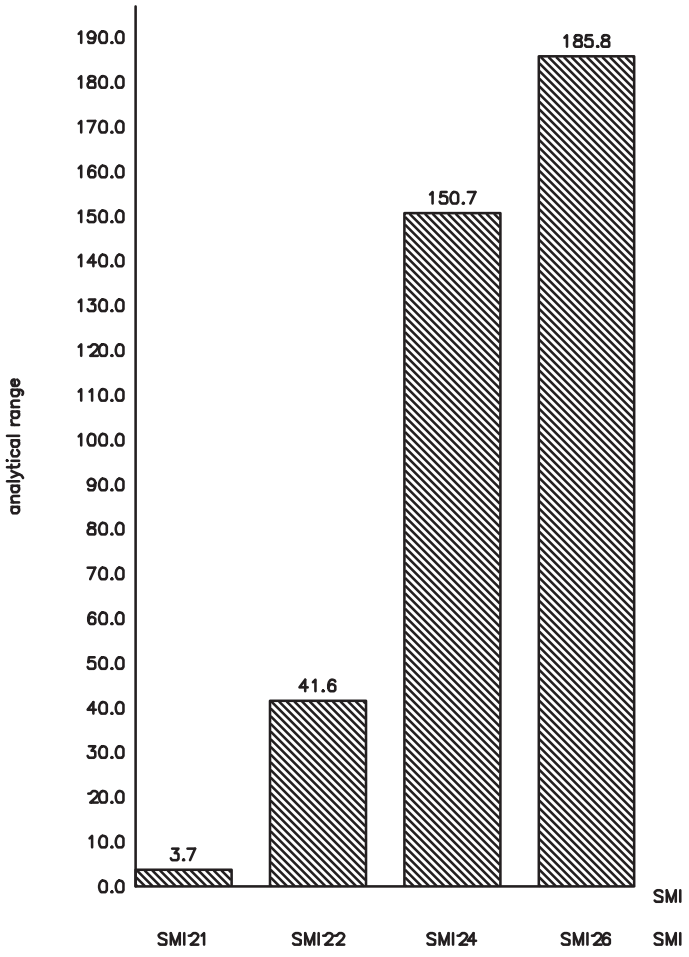

Figure 5.6: *The analytical range as determined by the signal–to–noise–ratio for the SMI antibodies binding to different epitopes on GFAP.*

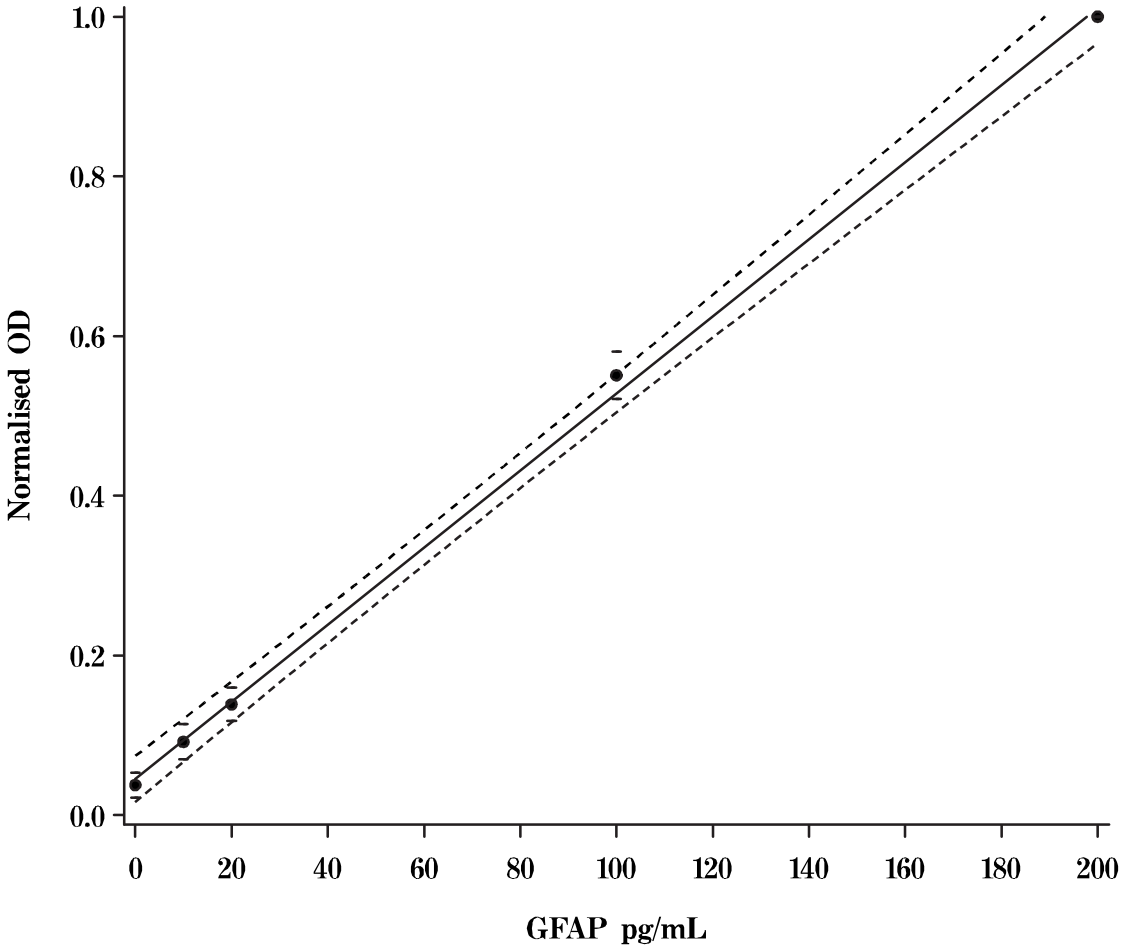

Figure 5.7: *Standard–curve for the GFAP^{SMI26} assay. Reproducibility of eight consecutive normalised calibration lines. The graph shows the mean values (dots) ± standard deviation (bars), linear regression line, 5% and 95% confidence interval curves.*

5.3.3 Precision

CSF samples (neat and spiked with GFAP) were used to calculate the within- and between-batch precision and recovery. Within–batch and between–patch precision was determined for high and low concentrations. The within–batch precision was 4.8% for 200 pg/mL, 7.2% for 40 pg/mL. The between–batch precision was 10.2% for 130 pg/mL. The sensitivity was 10 pg/mL. The recovery of GFAP^{SMI26} (50 pg/mL added) in CSF was 92% for pool 1 (130 pg/mL) and 96% for pool 2 (92 pg/mL), averaging to 94%.

5.3.4 Parallelism

Parallelism between calibrant and CSF was studied by quantifying reciprocal dilutions. Three CSF samples from SAH patients and three different pools of HPLC–purified GFAP diluted in sample buffer were used. The OD was normalised to the highest value of the series. The parallel relationship was shown and suggested the absence of endogenous binding between CSF–GFAP^{SMI26} and other CSF substrates (Figure 5.8).

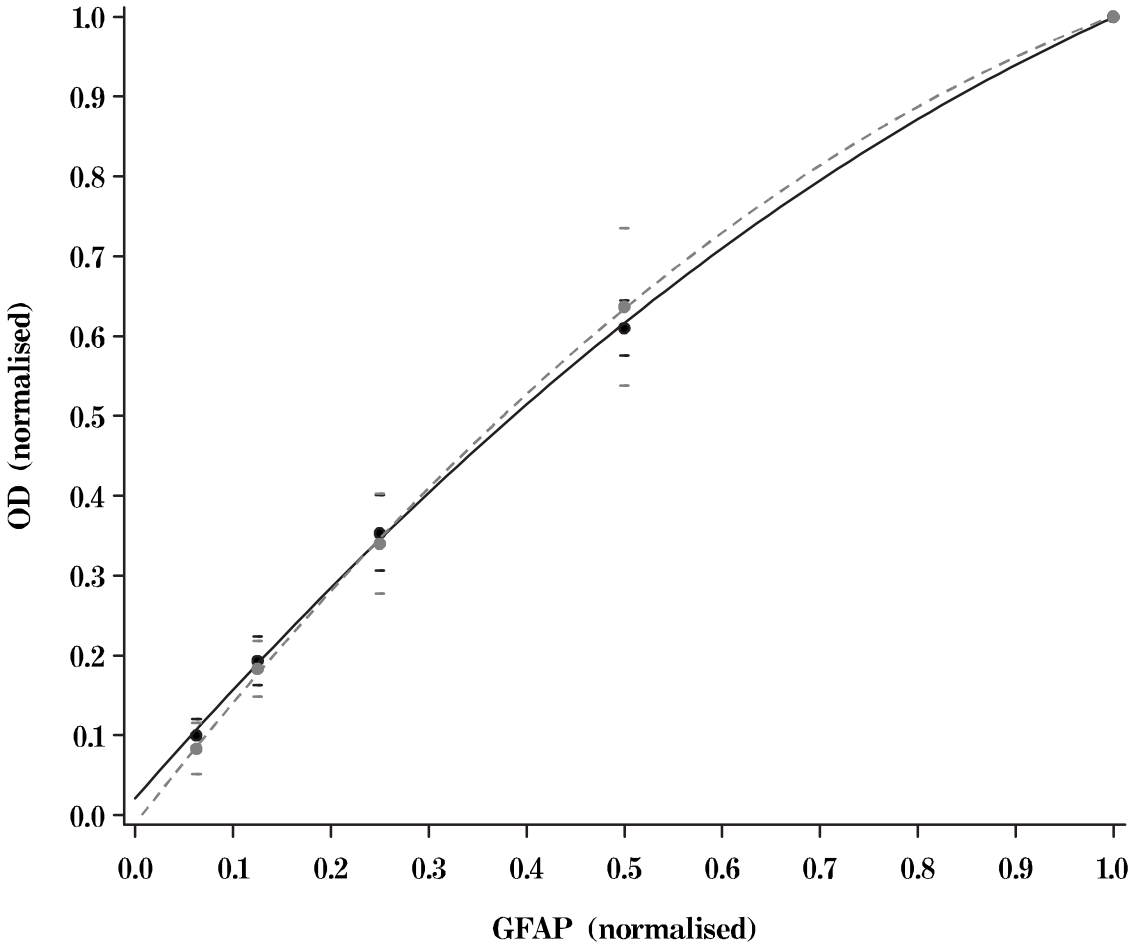

Figure 5.8: *Parallelism between calibrant (dots) and CSF (circles), linear regression.*

5.3.5 Stability of CSF samples

Stability was tested at room temperature (RT), 4°C and -70°C. CSF samples spiked with GFAP^{SMI26} were frozen in duplicates at -70°C, thawed on subsequent days and stored at 4°C and RT (Figure 5.9 A). Linear regression analysis of the 7–day observation period demonstrated no significant decrease in GFAP^{SMI26} at -70°C and 4°C. At RT there was however a significant ($p<0.05$) decrease in the measured GFAP^{SMI26} concentration.

No problems were found with stability of antibodies. To minimise any problems with cumulative contamination the antibodies were stored in 100 μL aliquots and each aliquot was used within 4 weeks. All buffers where used within 1 week and stored at 4°C.

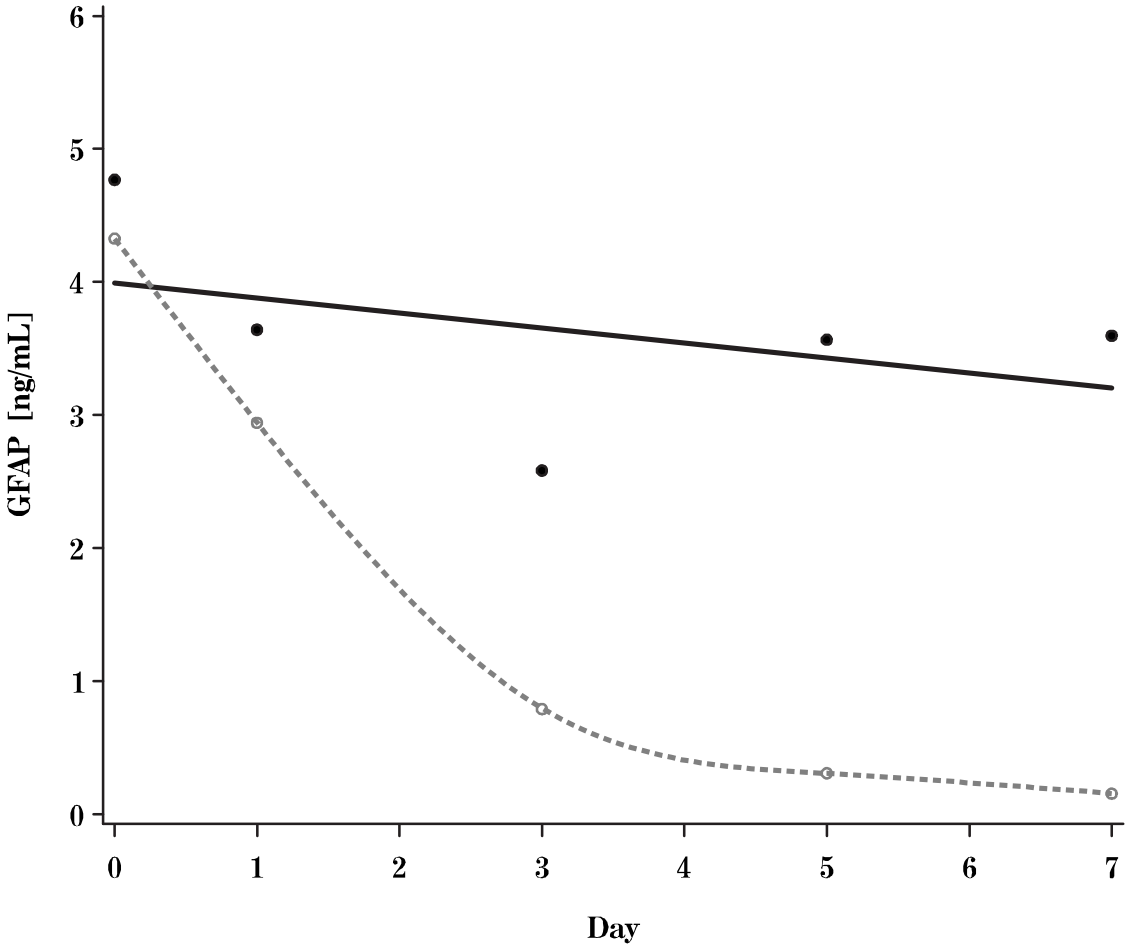

Figure 5.9: *Stability profile of GFAP^{SMI26} in CSF at 4°C (continuous line) and at room temperature (dotted line) over 7 days.*

5.3.6 Reference population

The top 10% of the 348 analysed samples were removed in order to obtain a representative reference population as discussed for the neurofilament ELISA (section 4.3.9 on page 111).

The mean age of the reference population was 44.7±15.9 years, with a median of 43.5 (IQR 33-56) years. The date of birth was not provided for 19 patients. There was no correlation between the age and CSF GFAP^{SMI26} levels (R=0.004, p=0.93). Fifty-nine percent (182/313) were female and 39% (122/3131) male and in 9 (3%) patients no gender was stated. There was no significant difference of CSF GFAP^{SMI26} levels between the 2 genders (Z=-0.59, p=0.27).

The distribution of the reference population for CSF GFAP^{SMI26} is shown in Figure 5.10. The upper–reference value was calculated as shown for the NfH^{SMI35} assay (page 111). The 97.5 percentile corresponded to 6 pg/mL (Figure 5.10, dotted reference line).

5.3.7 Neurological disorders

The CSF levels of the patients with subarachnoid hemorrhage (SAH), traumatic brain injury (TBI), dementia (DEM), hydrocephalus (HC) and miscellaneous disorders of the peripheral nervous system (PNS) are shown in Figure 5.11.

The CSF GFAP^{SMI26} levels differed significantly between the groups

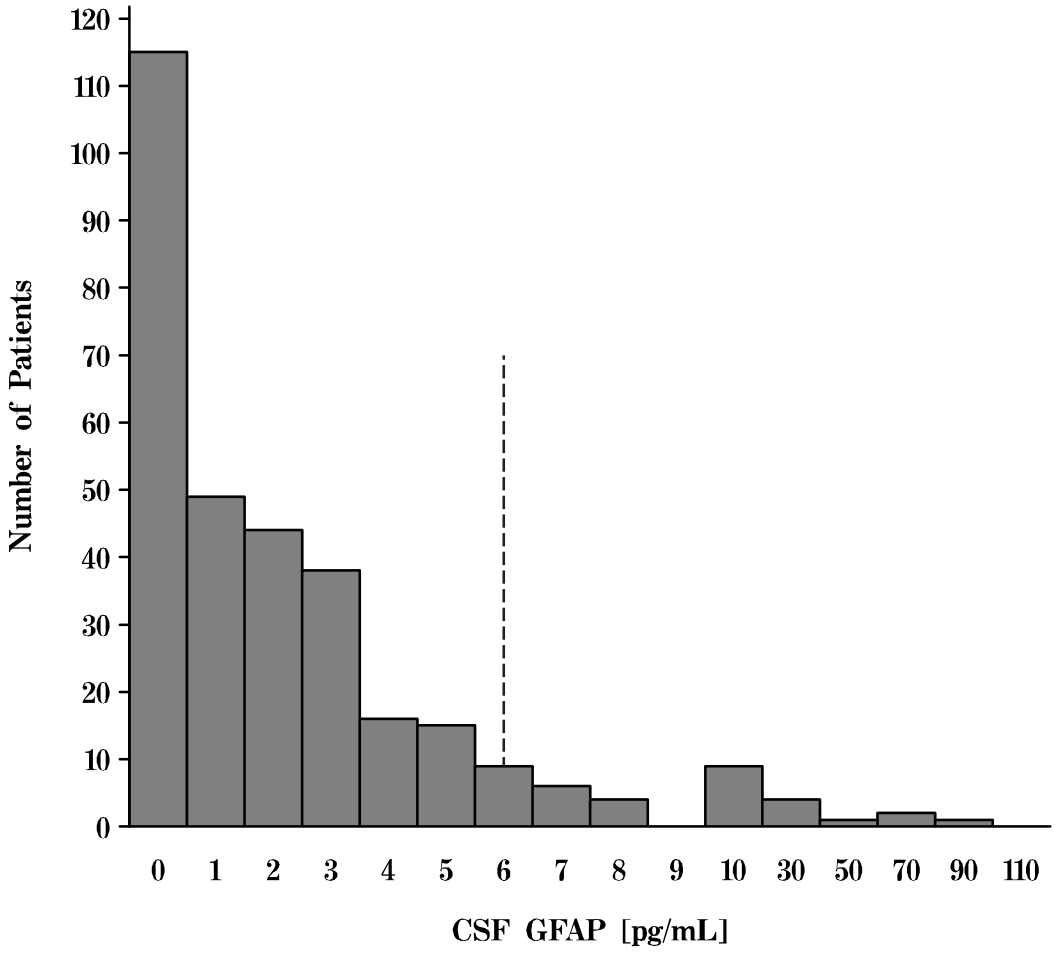

Figure 5.10: *Frequency histogram (bars) for the reference population. The cut–off for the upper reference limit of 6 pg/mL (dotted vertical line) is shown.*

(F(4,120)=9.88, p<0.001). The post–hoc analysis revealed that this was due to the higher values in SAH patients when compared to DEM (p<0.001), HC (p<0.001) and PNS (p<0.001). The levels of significance in the post–hoc analysis for TBI patients mirrored those of the SAH group. There was no significant difference of the GFAP^{SMI26} levels between SAH and TBI patients.

Table 5.1: *CSF GFAP^{SMI26} levels (mean±SD, range) in patients in patients with subarachnoid hemorrhage (SAH), traumatic brain injury (TBI), dementia (DEM), hydrocephalus (HC) and disorders of the peripheral nervous system (PNS). The number of patients with levels above the upper reference limit of 6 pg/mL is shown.*
Levels of significance comparing group means (⋆ p<0.001) or proportions († p<0.001) with the PNS group are indicated.

	CSF GFAP [pg/mL]+SD	**Range**	**Above reference**
SAH	18950±16078 ⋆	1550–40630	100% (5/5) †
TBI	16678±15022 ⋆	515–43730	100% (11/11) †
DEM	1374±11098	4–91540	94% (64/68) †
HC	1197±1226	0–2970	83% (10/12) †
PNS	1.4±1.9	0–6	0% (0/29)

The one outlier in the group of dementia patients had a GFAP^{SMI26} level of about 100 ng/mL (91540 pg/mL), a S100B level of 122000 pg/mL, was positive for 14-3-3 on the Western blot and had proved Creutzfeldt–Jakob disease on autopsy.

According to the previously defined reference limit of 6 pg/mL, 5/5 of the SAH, 11/11 of the TBI, 61/68 of the DEM, 10/12 of the HC and 0/29 of the PNS patients had CSF GFAP^{SMI26} levels above the upper reference limit. A significantly higher proportion of patients with SAH, TBI or DEM had CSF GFAP^{SMI26} levels above the reference limit when compared to the

numbers of PNS patients ($p<0.001$) (Table 5.1).

5.4 Discussion

The sandwich ELISA presented here is simple and based entirely on commercially available antibodies. The sensitivity of the assay is 5 pg/mL, the upper reference limit 6 pg/mL and the standard curve ranges from 0 to 200 pg/mL.

A previously described 4 to 5 layer assay[6] used in–house developed monoclonal antibodies[8] and a standard curve derived from human brain homogenate.[5,6] The GFAP range in the CSF of the control group was 2–14 ng/mL. The CSF GFAP levels in MS patients with acute relapse (10–21) or progressive disease (10–11) where not significantly different from the control group. The authors found significantly higher CSF GFAP levels in children with normal pressure hydrocephalus, which has been confirmed in a subsequent study[7] and is consistent with the results of the present study. Their assay has also been used successfully in determining GFAP levels in amniotic fluid,[6] but unfortunately we could not find any further studies using this assay. This assay is similar to two radio–immune assays and had a sensitivity of 0.5–1 ng/mL.[6,99,297]

A sensitivity of 16 pg/mL was achieved by using a three–layer sandwich ELISA based on in–house produced hen and rabbit anti–GFAP antibodies.[332] These authors used HPLC purified GFAP[333] for their standards. The

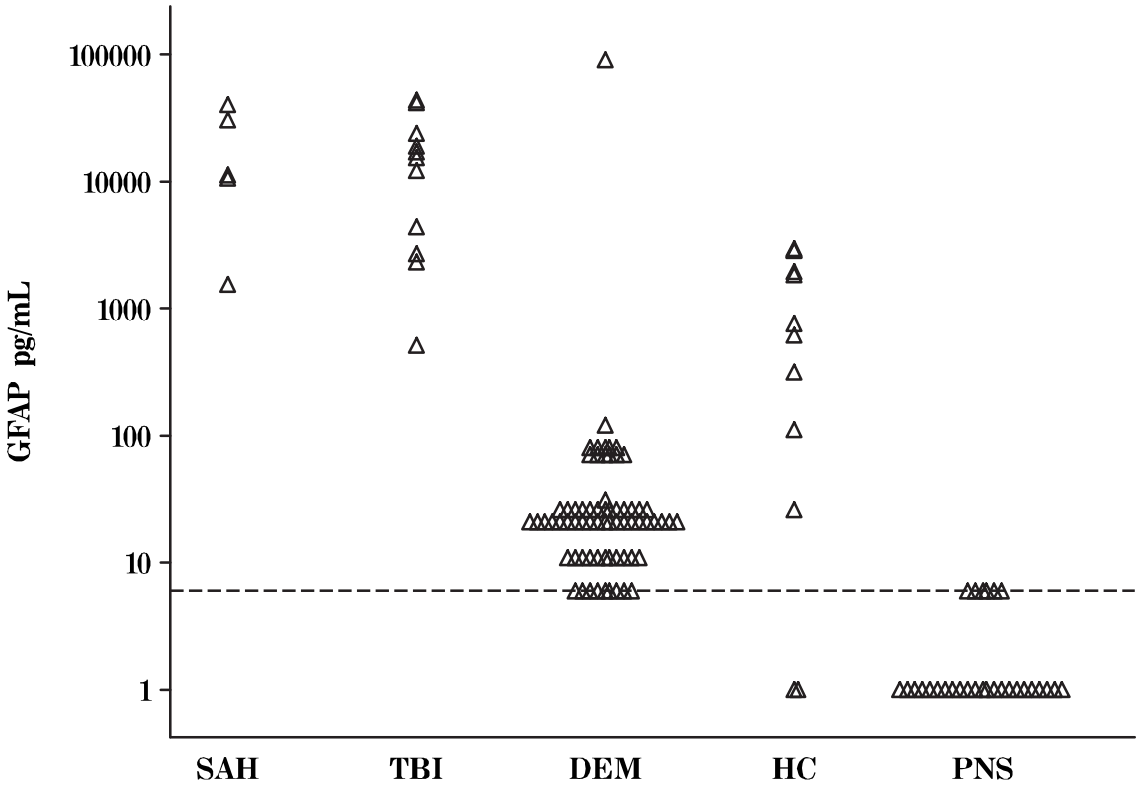

Figure 5.11: *CSF GFAP^{SMI26} (pg/mL; scale = $\log_{10}$) in patients with subarachnoid hemorrhage (SAH), dementia (DEM), hydrocephalus (HC) and a miscellaneous group of patients with disorders of the peripheral nervous system (PNS). The horizontal reference line (dotted) represents the upper reference limit of 6 pg/mL.*

assay was modified and a linear range for the standard–curve was obtained for 32–4000 pg/mL[337] with the sensitivity reported to be below 32 pg/mL. Using this method the authors were able to show elevated CSF GFAP levels in multiple sclerosis,[336] encephalopathy[92] and neuropsychiatric disorders.[3] This assay requires two overnight incubation steps.

So far the independent confirmation of results derived by this group has been hampered by the non–availability of their in–house developed antibodies. The present assay uses well–characterised and commercially available antibodies. In particular the capture antibody cocktail contains the original and well–described three IgG_{2b} Bigner–Eng clones MA1B4, MAb2E1, MAb4A11[264,302,413] and the IgG_1 SMI 22. No cross–reactivity with other intermediate filaments has been observed for the SMI26 antibody cocktail.

We and others[6,99,297] have not been able to demonstrate a correlation between CSF GFAP and age as described twice by one group.[332,337] However this group used an unique set of CSF samples from 25 healthy controls[337] and CSF GFAP levels started to rise at 48 years of age. It is of note that the other reported correlation of CSF GFAP and age in children[332] is due to 2 outliers in a rather small sample size (n=10) and no such correlation was observed in the larger group of children with autism (n=47). Thus the age effect might only become important after about the age of 50. Further studies are needed to clarify the influence of age on CSF GFAP levels. In particular one would need to take care to avoid bias by age of onset of disease, speed of

progression or severity of the underlying pathological process. This would have implications for the interpretation of CSF GFAP levels in patients with dementia.

Comparing the results for CSF GFAP levels in patients with dementia one would need to define an upper reference limit for Rosengren's population. The highest value for CSF GFAP of the healthy control group of Rosengren was 1200 pg/mL (see Figure 4 in[337]). The 97.5% quarantile corresponds to about 800 pg/mL. Using 800 pg/mL as upper reference limit, 13/16 (81%) of Rosengren's dementia patients had pathologically elevated CSF GFAP levels (see Figure 5 in[337]), which is a significantly higher proportion than in the control group ($p<0.001$, post–hoc analysis, Fisher's exact test). This post–hoc analysis is consistent with the finding that CSF GFAP^{SMI26} levels were elevated in a significant number of dementia patients (94%). The slightly higher percentage revealed in the present study might be due to a patient selection bias because the National Hospital of Neurology and Neurosurgery is a tertiary referral centre. In a subsequent analysis the same group subsequently reported significantly elevated CSF GFAP levels in patients with vascular dementia, senile dementia of the Alzheimer type and 'pure' Alzheimer's disease.[416]

The striking elevation of CSF GFAP^{SMI26} levels in patients with TBI and SAH has to our knowledge not previously been reported. For TBI patients high CSF GFAP^{SMI26} levels are likely to be related to direct parenchymal

destruction. It is however difficult to explain why CSF GFAP should be 4 orders of magnitude above the upper reference limit. One could speculate on a direct toxic effect of the blood released into the subarachnoid space onto a large surface of astrocytes. On the basis that the astrocyte maintains brain homeostasis, SAH astrocytotoxity could have a devastating impact on patient survival. We have previously shown that rise in serum S100B, another astrocytic marker was related to rise in ICP and mortality.[308] In this context CSF GFAP^{SMI26} could emerge as a second "astrocytic CSF marker" alongside S100B and contributes to increase the diagnostic specificity in conditions where the release of S100B from extra cranial sources such as adipose tissue, testis and skin[149,268,390] are problematic.[86,164] Certainly this new finding of high CSF GFAP^{SMI26} levels in SAH warrants further investigation.

In summary the present assay is reliable, reproducible and based entirely on commercially available antibodies. Such an assay is needed in order to clarify the issues discussed and advance the understanding of astrogliosis in neurological disorders.

Chapter 6

Established methods

6.1 S100B ELISA

indexELISA S100B was measured in the CSF as previously described[129]: Briefly, 96–well microtitre plates were coated with 200 μL 0.05 M carbonate buffer containing monoclonal anti S100B (Affiniti Research Products, Exeter, UK). The plates were washed with 0.67 M barbitone buffer containing calcium lactate, 0.1% BSA and 0.05% tween and then blocked with 2% BSA and washed again. Diluted serum (1:1) in 0.67 M barbitone buffer containing 1mM calcium lactate was added in duplicate. After incubation and washing HRP–conjugated polyclonal anti S100B (Dako, Copenhagen, Denmark) was used as detecting antibody. The colour reaction was stopped with 1 M hydrochloric acid and the absorbances read. The antigen concentration was calculated from an internal standard curve ranging from 0 to 2.5 ng/mL.

6.2 Ferritin ELISA

CSF ferritin was quantified using a previously described in–house ELISA technique.[185] The standards ranged from 0-20 μg/L ferritin and were prepared by diluting Lyphocheck Control serum Level 1 (Bio–Rad, Hemel Hempstead) in 0.85% W/V sodium chloride (saline) containing 0.1% BSA and 0.01% w/v sodium azide.

96–well microtitre plates were coated overnight at 4°C with 100 μL 0.05 M carbonate buffer (pH 9.5) containing 50 μg of polyclonal rabbit anti–ferritin serum (Dako Ltd., No A133). The plates were blocked with 250 μL 0.85% w/v sodium chloride (saline) containing 1% BSA and 1% gelatine for 1 hour. After washing with 250 μL saline containing 0.1% BSA, 0.1% gelatine and 0.1% tween 100μL of undiluted CSF was added in duplicate. After incubation and washing HRP–conjugated polyclonal rabbit anti–human ferritin (DAKO) was used as detecting antibody. The colour reaction with 100μL of *o*–phenylenediamine in 0.02 M acetate buffer (pH 5.1) was stopped with 50μL of 1 M hydrochloric acid. The absorbances were read at 492 nm against a reference wavelength of 405 nm. The antigen concentration was calculated from the internal standard curve.

6.3 Albumin rockets

CSF and serum albumin were quantified by a standard Laurell "rocket" electro immuno–assay. Briefly, 300 μL of goat anti–human albumin serum

(Incstar Ltd., Wolkingham; No 81900) were added to 30 mL molten 1.2% w/v medium electroendosmosis agarose (Flowgen Instruments Ltd., Sittingbourne; No 50013) in pH 8.6 barbitone electrophoresis buffer[170] containing 3% w/v polyethylene glycol 600. The mixture was then cast on 203 mm wide GelBond (Flowgen Instruments Ltd., Sittingbourne, product code 53760) using a casting frame prepared from two glass plates, 195 mm × 195 mm × 3 mm, separated by three thicknesses of Dymo tape and sealed around three edges with Scotch electrical tape. The glass plates were partially submerged in a water bath at 65°C and the agarose solution was added using a Pasteur pipette. After cooling to room temperature the gel was allowed to set at 4°C for a further 2 h before being used. The casting assembly was dismantled and 80 wells punched in the gel in five ranks of 16 wells. Each well was 2 mm in diameter and separated from its neighbour in the rank by 10 mm (centre to centre). Ranks were separated by 30 mm. Wells in adjacent ranks were staggered so that the rocket peak from one well would lie between two wells of the rank in front. The gel plugs were removed by suction. Standards were prepared from SPS01 (Protein Reference Units, Central Antiserum Purchasing Unit, Sheffield) diluted to values of 50, 100, 200, 300, 400, 500 mg/L. Samples of 2 μL undiluted CSF (unless the total protein was greater than 1 g/L in which case the CSF was diluted) or serum diluted 1:200 in 0.85% w/v sodium chloride (saline) were added to each well. Electrophoresis was carried out overnight at 150 V with cooling. After electrophoresis

the gel was pressed, washed for 30 min in saline, pressed again, then dried and stained using Coomassie Brilliant Blue. Albumin concentrations were calculated from the internal standard curve.

6.4 Total protein

Total protein was measured by a modification of the Lowry method[234] using the Bio–Rad DC Protein assay (Bio–Rad, Hemel Hempstead). Briefly, standards were prepared from BSA (Sigma) diluted into values of 225, 450, 900, 1250, 1500 mg/mL in saline. Five μL of undiluted CSF or diluted serum (1:100 in saline) were pipetted in duplicates into a 96–well microtitre plate. Twenty–five μL of an alkaline copper tartate solution (reagent A) were added into each well, the plate was shaken and 200 μL of a dilute folin reagent (reagent B) were added. The plate was incubated for 15 minutes on a plate shaker and absorbances were read at 750 nm.

6.5 Oligoclonal bands

CSF and serum immunoglobulins were separated using standard and consented methods.[16] Briefly, on glycerol (Sigma, No 80261), sorbitol (Sigma, No S-0900) agarose IEF (Pharmacia, No 7-0468-01) gels. Gels were prepared, cast and dismantled as described above. A sample application foil with 20 punched holes (10mm centre to centre distance) were layered 3 cm from the anodic edge of the gel to ensure equilined sample application. 3 μL of paired and time matched CSF (undiluted) and serum (diluted 1:400

in water) samples were added to each application slot. A strip of Postlip paper soaked in 0.05M sulphuric acid was placed on the outermost edge of the anodic and a Postlip paper soaked in 1M sodium hydroxide on the cathodic side of the gel. Isoelectric focusing was carried out at 1250 V, 150 mA and 20 W for 1100 volt–hours. At 850 volt–hours the run was stopped and IgG was passively plotted onto nitrocellulose for 30 minutes. Nitrocellulose was blocked with 2% milk in saline for 1 hour, washed with distilled water and incubated with polyclonal rabbit anti–goat immunoglobulin antibody (1:1000 in saline) for 1 hour. After another washing step, amino–ethyl carbazol was added as colour developer. After a final wash the nitrocellulose membrane was dried.

IgG patterns were stratified according into 7 groups. Samples without IgG in CSF/serum were called OCB -/-, samples with equal number of IgG bands in CSF/serum were called OCB +/+, samples with IgG bands present only in the CSF were called OCB +/-, samples with slightly more IgG bands in the CSF than in the serum were called OCB ++/+, samples with considerably more IgG bands in the CSF than in the serum were called OCB +++/+, samples with one single clone of IgG (monoclonal) in the CSF but not in the serum were called OCB m/- and samples with the same single clone of IgG in serum and CSF were labelled OCB m/m.

Chapter 7

Data management and analysis

7.1 Data management

The amount of raw data of the clinical studies required a systematic approach to establish data integrity. The SAS system provides powerful data management engines. Of particular importance is access to all major databases such as Microsoft ACCESS, SQL, Excel, DBase, etc. Information on patients was stored on the Sunquest system of UCLH and in the ACCESS database of the Department of Neuroimmunology. Experimental results were stored on Excel spread–sheets. These datasets were combined and stored within SAS because SAS datasets are optimised to enhance database performance and provide a close link to the statistical packages.

According to the MRC guidelines for data handling in the UK all patient data must be stored anonymously. Therefore a unique code was assigned to each patient. The patient names, hospital numbers and contact details (if available) were stored locally. Access to confidential information such as

names, addresses, etc. was protected. For collaborative studies the confidential database was stored locally in each centre. Frequent exchange of data was necessary and performed with coded protocols on the internet. Only datasets where anonymity of the patient was guaranteed by the unique identifier were exchanged. Statistical analysis was performed on virtual datasets merged directly prior to analysis.

7.2 Statistical analysis

All statistical analyses and graphs were done using SAS software (SAS version 6.12 and version 8.2, SAS Institute, Inc., Cary, North Carolina, USA).[65]

Descriptive statistics Descriptive statistics were performed using the `proc univariate` procedure. Normal distribution was tested using the Shapiro–Wilk test for n<2000.

All mean values were given ± the standard deviation (SD) or the standard error if n<10. Skewed data were presented as mean and 25–75% interquartile range (IQR) for n>10 and the 0–100% total range when n was smaller than 10. The presentation in tables then followed the notation: *median (range), number*. The box (median and 25%–75% cumulative frequency) and whisker (1%–100% cumulative frequency) were shown in the graphs. Dots were plotted adjacent to each other (jittered) if 2 or more observations showed the same value.

Correlation and regression The strength of the linear relationship between 2 continuous variables was evaluated using the Pearson correlation coefficient (α=0.05) for normally distributed and the Spearman rank correlation (α=0.05) for non–Gaussian distributed observations. For multiple comparisons a correlation matrix was calculated using the `proc corr` procedure with the appropriate correlation coefficient. Significance of the correlations was tested by analysing the scatter plot for outliers and ceiling effects.

Linear regression analysis was performed using the least–squares method (`proc reg`). The 95% confidence interval for the slope was calculated by taking approximately two standard errors above and below the mean if n >30. When n was < 30 the number of standard errors above and below the mean were taken from a t–table. Significance was tested by analysing the residuals. If the root MSE (square root of the error variance or standard deviation of the residuals) was high or the distribution of the residuals was dubious the results were rejected.

Partial correlations were performed when a group difference could have been biased by significant correlations of the independent variable with age (age at onset of disease, etc.) or significant gender differences. This was done by applying the `partial` option to the `proc corr` procedure.

T-tests and nonparametric comparisons Means of normally distributed, independent variables with similar variance were compared using the t–test (`proc ttest`). The one–tailed t–test was applied if the alternative hypothesis stated that one specific mean would be greater. If the alternative hypothesis was that the two means were different, a two–tailed t–test was performed. For dependent variables the paired t–test was used via the `proc means` procedure with the options `n mean stderr t prt`.

For non–normally distributed, independent variables the two-sample exact Wilcoxon rank-sum test was used (`proc npar1way` with the option `wilcoxon`).

For multiple comparisons the probability of at least one significant difference by chance alone is 0.64 for an α of 0.05 and all analyses were done by ANOVA.

Analysis of Variance For more than 2 groups and multiple comparisons ANOVA (`proc anova`) was used if the groups were independent, the sampling distribution were Gaussian and the groups were derived from populations with equal variances (homogeneity). If either of these assumptions was not met or if the populations were not homogeneous and were unbalanced (different number of subjects per group), the unbalanced two-way ANOVA (general linear model) was applied using the `proc glm` procedure.

Post–hoc or multiple comparison tests were done using Duncan's mul-

tiple range test for ANOVA and the least–square adjusted means for main effects for the general linear model (options `lsmeans pdiff`).

Categorical data analysis Proportions were compared by the χ^2 test using the `proc freq` procedure with the option `/ chisq` in the `table` statement. If the number per cell was less than 5, Fisher's exact test was used with α=0.05 (option `/ chisq FISHER`). The test was one–tailed if the alternative hypothesis was rational and clear before the analysis. A two–tailed test was performed if the alternative hypothesis stated only that the two groups might be different.

Trend analysis was done using the Mantel–Haenszel (M-Hχ^2) test (option `/ chisq all`).

Odds ratios were calculated by applying the Cochran–Mantel–Haenszel option `/ chisq CMH`. The Mantel–Haenszel value and the 95% CI were given.

Part III

Results

Chapter 8

Experimental autoimmune encephalomyelitis

8.1 Background

Experimental allergic encephalomyelitis (EAE) is a well established model of a CNS autoimmune demyelinating disease. Although possibly different from multiple sclerosis (MS) in aetiology, the underlying neurodegenerative processes that occur in EAE allow for some comparisons with the pathological changes that are observed in MS.

The principal advantage of studying brain–specific proteins (BSP) in CNS tissue from mice induced with EAE is that this tissue can be snap–frozen immediately after sacrifice of the animal. Therefore confounding variables such as variability in the post–mortem time and auto–proteolysis are better controlled than for human post–mortem tissue.

The model chosen for this study was the EAE in ABH mice .[28] In this model the spinal cord is the primary site of demyelination. The animal presents with clinical relapses and chronic disease progression (Figure 8.1).

Figure 8.1: *Disease progression in 11 CREAE animals followed up for 120 days with 28 relapses. The arrow indicates the time when the spinal cord sample was taken for this study.*

The chronic phase is of particular interest for understanding the relapse–independent relationship between cumulative axonal damage and loss of function. In addition the quantitative relations between axonal loss, glial activation and gliosis can be evaluated. As outlined in sections 2.2–2.3 (page 59 ff.) astrocytic activation might be a double–edged sword, beneficial if moderate, but preventing remyelination and axonal sprouting if astrocytic transformation occurs and a gliotic scar develops. The severity of spinal cord axonal loss and astrogliosis makes mice with chronic relapsing EAE (CREAE)[28] an ideal model to study these markers.

Failure to halt MS disease progression with immunomodulating agents has demonstrated that neurodegeneration is an important pathogenic component of MS.[41,438] This provides the impetus for designing and assessing treatment paradigms in animal models. Axonal loss correlates with permanent neurological disability in CREAE[438] and is typically assessed using time–consuming immunohistology.[41,438] Therefore a simple quantitative surrogate would be advantageous. This study examines the potential of the ELISA–based methods presented in chapters 4–6.4 (page 73 ff.) to assess the neurodegeneration that occurs in CREAE.

8.2 Methods

Animals Adult Biozzi ABH mice (6–8 weeks old) were supplied by the Department of Neuroinflammation, University College London (David Baker, Gareth Pryce). The mice were housed in a light- and temperature–controlled room and matched for age in the experiment.[28]

Induction or CREAE Syngeneic spinal cord homogenate (1 mg lyophilised spinal cord) was diluted in 0.15 mL PBS and Freund's incomplete adjuvant (Difco Laboratories) containing 60 μg killed Mycobacteria (*Mycobacterium tuberculosis H37Ra* and *M. butyricum* (8:1)). Two subcutaneous inoculations were given.[28] Animals were scored clinically on a scale ranging from 0 to 6, where 0 indicated a normal animal, 1 a limp tail, 2 loss of the inverted righting reflex, 3 partial hind limb paralysis, 4 complete hindlimb paralysis,

5 moribund and 6 death.[28] After 60–80 days post inoculation the chronic phase of the disease had been reached (arrow in Figure 8.1) and the animals were sacrificed by CO_2^- intoxication.

Preparation of spinal cord homogenate Immediately after death incisions were made in the spinal column at the level of the the lumbar and cervical regions. A needle was inserted into the lumbar vertebral column and the spinal cord ejected into an Eppendorf tube by a pressurised injection of saline. The spinal cord which is the site of pathology[28] was snap–frozen and stored at -70°C until further analysis.

Cytochemistry Frozen tissue was used for immunocytochemistry as described using polyclonal rabbit anti–cow GFAP IgG (DAKO, Denmark) or polyclonal rabbit anti–bovine NfH IgG (Sigma, UK) and FITC labelled swine anti–rabbit IgG (Dako).[28,29] Photographs of the fluorescin images were digitally transformed into black–and–white slides for better visualisation.

Protein extraction The spinal cord was suspended in sample buffer 1:5 v/w containing a protease inhibitor cocktail (Sigma, No P 8340). Samples were homogenised on ice by sonication and triturated 3 times through 19 and 21 gauge needles. In order to separate myelin protein, di–iso–propyl ether (1:5,000) was added. After extensive mixing the sample was spun at

20,000 g. The supernatant was covered by a myelin layer. A needle was put through the myelin layer and the supernatant drawn up into a 1 mL syringe. The supernatant was aliquoted into triplicates of 1:1,1000, 1:5,000, 1:10,000 and 1:100,000 dilutions. The aliquots were stored at -70°C until further analysis.

Assays S100B (page 146), ferritin (page 147), GFAP (page 121), NfH^{SMI35} (page 73) and total protein (page 149) were measured as described.

Statistical analysis Data were managed and analysed as described (Chapter 7, page 151). The median and 0–100% range are shown because of the non–normal distribution and n< 10. The cutoff for categorical data analysis was set to the 0% or 100% cumulative frequency of the control group as appropriate.

8.3 Results

A 3–fold increase of median GFAP levels (13 ng/mg protein) in chronic EAE animals was observed if compared to control animals (4.5 ng/mg protein, Fig. 8.2). In addition a more intense immunocytochemical staining was observed in CREAE mice. The white matter of CREAE animals showed intense staining for GFAP and widespread astrogliosis. Astrocytes of the CREAE grey matter were of larger configuration with a greater number of extending processes (Figure 8.6 A).

Levels of NfH^{SMI35} were approximately 3–fold lower in CREAE (21 ng/mg protein) than in control mice (63 ng/mg protein, Fig. 8.3). The staining for NfH was more intense in the white matter of control animals (Figure 8.6 B). It is of note that the continuity of axonal projections could be followed. In CREAE animals NfH staining was less intense, axonal continuity almost disappeared and many axonal ovoids were observed (Figure 8.6 B).

Ferritin was less then 2–fold lower in CREAE (547 ng/mg protein) compared to CTRL mice (858 ng/mg protein, Fig. 8.5), a median S100B levels were about 2.6–fold lower in CREAE (786 ng/mg protein) than in CTRL mice (2080 ng/mg protein, Fig. 8.4).

In order to compare the proportions of abnormal samples, the cut–off was defined as the 100% cumulative frequency of the control group for GFAP and as the 0% cumulative frequency for S100B, ferritin and NfH^{SMI35}. For statistical analysis, numbers of samples were compared for values for each group above versus below the defined cut–off (reference lines in Figure 8.2 to 8.5).

Table 8.1: *Control (CTRL) and* CREAE ABH mice *spinal cord homogenate. Levels of brain–specific proteins are shown in ng/mg protein. Median (range).*

Protein ng/mg protein	**CTRL mice**	**CREAE mice**
GFAP	4.5 (1.4–5.2)	13 (5.0–26.4)
S100B	2080 (852–3107)	786 (219–1466)
NfH^{SMI35}	63 (53–84)	21 (9–44)
Ferritin	858 (794–1801)	547 (355–963)
Number	7	8

Seven out of 8 (88%) of CREAE animals had GFAP levels above the cut–off and by definition none (0%) of the control animals had GFAP levels above the cut–off ($p<0.001$). For NfH^{SMI35} 0/8 (0%) of the CREAE and 7/7 (100%) of the control animals had levels above the cut–off ($p<0.001$). For ferritin 1/7 (13%) of the CREAE and 7/7 (100%) of the control mice had levels above the cut–off ($p<0.001$). For S100B 3/8 (38%) of the CREAE and 0/7 (100%) of the control mice had levels above cut–off, but this did not reach statistical significance.

As suggested by the inverse pattern shown for GFAP and NfH^{SMI35} (Figure 8.2) a negative correlation existed between these two proteins ($R=-0.54$, $p<0.05$, Figure 8.7 F). Strong positive correlations ($R>0.8$) between levels of NfH^{SMI35} , S100B and ferritin were found. Figure 8.7 shows the correlations, R–values and the level of significance for each comparison. Importantly neither S100B nor ferritin correlated with GFAP.

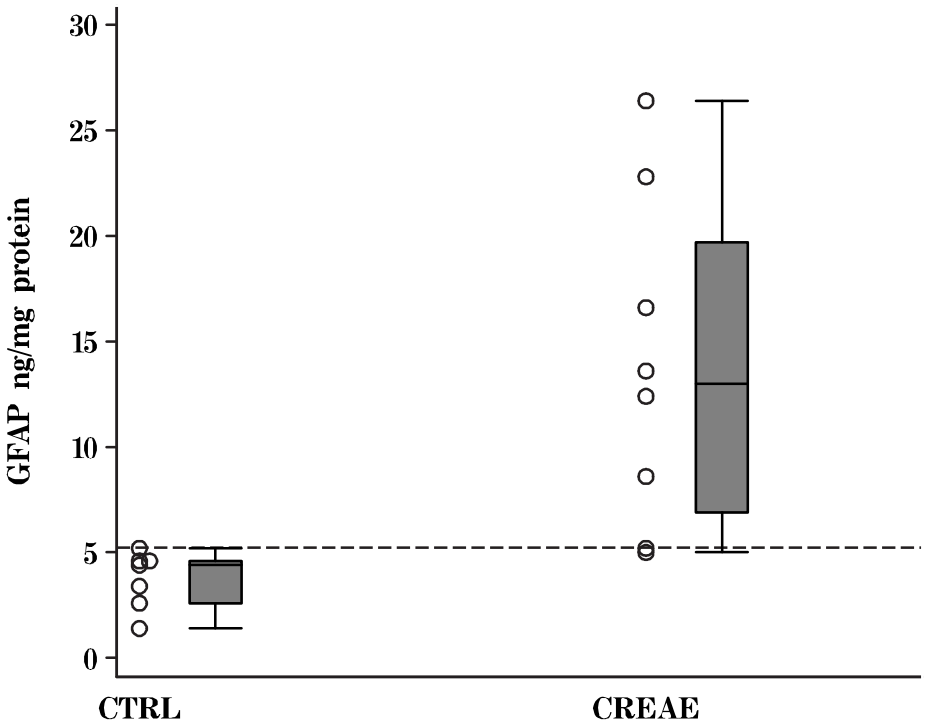

Figure 8.2: *Mice spinal cord tissue homogenates. Scatter and box and whisker plot for GFAP (ng/mg protein) levels in control (CTRL) and chronic EAE (CREAE) mice.*

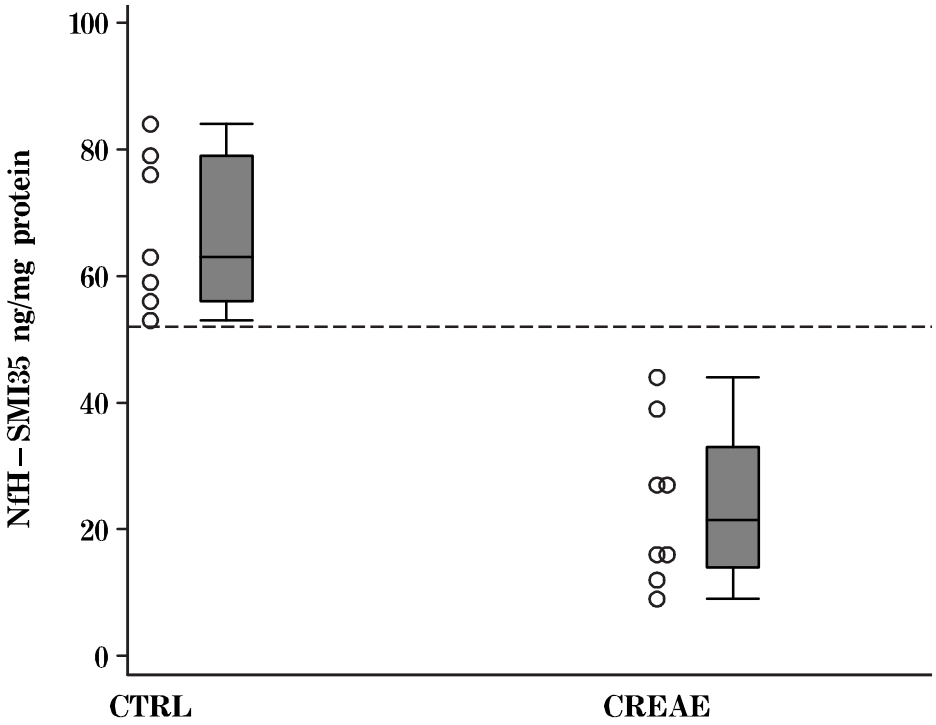

Figure 8.3: *Mice spinal cord tissue homogenates. Scatter and box and whisker plot for NfH^{SMI35} (ng/mg protein) levels in control (CTRL) and chronic EAE (CREAE) mice.*

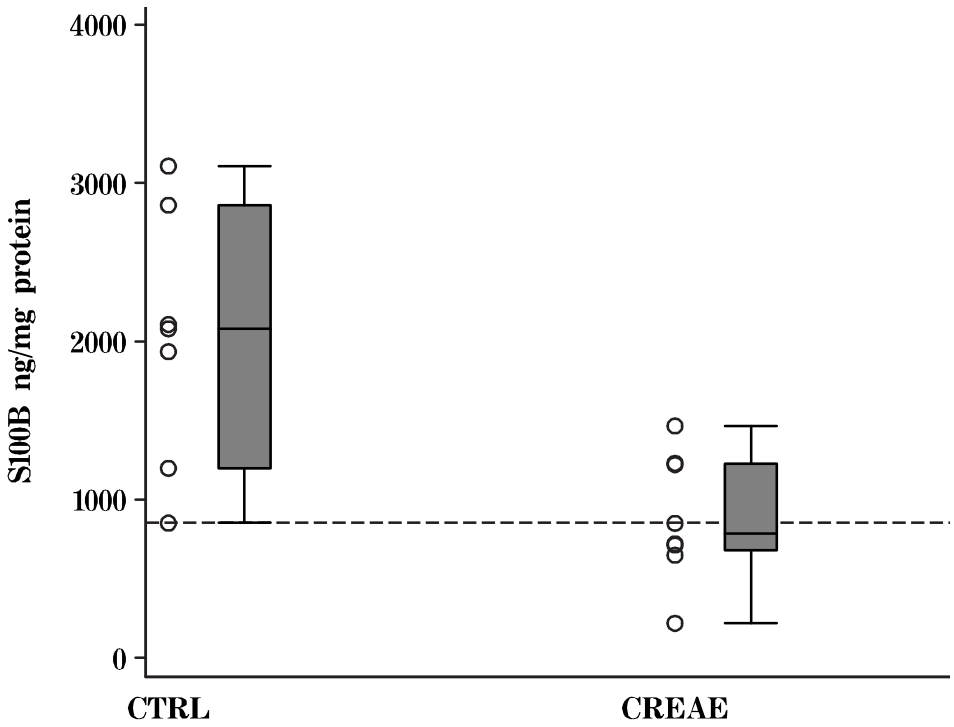

Figure 8.4: *Mice spinal cord tissue homogenate. Scatter and box and whisker plot for S100B (ng/mg protein) levels in control (CTRL) and chronic EAE (CREAE) mice.*

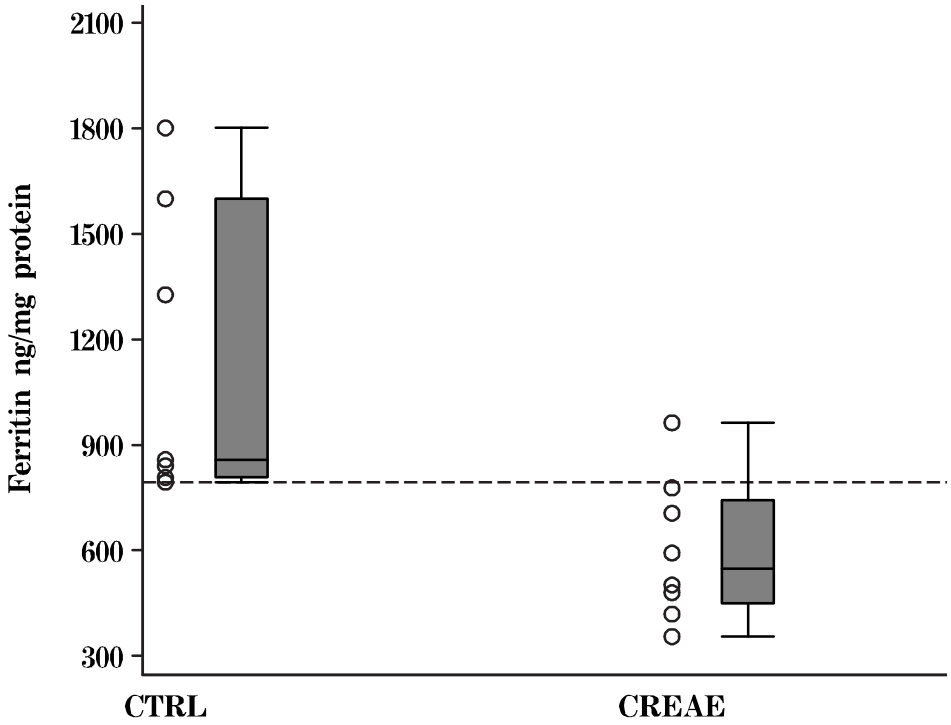

Figure 8.5: *Mice spinal cord tissue homogenate. Scatter and box and whisker plot for ferritin (ng/mg protein) levels in control (CTRL) and chronic EAE (CREAE) mice.*

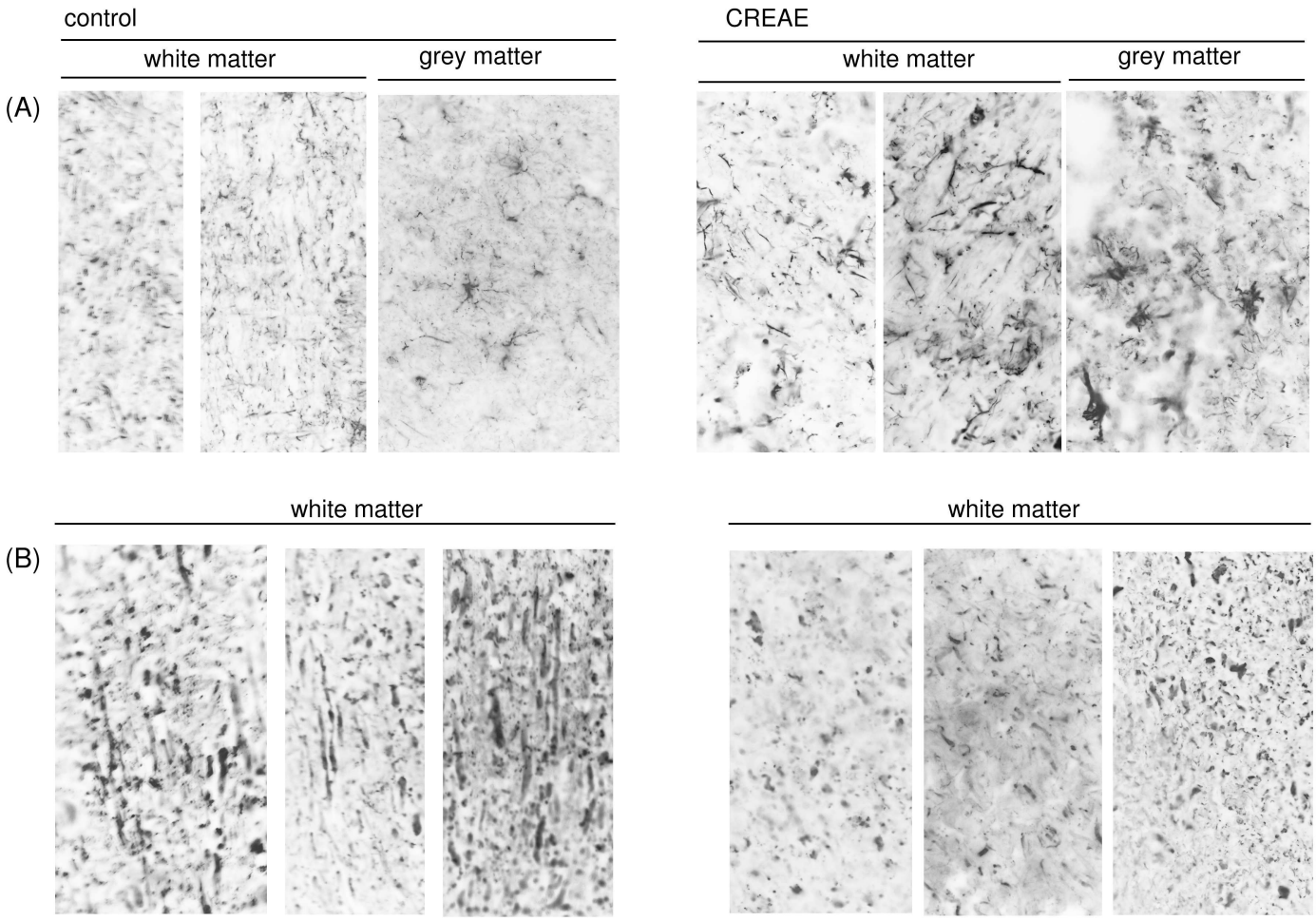

Figure 8.6: *Immunocytochemistry on longitudinal fresh frozen spinal cord sections of 3 control and 3 CREAE animals (x40). (A) GFAP staining for white and grey matter. More intense staining is observed in the CREAE spinal cord: in particular, the grey matter astrocytes are larger with more and longer processes. (B) NfH staining in white matter. Axonal tracts can be followed in control but not in CREAE animals. The staining in CREAE animals is less intense and many axonal ovoids are seen.*

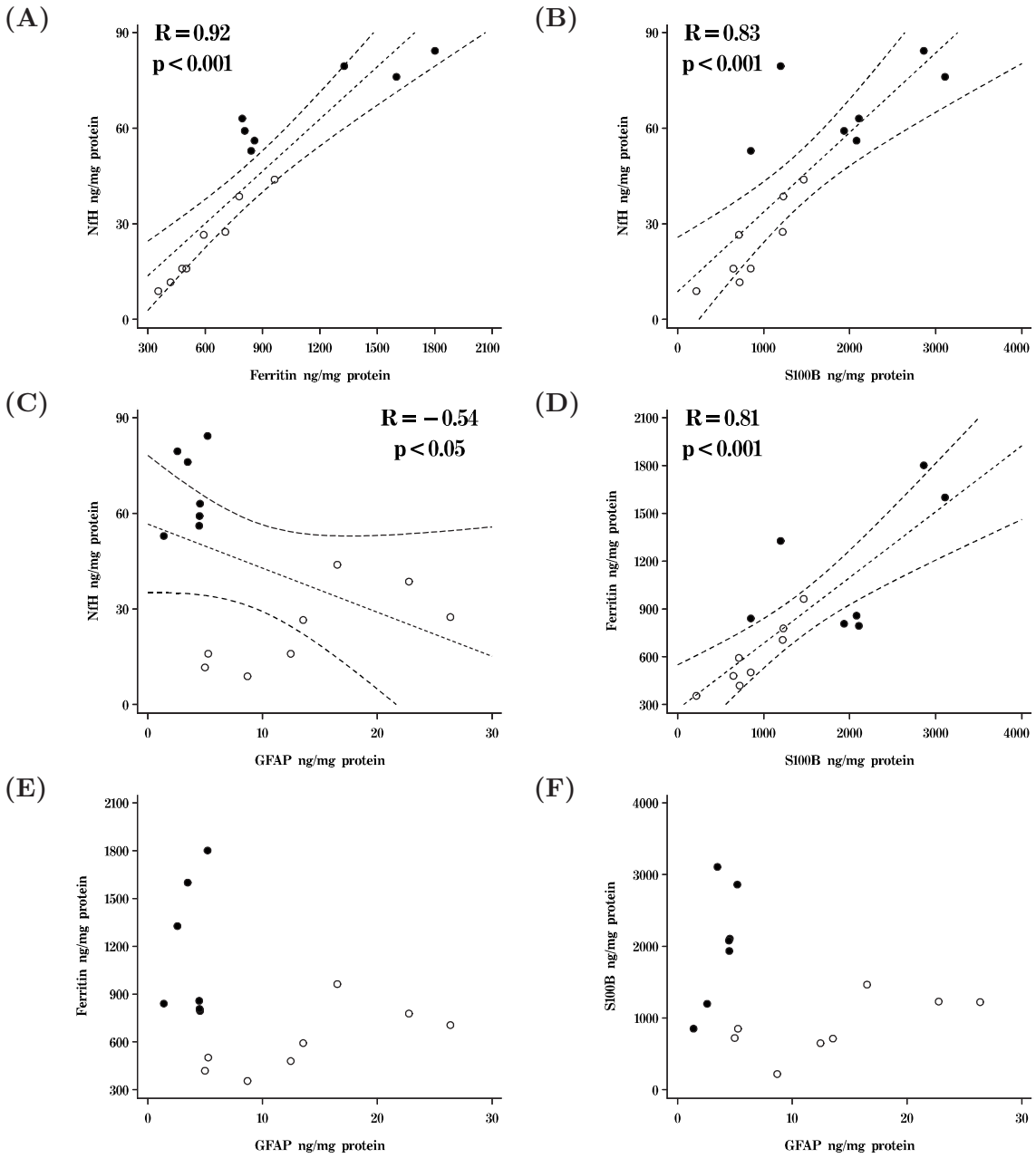

Figure 8.7: *Correlations of NfH^{SMI35} (ng/mg protein) with (A) ferritin (ng/mg protein), (B) S100B (ng/mg protein), (C) GFAP (ng/mg protein) and in (D) the correlation between Ferritin (ng/mg protein) with S100B (ng/mg protein). GFAP did not correlate with either (E) Ferritin (ng/mg*

8.4 Discussion

The observation that GFAP levels are 3–fold elevated in the spinal cord of mice with CREAE when compared to control animals of the same strain is in keeping with the observation of gliosis being the histological hallmark of the late disease stages.[61] However gliosis is difficult to quantify by immuncytochemical techniques and usually done by counting cells, and the number and length of extending processes (Figure 8.6 A). The present results would suggest that GFAP levels could be a "bulk–marker" for astrogliosis of the CNS. The finding of grey matter astrogliosis and elevated GFAP levels is in line with the results from human multiple sclerosis post–mortem tissue (Chapter 9).[307]

Importantly the NfH^{SMI35} levels were significantly lower in CREAE animals when compared to controls. The decrease confirms on a quantitative biochemical basis the immunhistologically observed loss of axons.[28,438] In the light of recent data on axonal loss in MS[41,398] and severe axonal loss in the spinal cord of EAE,[438] it is of particular interest that not only the overall staining intensity for NfH decreased, but also that axonal continuity almost completely disappeared. Counting axons might be particularly difficult in these situations and would only represent an estimate at site of section. The measurement of the total NfH^{SMI35} content is likely to be a more robust overall estimate of the bulk of remaining axons.

The finding that one astrocytic protein (GFAP) was elevated whilst the

other (S100B) was decreased could possibly be explained by S100B being a cytokine[86] (Figure 2.3 on page 63) and GFAP a structural protein[95] ((Figure 2.2 on page 61). There was no correlation whatsoever between S100B and GFAP. In contrast the correlations between S100B and ferritin with NfH^{SMI35} were strong (R>0.8). All three of these BSP were decreased in the spinal cord of CREAE animals. This suggests that at an advanced stage of the disease astrocytes, microglia and axons appear to be affected in parallel, i.e. severe axonal loss could be associated with a reduction of the potential to derive neurotrophic factors from glia which have been transformed into a gliotic scar.

8.5 Conclusion

Spinal cord tissue from EAE mice provide an important model for studying brain–specific proteins, particularly because confounding variables such as the post–mortem interval and autoproteolysis can be better controlled than in humans. In summary, this study demonstrates that axonal loss and gliosis can be measured biochemically by quantifying NfH^{SMI35} and GFAP levels in the spinal cord tissue of animals with CREAE. These findings support the concept of CSF BSP as putative surrogate markers and secondary outcome measures in patients with MS and also be used in animal models.

Chapter 9

Post–mortem study

9.1 Background

General introduction Despite the fact that GFAP was initially discovered in MS plaques[96, 288] no systematic study of a quantitative profile of BSP in histologically classified MS [289] lesions has yet been reported. In order to extend the animal study (Chapter 8) and to prepare for the human CSF studies (Chapters 10 to 12), this chapter presents BSP levels in human MS brain tissue. It was hypothesised that BSP levels differed between lesion types, normal–appearing MS and control brain tissue. The second aim was to find those proteins which are associated with acute lesions, because they would be of particular importance in a human CSF study.

Axonal damage and NfH phosphoforms Chapter 2.1 introduced the general relation of Nf to axonal damage. Since the use of specific monoclonal antibodies permits us to detect distinct Nf epitopes, the distribution of different NfH phosphoforms was studied in axonal pathology and in neu-

rodegeneration. It is on the background of this research that Sternberger *et al.* (1985) proposed the classification of the antibodies recognising these NfH phosphoforms according to their cellular distribution into 4 groups:

1. Group I antibodies stain cells and structures in the grey matter (GM).

2. Group II antibodies stain for projecting axons, but not for neuronal perikarya, dendrites or proximal axons.

3. Group III antibodies stain for perikarya, dendrites and proximal axons. Only little overlap with group II antibodies.

4. Group IV antibodies stain for all structures revealed by group II and group III antibodies.

These properties of the SMI antibodies have been discussed into detail in Chapter 4.

Attempts to relate NfH phosphoforms to axonal pathology have revealed everything but a unifying theory. It appears that there is considerable heterogeneity of axonal pathology in different diseases:

MS: In multiple sclerosis (MS) axonal injury has been related to increased staining by NfH^{SMI32} [398, Figure 8B, page 282]. NfH^{SMI32} was particularly abundant in axonal ovoids which indicate the site of axonal transection.

MND: In motor–neuron (MND) disease increased staining for phosphorylated NfH (i.e. NfH^{SMI34} , NfH^{SMI35}) has been shown in axons and the neuronal cell bodies. There is evidence for accumulation of phosphorylated NfH in the degenerating motor neurons.[282,339] However Nf dephosphorylation has been reported to precede excitotoxicity in a spinal cord cell culture model of MND.[396,410] Extending their work, this group has recently reported an increase of staining for NfH^{SMI32} in cultured spinal cord neurons after exposure to CSF from patients with MND.[397] Interestingly 3 of the 6 control CSF samples were from patients with MS, but the individual breakdown of the data has not been published.[397]

AD: In Alzheimer's disease (AD) increased staining for phosphorylated NfH is evident in the proximal axon and the perikaryon.[379,386,387,446] The staining for phosphorylated NfH has been shown in the proximal axon elongating from AD plaques.[378,386,387] This has been interpreted as evidence for early axonal injury remote (neuron proximal) to the plaque which exhibits toxic properties .[386,387] In addition there is evidence that NfH^{SMI32} positive neurons are selectively lost in AD .[126,151,280] In cell culture experiments this has been related to selective hypervulnerability of these NfH^{SMI32} positive neurons to kainate.[126]

A common methodological approach to reveal the phosphorylation state of Nf was to incubate the tissue with alkaline phosphatase (ALP) .[246,246,376–379,386,387,446]

These experiments have been summarised for the non–phosphorylated NfH SMI epitopes in Table 9.1, and for the phosphorylated NfH epitopes in Table 9.2. In order to allow for comparison with experiments using antibodies distinct from the Sternberger archive, Table 9.3 summarises some representative studies. For each NfH phosphoform the antibody source and main effects as observed by immunocytochemistry were summarised with regard to ALP–treated versus non–treated tissue sections. Because the applied method of dephosphorylation varied considerably (e.g. incubation times from 2.5 to 18 hours), the exact protocol is referred to in the footnotes of Tables 9.1 and 9.3.

The common finding in MS, MND and AD is that NfH^{SMI32} seems to indicate vulnerable or pre–damaged axons/neurons.[126,151,280,396–398,410] The finding of NfH^{SMI34} or NfH^{SMI35} positive axons in AD is either related to plaques or neurofibrillary tangles (NFT)[73,379,386,387,446] or an entire axon–proximal finding.[246,282,339,379,386,387,446]

Three NfH phosphoforms* emerge from Table 9.1 and 9.2 as the most interesting to be studied in MS brain tissue: NfH^{SMI32}, NfH^{SMI34} and NfH^{SMI35}.

*The labelling of the commercially available SMI antibodies has changed since the earlier publications. SMI31 was 02–135, SMI33 was 02–40, SMI34 was 07–5, SMI35 was 03–4, SMI36 was 06–68, SMI 37 was 06–32, SMI38 was 10–1. For reasons of consistent nomenclature (see section 2.1.1 on page 54) the currently used names are shown in Table 9.1 and 9.2.

Table 9.1: *Non–phosphorylated Nf stained in immunocytochemistry by the SMI clones. Characterisation of the antibody staining pattern in untreated and ALP, N.D. = not determined, N/A = not available/ data was not shown, GM = grey matter, WM = white matter, + = positive, - = negative, ↓ less intense after ALP treatment.*

Antibody	**Model**	**Not treated**	**Treated**
NfH^{SMI32}	ctrl	thick axons (+)[376–378]	thick axons (+)[†]
	ctrl	neuron/dendrites (++)[376–378]	neuron/dendrites (++)
NfH^{SMI32}	cell culture	vulnerable GABAergic axons (+++) [126]	N.D.
NfH^{SMI32}	MS	demyelinated axons (+++)[398]	N/A
NfH^{SMI32}	MS	axonal ovoids (+++)[398]	N/A
NfH^{SMI32}	AD	plaques (+)[387]	plaques +++
NfH^{SMI32}	AD	dystrophic neurons (+)[386]	++ [‡ §]
NfH^{SMI33}	AD	data not shown[386]	N/A
NfH^{SMI33}	MND	Spine: ctrl > ALS[246]	staining ↓↓[¶]
NfH^{SMI33}	AD	GM ++: AD = CTRL[73]	N.D.
NfH^{SMI33}	AD	WM +: AD = CTRL[73]	N.D.
NfH^{SMI33}	AD	pyramidal neurons, no NFT +++: AD <<< CTRL[73]	N.D.
NfH^{SMI33}	AD	pyramidal neurons, with NFT +: AD = CTRL[73]	N.D.

[†]Alkaline phosphatase treatment: 43μL calf intestinal alkaline phosphatase (type VII, Sigma) per mL in 0.1 M Tris–HCl, pH 8.0, 0.01 M phenylmethylsulfonyl fluoride, at 32°C for 18 hours.

[‡]NfH was also detectable in plaques which did not stain for tau/PHF.

[§]Alkaline phosphatase treatment: 400 μg/mL calf intestinal alkaline phosphatase (type VII, Sigma) in 0.1 M Tris–HCl, pH 8.0, at 37°C for 1.5–2 hours.

[¶]Alkaline phosphatase treatment: 400 μg/mL calf intestinal alkaline phosphatase (type VII, Sigma) in 0.1 M Tris–HCl,0.01 M phenylmethylsulfonylfluoride, pH 8.0, at 32°C for 2.5 hours. Similar results were found for pretreatment with trypsin (GIBCO), 400 μg/mL in 0.05 M Tris–HCL, 0.3 M sodium chloride, 0.02 M CaCl, pH 7.6, 37°C for 10 minutes.

Table 9.2: *Phosphorylated Nf stained in immunocytochemistry by SMI clones. Characterisation of the antibody staining pattern in untreated and ALP treated samples.*

Antibody	**Model**	**Not treated**	**Treated**
NfH^{SMI31}	MND	Brain: ctrl > ALS[246]	staining ↓↓
NfH^{SMI31}	AD	GM +: AD = CTRL[73]	N.D.
NfH^{SMI31}	AD	WM +++: AD = CTRL[73]	N.D.
NfH^{SMI31}	AD	pyramidal neurons, no NFT —: AD = CTRL[73]	N.D.
NfH^{SMI31}	AD	pyramidal neurons, with NFT —: AD = CTRL[73]	N.D.
NfH^{SMI31}	AD	data not shown[387]	N/A
NfH^{SMI31}	AD	(+)[386]	N/A
NfH^{SMI34}	ctrl	thick axons (+++)[376–378]	staining abolished
		thin axons (++)[376–378]	staining abolished
		basket cell dendrites (+)	staining abolished
NfH^{SMI34}	AD	GM ±: AD = CTRL[73]	N.D.
NfH^{SMI34}	AD	WM ±: AD = CTRL[73]	N.D.
NfH^{SMI34}	AD	pyramidal neurons, no NFT —: AD = CTRL[73]	N.D.
NfH^{SMI34}	AD	pyramidal neurons, with NFT +++: AD >>> CTRL[73]	N.D.
NfH^{SMI34}	MND	Spine: ctrl = ALS[246]	staining ↓↓
NfH^{SMI34}	MND	Brain: ctrl >> ALS[246]	staining ↓↓
NfH^{SMI35}	MND	Brain: ALS >>> CTRL[246]	staining ↓↓
NfH^{SMI35}	ctrl	thick axons (++)[376–378]	staining reduced
NfH^{SMI35}	ctrl	thin axons (+++)[376–378]	staining reduced
NfH^{SMI35}	ctrl	neuron/dendrites (+/—)	staining abolished
NfH^{SMI35}	AD	GM +: AD = CTRL[73]	N.D.
NfH^{SMI35}	AD	WM ++: AD << CTRL[73]	N.D.
NfH^{SMI35}	AD	pyramidal neurons, no NFT —: AD = CTRL[73]	N.D.
NfH^{SMI35}	AD	pyramidal neurons, with NFT ++: AD >> CTRL[73]	N.D.
NfH^{SMI310}	ALS	inconsistent results[246]	staining ↓↓
	AD	intraneuronal tangles (++)[379, 446]	staining abolished
NfH–P*	stroke	early neuronal damage ++[145]	N.D.

*The antibodies NfH^{SMI35}, NfH^{SMI34}, NfH^{SMI31} were used, but the authors did not specify in the results section which antibody stained for which condition.

Table 9.3: *Neurofilament antibodies other than then the SMI clones used for immunocytochemistry.*

Antibody	**Model**	**Not treated**	**Treated**
NfH^{N4142*}	AD	data not shown[387]	N/A
NfH^{RT9717}	nerve injury	+++: neurons with crushed nerves >>> CTRL neurons[281]	N.D.
NfH^{RT9717}	AD	Cerebellum +[144]	staining ↓ [†]
NfH^{RT9717}	AD	Hippocampus +[144]	staining ↓↓
NfH^{RT9717}	AD	Hippocampus NFT +[144]	staining ↓
NfH^{BF1017}	AD	Cerebellum +[144]	staining ↓
NfH^{BF1017}	AD	Hippocampus +[144]	staining ↓
NfH^{BF1017}	AD	Hippocampus NFT +[144]	+
NfH^{BF14717}	AD	Cerebellum +[144]	staining ↓
NfH^{BF14717}	AD	Hippocampus +[144]	staining ↓↓
NfH^{BF14717}	AD	Hippocampus NFT —[144]	staining —
NfH^{1D285}	CJD	swollen neurons: +[284]	— [‡]
NfH–P [§]	WHD	early damage in LMN ++[226]	N.D.
NfH$^{mab1.1.123}$	AD	AD +, CTRL: —[389]	N.D.
NfH^{MAB14717}	tractotomy	affected neurons: +[248]	N.D.

Glial axonal interactions There is emerging evidence of overlap between axonal and glial pathology. The secondary aim of this study was to investigate the relation of axonal and glial markers. This was done within different types of lesions. On basis of the results on CREAE model (chapter 8) it was hypothesised that in chronic plaques, correlations similar to that found for the atrophic CREAE spinal cord should be found, i.e. low NfH and high GFAP levels. However in acute lesions the relation between glial and

*Sigma, rabbit polyclonal anti NfH.

†Alkaline phosphatase treatment: 100μL calf intestinal alkaline phosphatase (Supplier not given) in 0.1 M Tris–HCl, pH 8.0, at 37°C for 2.5 hours.

‡Alkaline phosphatase treatment: 20 IU/mL alkaline phosphatase (Supplier not given) in 0.1 M Tris–HCl, 5 mM phenylmethylsulfonyl fluoride pH 8.0, at room temperature for 24 hours.

§The author did not specify which one of the SMI anti–phosphoneurofilament antibodies he used.

axonal markers might be very different. Trapp *et al.* (1988) found about an 660–fold increase of axonal transections in active lesions (11236±2775) versus normal–appearing white matter (17±28). Because the axonal ovoids indicates the site of transection it was hypothesised for the present study that there is at least one NfH phosphoform which should be increased in active lesions. In addition one would expect that in active lesions the relation of NfH phosphoforms to glial markers would be different to the relation in chronic lesions or NAWM.

9.2 Methods

9.2.1 Brain tissue preparation

Unfixed post–mortem brain tissue was obtained from 12 clinically and histologically definite MS patients and 8 controls. These specimens were kindly provided by the MS Society Tissue Bank at the Institute of Neurology. All MS cases where classified as secondary progressive MS with significant disability (EDSS 9–10).[138] The mean age of the MS patients was 48.6 (29–65) years, with a mean disease duration of 19.5 (7–43) years and a post-mortem interval of 30.2 (9–52) hours. The mean age in the control group was 56.7 (37–71) years and the mean post-mortem interval 26.9 (1–40) hours. The brain tissue was histologically classified into normal appearing white matter (NAWM), acute lesions (AL), subacute lesions (SAL), chronic lesions (CL) and normal appearing grey matter (NAGM) from MS patients using previously published criteria.[289] Normal control grey (NCGM) and white matter

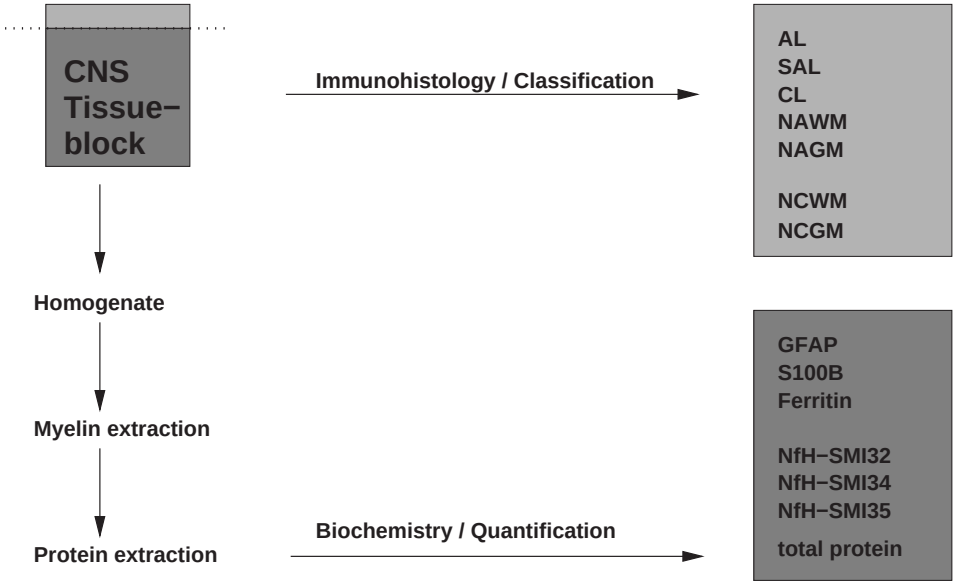

Figure 9.1: *Sample preparation: the top layer of a frozen CNS tissue block was analysed immunohistologically in order to classify the MS lesion. The adjacent tissue was homogenised and analysed biochemically.*

(NCWM) were obtained from control subjects without neurological diseases. Adjacent pieces of each type of tissue were excised and homogenised for BSP analysis as outlined in Figure 9.1.

Immunocytochemistry: For immunocytochemistry, sections were immunoperoxidase stained with antibodies directed against GFAP,[288] 14E for oligodendrocytes and reactive astrocytes.[290] Cryostat sections were fixed in methanol (-20°C, 10 min), incubated with primary antibody overnight (4°C) and stained using a three-step peroxidase method.

Protein extraction Snap-frozen blocks of brain tissue from MS and control cases of between 0.5 and 1g wet weight, were cut and re-suspended at 1:5 g/mL in Tris-HCl buffer (100mM Tris, pH 8.1 with 1% Triton X-100). Samples were homogenised on ice by sonication, triturated 3 times through 19 and 21 gauge needles and spun at 20,000g. In order to separate myelin protein, di–iso–propyl ether (1:5,000) was added. After extensive mixing the sample was spun at 20,000 g. The supernatant was covered by a myelin layer. A needle was put through the myelin layer and the supernatant drawn up into a 1 mL syringe. A protease inhibitor cocktail containing *AEBSF* for inhibition of trypsin and chymotrypsin, *aprotinine* for inhibition of trypsin, chymotrypsin, plasmin, trypsinogen, urokinase and kallikrein, *leupeptin* for inhibition of calpain, trypsin, papain and cathepsin B, *bstatin* for inhibition of aminopeptidases, *pepstatin A* for inhibition of acid proteases and *E–64* for inhibition of cysteine proteases (Sigma, P 8340) was added in a dilution 1:100 to supernatant. After dilution into aliquots of 1:1,1000, 1:5,000, 1:10,000 and 1:100,000 the samples were stored at -70 °C.

Assays S100B (page 146), ferritin (page 147), GFAP (page 121) and total protein (page 149) were measured as described.

The NfH phosphoforms NfH^{SMI32}, NfH^{SMI35} and NfH^{SMI34} were measured as described (Figures 4.1 to 4.9 on page 85–93).

Statistical analysis Data were managed and analysed as described (Chapter 7, page 151). Because of the small sample size no Gaussian curve with valid 95%CI could be calculated. Therefor the cut–off for categorical data analysis (Fisher's exact test) was set to the 100% cumulative frequency of the group with the lowest values.

9.3 Results

9.3.1 White matter

Axonal markers The median NfH^{SMI34} and NfH^{SMI35} levels were about 2–4 fold elevated in AL when compared to NCWM and NAWM (Table 9.4). For NfH^{SMI34} the lowest values for all NfH phosphoforms were found in CL (Table 9.4, see top–range). Therefore the 100% cumulative frequency of for NfH^{SMI34} was taken as the cut–off (Figure 9.2 A, dotted line). Significantly more samples taken from AL had NfH^{SMI34} levels above the cut–off (Figure 9.2 A) if compared to CL ($p<0.001$) or NAWM ($p<0.05$). Although median NfH^{SMI34} levels appeared to be about 3–fold higher in NCWM when compared to NAWM, this did not reach statistical significance on a rigorous categorical level.

NfH^{SMI35} levels were 3–fold higher in AL if compared to CL, NAWM or NCWM. The cut–off was determined as above. Significantly more samples taken from AL had NfH^{SMI35} levels above the cut–off (Figure 9.2 B) when compared to CL ($p<0.001$), NAWM ($p<0.001$) or NCWM ($p<0.001$). The median NfH^{SMI35} levels were about 2–fold higher in SAL if compared to CL.

A significantly higher number of SAL samples had NfH^{SMI35} levels above the cut–off when compared to CL ($p<0.05$). There was no difference in NfH^{SMI35} levels between NCWM and NAWM (Table 9.4).

Levels of NfH^{SMI32} were generally low and no statistically significant difference was found between the lesion types.

Table 9.4: *Levels of neurofilament phosphoforms in ng/mg protein in homogenised brain tissue. The median (range, number) for normal control white matter (NCWM), normal–appearing white matter (NAWM), acute lesions (AL), subacute lesions (SAL), chronic lesions (CL) and values for grey matter from control and MS tissue are shown. Level of significance are indicated as revealed by Fisher's exact test comparing proportions of samples.*

ng/mg protein	**White matter**				
	NCWM	NAWM	AL	SAL	CL
NfH^{SMI32}	1.72(0.17–14.70),6	2.08(0.00–115.81),6	2.03(0.12–5.93),6	3.66(0.80–161.637),6	1.01(0.33–2.17),6
NfH^{SMI34}	68.20(2.44–213.13),6	24.05(1.74–325.99),6	287.6(77.9–548.7),6	91.64(21.67–438.18),6	29.66(3.78–80.20),6
		|——— **p < 0.05** ———|		|——— **p < 0.001** ———|	
NfH^{SMI35}	54.72(13.60–101.82),6	51.54(6.44–120.53),6	128.6(89.4–575.4),6	87.92(2.10–289.58),6	55.22(17.33–72.52),6
		|——— **p < 0.001** ———|		|——— **p < 0.001** ———|	
			|——— **p < 0.05** ———|		

μg/mg protein	**Grey matter**	
	CTRL	MS
NfH^{SMI32}	1.78(0.50–13.52),6	2.03(0.10–4.43),5
NfH^{SMI34}	4.18(0.06–31.44),6	2.41(1.09–6.44),6
NfH^{SMI35}	11.53(1.02–30.34),6	20.77(6.97–33.83),6

Glial markers Each glial marker had about 2 to 3–fold higher median levels in MS lesion if compared to control brain tissue. For S100B and ferritin this was also true comparing NAWM and NCWM (Table 9.5). Note that all values are given as μg/mg protein as opposed to the NfH phosphoforms which were in ng/mg protein. The top range for S100B was lowest in SAL and for ferritin in NCWM, which have therefore been taken as the cut–off for subsequent categorical data analysis.

S100B levels were approximately 2–fold higher in acute plaques than in SAL (Table 9.5). Significantly more AL than SAL had S100B levels above the cut–off ($p<0.001$, Figure 9.4A).

Ferritin levels were higher in all MS lesions types compared to controls (Table 9.5). A significantly higher proportion of samples from NAWM had ferritin levels above the cut–off when compared to control WM tissue ($p<0.05$, Figure 9.4 B).

Table 9.5: *Levels of S100B, GFAP and ferritin in μg/mg protein in homogenised brain tissue. The median (range, number) values for normal control white matter (NCWM), normal–appearing white matter (NAWM), acute lesions (AL), subacute lesions (SAL), chronic lesions (CL) and values for grey matter from control and MS tissue are shown. Level of significance are indicated as revealed by Fisher's exact test comparing proportions of samples.*

μg/mg protein	**White matter**				
	NCWM	NAWM	AL	SAL	CL
S100B	2.4(1.5-5.6), 5	4.8(2.6-7.1), 5	5.2(4.0-6.4), 6	3.4(2.4-4.1), 4	3.9(2.0-8.0), 7
			|—— **p < 0.001** ——|		
GFAP	1.7(1.1-5.9), 5	1.4(0-6.0), 5	5.3(2.6-6.7), 6	3.9(2.5-5.4), 4	4.0(0.4-11.4), 7
Ferritin	3.6(2.5-4.7), 5	7.0(4.8-9.4), 5	5.2(3.7-11.2), 6	5.1(3.9-7.0), 4	5.7(4.0-13.2), 7
	|—— **p < 0.05** ——|				

μg/mg protein	**Grey matter**	
	CTRL	MS
S100B	1.1(0.9-1.5, 4)	2.2(1.6-3.5, 6)
	|—— **p < 0.001** ——————|	
GFAP	0.8(0.5-1.2), 4	2.4(0.2-5.0), 6
	|—— **p < 0.05** ——————|	
Ferritin	3.1(1.3-4.1), 4	4.8(2.5-12.3), 6

9.3.2 Grey matter

GFAP and S100B were elevated 2- to 3–fold in NAGM compared to NCGM (Figure 9.6, Table 9.5). Significantly more NAGM samples had S100B and GFAP levels above the cut–off when compared to NCGM ($p<0.001$, $p<0.05$, respectively). Ferritin levels were higher in NAGM than in control GM. There were however no differences between NAGM versus NAWM or NCGM versus NCWM ferritin levels.

NfH^{SMI34} levels appeared slightly elevated in NCGM if compared to NAGM, whilst the NfH^{SMI35} levels were lower in NCGM (Table 9.4). How-

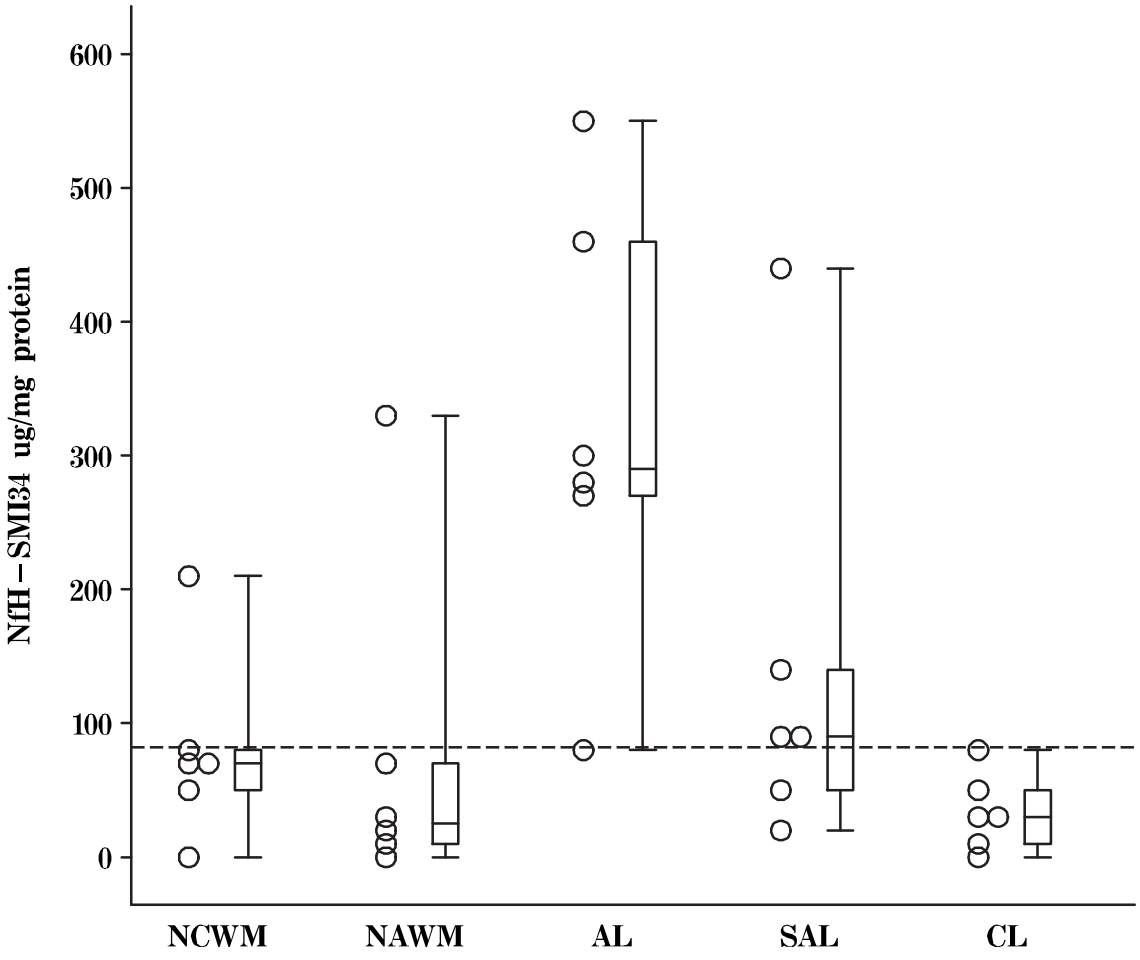

Figure 9.2: *White matter NfH^{SMI34} levels. Significantly more samples from AL had NfH^{SMI34} levels above the cut–off (79.9 ng/mg protein, dotted line) when compared to NAWM or CL.*

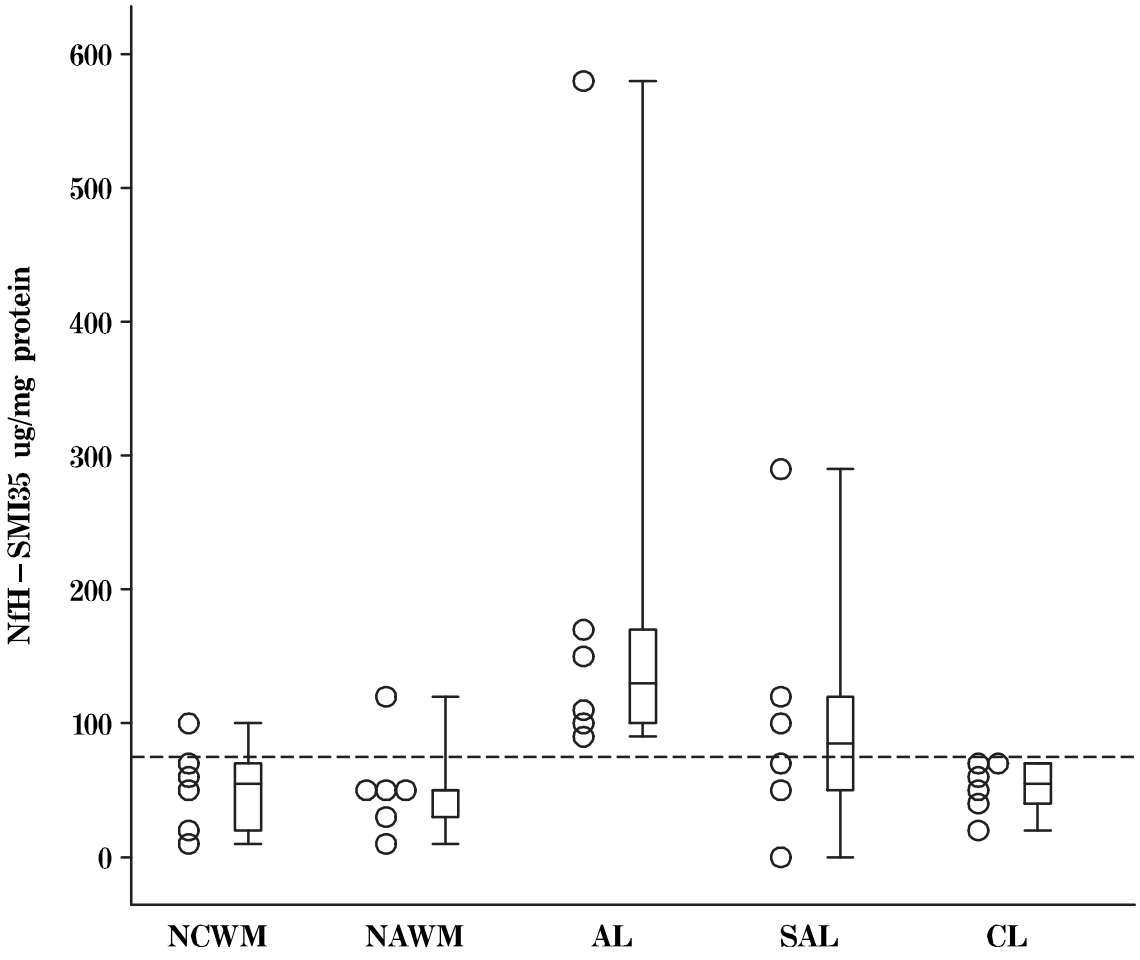

Figure 9.3: *White matter NfH^{SMI35} levels. Significantly more samples from AL had NfH^{SMI35} levels above the cut–off (75.5 ng/mg protein, dotted line) when compared to NCWM, NAWM or CL.*

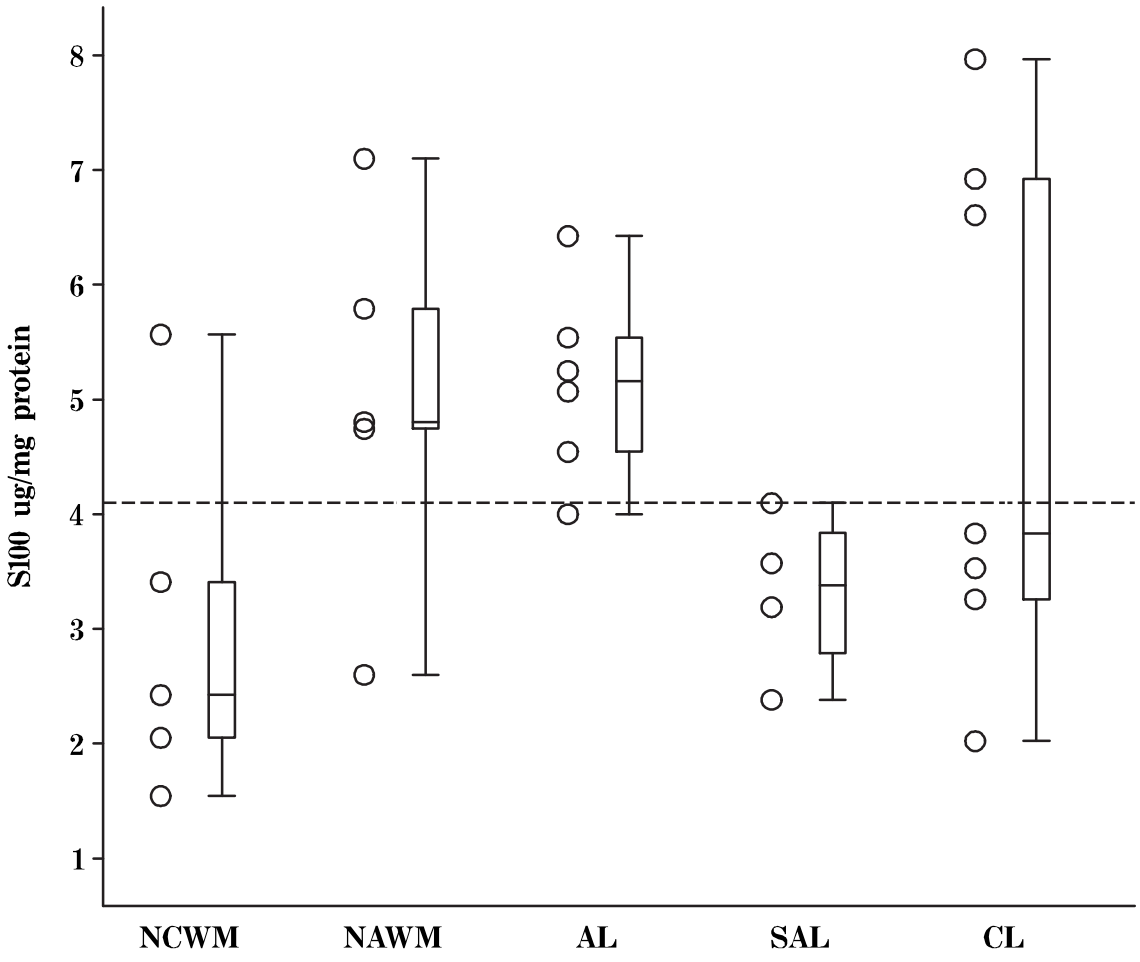

Figure 9.4: *White matter S100B levels. Significantly more samples from acute plaques have S100B levels above the cut–off (4.1 μg/mg protein, dotted line) than subacute plaques ($p<0.001$). (B) White matter ferritin levels.*

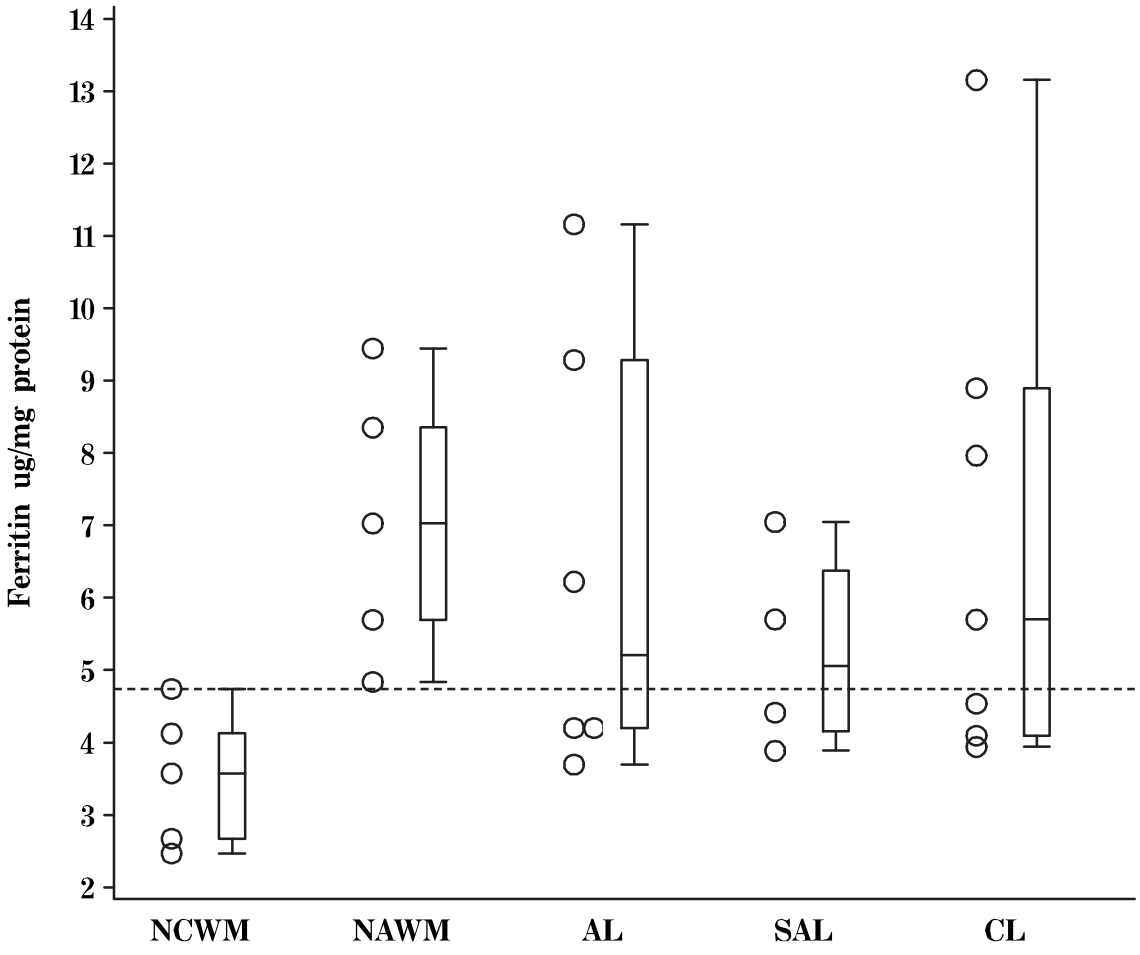

Figure 9.5: *White matter ferritin levels. Significantly more samples from NAWM had ferritin levels above the cut–off (4.7 μg/mg protein, dotted line) compared to control white matter ($p<0.001$).*

ever this did not reach statistical significance. There were no differences in NfH^{SMI32} levels between NAGM and NCGM. One sample had to be excluded from the analysis of NfH^{SMI32} because of contamination.

9.3.3 Relation of BSP

The correlation anaylsis was motivated by the results of Chapter 8. As suggested by the correlations found in CREAE (Figure 8.7 on page 169) S100B correlated with both phosphorylated NfH phosphoforms (Figure 9.8 and 9.9). For the correlation of S100B with NfH^{SMI35} (R=0.55, p<0.001) two outliers with NfH^{SMI35} levels above 200 ng/mg protein were observed. Removal of these outliers did improve the correlation to R=0.62, p<0.001 (dotted line in Figure 9.9).

The same outliers affected 3 further correlations: NfH^{SMI35} with NfH^{SMI34} (Figure 9.12 R=0.64, p<0.001) which was reduced to R=0.6, p<0.001 after removal (dotted line in Figure 9.12). The correlation of NfH^{SMI35} with GFAP (R=0.43, p<0.05, Figure 9.14), which improved to R=0.45, p<0.01 after removal (dotted line in Figure 9.14). The correlation of NfH^{SMI35} with ferritin (R=0.39, p<0.05, Figure 9.16), which was reduced to R=0.36, p<0.05 after removal (dotted line in Figure 9.16).

The strong correlation between ferritin and phosphorylated NfH (R=0.92, Figure 8.7 A) observed in the CREAE model was weaker in this human study, with R=0.39, p<0.05 for ferritin with NfH^{SMI35} and R=0.33, p<0.05 for ferritin with NfH^{SMI34} .

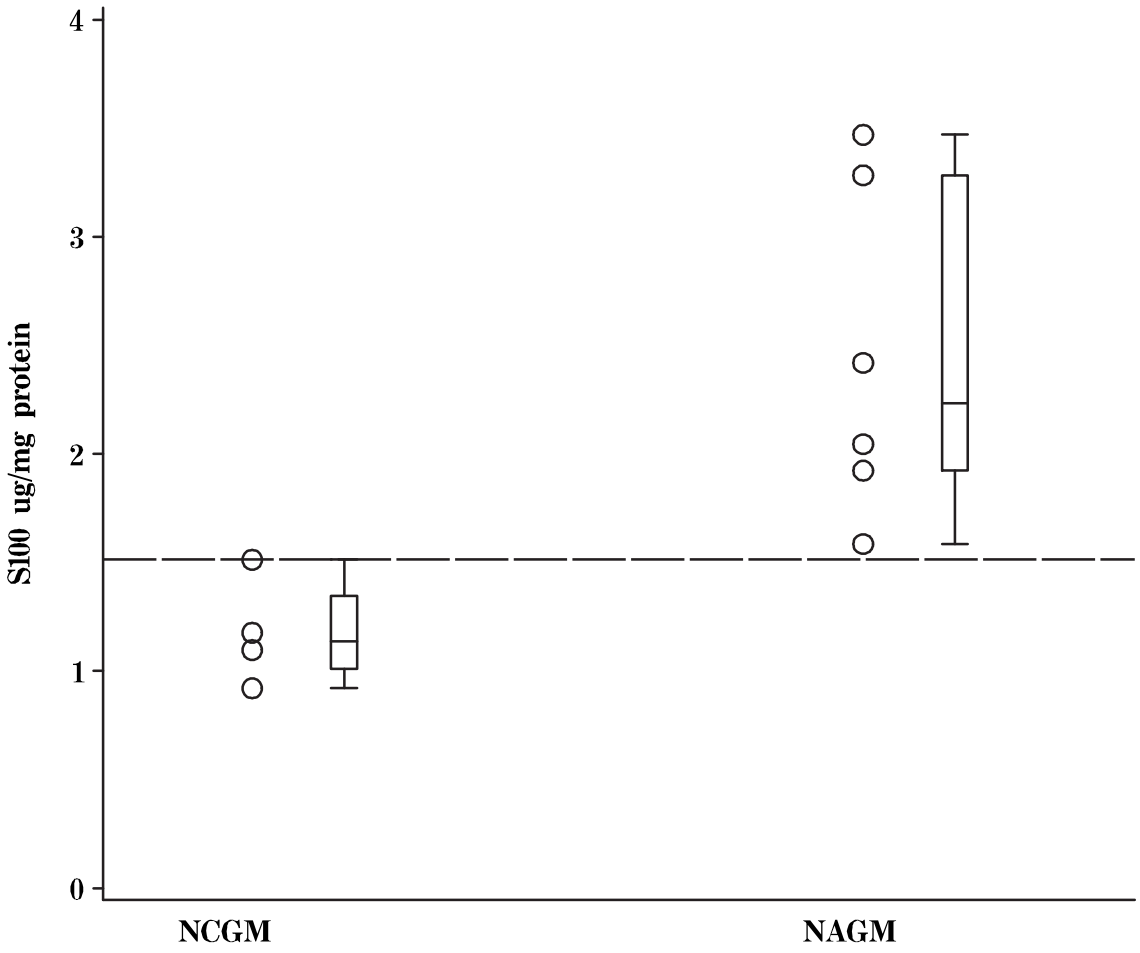

Figure 9.6: *Grey matter S100B: comparing levels of S100B in cortical MS versus controls a 2-fold increase was observed. Significantly more cortical samples from MS than controls had S100B levels above the cut–off (1.5 μg/mg protein, dotted line, $p<0.001$).*

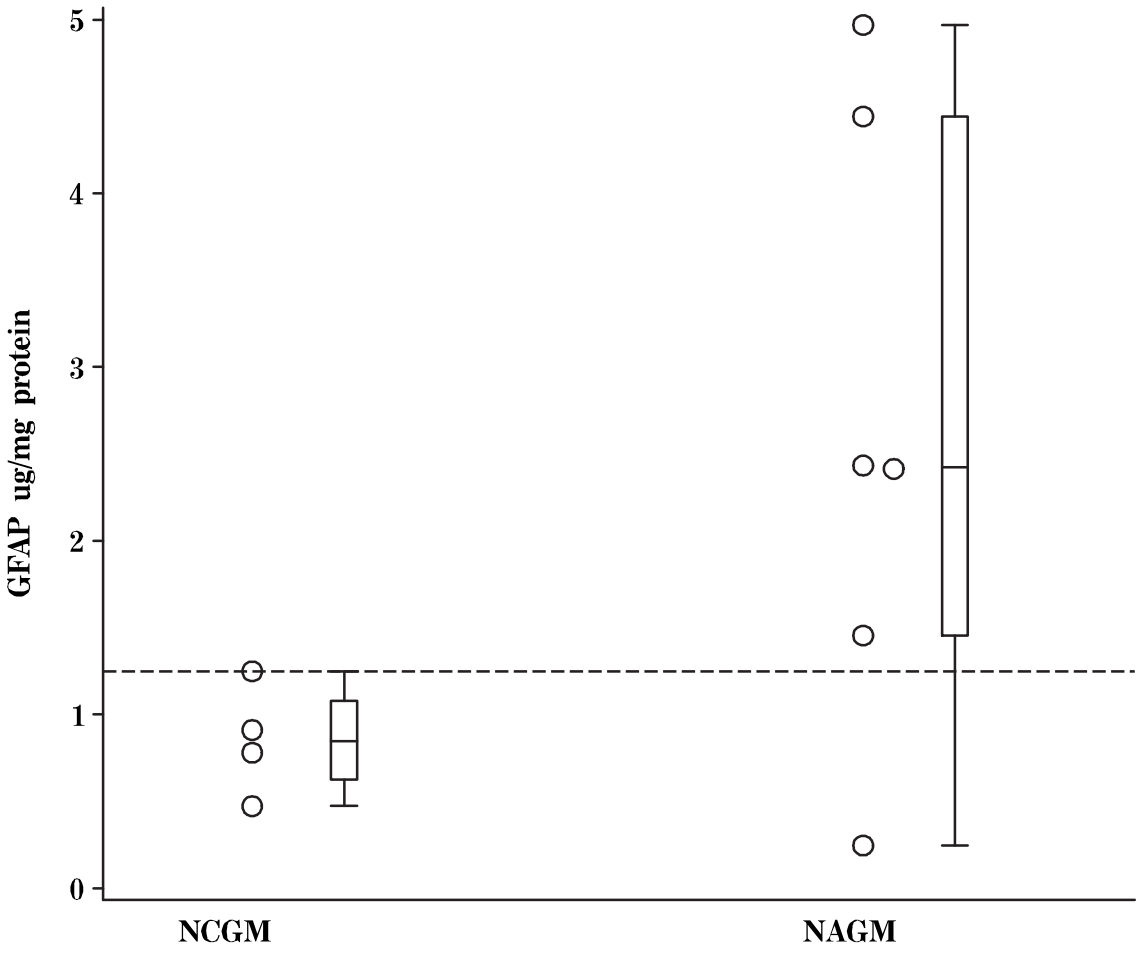

Figure 9.7: *Grey matter GFAP: comparing levels of GFAP in cortical MS versus controls a 3-fold increase is observed. Significantly more cortical samples from MS than controls had GFAP levels above the cut–off (1.2 μg/mg protein, dotted line, $p<0.05$).*

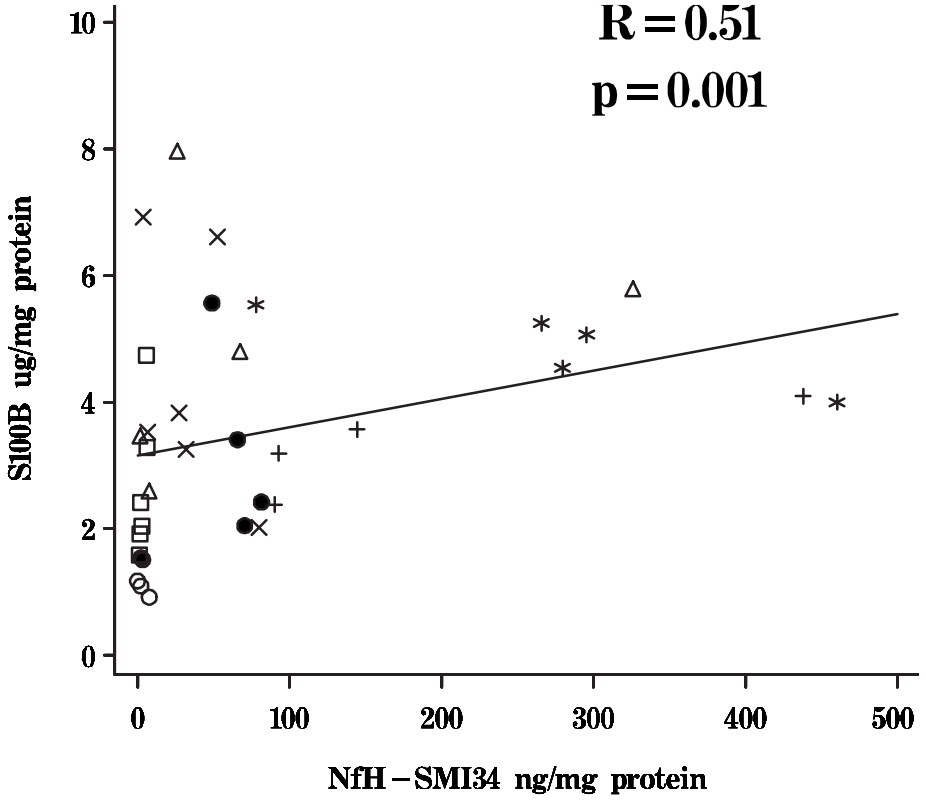

Figure 9.8: *Correlation of S100B (μg/mg protein) with NfH^{SMI34} (ng/mg protein). NCWM = $\bullet$, NCGM = $\circ$, NAWM = $\triangle$, NAGM = $\square$, AL = $*$, SAL = $+$, CL = $\times$.*

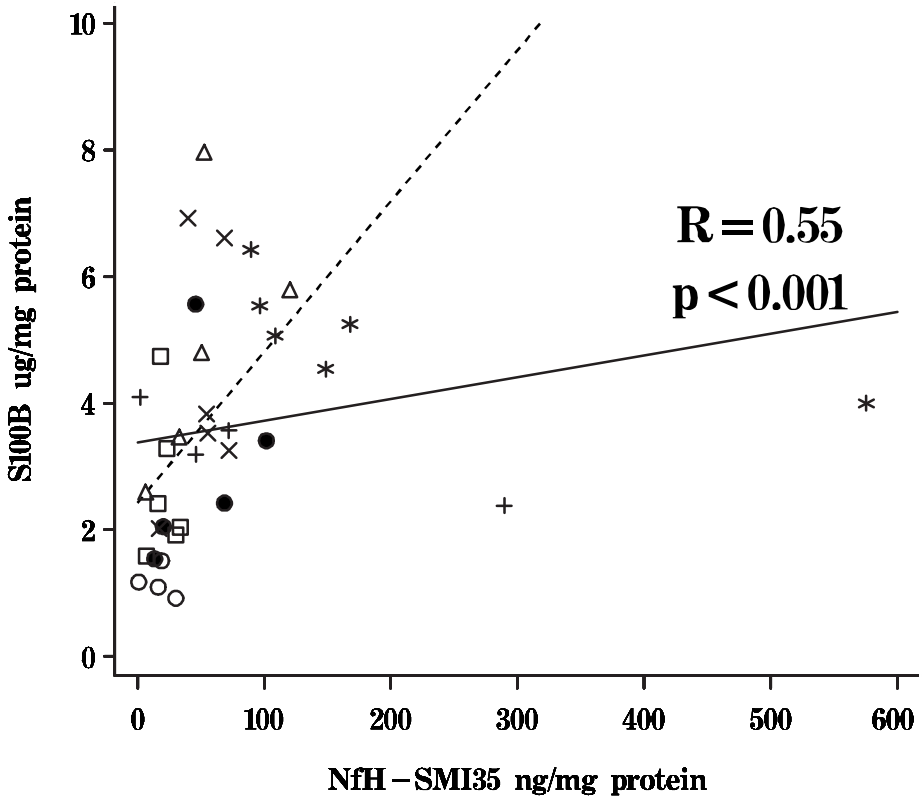

Figure 9.9: *Correlation of S100B (μg/mg protein) with NfH^{SMI35} (ng/mg protein). NCWM = $\bullet$, NCGM = $\circ$, NAWM = $\triangle$, NAGM = $\square$, AL = $*$, SAL = $+$, CL = $\times$. The straight line shows the regression over all data. The dotted line represents the correlation after removal of the outliers (see text).*

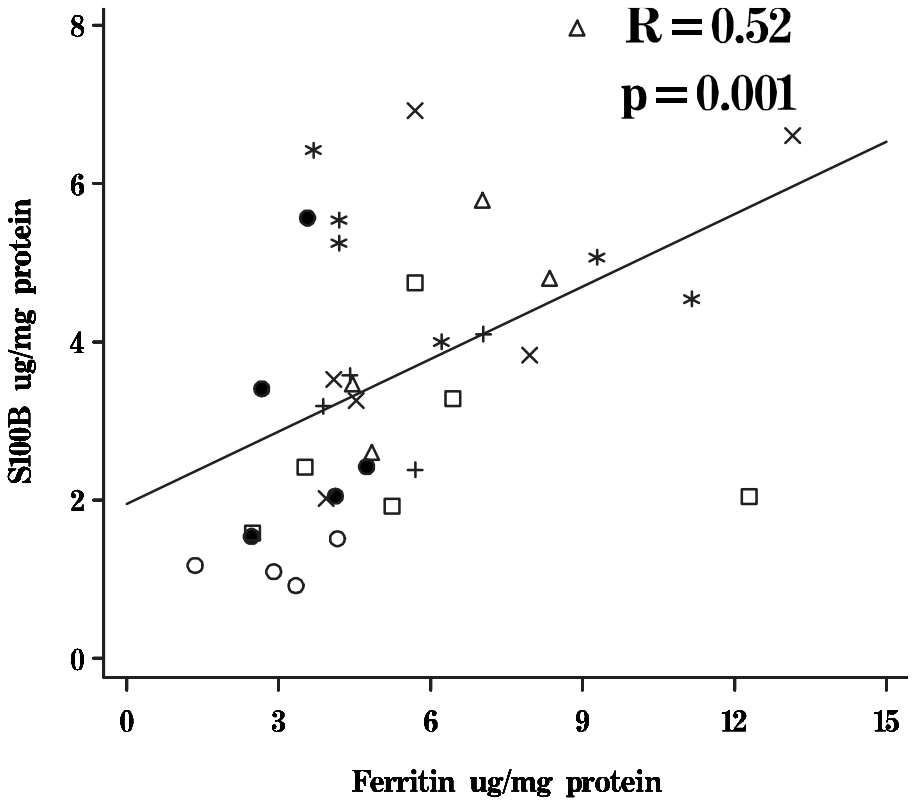

Figure 9.10: *Correlation of S100B (µg/mg protein) with Ferritin (µg/mg protein). NCWM = •, NCGM = ∘, NAWM = △, NAGM = □, AL = ∗, SAL = +, CL = ×.*

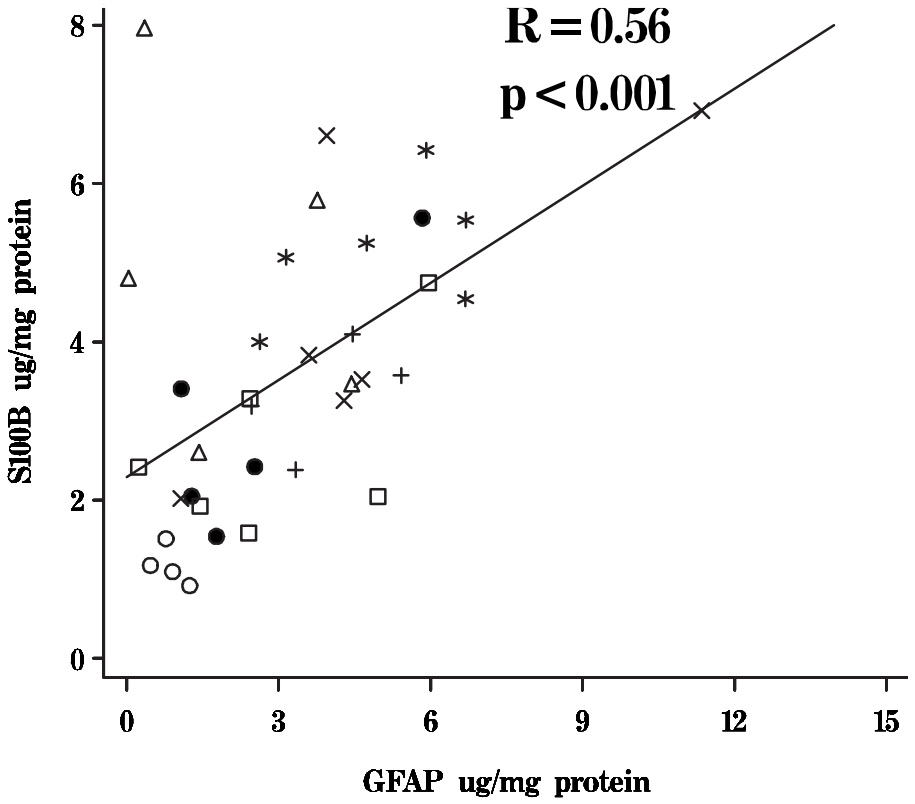

Figure 9.11: *Correlation of S100B (µg/mg protein) with GFAP (µg/mg protein). NCWM = •, NCGM = ∘, NAWM = △, NAGM = □, AL = ∗, SAL = +, CL = ×.*

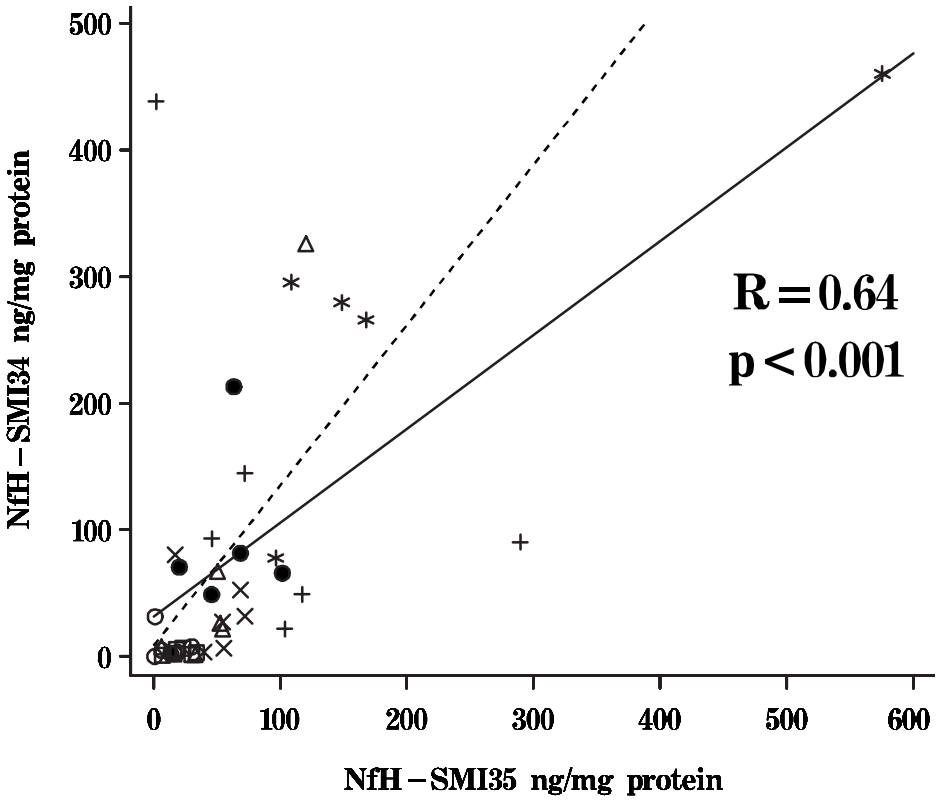

Figure 9.12: *Correlation of NfH^{SMI34} (ng/mg protein) with NfH^{SMI35} (ng/mg protein). NCWM = •, NCGM = ∘, NAWM = △, NAGM = □, AL = ∗, SAL = +, CL = ×. The straight line shows the regression over all data. The dotted line represents the correlation after removal of the outliers (see text).*

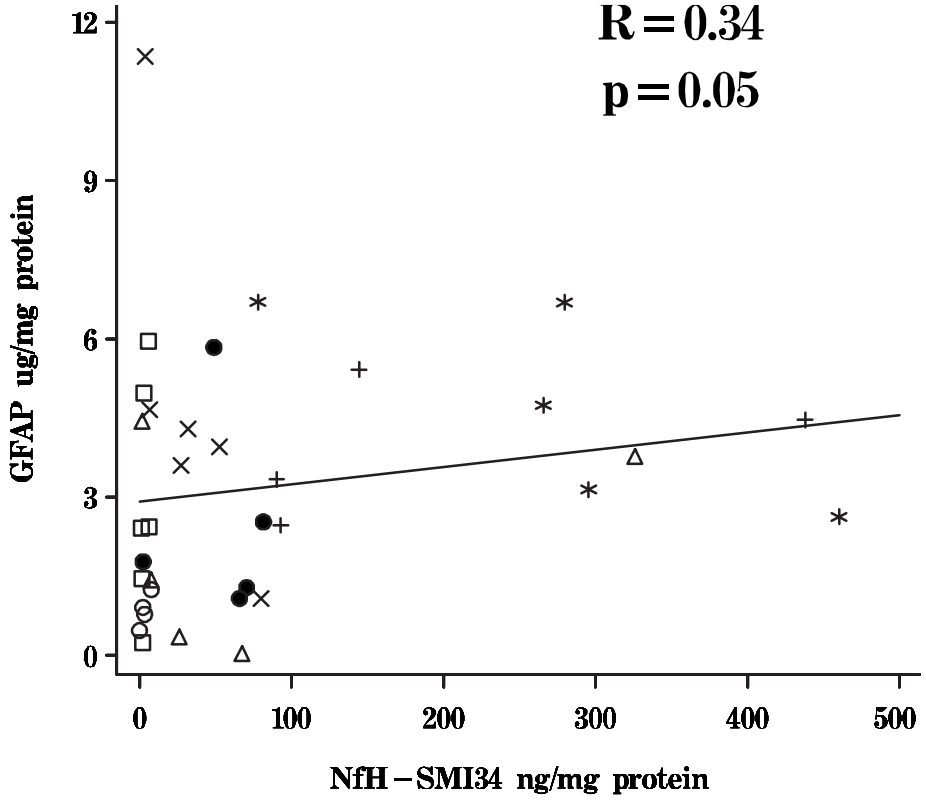

Figure 9.13: *Correlation of GFAP (μg/mg protein) with NfH^{SMI34} (ng/mg protein). NCWM = $\bullet$, NCGM = $\circ$, NAWM = $\triangle$, NAGM = $\square$, AL = $*$, SAL = $+$, CL = $\times$.*

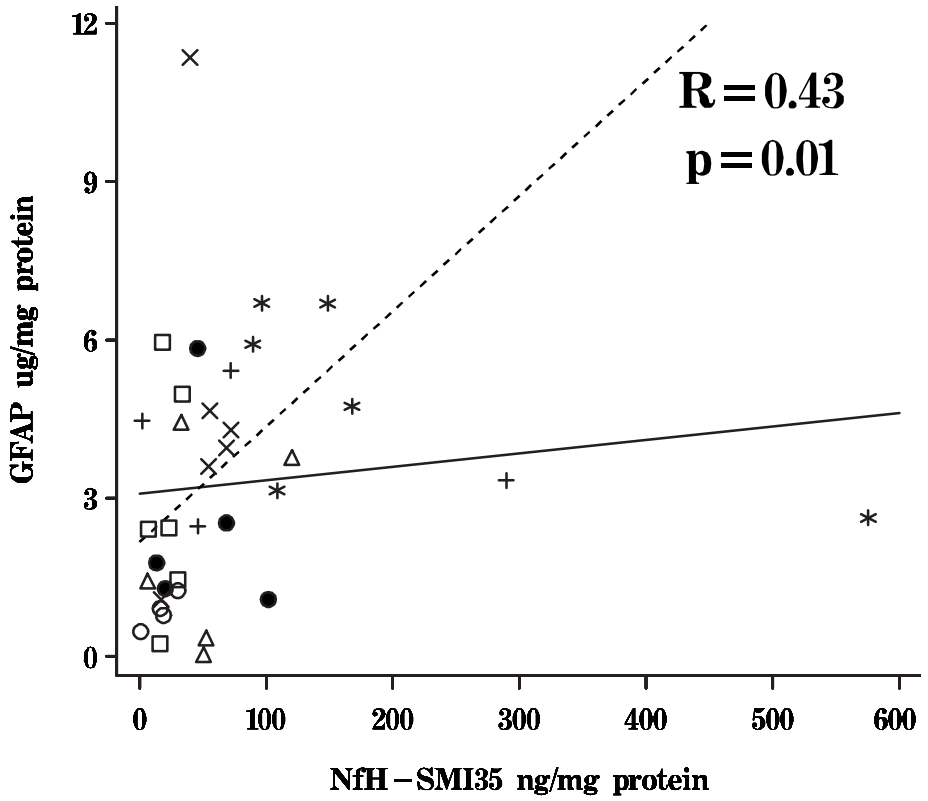

Figure 9.14: *Correlation of GFAP (μg/mg protein) with NfH^{SMI35} (ng/mg protein). NCWM = $\bullet$, NCGM = $\circ$, NAWM = $\triangle$, NAGM = $\square$, AL = $*$, SAL = $+$, CL = $\times$. The straight line shows the regression over all data. The dotted line represents the correlation after removal of the outliers (see text).*

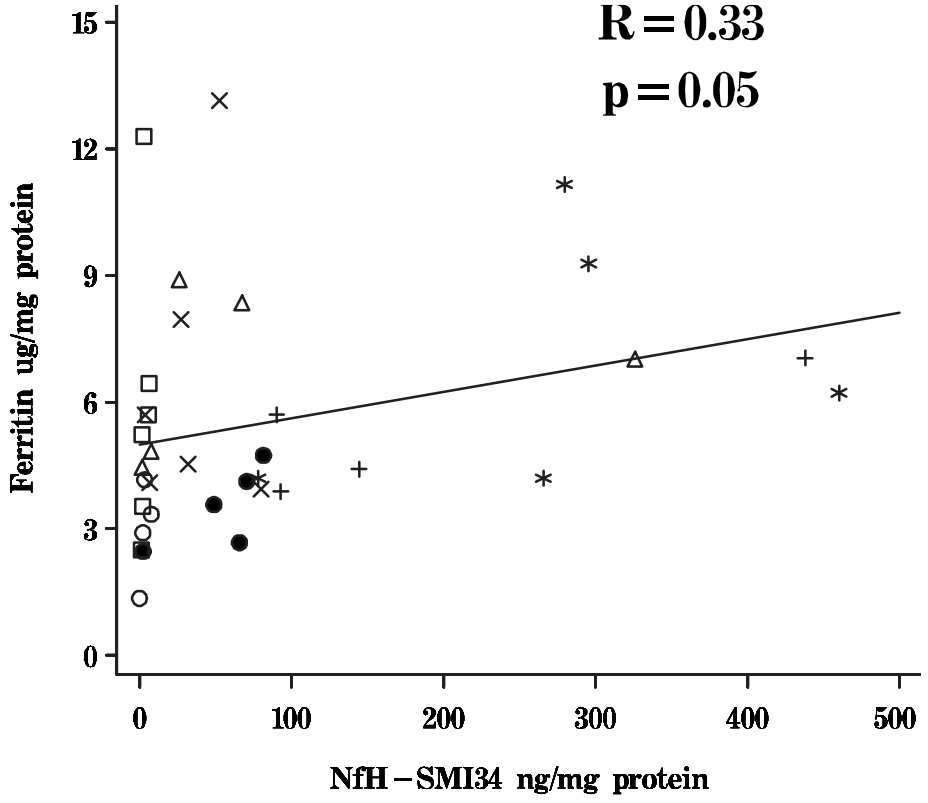

Figure 9.15: *Correlation of Ferritin (µg/mg protein) with NfH^{SMI34} (ng/mg protein). NCWM = •, NCGM = ∘, NAWM = △, NAGM = □, AL = ∗, SAL = +, CL = ×.*

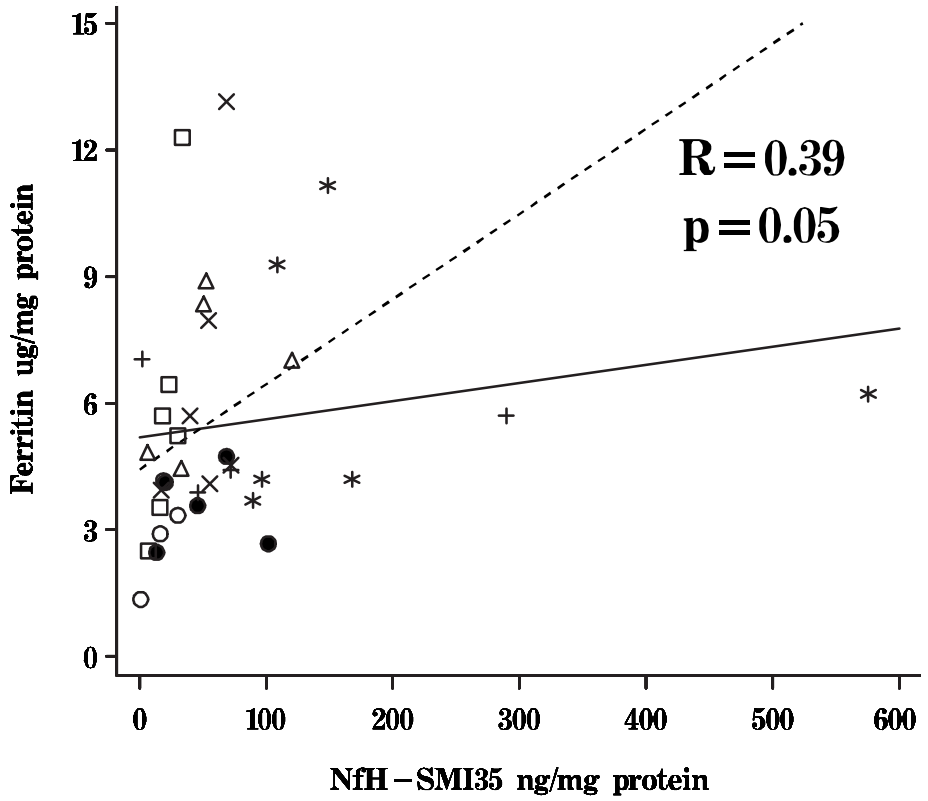

Figure 9.16: *Correlation of Ferritin (μg/mg protein) with NfH^{SMI35} (ng/mg protein). NCWM = $\bullet$, NCGM = $\circ$, NAWM = $\triangle$, NAGM = $\square$, AL = $*$, SAL = $+$, CL = $\times$. The straight line shows the regression over all data. The dotted line represents the correlation after removal of the outliers (see text).*

From the CREAE study no correlation between GFAP and S100B was expected (Figure 8.7 F). However, for the post–mortem study a good correlation between these proteins was found (Figure 9.11, R=0.56, p<0.001).

The positive correlation of S100B with ferritin (R=0.52, p<0.001) was consistent with the finding in CREAE (R=0.81, Figure 8.7 D). Also consistent with the CREAE study, no correlations were found between ferritin and GFAP.

9.4 Discussion

White matter The finding that two axonal markers (NfH^{SMI35} , NfH^{SMI34}) and one glial marker (S100B) were significantly increased in AL has to be regarded as the most important finding of this study because in patients this type of lesion is the most closely related to an "acute" clinical relapse. The relevance of these results is heightened by the significant correlation of S100B with both NfH phosphoforms (NfH^{SMI34} , NfH^{SMI35}) and of the latter two with each other.

The finding that S100B levels in SAL decreased to the range found for NCWM supports the notion that S100B is an "acute phase" protein. The decrease could partly be explained by the small molecular size (12 kDa), high solubility and rapid wash–out of the protein as suggested by studies from cardiovascular operations .[10,11,15,45,165,188,202,228,319,327,417,428,429]
In contrast NfH^{SMI34} and NfH^{SMI35} remained high in SAL. The longer per-

sistence in the tissue could also be due to the higher molecular weight (above 190 kDa) and the lower solubility of the protein. Therefore NfH^{SMI35} and NfH^{SMI34} could emerge as potential markers for acute to subacute axonal damage. It is of note that immunocytochemistry did not show an increase of either NfH^{SMI34} or NfH^{SMI35} staining in the core of AL, but at the lesion border. The high levels measured biochemically could thus represent either a high concentration of NfH^{SMI34} /NfH^{SMI35} from the AL borders and/or a higher concentration in the extracellular matrix. Certainly disintegration of the axonal membrane would cause release of axonal proteins into the extracellular space. The presence of damage–related extracellular NfH^{SMI35} or NfH^{SMI34} is a *sine qua non* for any attempt to measure either phosphoform in the CSF. Consistent with the findings that NfH^{SMI32} is highly susceptible to proteolysis, NfH^{SMI32} were substantially lower in all lesions. It is conceivable that for this reason no differences were found for NfH^{SMI32} between the lesion types.

Ferritin is consistently higher in MS than in control brain tissue and was significantly higher in MS NAWM compared to control WM. This suggests that ferritin is a sensitive but non–specific marker for microglial activity in NAWM. The correlation of ferritin with NfH^{SMI34} and NfH^{SMI35} is consistent with the model of Wallerian degeneration (Figure 1.2 on page 33). The bulk of axonal protein release occurs during the early and mature glial/macrophage response (Figure 1.2 C, D).

Grey matter The levels of all glial markers appear to be increased in NAGM. This was significant for S100B and GFAP. The involvement of GM in MS has been recognised for a long time.[30,247] One paper describes seven distinct lesion patterns,[189] which has been reduced to 3 major types by others.[305] Importantly Peterson *et al.* (2001) using immunocytochemistry, detected a significant activation of cortical astrocytes and microglia [305] which is consistent with the present results of a 2- to 3–fold increase in GFAP and S100B levels in NAGM.

Relation of BSP With 2 exceptions the findings of the post–mortem study were consistent with the findings for the CREAE model. In order to facilitate the comparsion between these two studies the Spearman correlation coeffiencents have been summarised in Table 9.6.

The positive correlation found for GFAP with NfH^{SMI35} (Figure 9.16 on page 202) was at first glance contradictory to the finding of a negative correlation for the same proteins in the CREAE study (Figure 8.7 C, on page 169). It appears however from Figure 8.7 C that the negative correlation is really due to the CREAE animals having lower NfH^{SMI35} levels then the control animals. For the CREAE animals alone a positive correlation is suggested by the scatter of the points. The post–hoc analysis revealed that this was significant ($R=0.79$, $p<0.05$). Whereas for the animal study the number of the CREAE to control mice was relative balanced, in the post–

mortem study 27 samples from MS patients outweighted the 9 samples from control brain tissue.

Table 9.6: *Correlations between BSP in the CREAE and human post–mortem study.*

BSP	**CREAE**	**Post-mortem**	**Consistent**
NfH^{SMI35} with S100B	0.83	0.55	yes
NfH^{SMI35} with GFAP	-0.54	0.43	no
NfH^{SMI35} with Ferritin	0.92	0.39	yes
Ferritin with S100B	0.81	0.52	yes
Ferritin with GFAP	N.S.	N.S.	yes
GFAP with S100B	N.S.	0.56	no

The situation is more complex for the comparison of S100B with GFAP. The post–hoc analysis for CREAE animals alone is not significant (R=0.55, p=0.16). Whilst the values for GFAP were spread out relatively wide in the CREAE mice (5.0–26.4 μg/mg protein) the scatter was narrower for the control mice (1.4–5.2 μg/mg protein, Table 8.1 on page 163). In the post–mortem study the correlation between S100B and GFAP was due to low values for GFAP and S100B in NAGM and NCWM which are contrasted by higher values in AL, SAL and NAGM (Figure 9.10 and 9.11). Again the distribution for GFAP in MS brain tissue is broad (0.1–11.4). In contrast, if one disregards one outlier for the NCWM with a GFAP level of about 5.9 μg/mg protein the distribution for GFAP in the control tissue is narrower, ranging from (0.9–2.8 μg/mg protein).

Taking all this together it appears that the findings for BSP in an animal study and in a human post–mortem study are highly consistent. However,

the strength of the correlations is weaker in the post-mortem study. This could possibly be due to the heterogeneity of the lesions, or to autoproteolysis during the variable post–mortem interval.

9.5 Conclusion

The results of this postmortem study provide evidence for NfH^{SMI35} and NfH^{SMI34} being practical markers for axonal damage in the acute and subacute phase of the disease. The probable accumulation in the extracellular matrix would allow for diffusion into the CSF, therefore providing a testable hypothesis for any CSF study.

The relation of the different NfH phosphoforms to NAWM versus AL and SAL suggests heterogeneity of axonal pathology in MS.

S100B could be associated with AL, whilst ferritin is generally elevated in MS white matter.

Chapter 10

Disease heterogeneity: Cross–sectional

10.1 Background

The concept of disease heterogeneity in MS has important prognostic and therapeutic implications. The clinical heterogeneity originates in the wide spectrum of disorders presenting with symptoms consistent with demyelination. This has been discussed in Chapter 1.1 and is briefly recapitulated in Table 10.1. Careful examination of MS plaques revealed distinct immunohistological patterns of demyelination (Table 1.1 on page 28).[112,238] The profile of glial and axonal markers in different MS lesions (Chapter 9) further supported this notion. Heterogeneity of lesions was also apparent in magnetic resonance imaging (MRI) and magnetic resonance spectroscopy (MRS) studies.[50,217] Furthermore, treatment response is not homogeneous.[91,298] It is probable that the pathological features associated with demyelination are not exclusive, but occur simultaneously at different phases of the disease. These include inflammation, glial reaction and axonal injury. The balance of

pathological processes might partly account for the clinical phenotype and influence treatment response.

Quantification of CSF levels of biomarkers for reactive astrocytosis (Section 2.3, page 62), microglial activation (Section 2.4, page 66), astrogliosis (Section 2.2, page 59) and axonal injury (Section 2.1, page 50) could potentially be relevant for understanding *in vivo* factors contributing to disease heterogeneity in MS.

However the design of previous studies did not allow sufficiently detailed analysis of both disease subtype and disability in relation to CSF levels of glial[171,172,222,251,270,336] and axonal markers.[172,212,242,278,353] Consequently most authors had not shown any statistically significant difference between clinical subgroups . A detailed summary has been presented in Tables 1.2 to 1.4. The post–hoc analyses for two studies[251,270] showed (Table 1.2 on page 45) that there is evidence that S100B is elevated in acute disease. Another study used a sophisticated composite score in order to distinguish clinical subtypes of MS .[172]

Table 10.1: *Idiopathic inflammatory demyelinating diseases of the CNS. Adapted † from Weinshenker and Miller (1997).*[427]

Acute	**Intermediate**	**Chronic**
ADEM	RR MS	Chronic myelopathy
Marburg's	SP MS	Balo's
Optic neuritis	Benign MS	Relapsing myelitis
Transverse myelopathy		Cerebellar syndrome
Devic's		

In this study CSF levels of S100B, GFAP^{SMI26} and ferritin were quanti-

fied for the first time in all three principal clinical subgroups of MS (Figure 1.1 on page 23), which were not heavily biased by patients having acute relapses. This is important because release of biomarkers during the acute phase of disease are slanted towards relapse–related tissue destruction. As a result regression to the mean might be the main effect seen.

The purpose of this cross–sectional study was to determine levels of CSF BSP in MS patients and to evaluate their relation to the clinical subtype. The relation of the same BSP to disability was also investigated, but for reasons of clarity this will be presented separately in Chapter 11.

10.2 Methods

Patients One-hundred and two patients with neurological disease were included in the study. In response to an article in the journal of the Dutch Society of MS, 65 MS patients volunteered to undergo lumbar puncture. Fifty-one patients in whom a diagnosis of clinically definite MS could be made were included in the study. MS patients were classified as having relapsing remitting (RR), secondary progressive (SP) or primary progressive (PP) disease according to previously published criteria.[236]

Due to restricted sample size glial markers (S100B, GFAP^{SMI26} and ferritin) and neurofilament phosphoforms were measured in two different control groups. The control group for glial markers consisted of 51 patients with other neurological disorders: One patient had aphasia, 1 ataxia, 1 back

pain, 1 benign intracranial hypertension (BIH), 1 chorea, 2 cerebral infarction, 2 dementia, 1 dysphagia, 12 headache, 4 motor symptoms, 2 peripheral neuropathies, 1 sarcoid, 1 transient ischaemic attack and 21 non–specific sensory symptoms presumably of a functional basis. The control group for neurofilament phosphoforms consisted of 9 patients with cluster headache syndrome in whom no other pathology could be revealed. All these samples were obtained from a library of CSF from patients undergoing diagnostic lumbar punctures at the National Hospital for Neurology and Neurosurgery, London.The CSF samples were coded and anonymised in accordance with the MRC guidelines on the ethical use of biological specimen collections in clinical research.

Patient demographics are shown in Table 10.2. The demographics of the control patients are shown in Table 10.3.

Table 10.2: *Demographic data from MS patients: median (range). MS patients are classified into clinical subgroups : PP = primary progressive, SP = secondary progressive, RR = relapsing remitting disease.*

		Clinical classification		
	MS	**RR**	**SP**	**PP**
Age (years)	46(27–65)	40(27–55)	46(28–65)	51(43-55)
Gender (f, m)	28, 23	11, 9	10, 11	7, 3
Age at onset (years)	29(17–45)	28(22–45)	28(17–42)	38(24–44)
Disease duration (years)	13(0–35)	8(0–27)	18(6–35)	15(6–27)
Time from last relapse (months)	37(1–228)	15(1–79)	77(4–228)	N/A
Number	51	20	21	10

Table 10.3: *Demographic data from control patients: median (range. OND represents a heterogeneous group with other neurological diseases and headache a well defined group of patients with cluster headache syndrome.*

	OND	**Headache**
Age (years)	41(27–63)	37 (25–44)
Gender (f, m)	37, 14	8, 1
Number	51	9

Samples Samples of CSF were obtained by routine lumbar puncture. CSF was centrifuged and aliquots of the supernatant were stored at -70°C until assayed. Approval for the study was obtained from the local Ethics Committees. Written informed consent was obtained from all MS patients.

Assays S100B (page 146), ferritin (page 147), GFAP^{SMI26} (page 121), NfH (page 73), albumin (page 147) and oligoclonal bands (page 149) were measured as described.

Statistical analysis Data were managed and analysed as described (Chapter 7, page 151). Because of the small sample size a Gaussian curve with valid 95%CI could not be calculated. Therefore the cut–off for categorical data analysis (Fisher's exact test) was set to the 100% cumulative frequency of the indicated control group.

10.3 Results

Oligoclonal bands The CSF and serum IEF patterns were classified according to whether the patients had evidence of intrathecal IgG synthesis (OCB+), evidence of a systemic oligoclonal response with matched bands in the serum and CSF (OCB*), i.e. a "mirror pattern" or no evidence of an intrathecal or systemic oligoclonal response (OCB-). Forty–six out of 51 MS patients (90%) had intrathecal oligoclonal IgG synthesis. Four (8%) of the MS patients had a mirror pattern OCB(*) and one (2%) had no evidence of a local or systemic oligoclonal IgG response. None of the control patients had evidence of intrathecal IgG synthesis.

Brain–specific proteins CSF levels of BSP did not correlate with age, age at onset of disease, disease duration or time from last relapse in the MS patients. In the subgroup analysis CSF ferritin levels in SP MS patients correlated with disease duration ($R=0.46$, $p<0.05$). There was a pseudo–correlation between S100B and NfH^{SMI35} ($R=-0.3$, $p<0.05$) due to two outliers. Removal of the outliers abolished the correlation. There was no other correlation between the different BSP. The CSF to serum albumin ratio was normal.

Table 10.4: *CSF levels of S100B, ferritin, GFAP^{SMI26}, NfH^{SMI34} and NfH^{SMI35} in RR, SP and PP MS patients: median (range), number.*

			Clinical classification		
	OND	**MS**	**RR**	**SP**	**PP**
S100B ng/mL	0.25(0–0.4),51	0.3(0.1–2),51	0.3(0.1–2),20	0.27(0.2–1.4),21	0.25(0.1–0.4),10
	|—— **p<0.05** ——|				
	|—— **p<0.01** ——————————|				
Ferritin ng/mL	5(3–7), 51	5(1–20),51	4.5(1–20),20	6(1–19),21	5.5(3–13),10
	|—— **p<0.01** ——————————————|				
GFAP^{SMI26} pg/mL	1(0–13),51	3(0–16),51	3(0–11),20	2(0–16),21	0.5(0–11),10
	Headache	**MS**	**RR**	**SP**	**PP**
NfH^{SMI34} pg/mL	684(0–964),9	11(0–47),51	8.5(0–37),20	11(5–44),21	11(5–47),10
	|—— **p<0.001** ——|				
NfH^{SMI35} pg/mL	0(0–151),9	53(0–1386),51	74.5(0–1386),20	42(11–240),21	95(7–155),10
	|—— **p<0.001** ——|				

10.3.1 Controls

CSF S100B was significantly higher in MS compared to OND patients ($p<0.05$, Table 10.4). CSF GFAP^{SMI26} levels did not distinguish significantly between OND and MS patients. CSF ferritin levels tended to be higher in MS compared to control patients, but this was not significant. MS patients had significantly higher CSF Nf-SMI35 levels than patients with cluster headache ($p<0.01$). Conversely cluster headache patients had significantly higher NfH^{SMI34} levels than MS patients ($p<0.001$).

10.3.2 Relapsing disease

RRMS patients had higher median CSF S100B and GFAP^{SMI26} levels compared to the other clinical subgroups (Table 10.4).

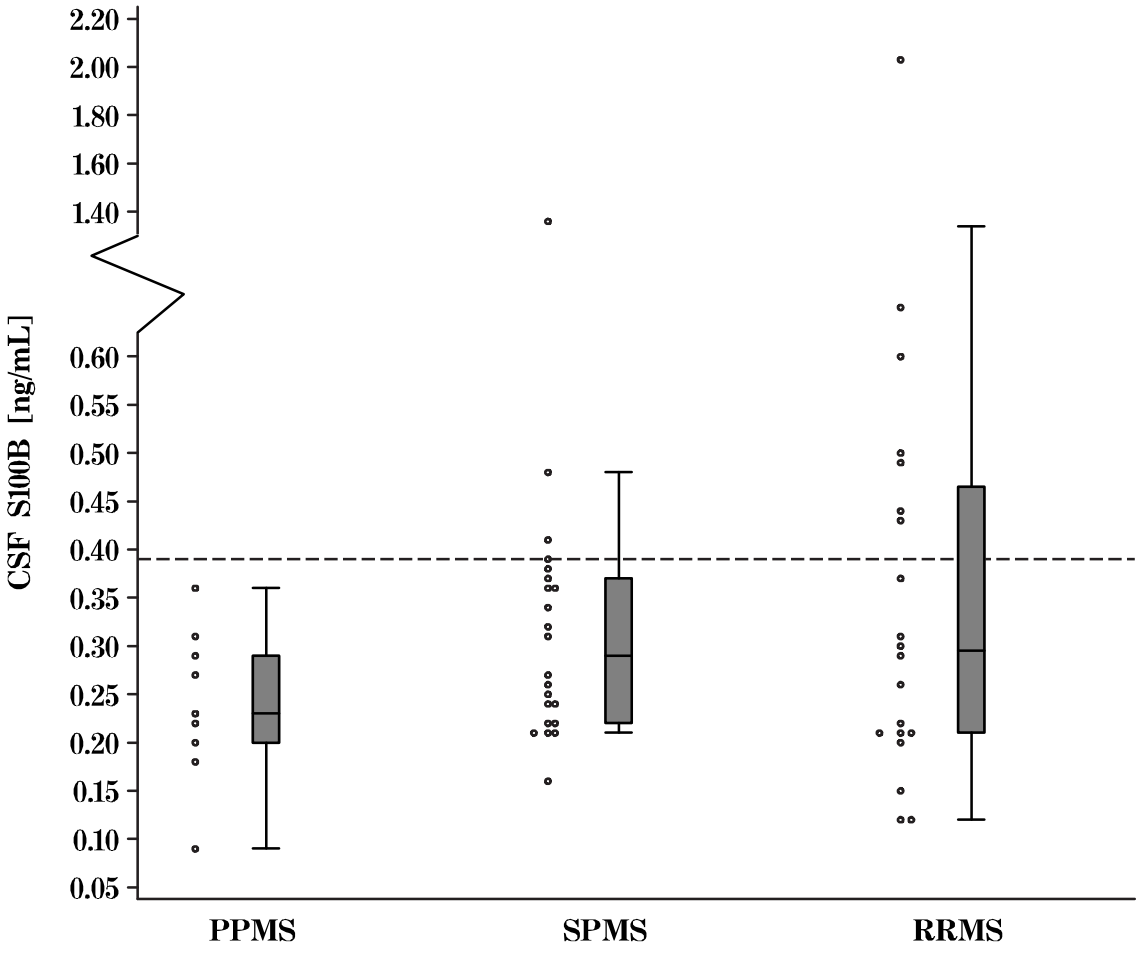

Figure 10.1: *Scatter and box-whisker plot for CSF S100B. The trend for stepwise increase of S100B levels in proportions of patients from PP to SP to RR MS is significant ($p<0.05$).*

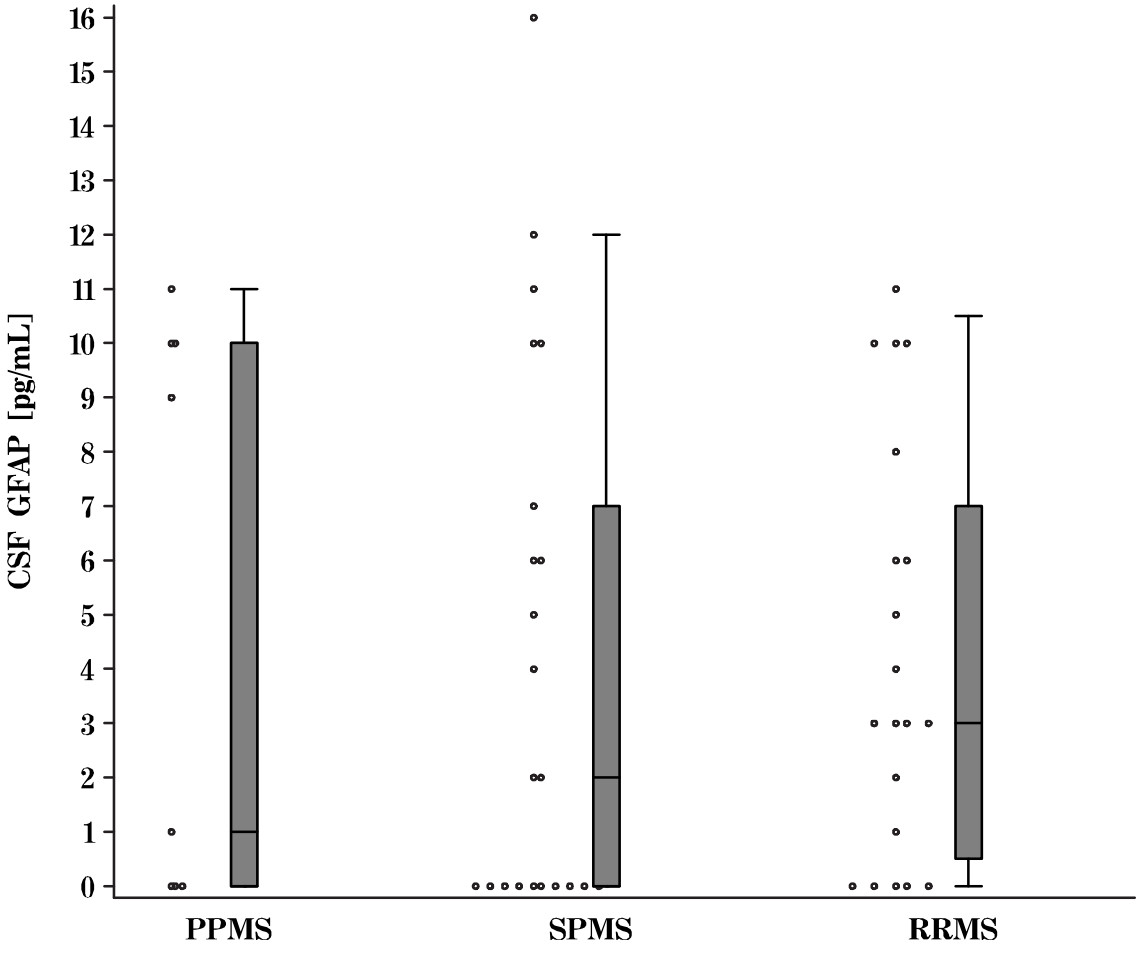

Figure 10.2: *Scatter and box-whisker plot for CSF GFAP^{SMI26}. There was no significant difference for GFAP^{SMI26} levels between the clinical subgroups.*

S100B levels were significantly different between the clinical subgroups and controls

($F(3,105)=2.77$, $p<0.05$). The post–hoc analysis showed that this significance originated from higher levels present in RR MS when compared to control patients ($p<0.01$). Mean S100B levels in RR patients were nearly 2–fold higher compared to PP and 1.5–fold compared to SP MS patients, but these differences did not reach statistical significance. There was however a trend for a stepwise increase of S100B levels from PP to SP to RR MS patients (Figure 10.1). None (0/10) of the PP, 14% (3/21) of the SP and 35% (7/20) of the RR MS patients had S100B levels above the cut–off of 0.39 ng/mL. This trend for linear increase was significant (M-Hχ^2=5.633, $p<0.05$). Importantly S100B did not correlate with time from last relapse in either of the clinical subgroups.

GFAP^{SMI26} levels were not significantly different between the clinical subgroups (Figure 10.2). A bimodal distribution for GFAP^{SMI26} was observed in PP MS patients. PP MS patients with high GFAP^{SMI26} levels were however not clinically more disabled when compared to those with low GFAP^{SMI26} levels (see Section 11.3.1, page 231). In particular there was no statistical significant difference regarding age, age at onset of disease, EDSS, 9HPT or AI. PP MS patients with high GFAP^{SMI26} levels had a slightly longer disease duration (17.6±8.6 years) when compared to PP MS patients with lower GFAP^{SMI26} levels (11.8±3.3 years), but this failed to

reach statistical significance.

10.3.3 Progressive disease

SP patients had the highest median CSF ferritin levels of the clinical subtypes (Figure 10.3). Ferritin levels in progressive MS patients (SP and PP) were higher than in RR MS patients, which was inverse to the levels observed for S100B (Table 10.4). Consequently a ratio of $\frac{S100B}{ferritin}$ distinguished significantly between clinical subgroups ($F(3,98)=6.45$, $p<0.001$). The $\frac{S100B}{ferritin}$ ratio was significantly higher in RR (1.0 ± 0.8) than in SP (0.7 ± 0.6) or in PP (0.5 ± 0.3) and control (0.5 ± 0.2) patients ($p<0.05$, $p<0.01$ and $p<0.001$, respectively, Figure 10.6). None (0/10) of the PP, 19% (4/21) of the SP and 45% (9/20) of the RR MS patients had a $\frac{S100B}{ferritin}$ ratio above the cut-off. The trend analysis revealed a significant linear increase of the $\frac{S100B}{ferritin}$ ratio from PP to SP to RR MS patients (M-H$\chi^2=7.7$, $p<0.01$).

In PP patients ferritin and GFAP^{SMI26} were slightly elevated, but the difference from the control patients did not reach statistical significance. S100B in PP MS patients was similar to the control group.

No overall statistically significant difference was observed for the three clinical subgroups regarding CSF levels of either NfH^{SMI34} or NfH^{SMI35}. One outlier of 1386 ng/mL was observed for NfH^{SMI35} (Figure 10.4). Removal of this outlier decreased the median CSF NfH^{SMI35} level in the RR MS group to 53 (0–196) ng/mL without altering the statistics.

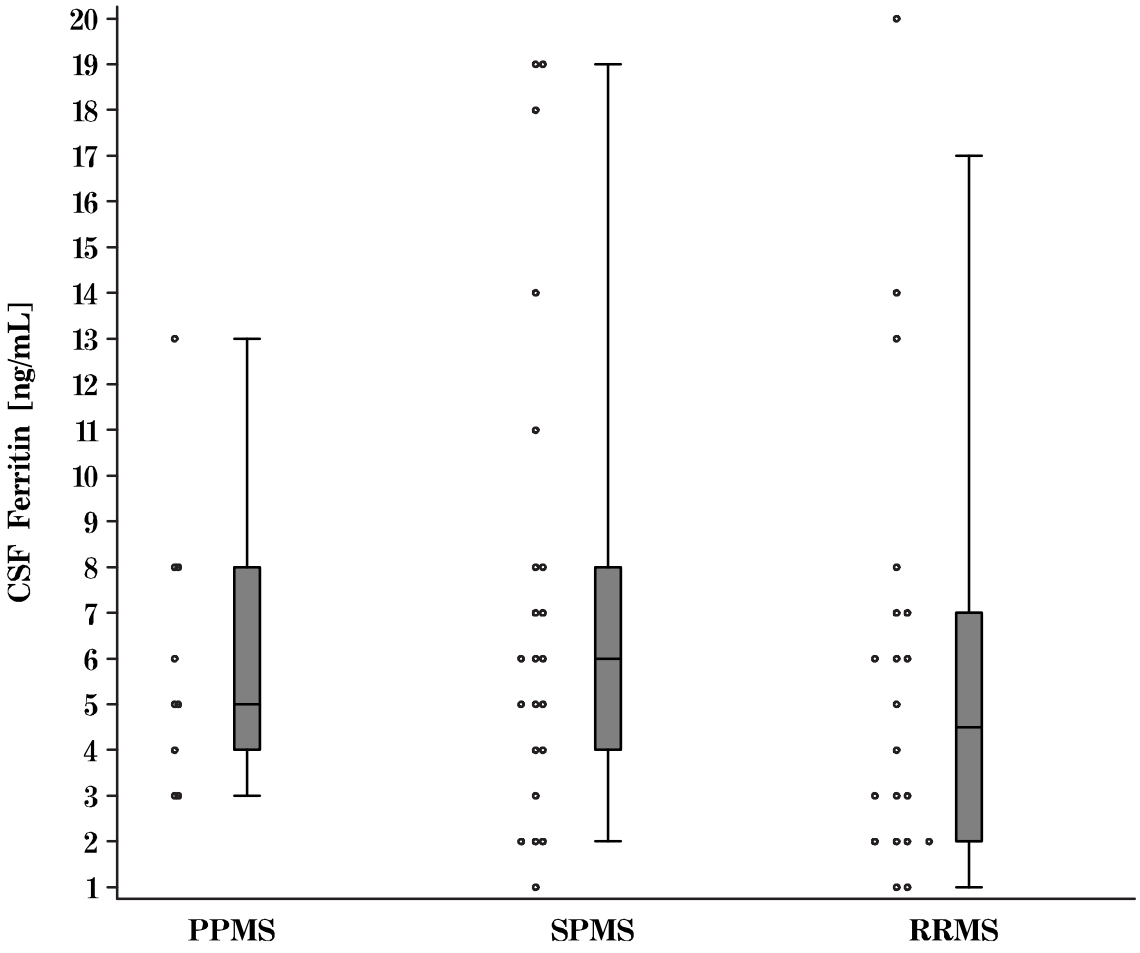

Figure 10.3: *Scatter and box and whisker plot for CSF ferritin. The median ferritin levels are slightly higher in progressive than in relapsing MS patients.*

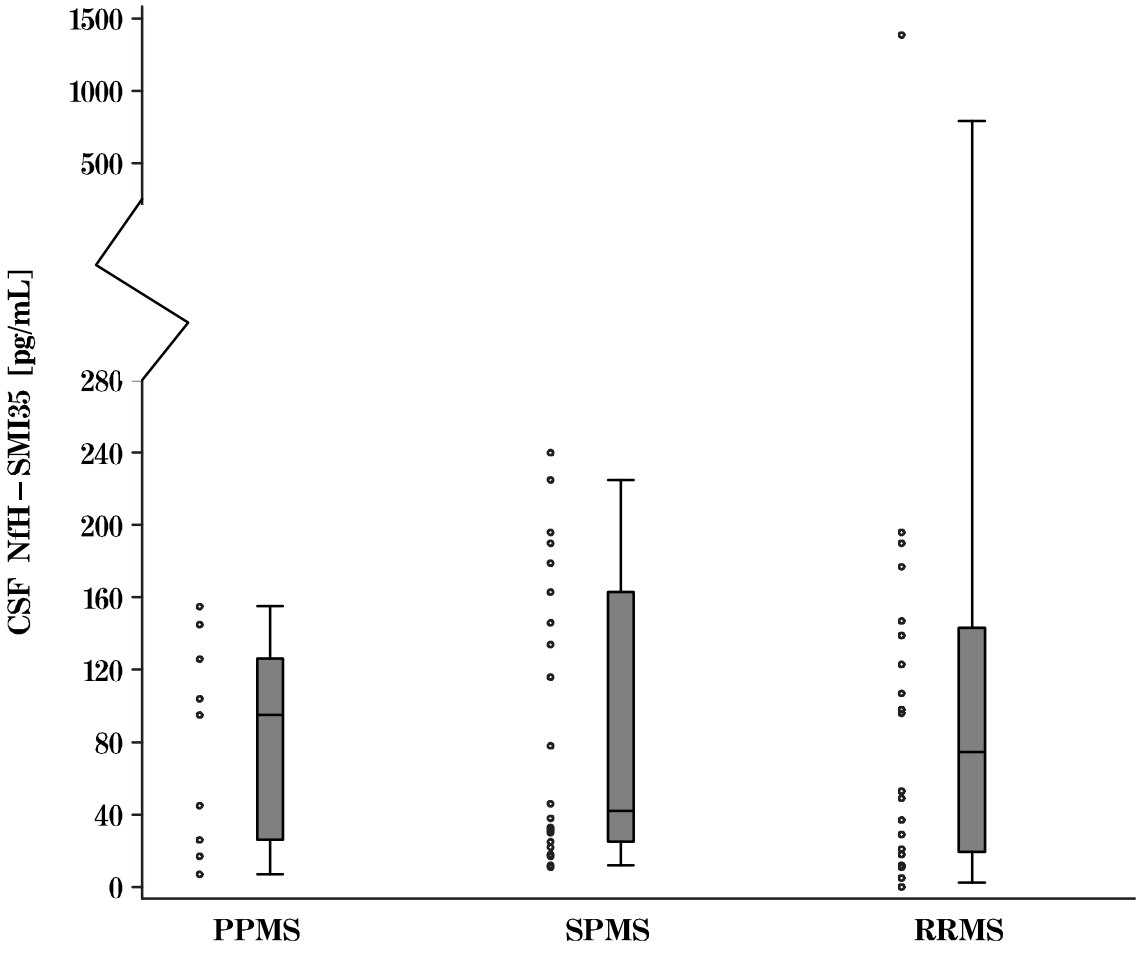

Figure 10.4: *Scatter and box and whisker plot for CSF NfH^{SMI35}. No statistically significant difference is observed for the three clinical subgroups.*

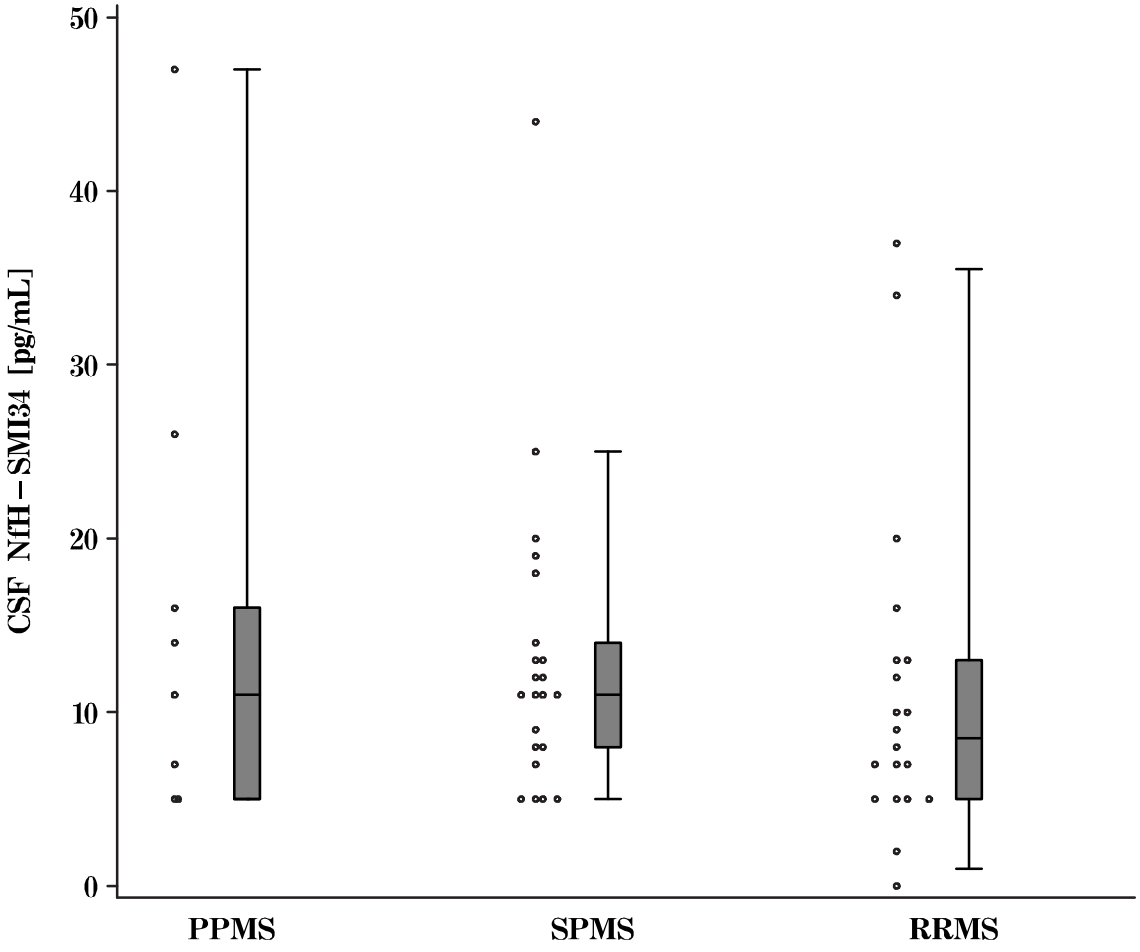

Figure 10.5: *Scatter and box and whisker plot for CSF NfH^{SMI34} . No statistically significant difference is observed for the three clinical subgroups.*

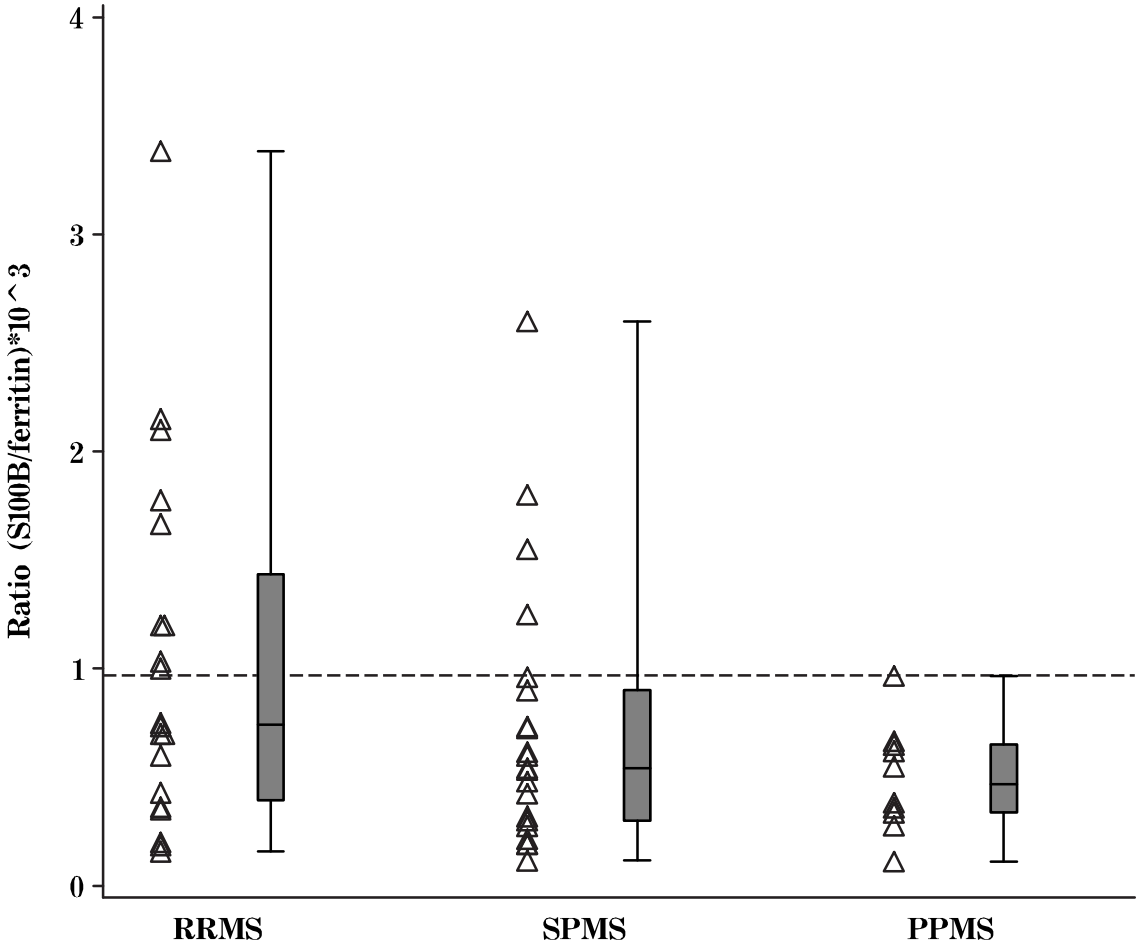

Figure 10.6: *Scatter and box and whisker plot for the CSF* $\frac{S100B}{ferritin}$ $[\times 10^3]$ *ratio. The* $\frac{S100B}{ferritin}$ *ratio was significantly higher in RR than in SP ($p<0.05$) or in PP MS ($p<0.01$) patients. 0% of PP, 19% of SP and 45% of RR MS patients have S100B levels above the cut-off of 0.97. The trend for linear stepwise increase (PPMS to RRMS) is significant ($p<0.01$).*

10.4 Discussion

The results provide evidence that biomarkers for astrocytic and microglial activation have the potential to distinguish between patients with relapsing remitting (RR) and progressive MS (PP and SP). There was a significant trend for increasing S100B levels from PP to SP to RR MS patients, with RR MS patients having significantly higher S100B levels than control patients. Ferritin levels were significantly higher in SP MS patients than in control patients (Table 10.4). Consequently a $\frac{S100B}{ferritin}$ ratio was capable of distinguishing RR from SP MS patients. This suggests that astrocytic activation predominates in relapsing disease and microglial activation in progressive disease.

MS patients had significantly elevated CSF S100B levels compared to control patients, which was principally due to the high S100B levels in RRMS patients. This result confirms most previous studies.[211,250,251,270] The median relapse–free interval in our study was 15 months in the RR and 77 months in the SP MS patients. Therefore the CSF S100B levels represent relapse–independent astrocytic activity. *In vitro* astrocytes have been shown to increase their expression of S100B after exposure to adrenocorticotropic hormone (ACTH),[388] which has shown to be an effective drug in MS .[107] The results of Chapter 9 (page 172) where high S100B levels have been shown in NAWM (Figure 9.4) are in keeping with this argument.

The dynamics of clearance of all investigated markers from the extracel-

lular space via the CSF are unknown, but one would assume that because of dilution the extracellular concentration at the site of release is much higher than that in the CSF. Nanomolar levels S100B have neurotrophic activity whilst micromolar S100B levels have cytotoxic properties.[86] This could be of pathological and therapeutic relevance.

It is of note that elevated levels of S100B due to head injury or rapid parenchymal destruction have been reported in epilepsy,[212,373] Creutzfeldt–Jakob disease,[127,301] stroke [22,439] and acute brain injury[148] (Chapter 2.3 on page 62). These levels should however be distinguished from those in slowly progressive diseases where S100B might play a different pathogenic role i.e. by modulating the inflammatory response through stimulation of inducible nitric oxide synthetase (iNOS) [2,86] or modify disease progression by yet unknown mechanisms, e.g. in Down's syndrome or Alzheimer's disease.[86,128,132] Although extra–cranial sources of S100B such as adipose tissue, testis and skin are known[149,268,390] and are potential confounding factors in the interpretation of serum S100B levels,[86,164] these are unlikely to be a problem for CSF levels in this study because the BBB (as determined by CSF/serum albumin ratio) was intact and all of the MS patients were outside acute relapse.

In the present study CSF ferritin was significantly higher in SP MS patients than in the control group. Medline, Embase and reference research revealed only one other study where ferritin levels have been measured in

MS patients and found them to be elevated in progressive patients.[222] This result is in keeping with the findings in MS brain homogenate where NAWM ferritin concentrations were significantly increased when compared to control WM (Figure 9.4 B, page 189). As NAWM contributes the bulk of brain tissue equilibrating with the CSF the result in CSF of MS patients is not surprising. Interestingly Hulet (1999) found decreased binding of ferritin to white matter within the MS lesion.[160] The oligodendrocyte requires iron for the synthesis of myelin ,[71] therefore upregulated ferritin levels in MS brain could reflect a physiological reaction to decreased binding and metabolic needs.

In contrast to one study[336] using the CSF of 5 healthy volunteers as controls, this study together with others[7,296] did not find any significant difference between CSF GFAP^{SMI26} levels in MS and the control group consisting of patients with other neurological disorders. GFAP^{SMI26} has also been found to be elevated in dementia,[97] normal pressure hydrocephalus ,[7] asphyxiated newborns,[44] post head injury ,[276] brain infarction[22] Lyme–borreliosis,[87] trypanosomiasis[220] and MS .[336] GFAP^{SMI26} should therefore be regarded as a non–specific biomarker of CNS tissue injury, probably astrocytic activation [199,383] and astrogliosis (Chapters 8 and 9).

The poor discriminatory power of NfH phosphoforms for the clinical subgroups of MS suggests that axonal injury is a uniform phenomenon in MS. The only other study measuring Nf, albeit the light chain in CSF of different

clinical types, by Semra *et al.* (2002) also did not reveal a statistical significant difference between RR and SP/PP MS patients.[353] However in Semra's and the present study the median/mean NfL/ NfH levels were slightly higher in progressive compared to relapsing MS patients. An important question to ask is how axonal damage develops during progression of the disease, i.e. if the dynamics of axonal injury in SP/PP MS are distinct from those in RR MS. This will be possible in the longitudinal study presented in Chapter 12.

10.5 Conclusion

This study investigated the relationship between biomarkers for different glial cell responses and the clinical subgroups of MS.

There was a significant trend for increasing S100B levels from PP to SP to RR MS ($p<0.05$). S100B was significantly higher in RR MS than in control patients ($p<0.01$), whilst ferritin levels were significantly higher in SP MS than in control patients ($p<0.01$). The $\frac{S100B}{ferritin}$ ratio discriminated between patients with RR MS and those with SP, PP or control patients ($p<0.05$, $p<0.01$ and $p<0.01$, respectively).

S100B was a good marker for the relapsing phase of the disease (confirmed by post–mortem observation in chapter 9) as opposed to ferritin which is elevated throughout the entire course. The results of this study might be considered in future classifications of MS subgroups.

Chapter 11

Disability: Cross–sectional

11.1 Background

In his remarkable 1868 papers Charcot distinguished three steps in the pathology of his disease, *la sclérose en plaques* (multiple sclerosis): (1) initial astrocytic and microglial activation: *"la multiplication des noyaux et l'hyperplasie concomitante des fibres réticulées de la névroglie sont le fait initial"*, (2) secondary neuro–axonal degeneration: *"l'atrophie dégénerative des éléments nerveux est secondaire"* and (3) astrogliosis: *"la névroglie fait place au tissu fibrillaire"* (Figure 11.1), which he considered to represent the anatomical substrates of progressively impaired locomotor activity: *"est considérée à juste titre comme le substratum anatomique de l'ataxie locomotrice progressive."*[61]

Out of these, axonal damage has become one of the most intensely studied aspects of recent MS research and will be investigated in Chapter 12. Moreover the clinical relevance of the glial response has received less attention despite recent evidence that glial pathology can precede secondary

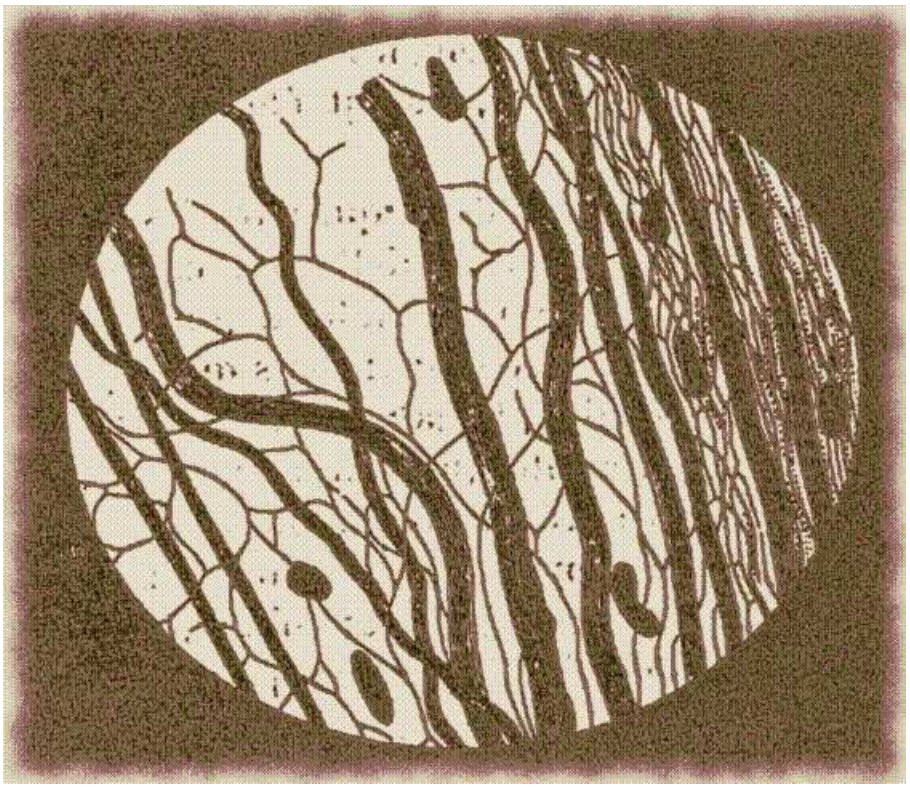

FIG. 11.1 – Elle représente une préparation fraîche, provenant du centre d'une plaque scléreuse, coloriée par le carmin et traitée par delacération. Au centre, *vaisseau capillaire* portant plusieurs *noyaux*. A droite et à gauche, *cylindres d'axe*, les uns volumineux, les autres d'un très–petit diamètre, tous dépouillés de leur myéline. Le vaisseau capillaire et les cylindres d'axe étaient fortement colorés par le carmin. Les cylindres d'axe ont des bords parfaitement lisses, ne presentant aucune ramification. Dans l'intervalle des cylindres d'axe, membranes fibrilles de formation récente, à peu près parallèles les unes aux autres dans la partie droite de la préparation, formant à gauche et au centre, une sorte de réseau résultant, soit de l'enchevêment, soit de l'anastomose des fibrilles. Celles–ci se distinguent des cylindres d'axe, 1° par leur diamètre qui est beaucoup moindre ; 2° par les ramifications qu'elles offrent dans leur trajet ; 3° parce qu'elles ne se colorent pas par le carmin. — Çá et et là, *noyaux* disséminés. Quelques–uns paraissant en connexion avec les fibrilles conjonctives ; d'autres ayant pris une forme irrégulière, due à l'action de la solution ammoniacale du carmin.[60]

axonal degeneration.[111]

Previously only one attempt has been made to relate a glial marker to disability (Table 1.2 on page 45). Confirmation of this result was hampered by the use of tests which were only available to the original laboratory.[332,336]

In this chapter the CSF levels of S100B, GFAP^{SMI26} and ferritin quantified in the clinical MS subtypes described in Chapter 11 were related to the degree of disability as quantified by different clinical scales. The hypotheses underlying the study were that CSF BSP levels relate to the degree of disability.

11.2 Methods

Patients As described in Chapter 10.2 (page 208). Patient demographics and baseline characteristics are shown in Table 11.1.

Clinical assessment The Amsterdam group assessed all the MS patients. An ambulation index (AI),[14] an expanded Disability Status Scale score (EDSS)[206] and a 9–hole PEG test (9HPT) for both hands[14,177] were performed on all patients within one week of the lumbar puncture. The AI classified the gait on a scale ranging from 0 (no impairment) to 9 (restricted to wheelchair without independent transfer). The 9HPT is a measure of upper limb motor function. The 9HPT was performed twice with each hand. The quickest performance for each hand was taken to calculate an average value.[177]

CSF analysis As described in Chapter 10.2.

Statistical analysis Data were managed and analysed as described (Chapter 7, page 151). Because of the small sample size a Gaussian curve with valid 95%CI could not be calculated. The cut–off for categorical data analysis (Fisher's exact test) was therefore set to the 100% cumulative frequency of the indicated control group.

Table 11.1: *Demographic and clinical data: median (range, number). MS patients are classified into clinical subtypes: PP = primary progressive, SP = secondary progressive, RR = relapsing remitting disease. AI = ambulation index, EDSS = Kurtzke's extended disability status score, 9HPT = 9–hole PEG test (see text).*

			Clinical classification		
	CTRL	**MS**	**RR**	**SP**	**PP**
Age (yrs)	41(27-63),51	46(27-65),51	40(27-55),20	46(28-65),21	51(43-55),10
Gender (f, m)	37, 14	28, 23	11, 9	10, 11	7, 3
AI	N/A	4.5 (0–10),44	1.5 (0–10),18	6.5 (1–9),18	4 (1–9),8
EDSS	N/A	3.5 (0–8),51	1.75 (0–6.5),2)	6 (1–8),21	6 (1.5–8),10
			|— **p<0.001** ——————————————|		
			|— **p<0.001** ——————|		
9HPT	N/A	25 (17–84),49	20 (18–29),18	29 (17–84),21	26 (17–36),10
			|— **p<0.01** ————|		

11.3 Results

Patients were categorised according to the frequency distribution on the clinical scales (Figure 11.2). The distribution of the AI and EDSS was trimodal. Patients were therefore classified into those with good (AI $\leq$2), moderate (3-6) and poor ($\geq$7) ambulation. The EDSS was classified as indicating mild (0–3), moderate (3.5–6.5) and severe disability (7–10).

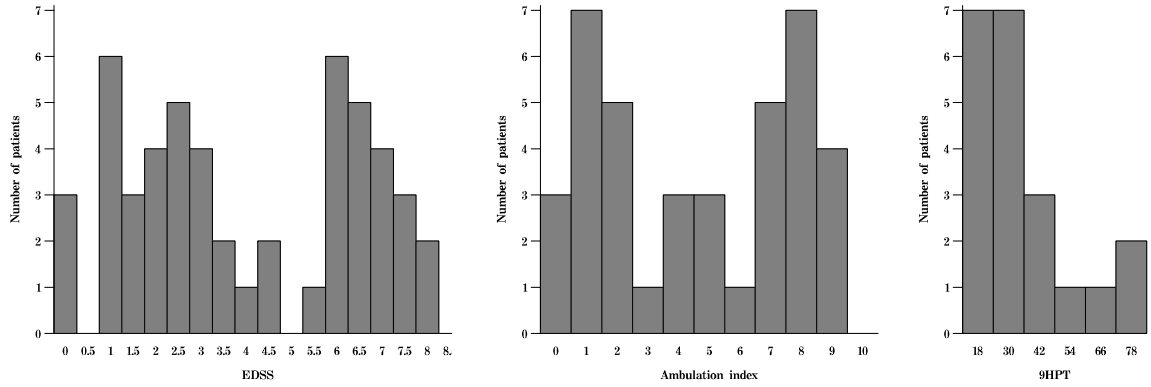

Figure 11.2: *Frequency plot of the clinical scales: (A) EDSS, no patient had an EDSS above 8.5, (B) Ambulation index and (C) 9HPT. The number of patients is indicated on the ordinate.*

11.3.1 Ambulation index

There was a significant difference in CSF GFAP^{SMI26} levels between MS patients classified according to the AI and control patients (F(3,64)=5.49, p<0.001, Table 11.2). In the post–hoc analysis MS patients with poor ambulation had significantly higher CSF GFAP^{SMI26} levels than control patients (p<0.001) or MS patients with good ambulation (p<0.05). The subgroup analysis revealed that this significance was due to the 9 SP MS patients with poor ambulation, which had nearly 6-fold elevated median GFAP^{SMI26} levels when compared to control patients (p<0.05, Table 11.2). Significantly elevated GFAP^{SMI26} levels were also present in poorly ambulating RR MS patients compared to control patients (p<0.01), but not in poorly ambulating PP MS patients.

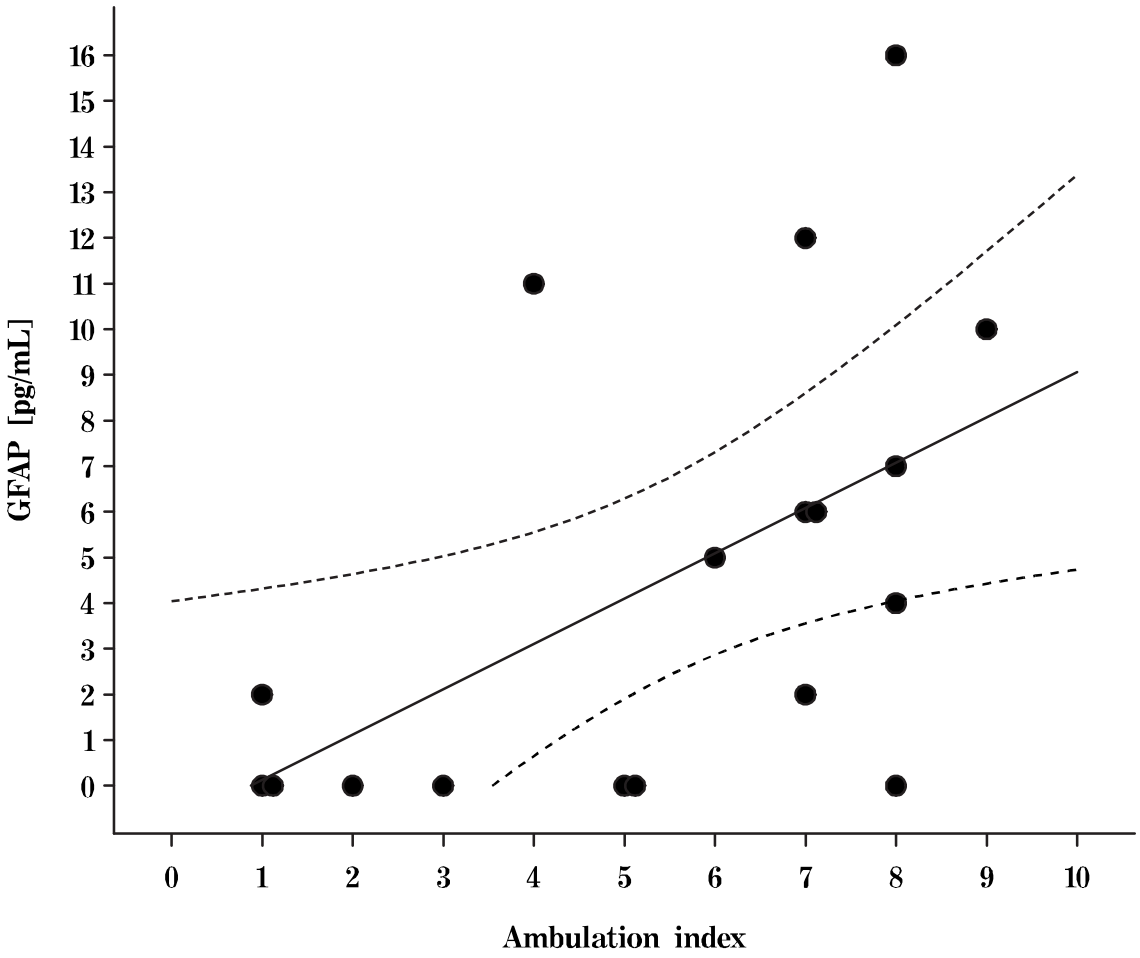

Figure 11.3: *CSF GFAP^{SMI26} levels correlated significantly with the AI in SP MS patients (R=0.57, p<0.01). Data points are horizontally adjacent if observations overlapped. The linear regression line, the 5% lower and 95% upper confidence curves are shown.*

In SPMS patients disability measured by the AI correlated with levels of GFAP^{SMI26} (R=0.57, p<0.01, Figure 11.3). The 100% cumulative frequency (2 pg/mL) of the CSF GFAP^{SMI26} levels of patients with good ambulation was taken as cut–off for the trend–analysis. None (0/4) of patients with good, 40% (2/5) of patients with moderate and 78% (7/9) of patients with poor ambulation had CSF GFAP^{SMI26} levels above this cut–off. The trend analysis revealed a significant linear increase within these 3 AI categories (M-Hχ^2=6.6, p<0.01).

11.3.2 EDSS

There was a significant difference in CSF GFAP^{SMI26} levels between MS patients classified according to the EDSS and control patients (F(2,57)=5.06, p<0.01, Table 11.2). Severely disabled MS patients had significantly higher GFAP^{SMI26} levels than control patients (p<0.01). The post–hoc analysis revealed that this was caused by the approximate 6-fold elevation in median GFAP^{SMI26} levels in severely disabled SP MS patients when compared to control patients (p<0.01). The post–hoc analysis also revealed significantly elevated GFAP^{SMI26} levels in severely disabled compared to moderately disabled MS patients (p=0.05). There was no linear correlation between the EDSS and GFAP^{SMI26} levels and the trend analysis was not significant.

In SP MS patients ferritin correlated with the EDSS (R=0.45, p<0.05). Because of the previously indicated correlation between disease duration and ferritin levels, a partial correlation correcting for disease duration was

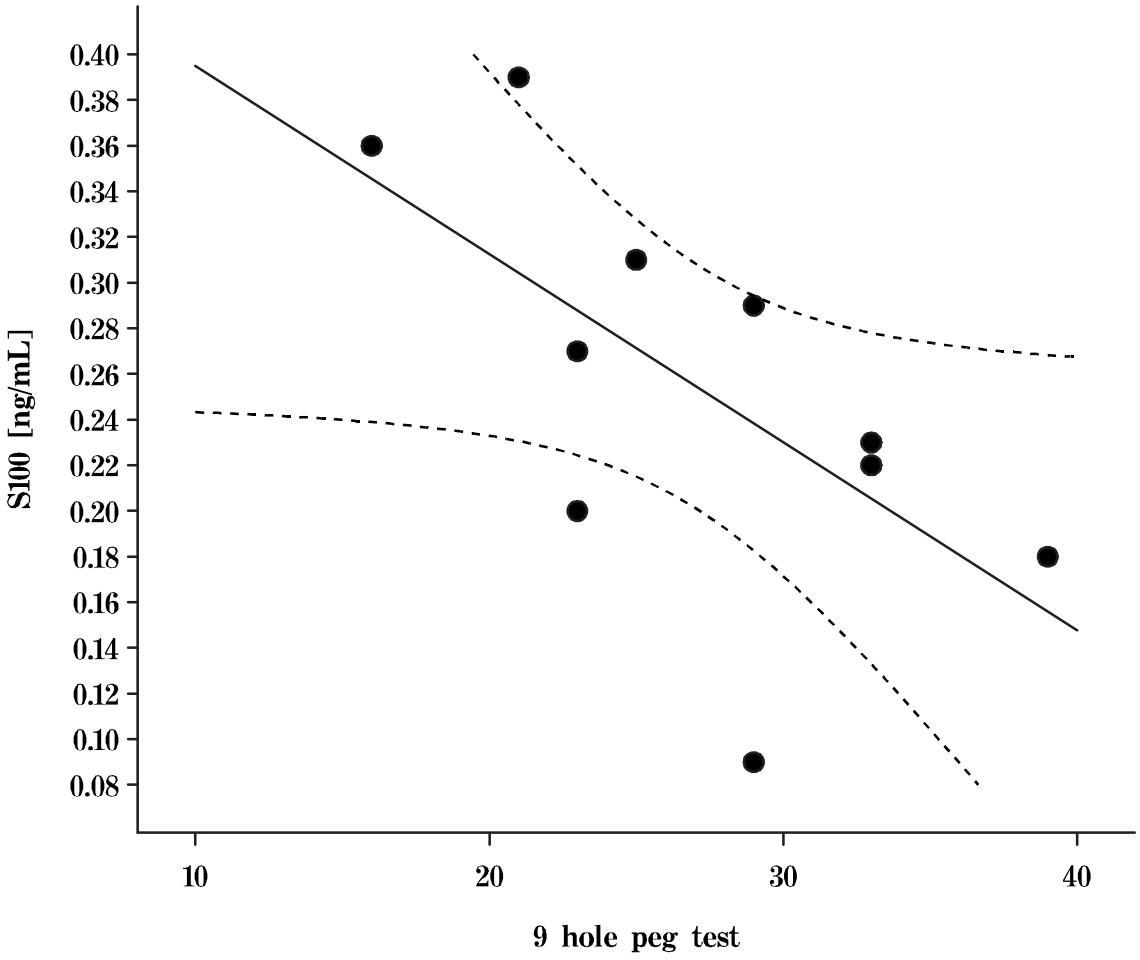

Figure 11.4: *CSF S100B levels correlated significantly with the 9HPT of the dominant hand in PP MS patients (R=-0.85, p<0.01). The linear regression line, the 5% lower and 95% upper confidence curves are shown.*

performed which abolished the correlation between EDSS and ferritin.

11.3.3 9–hole PEG test

CSF ferritin levels were about 2-fold higher in patients with a test performance $>$ 55 seconds (12.3±5.1 ng/mL) than in "quick" (6.2±4.8 ng/mL) patients ($p<0.05$, Wilcoxon rank sum test). Because there were only 4 "slow" patients the results were checked by the Fisher's exact test and no significance could be demonstrated. CSF S100 correlated negatively with the 9HPT in PP MS patients ($R=-0.85$, $p<0.01$, Figure 11.4).

Table 11.2: *CSF GFAP^{SMI26} levels in control, MS patients and clinical subtypes: median (range), number. GFAP^{SMI26} distinguishes significantly the grades of disability in clinical subtypes (post–hoc analysis) from those in control patients (AI: F(3,64)=5.49, p<0.001; EDSS: F(2,57)=5.06, p<0.01).*

GFAP^{SMI26} [pg/mL]		**Ambulation index**		
	CTRL	**< 2**	**2–6**	**> 6**
MS	1(0–13),51	2(0–11),19	0(0–11),8	6(0–16),17
				p<0.001
				p<0.05
SP		0(0–2),4	0(0–11),5	6(0–16),9
				p<0.001
				p<0.05
PP		0(0–11),3	4.5(0–9),2	1(0–10),3
RR		3(0–10),12	0(0),1	6(3–11),5
				p<0.01

	EDSS		
	< 3.5	**3.5-6.5**	**> 6.5**
MS	3(0–11),27	0(0–11),15	6(0–16),9
			p<0.01
			p=0.05
SP	2(0–10),5	0(0–11),9	6(0–16),7
			p<0.01
PP	0(0–11),4	4.5(0–10),4	5.5(1–10),2
RR	3.5(0–11),18	0(0),2	N/A

11.4 Discussion

Patients with poor ambulation had significantly higher CSF GFAP^{SMI26} levels than patients with good ambulation and control patients (Table 11.2). Also severely disabled patients had significantly higher CSF GFAP^{SMI26} levels compared to mildly disabled patients. This is suggestive of increased astrogliosis within the spinal cord of poorly ambulating or disabled patients. Compared to the control group these were the only patients with significantly higher GFAP^{SMI26} levels. The subgroup analysis revealed that this was most marked in patients with SP MS. This study revealed a significant correlation between GFAP^{SMI26} and individual scoring on the AI for SP MS patients (R=0.57, Figure 11.3). The lack of correlation in PP MS may relate to the small number of cases studied. We interpret the results as showing a direct relationship between GFAP^{SMI26} and astrogliosis, which is expressed clinically as disability.

The reason why a direct correlation was found between GFAP^{SMI26} and individual points on the AI but not with the EDSS may be explained by the physiological basis of these clinical scales. The AI essentially measures gait. The EDSS in contrast includes other neurological functions which are outside (rostral) the anatomical parts of the CNS which equilibrate with the CSF in the lumbar sac. This "CSF analytical brain" consists of the inner half of the telencephalon, the basal cortex, the cerebellum, the brain stem and the spinal cord.[104] Each lost axon innervating the lower limb could potentially

be replaced by a gliotic scar about 1 meter long.[198] Therefore a considerable amount of gliotic tissue would form the source of GFAP^{SMI26} release and would hence parallel the decline in ambulation. Thus almost all changes measured by the AI, but only some assessed by the EDSS, would be reflected in a change of lumbar CSF GFAP^{SMI26} levels.

This was also demonstrated by the study of Rosengren (1995) who studied serial CSF samples in 10 RRMS patients.[336] The scale applied to assessing disability, the regional functional score system (RFSS) includes visual and mental functions. Contradictory changes in the RFSS and lumbar CSF GFAP^{SMI26} levels can be observed in 8 out of the 10 patients studied. Importantly this study on serial CSF samples (7 lumbar punctures per patient over a 2 year period) did not reveal any relationship between CSF GFAP^{SMI26} levels and the time from relapse.

The strong negative correlation between S100B and the 9HPT in PP MS patients which has not previously been observed and is difficult to explain. None of the previous studies investigated the relation of CSF S100B with disability (see Table 1.2 on page 45). The neurotrophic role of S100B in nanomolar concentrations is well described.[86,139] One might speculate whether there is an association between the treatment response to ACTH in MS[107] which upregulates of S100B excretion *in vitro*.[388] In this context high levels would have to be associated with relapse and possible toxic effects, whilst low levels would be related to failure of initiating an adequate cellular

response (Chapter 8). These results need to be confirmed by other groups to assess whether the correlation of S100B with disability is a consistent finding.

11.5 Conclusion

Disease progression in MS occurs within the interface of glial activation and gliosis. This study aimed to investigate the relationship between biomarkers of different glial cell responses to disability.

MS patients with poor ambulation (AI$\geq$7) or severe disability (EDSS $>$ 6.5) had significantly higher CSF GFAP^{SMI26} levels than less disabled MS patients or controls ($p<0.01$, $p<0.001$, respectively). There was a correlation between GFAP^{SMI26} levels and ambulation in SP MS ($R=0.57$, $p<0.01$) and S100B and the 9HPT in PP MS patients ($R=-0.85$, $p<0.01$).

CSF GFAP^{SMI26} may therefore be a marker for irreversible damage due to a gliotic scar as already suggested by Charcot in 1868. The results of this study have broader implications for finding new and sensitive outcome measures for treatment trials which aim to delay the development of disability.

Chapter 12

Axonal pathology: Longitudinal

12.1 Background

The new insight from recent studies into axonal pathology in multiple sclerosis (MS) is that a high number of transected axons was already present in acute lesions ,[106,398] in patients with a short clinical course [42,398] and independently from demyelination.[40] Axonal damage/loss results in atrophy of the spinal cord,[231] cerebellum[230] and cortex,[113] all of which correlate with disability.[113,230,231]

The neuron relies on the axonal compartment to maintain function over long distances in an ever–changing environment. It does so by exploiting functional properties of proteins, which can be modulated locally in the axon, e.g. by phosphorylation and dephosphorylation of proteins such as Nf (Chapter 2.1 on page 50). Of the three Nf subunit proteins NfH is highly phosphorylated and its KSP (Lys-Ser-Pro) repeat–enriched tail domain constitutes a target for a range of protein kinases .[27,34,119,136,169,223,293,411] In

the healthy axonal compartment NfH^{SMI35} dominates.[214,294,404] After axonal injury the relative amount of NfH^{SMI32} increases in the proximal axon and intense staining for hypophosphorylated NfH isoforms is observed at the site of injury[398,404] (Table 9.1 on page 176). Disintegration of the axonal membrane results in release of Nf (Chapter 9). CSF Nf levels are therefore putative markers for axonal damage.[131,242,353] Using two discrete monoclonal antibodies we have monitored phosphorylated (NfH^{SMI35}) and extensively phosphorylated (NfH^{SMI34}) NfH not just in relation to each other (as a ratio) but also the changes in levels over time (Δ NfH).[377,378]

This prospective study presents the 3–year follow–up data of the cross–sectional study in Chapters 10 and 11. The longitudinal study was stimulated by 3 questions[256,424]: (1) Can *clinical subgroups* of MS be distinguished on the basis of axonal damage? (2) Does *disability* correlate with markers of axonal pathology? And (3) Can we predict loss of function by using biomarkers for axonal injury as *prognostic* indicators?

12.2 Methods

Patients Twenty–eight patients from the cohort presented in Chapters 10 and 11. A second CSF sample was available from those patients who agreed to another lumbar puncture at 3–years follow–up. To avoid measuring regression to the mean CSF was analysed only in those patients who had a relapse–free interval of at least 2 months prior to lumbar puncture, by

which time CSF NfL is known to return to baseline levels.[242] MS patients were classified as having relapsing remitting (RR), or progressive (SP/PP) disease.[236] Approval for the study was obtained from the local Ethics Committees. Written informed consent was obtained from all patients. In 8 of the MS patients (5 RR, 3 SP) treatment with interferon beta (IFN) had been started since 1996. The control group consisted of the 9 patients with cluster headache presented in Chapter 10. The demographic data of the patients are shown in Table 12.1.

Table 12.1: *Baseline characteristics of the patients. The median (IQR) is shown.*

	CTRL	**MS**	**SP/PP**	**RR**
Female:Male	8:1	13:15	9:9	4:6
Age (years)	37 (25–44)	46.3 (39.7–51)	48.5 (42.5–51.5)	39.8 (38.3–47.7)
Disease duration (years)	N/A	14 (8.0–19.9)	18.1 (12.6–27.6)	8.8 (7.4–13)
Relapse–free interval (months)	N/A	38 (8–96)	96 (47.5–150.5)	11.5 (6–38)
No of patients	N=9	N=28	N=18	N=10

Clinical assessment The patients were reassessed as described in Chapter 11 at the 3–year follow–up visit. All clinical evaluations were performed on all patients within one week of each lumbar puncture. Patients were classified as clinically advancing if the EDSS had increased by at least 1 point[166] over the 3 years.

Assays The NfH phosphoforms NfH^{SMI34} and NfH^{SMI35} were analysed as described in Chapter (page 73). Albumin (page 147) and oligoclonal bands (page 149) were measured as described.

Data analysis Data were managed and analysed as described (Chapter 7, page 151). Because of the small sample size a Gaussian curve with valid 95%CI could not be calculated. The cut–off for categorical data analysis (Fisher's exact test) was therefore set to the 100% cumulative frequency of the indicated control group. Independent variables were compared using the non-parametric two-sample exact Wilcoxon rank-sum test or the unbalanced two-way ANOVA (general linear model) for more than two groups[65] which were done in the following order (1) controls, RR, SP/PP MS; (2) control, RR (stable), RR (advancing), SP MS; (3) control, RR (disease course maintained), RR (RR to SP conversion).

The change of NfH levels between baseline and follow–up was expressed as the difference:

$$\Delta NfH = NfH_{follow-up} - NfH_{baseline}$$

A positive number indicated an increase in NfH follow–up levels. The phosphoform ratio is a measure of the degree of phosphorylation and was expressed as a cross–sectional measure:

$$RATIO = \frac{NfH^{SMI34}}{NfH^{SMI35}}$$

A ratio <1 indicates an overall decrease in the level of phosphorylation. Values with zero deliminator (or NfH at baseline and follow–up below assay sensitivity) could not be calculated and were excluded from this analysis. For each variable the numbers of valid observations were therefore shown in the table.

12.3 Results

At baseline the CSF levels of $\text{NfH}^{SMI35}_{baseline}$ were higher in all MS patients when compared to controls ($p<0.01$, Table 12.2). Comparing clinical subgroups ($F(3,33)=3.38$, $p<0.05$) and progression ($F(3,33)=3.38$, $p<0.05$) this was due to higher $\text{NfH}^{SMI35}_{baseline}$ levels in SP/PP MS patients ($p<0.05$, Table 12.2) and in patients with clinically advancing RR MS ($p<0.05$, Table 12.3).

At baseline the CSF levels of NfH^{SMI34} were higher in control subjects compared to MS patients ($p<0.001$). Comparing MS clinical subgroups ($F(3,33) = 3.38$, $p<0.05$) with the control patients the same levels of significance were revealed for each subtype ($p<0.001$, Table 12.2).

Three RR patients converted to SP disease, accounting for 7 RR and 21 SP/PP MS patients at follow–up. Treatment with IFN had no significant effect on either NfH phosphoform levels, the ratio or the change of levels over time. No correlations were found between any Nf phosphoform or the ratio, with age, age at onset, disease duration or time from last relapse.

Table 12.2: *CSF levels and ratio of NfH phosphoforms (median, IQR, number). RR MS patients which showed a decrease of at least 1 point on the EDSS between baseline and follow–up were classified as advancing RR. Three of the RR MS patients converted to SP MS, explaining the change of patient numbers in the clinical subgroups at follow–up. At follow–up the change of NfH over time (ΔNfH) was also calculated.*

			Clinical subgroup	
	CTRL	**MS (all)**	**SP/PP**	**RR**
Baseline				
NfH^{SMI35} pg/mL	0	78	80.5	78
	(0-47) 9	(19.5-167) 28	(22-179) 18	(11-139) 10
	—— p<0.001 ——			
	—— p<0.05 ————————			
NfH^{SMI34} pg/mL	684	9	11	7
	(230-795) 9	(6.0-13) 28	(7.0-13) 18	(5-9) 10
	—— p<0.001 ——			
	—— p<0.001 ————————			
	—— p<0.001 ————————————			
Ratio	55.9	1.8	2.4	1
	(24.6-145.5) 4	(0.6-5.8) 27	(0.6-6.1) 18	(0.42-3.5) 9
	——— p<0.05 ———			
Follow–Up				
NfH^{SMI35} pg/mL	N/A	116.5	132	0
			——— p<0.05 ———	
		(0-178) 28	(96-209) 21	(0-120) 7
NfH^{SMI34} pg/mL	N/A	49.6	48	51
		(8.5-129.1) 28	(10-139) 21	(3-120) 7
Ratio	N/A	3.3	3.3	5
		(0.9-10.1) 18	(0.90-139) 16	(0.2-10) 2
Δ NfH^{SMI35} pg/mL	N/A	11.5	82	-49
		(-59-98) 28	(-11-104) 21	(-107-0) 7
Δ NfH^{SMI34} pg/mL	N/A	42.5	35	51
		(-1-123) 28	(-3-134) 21	(1-112) 7

12.3.1 Accumulation of axonal damage in progressive disease

An increase of NfH^{SMI35} from baseline to follow–up was observed in more cases with SP/PP MS (14/19, 74 percent, Figure 12.1, closed lines) when compared to RR patients (1/5, 20 percent), which was statistically significant (p<0.05). Two RR and 2 SP/MS patients were excluded from analysis

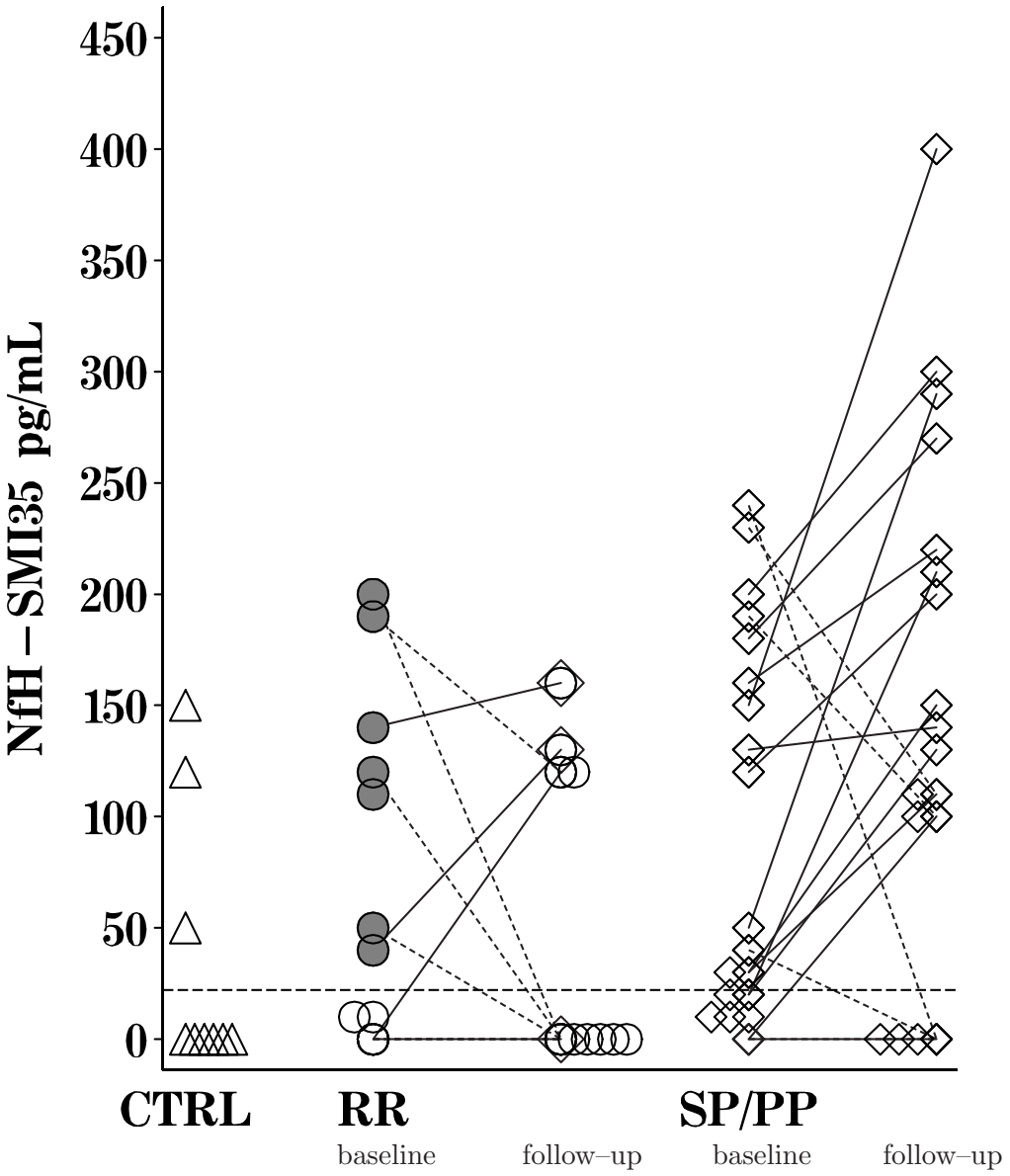

Figure 12.1: *CSF NfH^{SMI35} levels in patients RR (open circles) and SP/PP (diamonds) forms of MS. Three of the RR patients converted to SP MS at follow–up (superimposed diamonds). RR MS patients who experienced clinically advancing disease are indicated (grey circles). Increasing levels of NfH^{SMI35} between baseline and follow–up are indicated by closed lines and decreasing levels by dotted lines. The control group consists of patients with cluster headache (triangles). The sensitivity of the NfH–assay is 20 pg/mL (horizontal reference line).*

because NfH levels were below assay sensitivity for both measurements (horizontal reference line, Figure 12.1).

The distribution of NfH^{SMI35} was bimodal for RR and SP/PP MS patients both at baseline and follow–up with no levels observed between 50–100 pg/mL (Figure 12.1). No statistical significant difference could be revealed for any demographic or clinical data explaining this bimodal distribution. There was no correlation between either of the NfH phosphoform concentration and blood–brain barrier dysfunction as measured by the ratio of $\frac{\text{CSF albumin}}{\text{Serum albumin}}$ (data not shown).

Table 12.3: *CSF levels and ratio of NfH phosphoforms (median, IQR, number) at baseline. RR MS patients are classified according to progression on the EDSS scale or the clinical classification.*

	Disability		**Clinical subtype**	
	Stable	Advancing	Maintaining RR	Converting to SP
NfH^{SMI35} pg/mL	5	23	49	123
	(0-11) 3	(49-190) 7	(5-190) 7	(37-139) 3
	—— p<0.001 ——			
NfH^{SMI34}	2	8	7	9
	(0-7) 3	(5.0-13) 7	(2-8) 7	(5.0-13) 3
Ratio	5.1	0.7	2.3	0.73
	(4.0-6.4) 2	(0.6-3.5) 7	(0.4-4) 6	(0.4-3.5) 3
	—— p<0.001 ——			

12.3.2 Axonal injury: correlation with disability

NfH^{SMI35} levels correlated with all clinical scales at follow–up (Figure 12.2 to 12.4). The correlation was strongest for the 9HPT (R=0.59, p=0.001), followed by the EDSS (R=0.54, p<0.01) and the AI (R=0.42, p<0.05). One outlier was observed for the 9HPT, exclusion of which did not change the significance of the analysis (R=0.55, p<0.01). No correlations were found

between $NfH^{SMI34}_{baseline}$ and any of the disability scales. The ratio of the NfH phosphoforms at follow–up correlated with the EDSS (R=0.52, p<0.05). At baseline no such correlation was demonstrated. The ratio could not be calculated in one patient at baseline (zero denominator). At follow–up the denominator was zero in 10 patients. By definition correlations with the change of NfH phosphoforms could only be calculated for the follow–up assessment. The (ΔNfH^{SMI35}) correlated with the 9HPT at follow–up (R=0.39, p<0.05) but not with the EDSS (R=0.36, p=0.06) or AI (R=0.23, N.S.). No correlations were found for ΔNfH^{SMI34} and any of the disability scales.

Table 12.4: *Disability as measured on the EDSS, AI and 9HPT at baseline and follow–up. As expected advancing RR patients were more disabled at follow–up then at baseline (p<0.01). There was no significant difference for AI and 9HPT between baseline and follow–up in the subgroups. Three of the RR patients converted to SP MS between baseline and follow–up, explaining the change of numbers of the groups. The data for the advancing versus stable RR MS patients are shown according to the baseline classification only.*

	MS	**Clinical subtype**		**RR** (baseline cohort)	
	all	SP/PP	RR	stable	advancing
Baseline					
EDSS	4.3	6	1.75	2	1
	(2–6.5) 28	(4.5–7) 18	(1–2) 10	(1.5–4) 3	(1–2) 7
AI	2	6	1	1	1
	(1–7) 25	(2–8) 15	(1) 10	(1) 3	(0–2) 7
9HPT	24.3	26.5	20	20.5	20
	(20–28.3) 28	(24–30) 18	(18–22) 10	(18–23) 3	(18–22) 7
Follow–up					
EDSS	4.5	6	3	3	3.5
	(3.4–6.3) 28	(4–7) 21	(2.5–4) 7	(1.5–4) 3	(3–4) 7
AI	2	4	1	1	2
	(2–6) 28	(2–7) 21	(1–2) 7	(0–2) 3	(1–2) 7
9HPT	23.5	24.5	20	21	20
	(20–29.3) 28	(21.5–31) 21	(18–22) 7	(16–21) 3	(18–25) 7

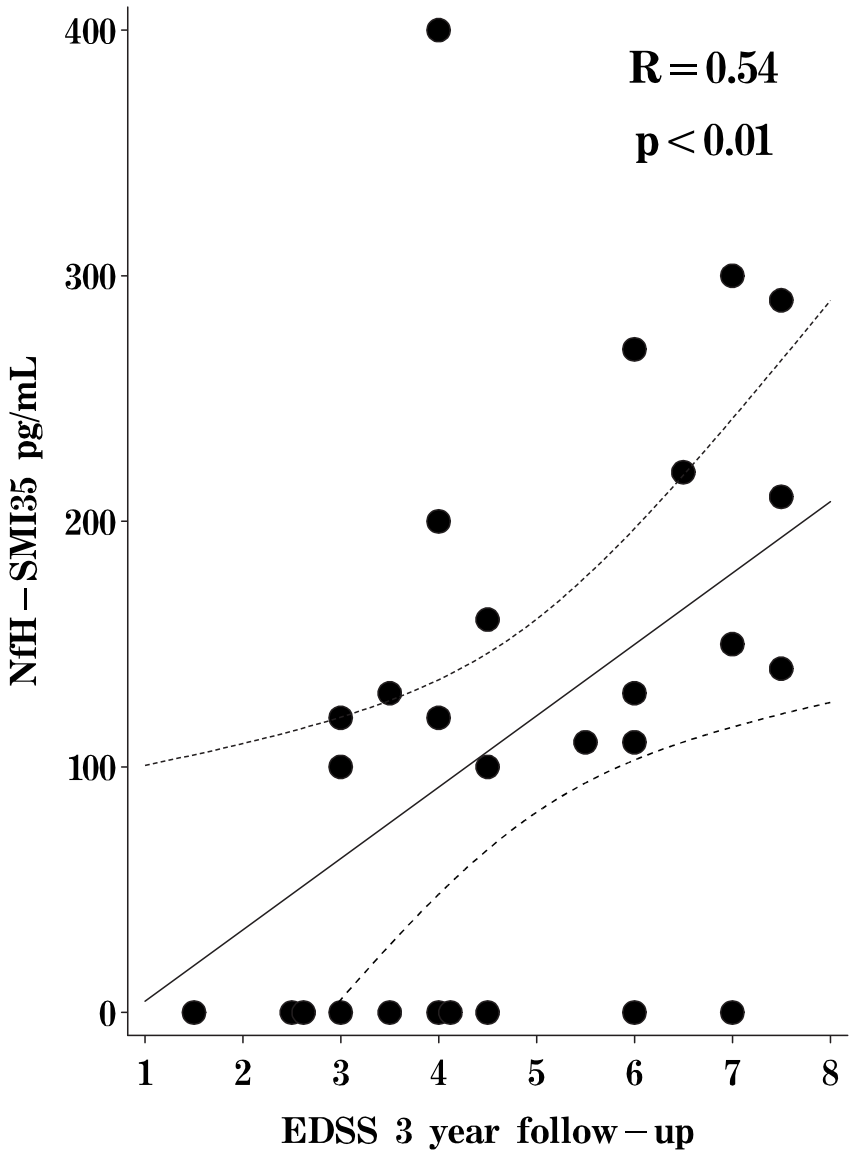

Figure 12.2: *Correlation between the NfH^{SMI35} and the EDSS at follow–up.*

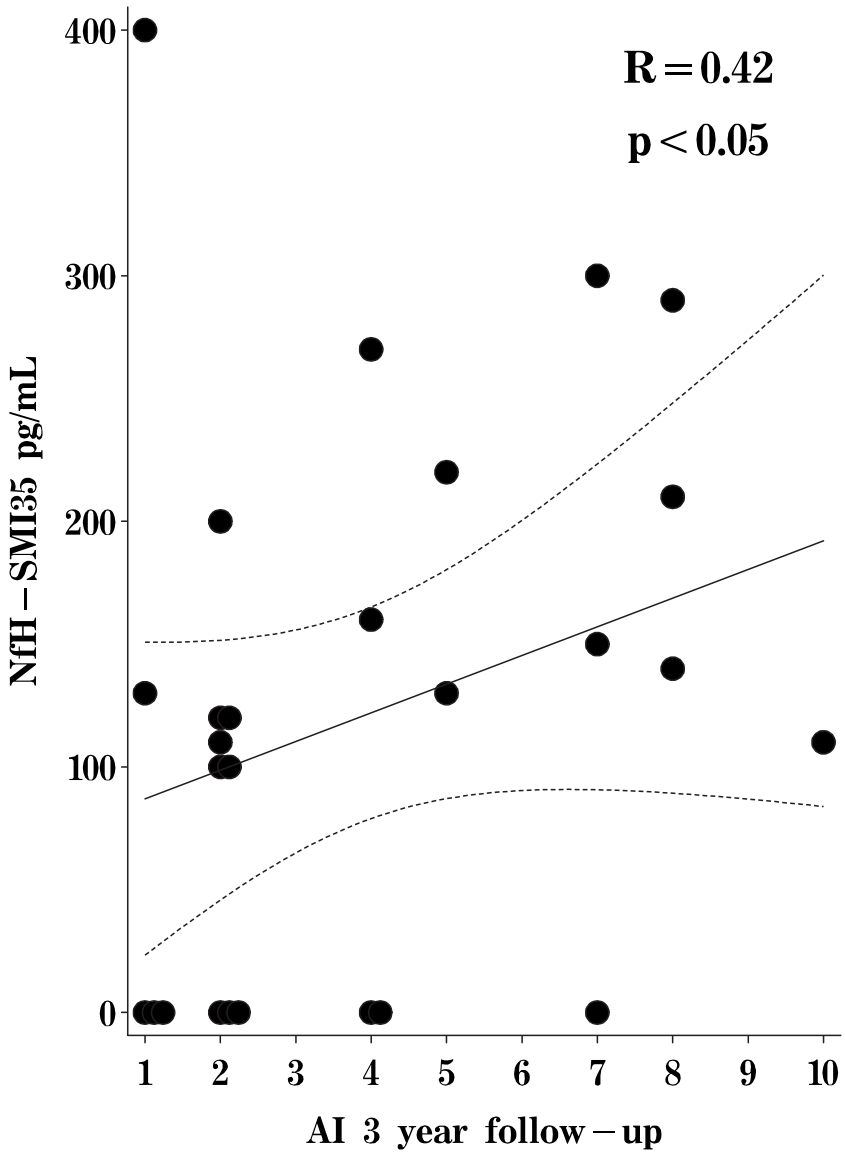

Figure 12.3: *Correlation between the NfH^{SMI35} and the AI at follow–up.*

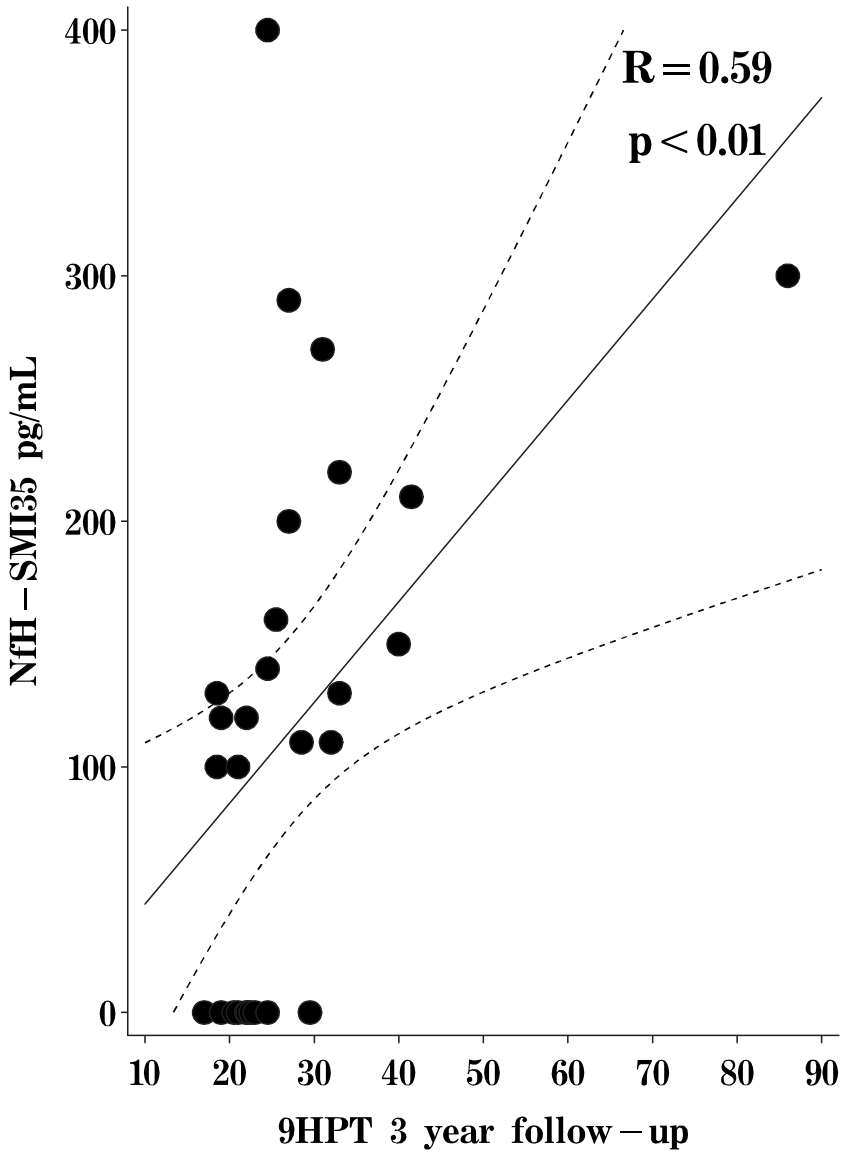

Figure 12.4: *Correlation between the NfH^{SMI35} and the 9HPT at follow–up.*

12.3.3 Early axonal injury: indicator of poor prognosis in RR MS

A significantly higher proportion 7/10 (70 percent) of RR MS versus 3/18 (17 percent) SP/PP patients progressed on the EDSS during the study ($p<0.001$). The median EDSS at 3–year follow–up was over 3-fold higher than at baseline for the advancing RR MS patients ($p<0.01$, Table 12.4). No significant change in the EDSS was observed for the SP/PP MS patients.

At follow–up all RR MS patients (7/7, 100 percent) who progressed had $NfH^{SMI35}_{baseline}$ levels above the assay sensitivity level (20 pg/mL, Figure 12.1, grey circles). None (0/3, 0 percent) of the clinically stable RR MS patients had $NfH^{SMI35}_{baseline}$ levels above this cut–off ($p<0.001$, Figure 12.1, open circles).

RR patients who converted to SP MS had higher baseline median NfH^{SMI35} levels when compared to non–converting RR patients, but this did not reach statistical significance (Table 12.3; Figure 12.1, circles with superimposed diamond).

Pooling RR and SP/PP MS patients in order to test for a general progression on the EDSS did not reveal any statistical significance for either NfH phosphoform, the ratio or change over time.

12.4 Discussion

The observation that NfH^{SMI35} levels were higher in SP/PP patients, who were more disabled compared to patients with RR MS, suggests that ax-

onal damage predominates in SP/PP MS. Additionally the significant higher proportion of SP/PP MS patients in whom NfH^{SMI35} levels increased from baseline when compared to RR patients suggests the accumulation of axonal injury during the 3–year observation period.

These findings provide further evidence that loss of neurological function is a consequence of axonal injury .[256,398,424] McDonald et al. (1992) hypothesised that axonal damage is a gradual cumulative process as the disease progresses.[258] However, uncertainty about this concept exists in the histological literature because some authors found little[106] whilst others found compelling evidence[398] for axonal damage in chronic lesions. This discrepancy may be due to the staining methods applied[399] and the dynamics of amyloid precursor protein which was used as a marker for axonal injury.[194] Our results would be in favour of cumulative axonal injury during SP/PP disease. A hypothesis supported by recent brain imaging studies.[31]

Interestingly, high CSF NfH^{SMI35} levels at the baseline were associated with the development of disability in RR MS patients 3 years later. Axonal staining for NfH^{SMI35} using the well–characterised Sternberger monoclonal antibodies[377,378] is an early sign of axonal injury[145] (Table 9.2 on page 177). This result confirms on a biochemical level the histological observation of axonal damage in acute lesions[42,106,398] and is consistent with the findings of Chapter 9. Those RR MS patients with elevated NfH$^{SMI35}_{baseline}$ levels advanced by a median of 2.5 points on the EDSS. Evidence of axonal damage early

in the disease course of RR MS should therefore be interpreted as a poor prognostic sign.

The correlation between $NfH^{SMI35}_{follow-up}$ and the EDSS extends this argument and confirms two previous reports on a different neurofilament subunit (the 68 kDa light chain, NfL) .[242,353] In the study of Lycke *et al.* CSF NfL correlated with the EDSS at baseline (R=0.27) and follow–up (R=0.34) in RR MS patients.[242] In the study by Semra *et al.* CSF NfL correlated with the EDSS (R=0.41) in progressive MS patients. Interestingly Trapp et. al (1998) described increased staining for hypophosphorylated NfH (SMI32 antibody) in demyelinated and transected axons as opposed to healthy axons.[398] Hypophosphorylated Nf are, however, prone to protease digestion[349,418] whilst the phosphorylated forms are relatively protected from proteolysis.[124,378] Phosphorylated NfH is reported to be more soluble then hypophosphorylated NfH or NfL.[403] Consequently the phosphorylated (NfH^{SMI35}) and extensively phosphorylated (NfH^{SMI34}) NfH phosphoforms have been measured.

The interpretation of the present data needs to take into account the fact that the patient group is population based (Chapter 10). Clinically there was no significant change in the EDSS of the SP/PP MS patients over 3 years. This represents a benign course compared to the more rapid progression observed in other cohorts of patients selected from hospital populations. The results must therefore be interpreted with caution and will need to be

cross–validated in other longitudinal studies. This would be particularly important for advancing the argument that axonal damage may accumulate despite a stable EDSS.

In contrast to RR MS patients no definite conclusion can yet be drawn regarding the prognostic value of high $NfH^{SMI35}_{baseline}$ levels in SP/PP MS patients. This might however be a consequence of the sensitivity of the clinical scales applied. The functional consequences of loss of axons on a clinical level will not necessarily be captured using the EDSS (as well as the AI or the 9HPT), particularly after an EDSS of 4–5 has been reached.[70,399] The EDSS in the SP/PP patients in this study was above this limit (median EDSS of 6 at baseline). The epidemiological observation that the disease course in MS progresses from EDSS 4 to 6 and from 6 to 7 with similar speed in SP/PP and RR patients[70] could thus be interpreted in 2 ways: Firstly the concept of inexorable axonal loss above a certain threshold[399] leads to SP disease, which is reflected by uniform progressing clinical disability.[70] Secondly these observations are biased by the method of quantification (EDSS), and the dynamics from axonal injury to axonal loss might provide a window for therapeutic intervention. The latter interpretation would be more in keeping with the binomial distribution observed for $NfH^{SMI35}_{baseline}$ in SP/PP MS patients in this study. However treatment with IFN in a small number of patients did not give rise to a significant change of CSF NfH phosphoform levels, but it is impossible to draw conclusions from this data.

Taking all these observations together, the results of this study are nevertheless in accordance with the current concept of progressive axonal degeneration in MS which is based on evidence from animal,[195] human post–mortem,[42,106,398] magnetic resonance spectroscopy,[409] magnetic resonance imaging[113,230,231,402] and epidemiological studies.[70,341]

The results of this prospective 3–year study further suggest that NfH^{SMI35} might be a valuable surrogate marker and has the potential to be used as a new secondary outcome measure in MS treatment trials. In addition CSF Nf levels may be used to select patients with a poor prognosis to improve the power of studies to detect a therapeutic effect in progressive MS. CSF levels of NfH phosphoforms could be exploited for evaluating neuroprotective treatment strategies in MS and potentially other neurodegenerative diseases.

12.5 Conclusion

This study aimed to investigate the relation of neurofilament phosphoforms as biomarkers for axonal injury to (1) disease heterogeneity, (2) disability and (3) as prognostic indicators.

A significantly higher proportion of patients with SP/PP disease experienced an increase in NfH^{SMI35} levels between baseline and follow–up compared to those who remained with RR disease. SP/PP patients at baseline and follow–up were found to have higher NfH^{SMI35} levels than stable RR MS patients at baseline or RR MS patients at follow–up. Median NfH^{SMI35} levels

at baseline were significantly higher in clinically advancing RR MS versus stable RR MS patients. NfH^{SMI35} correlated with the EDSS (R=0.54, p<0.01), the AI (R=0.42, p<0.05) and the 9HPT (R=0.59, p<0.01) at follow–up. The degree of phosphorylation (ratio) correlated with the EDSS (R=0.52, p<0.05) and ΔNfH^{SMI35} with the 9HPT (R=0.39, p<0.05).

The increase of Nf during the progressive phase of the disease together with the correlation of NfH^{SMI35} with all clinical scales at follow–up suggests that cumulative axonal loss is responsible for sustained disability. The results also suggest that early axonal injury is a poor prognostic sign. Measurement of NfH phosphoforms could be exploited for evaluating neuroprotective treatment strategies in those neurological disorders where axonal degeneration is of pathological relevance.

Part IV

Discussion

Chapter 13

General discussion

The diagnosis of MS is made on the basis of the appearance of demyelinating lesions separated by time and space.[257,311] The term multiple sclerosis provides most probably an umbrella for a heterogeneous group of CNS demyelinating diseases sharing certain pathological (Figure 1.4 on page 38) and phenotypical (Table 10.1 on page 209) features. The clinical course of MS is variable and classified into different patterns of progression of disability (Figure 1.1 on page 23).[236] The clinical course and prognosis remain difficult to predict.

This Ph.D. aimed to investigate whether the analysis of brain–specific proteins could contribute to a better understanding of two issues: *disease heterogeneity* and *disability*.

The purpose of the general discussion is to put the results obtained in the different chapters into a broader context. This will be accomplished by firstly comparing the consistency of the models studied, secondly by evaluating the value of BSP as biomarkers to describe disease heterogeneity and thirdly by

discussing the concept of BSP as surrogate markers for disability. Finally the advantages and disadvantages for each BSP as a surrogate marker will be summarised.

13.1 Consistency of the models studied

The basic idea followed in this subsection is, that for each BSP investigated the CV provides an estimate of the accuracy of the method upon the model studied. Three different models have been used in this Ph.D. project. Table 13.1 and Table 13.2 summarise the CVs found for each experiment. The lowest CVs were found for the mouse model with a range from 18.5–56.3. In the post–mortem study the CV ranged from 16.2–139.9 and in the human CSF study from 26.6–206.9. The methodological advantage of the mouse model was that tissue could be snap frozen directly after the animal was killed. For the post–mortem study a considerable variation of the post–mortem interval had to be taken into account. During the post–mortem interval auto–proteolysis of the brain poses a serious problem in particular for the analysis of proteins more susceptible to proteolysis. What are the implications for the results of Chapter 8 to 10?

Table 13.1: *The coefficient of variation (CV) of the results for the BSP studied in Chapter 8 to 10. The sample size (n) for each CV is given in brackets. P.M. = post–mortem, N.D. = not determined.*

Model	**Type**	**S100B**	**GFAP**	**Ferritin**	**NfH**^{SMI35}	**NfH**^{SMI34}
Mouse	CTRL	40.1 (7)	35.9 (7)	37.0 (7)	18.5 (7)	N.D.
Mouse	CREAE	45.4 (8)	56.3 (8)	34.0 (8)	53.9 (8)	N.D.
P.M.	NCWM	53.0 (5)	77.7 (5)	27.3 (5)	62.8 (6)	88.0 (6)
P.M.	MS (all)	41.0 (23)	64.5 (23)	44.3 (23)	136.8 (30)	136.0 (30)
P.M.	NAWM	42.5 (5)	100.0 (5)	30.0 (5)	71.4 (6)	75.1 (6)
P.M.	AL	16.2 (6)	35.7 (6)	48.0 (6)	94.8 (6)	51.3 (6)
P.M.	SAL	21.8 (4)	32.9 (4)	26.8 (4)	94.4 (6)	109.1 (6)
P.M.	CL	45.0 (7)	71.3 (7)	54.2 (7)	39.5 (6)	85.7 (6)

Table 13.2: *The coefficient of variation (CV) of the results for the different methods used to characterise MS patients. The sample size (n) for each CV is given in brackets.*

Method	**MS (all)**	**RR MS**	**SP MS**	**PP MS**
S100B	87.8 (51)	101.4 (20)	71.1 (21)	33.4 (10)
GFAP	105.6 (51)	90.0 (20)	119.7 (21)	114.1 (10)
Ferritin	75.3 (51)	85.6 (20)	74.6 (21)	52.0 (10)
NfH^{SMI34}	177.7 (51)	206.9 (20)	87.7 (21)	71.5 (10)
NfH^{SMI35}	78.3 (51)	84.8 (20)	67.0 (21)	91.4 (10)

Statistically the variation of the range of the CVs was reflected by the strength of the correlations found between the BSP. Although overall consistency was found for the investigation of tissue homogenate (Table 9.6 on page 206), the strengths of the correlations varied. For the mouse model the Spearman correlation coefficient ranged from R=0.81 to R=0.92 and there was one negative correlation with an R=-0.54 (Figure 8.7 on page 169). For the post–mortem study the Spearman correlation coefficient ranged from R=0.45 to R=0.64 (Figure 9.8–9.16 on page 194–202). Apart from a pseudocorrelation between NfH^{SMI35} and S100B with R=-0.3 (Chapter 10.3 on page 213) no such correlations were found in the CSF study. What conclusions can be drawn from the comparison of these data?

The CSF represents an overall average of proteins released from different lesion types. Furthermore the metabolism and the dynamics of these proteins through the CSF are different. The highly soluble S100B diffuses within minutes into the systemic circulation,[11] whilst less soluble proteins of higher molecular weight such as GFAP and NfH have different physiological dynamics.[104] The conclusion for future studies aiming to investigate the the relations between different BSP to each other is that a mouse model and possibly cell–cultures have to be regarded as a more reproducible model than human post–mortem material or CSF.

13.2 Disease heterogeneity

Disease heterogeneity in MS is observed by almost all clinical and paraclinical methods. From the review of the literature (Chapter 1.1 on page 24 ff.) it appeared that heterogeneity is greater in early MS.[12,30,78,84,184,187,247,310,330,342,344,427,427,444] In later disease stages heterogeneity seems to decrease. Epidemiological studies are in line with this concept and provided evidence that with the increase of disability a common final (degenerative ?) pathway might be present[68–70] (Figure 1.4 on page 38). This hypothesis is supported by pathological studies.[41,201,237,398] Schuller (1973) coined the term "MS a two–phase disease" .[351] Steinman (2001) recently reintroduced this terminology as "MS a two–stage disease".[375]

The results from the animal study are consistent with this concept. The

atrophied CREAE spinal cord could be distinguished from the control animals (Table 8.1 on page 163). GFAP was higher in the atrophied and gliotic spinal cord then in control animals. S100B, ferritin and NfH^{SMI35} were lower in the atrophic spinal cord.

In the post–mortem study AL, SAL, NCWM and MSGM could be distinguished with the aid of BSP (Table 9.4 on page 184 and Table 9.5 on page 186). In brief, the findings were that S100B, NfH^{SMI34} and NfH^{SMI35} were elevated in AL. Ferritin was generally higher in all MS lesions when compared to control tissue. GFAP and S100B were higher in MSGM when compared to control tissue. However, as suggested in the discussion of the consistency of the model (section 13.1) the distinction was less clear than for the animal experiment.

In MS patients there was a trend for increasing S100B levels from PP to SP to RR MS patients (Table 10.4 on page 214). This trend became more evident using a ratio of $\frac{S100B}{ferritin}$ (Figure 10.6 on page 222). However, the underlying pathology in MS patients when estimated by the measurement of CSF BSP does not permits us to distinguish the between subgroups as proposed by Lublin *et al.* (1996).[236] The measurement of BSP is more likely to be of value as a surrogate marker for disability as summarised in the next section.

13.3 Disability

Disability (i.e. "a restriction or lack... of ability to perform an activity in the manner of within the range considered normal for a human being")[300] is probably the most devastating result of MS in the life of a patient. Where cure is not possible, treatment should aim at holding or slowing down the progression of disability. The main caveat of surrogate markers currently used is that the most accurate relation is found between MRI measurements of atrophy and disability as estimated by clinical scales.[31,274] Correlation of other MRI measures with disability have been rather weak .[183] Consequently the value of MRI as a secondary outcome measure of MS trial has been discussed.[260] The conclusion was drawn that at present no single MRI measurement has been validated as a tool for distinguishing clinical subgroups of MS with acceptable speceficity. However, the use of multiple, new scanning sequences was put up higher on the research agenda.[260]

The problem using MRI measurements of CNS atrophy is that atrophy is non–reversible. The concept of biological surrogate markers tries to close this gap by enabling to monitor subclinical but relevant damage to the CNS.

The hypotheses behind employing BSP as surrogate markers in MS (Chapter 3 on page 69) were, in brief:

- Nf is a marker for axonal damage and should relate to disability
- GFAP is a measure for astrogliosis and should relate to the "total

lesion load" and relate indirectly to disability

- S100B is a measure of astrocytic activation and should be higher in patients with active disease

- Ferritin is a measure of microglial activation and should be higher in patients with active disease

The data presented in this study and the literature (see Tables 1.2 to 1.4 on pages 45–48, Table 11.2 on page 236, Table 12.3 on page 247 and Table 12.4 on page 248) show considerable variability in the strength of the assumed correlations between BSP and disability as estimated by clinical scales. The explanation that this was due to the different methods applied, would only be valid for the comparisons of studies between different groups.[241,307,353] It would however not explain the variability found for the present longitudinal data (Chapter 12). The present data suggest that axonal pathology might be a dynamic process. Degenerative and regenerative processes could be balanced, at least for a certain time. It was noted that once a critical threshold is reached, the inexorable loss of axons and neurons which had been integrated into the functional CNS network would surpass the potential for plasticity. It was hypothesised that this phase could possibly be reflected by the epidemiological finding that above an EDSS of about 4 the disease progress is uniform and inexorable.[70]

Taking these together the current concept of surrogate markers has an

important shortcoming: *it does not allow for improvement*. In other words the hypothesis that elevated levels of certain substances inevitable demonstrates damage which leads to irreversible disability might only be partly valid. In theory elevated levels of Nf could result from either release from a disintegrating axon or the growth cone of a regenerating axon. Similarly one could hypothesise that S100B could indicate astrocytic activation in response to damage, but also a physiological response necessary to for supplying regenerating axons with growth factors.[86] Neuroprotective properties are now attributed to a range of substances and mechanisms which have previously been related only to CNS tissue damage.[108,161,186,291]

In order to allow for these possibilities a concept of a surrogate which is expected to correlate more consistently with clinical measurements of disability should include a combination of markers for degeneration and regeneration. Two theoretical models for the interpretation of surrogate markers are postulated:

1. **A one–factor model:** Tissue damage leads to release of substances such as BSP. Therefore the quantification of BSP allows us to estimate the extent of CNS tissue damage. One would expect to find a relationship of baseline damage with disability at future time points as demonstrated for MRI measurements.[49] BSP could potentially be included as a secondary outcome measure in MS treatment trials. The hypothesis would be that an effective treatment reduces the levels of

BSP into the range found in normal control subjects.

2. **A two–factor model:** In the CNS, both tissue damage and regeneration lead to release of substances such as BSP. In order to maintain the plasticity of the CNS a permanent remodelling of the axon–dendritic tree can be expected.[4,63,178,180] The use of at least 2 functionally distinct isoforms of one protein could provide a way around the shortcomings of a linear model. One isoform would need to be predominantly released during tissue damage, whilst the other isoform would increase during regeneration. The advantage of quantifying different isoforms of one protein as opposed to different proteins is that molecular size, solubility, metabolism and therefore the physiological dynamics are likely to be similar, even though both protein isoforms would originate from the same cellular source. A ratio of the "degenerative isoform A" to the "regenerative isoform B" would then indicate the predominant pathological feature. Furthermore the measurement of these 2 isoforms at 2 time–points would allow to estimate the dynamics of these proteins over time. For the evaluation of treatment trials the dynamic model would allow us to define secondary outcome measures for halting disease progression and enhancement of neuroprotective features.

In conclusion a simple one–factor approach seems to be feasible in acute conditions (e.g. frequently relapsing MS) and can expected to be of great

value for neurological intensive care (e.g. subarachnoid–hemorrhage, traumatic brain injury and stroke). A more sophisticated two–factor approach, allowing for the dynamics of degeneration and regeneration would be of value for assessing more chronic conditions, such as present in the relapse independent progression of disability in MS.

13.4 The value of BSP as surrogate markers

13.4.1 Neurofilament proteins

CSF levels of NfH^{SMI35} correlated with disability in MS. This finding is consistent with two previous studies.[242,353] Additionally NfH^{SMI35} predicted development of disability in RR MS patients. NfH phosphoforms did not distinguish between MS subgroups on a cross–sectional basis, which is in keeping with one previous report.[353] However, there was evidence for increasing NfH^{SMI35} levels over time in progressive MS patients suggesting accumulation of axonal damage.

CSF NfH^{SMI35} should be regarded as a sensitive marker for axonal damage. The clinical value is likely to be the long–term prediction of disability. Correlations with disability should be regarded with caution as they might be a spurious finding. There is no evidence that NfH^{SMI35} could be a disease specific or diagnostic marker.

In this respect the finding of markedly elevated levels in SAH and in some GBS patients (Figure 4.23 on page 112) is of particular interest. NfH^{SMI35} might be an early indicator of axonal variant of GBS.[103]

13.4.2 Glial fibrillary acidic protein

CSF GFAP levels correlated with disability in progressive patients. The correlation with disability is consistent with the finding of the only other published study investigating this relationship.[336] GFAP did not distinguish between MS subgroups which is consistent with the only published study allowing for such a comparison.[5]

It is therefore of note that elevated CSF GFAP levels were found in another chronic progressive CNS disease, dementia (Figure 5.11 on page 142). However as the same Figure showed high CSF GFAP levels were also found in acute disorders such as SAH or TBI. Therefore CSF GFAP levels cannot be regarded as a "pure" marker for astrogliosis and the interpretation of the levels needs to be done in the light of any other acute CNS insult. In MS particular attention needs to be paid to the presence of relapses as revealed by either MRI or clinical observation.

CSF GFAP levels could be a marker for disability in relapse–free MS patients who have reached the progressive phase of the disease. However, the relation between CSF GFAP and disability is likely to reflect the "burnt–out" phase of the disease. Therefore the prognostic value of measuring CSF GFAP levels remains questionable.

13.4.3 S100B protein

CSF S100B levels were higher in MS patients than in controls, which is consistent with most[211,250,251,270] but not all[363] previous studies. This difference was explained by the higher S100B levels in RR MS patients. Although there was no clinical evidence for recent relapses in the present RR MS patient, the post–hoc analysis of the data from the literature indicated that elevated CSF S100B were associated to acute disease.[251,270,278] This notion is largely supported by studies into acute neurological disorders.[37,147,148,163,314,338,354,421]

CSF S100B should be regarded as a sensitive marker for acute impairment of CNS homeostasis. This can be caused by a wide range of conditions and CSF S100B is not a disease specific marker. In MS CSF S100B and possibly serum S100B might however prove a valuable indicator of relapses. There might also be a potential for identifying those patients with a higher disease activity, which might escape MRI or clinical observations, but who would profit and respond to early treatment. CSF S100B might become the "CRP of the brain". The biochemical advantages are high solubility, small molecular size and stability. The investigation of S100B levels in various body fluids and various diseases will become increasingly important.

13.4.4 Ferritin

CSF ferritin levels were higher in SP MS patients then in control patients which is consistent with the finding of elevated CSF ferritin levels in progressive MS patients.[222]

Because ferritin is primarily involved in iron metabolism, CSF ferritin has been shown to be elevated in patients with evidence for intracerebral bleed. Ferritin is of particular importance for diagnosing occult bleeding, such as present in CNS siderosis. Secondly ferritin is involved in the metabolism of myelin proteins by distributing iron as an essential cofactor and increased endocytotic ferritin uptake could be demonstrated in oligodendrocyte progenitor cells .[71,159] As outlined in the introduction (on page 66) oligodendrocytes contain the ferritin heavy chain (FTH), whilst microglia also express the light chain (FTL).

The role for measuring CSF ferritin in MS is not yet clarified, but it would be worthwhile to investigate if measurement of FTL and FTH would permit to identify MS patients with different potential to remyelinate. FTL and FTH are two candidates which should be investigated in a two–factor model model for surrogate markers as proposed above.

Bibliography

[1] S Acerklay, AJ Grierson, J Brownless, et al. Glutamate slows axonal transport of neurofilaments in transfected neurons. *J Cell Biol*, 150:165–176, 2000.

[2] C Adami, G Sorci, E Blasi, AL Agneletti, F Bistoni, and R Donato. S100B expression in and effects on microglia. *Glia*, 33:131–42, 2001.

[3] G Ahlsen, L Rosengren, M Belfrage, A Palm, K Haglid, A Hamberger, and C Gillberg. Glial fibrillary acidic protein in the cerebrospinal fluid of children with autism and other neuropsychiatric disorders. *Biol Psychiatry*, 33:734–743, 1993.

[4] L Aigner, S Arber, JP Kapfhammer, T Laux, C Schneider, F Botteri, HR Brenner, and P Caroni. Overexpression of the neural growth-associated protein GAP-43 induces nerve sprouting in the adult nervous system of transgenic mice. *Cell*, 83:269–278, 1995.

[5] M Albrechtsen and E Bock. Quantification of glial fibrillary acidic protein (GFAP) in human- body fluids by means of elisa employing a monoclonal-antibody. *J Neuroimmunol*, 8:301–309, 1985.

[6] M Albrechtsen, E Bock, and B Norgaardpedersen. Glial fibrillary acidic protein in amniotic fluids from pregnancies with fetal neural-tube defects. *Prenatal Diagnosis*, 4:405–410, 1984.

[7] M Albrechtsen, PS Sorensen, F Gjerris, and E Bock. High cerebrospinal–fluid concentration of glial fibrillary acidic protein (GFAP) in patients with normal pressure hydrocephalus. *J Neurol Sci*, 70:269–274, 1985.

[8] M Albrechtsen, AC von Gerstenberg, and E Bock. Mouse monoclonal antibodies reacting with human brain glial fibrillary acidic protein. *J Neurochem*, 42:86–93, 1984.

[9] H Aldskogius and EN Kozlova. Central neuron-glial and glial-glial interactions following axon injury. *Progress Neurobiology*, 55:1–26, 1998.

[10] M Ali, M Harmer, and R Vaughan. Serum S100 protein as a marker of cerebral damage during cardiac surgery. *Br J Anaesth*, 85:287–298, 2000.

[11] SM Ali, M Harmer, RS Vaughan, J Dunne, and IP Latto. Early release pattern of S100 protein as a marker of brain damage after warm cardiopulmonary bypass. *Anaesthesia*, 55:802–806, 2000.

[12] IV Allen, G Glover, and R Anderson. Abnormalities in the macroscopically normal white matter in cases of mild or spinal multiple sclerosis. *Acta Neuropathol (Berl)*, suppl VII:176–178, 1981.

[13] M Alter, TN Bryne, Daube JR, et al. Practice advisory on selection of patients with multiple sclerosis for treatment with Betaseron Report of the Quality Standards Subcommittee of the American Academy of Neurology. *Neurology*, 44:1537–1540, 1994.

[14] MP Amato and G Ponziani. Quantification of impairment in MS: discussion of the scales in use. *Mult Scler*, 5:216–219, 1999.

[15] RE Anderson, LO Hansson, J Liska, G Settergren, and J Vaage. The effect of cardiotomy suction on the brain injury marker S100beta after cardiopulmonary bypass. *Ann Thorac Surg*, 69:847–850, 2000.

[16] M Andersson, J Alvarez-Cermeno, G Bernardi, I Cogato, P Fredman, J Frederiksen, S Fredrikson, P Gallo, LM Grimaldi, M Gronning, et al. Cerebrospinal fluid in the diagnosis of multiple sclerosis: a consensus report. *J Neurol Neurosurg Psychiatry*, 57:897–902, 1994.

[17] BH Anderton, D Breinburg, MJ Downes, PJ Green, BE Tomlinson, J Ulrich, JN Wood, and J Kahn. Monoclonal antibodies show that neurofibrillary tangles and neurofilaments share antigenic determinants. *Nature*, 298:84–6, 1982.

[18] LC Ang, DG Munoz, D Shul, and DH George. SMI-32 immunoreactivity in human striate cortex during postnatal development. *Brain Res Dev Brain Res*, 61:103–9, Jul 1991.

[19] DR Archer, DF Watson, and JW Griffin. Phosphorylation-dependent immunoreactivity of neurofilaments and the rate of slow axonal-transport in the central and peripheral axons of the rat dorsal-root ganglion. *J Neurochem*, 62:1119–1125, 1994.

[20] DL Arnold, N de Stefano, PM Matthews, and BD Trapp. N-acetylaspartate: usefulness as an indicator of viable neuronal tissue. *Ann Neurol*, 50:823; discussion 824–805, 2001.

[21] Ak Ashbury, MK Gale, SC Cox, JR Baringer, and BO Berg. Giant axonal neuropathy: a unique case with segmental neurofilamentous masses. *Acta Neuropathol*, 20:237–247, 1972.

[22] A Aurell, LE Rosengren, B Karlsson, et al. Determination of S-100 and glial fibrillary acid protein concentration in cerebrospinal fluid after brain infarction. *Stroke*, 22:1254–1258, 1991.

[23] L Autilio-Gambetti, P Gambetti, and RC Crane. *Biological aspects of Alzheimer's disease*, chapter Paired helical filaments: relatedness to neurofilaments shown by silver staining and reactivity with monoclonal antibodies, pages 117–124. Cold Spring Harbor Laboratory, New York, 1983.

[24] AM Avellino, D Hart, AT Dailey, M MacKinnon, D Ellegala, and M Kliot. Differential macrophage response in the peripheral and central nervous system during wallerian degeneration of axons. *Experimental Neurology*, 136:183–198, 1995.

[25] O Bagasra, FH Michaels, YM Zheng, LE Bobroski, SV Spitsin, ZF Fu, R Tawadros, and H Koprowski. Activation of the inducible form of nitric oxide synthase in the brains of patients with multiple sclerosis. *Proc Natl Acad Sci USA*, 92:12041–12005, 1995.

[26] D Bahner, C Klucke, B Kitze, E Elitok, T Bogumil, A Dressel, H Tumani, F Weber, S Poser, and A Bitsch. Interferon-beta-1b increases serum interleukin-12 p40 levels in primary progressive multiple sclerosis patients. *Neurosci Lett*, 326:125–108, 2002.

[27] NP Bajaj and CC Miller. Phosphorylation of neurofilament heavy-chain side-arm fragments by cyclin-dependent kinase-5 and glycogen synthase kinase-3alpha in transfected cells. *J Neurochem*, 69:737–743, 1997.

[28] D Baker, JK O'Neill, SE Gschmeissner, CE Wilcox, C Butter, and JL Turk. Induction of chronic relapsing experimental allergic encephalomyelitis in Biozzi mice. *J Neuroimmunol*, 28:261–270, 1990.

[29] D Baker, G Pryce, JL Croxford, et al. Cannabinoids control spasticity and tremor in a multiple sclerosis model. *Nature*, 404:84–87, 2000.

[30] J Balo. Encephalitis periaxialis continua. *Arch Neurol*, 19:242–263, 1928.

[31] F Barkhof. The clinico–radiological paradox in multiple sclerosis. *Curr Opin Neurol*, 15:239–245, 2002.

[32] A Basu, JK Krady, M O'Malley, SD Styren, ST DeKosky, and SW Levison. The type 1 interleukin-1 receptor is essential for the efficient activation of microglia and the induction of multiple proinflammatory mediators in response to brain injury. *J Neurosci*, 22:6071–6082, 2002.

[33] J Baudier, C Delphin, D Grunwald, S Khochbin, and JJ Lawrence. Characterization of the tumor suppressor protein p53 as a protein kinase C substrate and a S100b–binding protein. *Proc Natl Acad Sci USA*, 89:11627–11631, 1992.

[34] JM Beaulieu, MD Nguyen, and JP Julien. Late onset death of motor neurons in mice overexpressing wild-type peripherin. *J Cell Biol*, 147:531–544, 1999.

[35] J Beck, P Rondot, L Catinot, et al. Increased production of interferon gamma and tumor necrosis factor preceedes clinical manifestation in multiple sclerosis: Do cytokines trigger off exacerbations? *Acta Neurol Scand*, 78:318–323, 1988.

[36] JC Betts, WP Blackstock, MA Ward, and BH Anderton. Identification of phosphorylation sites on neurofilament proteins by nanoelectrospray mass spectrometry. *J Biol Chem*, 272:12922–12907, 1997.

[37] P Biberthaler, T Mussack, E Wiedemann, KG Kanz, M Koelsch, C Gippner-Steppert, and M Jochum. Evaluation of S-100b as a specific marker for neuronal damage due to minor head trauma. *World J Surg*, 25:93–7, 2001.

[38] B Bielekova and R Martin. Multiple sclerosis: Immunotherapy. *Curr Treat Options Neurol*, 1:201–220, 1999.

[39] A Bitsch and W Bruck. Differentiation of multiple sclerosis subtypes: implications for treatment. *CNS Drugs*, 16:405–418, 2002.

[40] A Bitsch, J Schuchard, S Bunkowski, T Kuhlmann, and W Brück. Acute axonal injury in multiple sclerosis: correlation with demyelination and inflammation. *Brain*, 123:1174–1183, 2000.

[41] C Bjartmar, G Kidd, S Mork, R Rudick, and BD Trapp. Neurological disability correlates with spinal cord axonal loss and reduced N-acetyl aspartate in chronic multiple sclerosis patients. *Ann Neurol*, 48:893–901, 2000.

[42] C Bjartmar, RP Kinkel, G Kidd, RA Rudick, and BD Trapp. Axonal loss in normal-appearing white matter in a patient with acute MS. *Neurology*, 57:1248–1252, 2001.

[43] C Bjartmar and BD Trapp. Axonal and neuronal degeneration in multiple sclerosis: mechanisms and functional consequences. *Curr Opin Neurol*, 14:271–208, 2001.

[44] M Blennow, H Hagberg, and L Rosengren. Glial fibrillary acidic protein in the cerebrospinal-fluid - a possible indicator of prognosis in full-term asphyxiated newborn-infants. *Ped Res*, 37:260–264, 1995.

[45] S Blomquist, P Johnsson, C Luhrs, G Malmkvist, JO Solem, C Alling, and E Stahl. The appearance of S-100 protein in serum during and immediately after cardiopulmonary bypass surgery: a possible marker for cerebral injury. *J Cardiothorac Vasc A*, 11:699–703, 1997.

[46] P Bomont, L Cavalier, F Blondeau, C Ben Hamida, S Belal, M Tazir, E Demir, H Topaloglu, R Korinthenberg, B Tuysuz, P Landrieu, F Hentati, and M Koenig. The gene encoding gigaxonin, a new member of the cytoskeletal BTB/kelch repeat family, is mutated in giant axonal neuropathy. *Nat Genet*, 26:370–374, 2000.

[47] TW Bouldin, TS Earnhardt, and ND Goines. Sequential changes in the permeability of the blood–nerve barrier over the course of ricin neuronopathy in the rat. *Neurotoxicology*, 11:23–34, 1990.

[48] W Brück, M Schmied, G Suchanek, et al. Oligodendrocytes in the early course of multiple sclerosis. *Ann Neurol*, 35:65–73, 1994.

[49] PA Brex, O Ciccarelli, JI O'Riordan, M Sailer, AJ Thompson, and DH Miller. A longitudinal study of abnormalities on MRI and disability from multiple sclerosis. *N Engl J Med*, 346:158–64, 2002.

[50] PA Brex, GJ Parker, SM Leary, PD Molyneux, GJ Barker, CA Davie, AJ Thompson, and DH Miller. Lesion heterogeneity in multiple sclerosis: a study of the relations between appearances on T1 weighted images, T1 relaxation times, and metabolite concentrations. *J Neurol Neurosurg Psychiatry*, 68:627–632, 2000.

[51] H Brisby, K Olmarker, L Rosengren, CG Cederlund, and B Rydevik. Markers of nerve tissue injury in the cerebrospinal fluid in patients with lumbar disc herniation and sciatica. *Spine*, 24:742–746, 1999.

[52] W Bruck, P Porada, S Poser, P Rieckmann, F Hanefeld, HA Kretzschmar, and H Lassmann. Monocyte/macrophage differentiation in early multiple sclerosis lesions. *Ann Neurol*, 38:788–796, 1995.

[53] P A Calabresi, L R Tranquill, H F McFarland, and E P Cowan. Cytokine gene expression in cells derived from csf of multiple sclerosis patients. *J Neuroimmunol*, 89:198–205, 1998.

[54] DR Campbell, BS Skikne, and JD Cook. Cerebrospinal fluid ferritin levels in screening for meningism. *Arch Neurol*, 43:1257–1260, 1986.

[55] MJ Campbell, PR Hof, and JH Morrison. A subpopulation of primate corticocortical neurons is distinguished by somatodendritic distribution of neurofilament protein. *Brain Res*, 539:133–106, 1991.

[56] MJ Campbell and JH Morrison. Monoclonal antibody to neurofilament protein (SMI-32) labels a subpopulation of pyramidal neurons in the human and monkey neocortex. *J Comp Neurol*, 282:191–205, 1989.

[57] PB Carrieri, V Provitera, T De Rosa, G Tartaglia, F Gorga, and O Perrella. Profile of cerebrospinal fluid and serum cytokines in patients with relapsing-remitting multiple sclerosis: a correlation with clinical activity. *Immunopharmacol Immunotoxicol*, 20:373–382, 1998.

[58] R Carswell. *Pathological anatomy: illustrations on elementary forms of disease*. London: Longman, 1838.

[59] M Charcot. Histologie de la sclérose en plaques (i). *Gazette des hopitaux*, 14:554–555, 1868.

[60] M Charcot. Histologie de la sclérose en plaques (ii). *Gazette des hopitaux*, 14:557–558, 1868.

[61] M Charcot. Leçons sur les maladies chroniques du système nerveux: I – Des scléroses de la moelle épinière. *Gazette des hopitaux*, 14:405–406, 554–555, 557–558, 566, 1868.

[62] P Cheepsunthorn, C Palmer, S Menzies, RL Roberts, and JR Connor. Hypoxic/ischemic insult alters ferritin expression and myelination in neonatal rat brains. *J Comp Neurol*, 431:382–396, 2001.

[63] MS Chen, AB Huber, ME van der Haar, M Frank, L Schnell, AA Spillmann, F Christ, and ME Schwab. Nogo-A is a myelin-associated neurite outgrowth inhibitor and an antigen for monoclonal antibody IN-1. *Nature*, 403:434–409, 2000.

[64] M Clerici, M Saresella, D Trabattoni, L Speciale, S Fossati, S Ruzzante, R Cavaretta, M Filippi, D Caputo, and P Ferrante. Single-cell analysis of cytokine production shows different immune profiles in multiple sclerosis patients with active or quiescent disease. *J Neuroimmunol*, 121:88–101, 2001.

[65] PR Cody and JK Smith. *Applied Statistics and the SAS Programming Language*. Prentice-Hall, Upper Saddle River, New Jersey 07458, 4th edition, 1997.

[66] MP Coleman, L Conforti, EA Buckmaster, A Tarlton, RM Ewing, MC Brown, MF Lyon, and VH Perry. An 85-kb tandem triplication in the slow Wallerian degeneration (Wld(s)) mouse. *Proc Natl Acad Sci USA*, 95:9985–9990, 1998.

[67] M Comabella, J Imitola, HL Weiner, and SJ Khoury. Interferon-beta treatment alters peripheral blood monocytes chemokine production in MS patients. *J Neuroimmunol*, 126:205–212, 2002.

[68] C Confavreux, M Hutchinson, M M Hours, P Cortinovistourniaire, and T Moreau. Rate of pregnancy-related relapse in multiple sclerosis. *New Eng J Med*, 339:285–291, 1998.

[69] C Confavreux and S Vukusic. Natural history of multiple sclerosis: implications for counselling and therapy. *Curr Opin Neurol*, 15:257–266, 2002.

[70] C Confavreux, S Vukusic, T Moreau, and P Adeleine. Relapses and progression of disability in multiple sclerosis. *N Engl J Med*, 343:1430–1438, 2000.

[71] JR Connor and SL Menzies. Relationship of iron to oligodendrocytes and myelination. *Glia*, 17:83–93, 1996.

[72] LC Cork, NH Sternberger, LA Sternberger, MF Casanova, RG Struble, and DL Price. Phosphorylated neurofilament antigens in neurofibrillary tangles in Alzheimer's disease. *J Neuropathol Exp Neurol*, 45:56–64, 1986.

[73] LC Cork, NH Sternberger, LA Sternberger, et al. Phosphorylated neurofilament antigens in neurofibrillary tangles in alzheimer's disease. *J Neuropath Exp Neurol*, 45:56–64, 1986.

[74] S Couillard-Despres, Q Zhu, PC Wong, DL Price, DW Cleveland, and JP Julien. Protective effect of neurofilament heavy gene overexpression in motor neuron disease induced by mutant superoxide dismutase. *Proc Natl Acad Sci USA*, 95:9626–9630, 1998.

[75] A Cozzi, B Corsi, S Levi, P Santambrogio, A Albertini, and P Arosio. Overexpression of wild type and mutated human ferritin H-chain in HeLa cells: in vivo role of ferritin ferroxidase activity. *J Biol Chem*, 275:25122–25109, 2000.

[76] J Curveilhier, editor. *Anatomie pathologique du crops humain.* Paris: Bailliere, 1841.

[77] GR Cutter, ML Baier, RA Rudick, DL Cookfair, JS Fischer, J Petkau, K Syndulko, BG Weinshenker, JP Antel, C Confavreux, GW Ellison, F Lublin, AE Miller, SM Rao, S Reingold, A Thompson, and E Willoughby. Development of a multiple sclerosis functional composite as a clinical trial outcome measure. *Brain*, 122:871–882, 1999.

[78] RC Dale, C de Sousa, WK Chong, TC Cox, B Harding, and BG Neville. Acute disseminated encephalomyelitis, multiphasic disseminated encephalomyelitis and multiple sclerosis in children. *Brain*, 123 Pt 12:2407–2422, 2000.

[79] CM Dalton, PA Brex, KA Miszkiel, et al. Application of the new McDonald criteria to patients with clinically isolated syndromes suggestive of multiple sclerosis. *Ann Neurol*, 52:47–53, 2002.

[80] SE Davies, J Newcombe, SR Williams, WI McDonald, and JB Clark. High resolution proton NMR spectroscopy of multiple sclerosis lesions. *J Neurochem*, 64:742–748, 1995.

[81] J Dawson. The histology of disseminated sclerosis. *Trans Royal Soc Edin*, 50:517–740, 1916.

[82] P De Jonghe, I Mersivanova, E Nelis, J Del Favero, JJ Martin, C Van Broeckhoven, O Evgrafov, and V Timmerman. Further evidence that neurofilament light chain gene mutations can cause Charcot-Marie-Tooth disease type 2E. *Ann Neurol*, 49:245–249, 2001.

[83] E Debus, K Weber, and M Osborn. Monoclonal antibodies specific for glial fibrillary acidic (GFA) protein and for each of the neurofilament triplet polypeptides. *Differentiation*, 25:193–203, 1983.

[84] E Devic. Myélite aiguë compliequée de névrite optique. *Bull Méd*, 8:1033–1034, 1894.

[85] SM Dewaegh, VMY Lee, and ST Brady. Local modulation of neurofilament phosphorylation, axonal caliber, and slow axonal-transport by myelinating Schwann–cells. *Cell*, 68:451–463, 1992.

[86] R Donato. S100: a multigenic family of calcium-modulated proteins of the EF-hand type with intracellular and extracellular functional roles. *Int J Biochem Cell Biol*, 33:637–668, 2001.

[87] L Dotevall, T Hagberg, JE Karlsson, and LE Rosengren. Astroglial and neuronal proteins in cerebrospinal fluid as markers of CNS involvement in lyme neuroborreliosis. *Eur J Neurol*, 6:169–178, 1999.

[88] PC Dowling and SD Cook. Disease markers in acute multiple sclerosis. *Arch Neurol*, 33:668–670, 1976.

[89] DA Dyment, AD Sadnovich, and GC Ebers. Genetics of multiple sclerosis. *Human Molecular Genetics*, 6:1693–1698, 1997.

[90] GC Ebers, K Kukay, DE Bulman, et al. A full genome search in multiple sclerosis. *Nat Genet*, 13:472–406, 1996.

[91] G Edan, D Miller, M Clanet, et al. Therapeutic effect of mitoxantrone combined with methylprednisolone in multiple sclerosis: a randomised multicentre study of active disease using MRI and clinical criteria. *J Neurol Neurosurg Psychiatry*, 62:112–108, 1997.

[92] S Ehlers, M Kyllerman, and L Rosengren. Analysis of glial fibrillary acidic protein in the cerebrospinal fluid of children investigated for encephalopathy. *Neuropediatrics*, 25:129–33, 1994.

[93] GA Elder, VL Jr Friedrich, P Bosco, C Kang, A Gourov, PH Tu, VM Lee, and RA Lazzarini. Absence of the mid-sized neurofilament subunit decreases axonal calibers, levels of light neurofilament (NF-L), and neurofilament content. *J Cell Biol*, 141:727–739, 1998.

[94] GA Elder, VL Jr Friedrich, C Kang, P Bosco, A Gourov, PH Tu, B Zhang, VM Lee, and RA Lazzarini. Requirement of heavy neurofilament subunit in the development of axons with large calibers. *J Cell Biol*, 143:195–205, 1998.

[95] LF Eng, FE D'Amelio, and ME Smith. Dissociation of GFAP intermediate filaments in EAE: observations in the lumbar spinal cord. *Glia*, 2:308–317, 1989.

[96] LF Eng, B Gerstl, and JJ Vanderhaeghen. A study of proteins in old multiple sclerosis plaques. *Trans Amer Soc Neurochem*, 1:42, 1970.

[97] LF Eng and RS Ghirnikar. GFAP and astrogliosis. *Brain Pathol*, 4:229–237, 1994.

[98] LF Eng, RS Ghirnikar, and YL Lee. Inflammation in EAE: role of chemokine/cytokine expression by resident and infiltrating cells. *Neurochem Res*, 21:511–525, 1996.

[99] LF Eng, YL Lee, and LE Miles. Measurement of glial fibrillary acidic protein by a two-site immunoradiometric assay. *Anal Biochem*, 71:243–259, 1976.

[100] LF Eng, JJ Vanderhaeghen, A Bignami, and B Gerstel. An acidic protein isolated from fibrous astrocytes. *Brain Res*, 28:351–354, 1971.

[101] MM Esiri and D Gay. *Multiple Sclerosis*, chapter The Immunonocytochemistry of multiple sclerosis plaques, pages 173–186. Volume 1 of Raine et al.,[316] 1997.

[102] P Evers and HB Uylings. An optimal antigen retrieval method suitable for different antibodies on human brain tissue stored for several years in formaldehyde fixative. *J Neurosci Methods*, 72:197–207, 1997.

[103] TE Feasby, JJ Gilbert, WF Brown, CF Bolton, AF Hahn, WF Koopman, and DW Zochodne. An acute axonal form of Guillain-Barre polyneuropathy. *Brain*, 109:1115–1126, 1986.

[104] K Felgenhauer and W Beuche, editors. *Labordiagnostik neurologischer Erkrankungen*. Thieme Verlag Stuttgart, New York, 1999.

[105] PA Felts, TA Baker, and KJ Smith. Conduction in segmentally demyelinated mammalian central axons. *J Neuroscience*, 17:7267–7277, 1997.

[106] B Ferguson, MK Matyszak, MM Esiri, and VH Perry. Axonal damage in acute multiple sclerosis lesions. *Brain*, 120:393–399, 1997.

[107] G Filippini, F Brusaferri, WA Sibley, A Citterio, G Ciucci, R Midgard, and L Candelise. Corticosteroids or acth for acute exacerbations in multiple sclerosis. *Cochrane Database Syst Rev*, page CD001331, 2000.

[108] J Fisher, H Levkovitch-Verbin, H Schori, E Yoles, O Butovsky, JF Kaye, A Ben-Nun, and M Schwartz. Vaccination for neuroprotection in the mouse optic nerve: implications for optic neuropathies. *J Neurosci*, 21:136–42, 2001.

[109] D Franciotta, G Martino, E Zardini, R Furlan, R Bergamaschi, L Andreoni, and V Cosi. Serum and CSF levels of MCP-1 and IP-10 in multiple sclerosis patients with acute and stable disease and undergoing immunomodulatory therapies. *J Neuroimmunol*, 115:192–108, 2001.

[110] E Fuchs and DW Cleveland. A structural scaffolding of intermediate filaments in health and disease. *Science*, 279:514–519, 1998.

[111] JY Garbern, DA Yool, GJ Moore, et al. Patients lacking the major cns myelin protein, proteolipid protein 1, develop length-dependent axonal degeneration in the absence of demyelination and inflammation. *Brain*, 125:551–561, 2002.

[112] FW Gay, TJ Drye, et al. The application of multifactoral cluster analysis in the staging of plaques in early multiple sclerosis. Identification and characterization of the primary demyelinating lesion. *Brain*, 120:1461–1483, 1997.

[113] Y Ge, RI Grossman, JK Udupa, JS Babb, LG Nyul, and DL Kolson. Brain atrophy in relapsing-remitting multiple sclerosis: fractional volumetric analysis of gray matter and white matter. *Radiology*, 220:606–610, 2001.

[114] N Geisler, E Kaufmann, S Fischer, U Plessmann, and K Weber. Neurofilament architecture combines structural principles of intermediate filaments with carboxy-terminal extensions increasing in size between triplet proteins. *EMBO J*, 2:1295–1502, 1983.

[115] N Geisler and K Weber. Self assembly in vitro of the 68000 molecular weight component of the mammalian neurofilament triplet proteins into intermediate–sized filaments. *J Mol Biol*, 151:565–571, 1981.

[116] CP Genain, B Cannella, SL Hauser, and CS Raine. Identification of autoantibodies associated with myelin damage in multiple sclerosis. *Nat Med*, 5:170–105, 1999.

[117] R George and JW Griffin. Delayed macrophage responses and myelin clearance during wallerian degeneration in the central nervous system: the dorsal radiculotomy model. *Exp Neurol*, 129:225–236, 1994.

[118] R George and JW Griffin. The proximo-distal spread of axonal degeneration in the dorsal columns of the rat. *J Neurocytol*, 23:657–667, 1994.

[119] BI Giasson and WE Mushynski. Aberrant stress-induced phosphorylation of perikaryal neurofilaments. *J Biol Chem*, 271:30404–30409, 1996.

[120] SR Gill, PC Wong, MJ Monteiro, and DW Cleveland. Assembly properties of dominant and recessive mutations in the small mouse neurofilament (Nf-L) subunit. *J Cell Biology*, 111:2005–2019, 1990.

[121] G Giovannoni, SJ Heales, NC Silver, et al. Raised serum nitrate and nitrite levels in patients with multiple sclerosis. *J Neurol Sci*, 145:77–78, 1997.

[122] G Giovannoni, JW Thorpe, D Kidd, et al. Soluble e–selectin in multiple–sclerosis — raised concentrations in patients with primary progressive disease. *J Neurol Neurosurg Psychiatry*, 60:20–26, 1996.

[123] ME Goldstein, Sternberger; LA, and NH Sternberger. Varying degrees of phosphorylation determine microheterogeneity of the heavy neurofilament poypeptide (Nf–H). *J Neuroimmunol*, 14:135–148, 1987.

[124] ME Goldstein, NH Sternberger, and LA Sternberger. Phosphorylation protects neurofilaments against proteolysis. *J Neuroimmunol*, 14:149–160, 1987.

[125] T Gotow and J Tanaka. Phosphorylation of neurofilament H subunit as related to arrangement of neurofilaments. *J Neurosci Res*, 37:691–713, 1994.

[126] F Gottron, D Turetsky, and D Choi. Smi-32 antibody against non-phosphorylated neurofilaments identifies a subpopulation of cultured cortical neurons hypersensitive to kainate toxicity. *Neurosci Lett*, 194:1, 1995.

[127] AJ Green, EJ Thompson, GE Stewart, M Zeidler, JM McKenzie, MA MacLeod, JW Ironside, RG Will, and RS Knight. Use of 14-3-3 and other brain-specific proteins in CSF in the diagnosis of variant Creutzfeldt-Jakob disease. *J Neurol Neurosurg Psychiatry*, 70:744–748, 2001.

[128] AJE Green, RJ Harvey, EJ Thompson, and MN Rossor. Increased S100 beta in the cerebrospinal fluid of patients with frontotemporal dementia. *Neurosci Lett*, 235:5–8, 1997.

[129] AJE Green, G Keir, and EJ Thompson. A specific and sensitive ELISA for measuring S-100b in cerebrospinal fluid. *J Immunol Meth*, 205:35–41, 1997.

[130] JG Greenfield and LS King. Observations on the histopathology of the cerebral lesions in desseminated sclerosis. *Brain*, 59:445–458, 1936.

[131] JW Griffin, EB George, ST Hsieh, and JD Glass. *The axon: structure, function and pathophysiology*, chapter Axonal degeneration and disorders of the axonal cytoskeleton, pages 375–390. In Waxman et al.,[425] 1995.

[132] WS Griffin, LC Stanley, C Ling, L White, V MacLeod, LJ Perrot, 3rd White CL, and C Araoz. Brain interleukin 1 and s-100 immunoreactivity are elevated in Down syndrome and Alzheimer disease. *Proc Natl Acad Sci USA*, 86:7611–7605, 1989.

[133] DMA Gromwall. Paced auditory serial addition task: a measure of recovery from concussion. *Perceptual Motor Skills*, 44:367–373, 1977.

[134] N Gruener, O Gozlan, T Goldstein, J Davis, I Besner, and TC Iancu. Iron, transferrin, and ferritin in cerebrospinal fluid of children. *Clin Chem*, 37:263–205, 1991.

[135] RJ Guan, BS Khatra, and JA Cohlberg. Phosphorylation of bovine neurofilament proteins by protein- kinase fa (glycogen-synthase kinase-3). *J Biol Chem*, 266:8262–8267, 1991.

[136] S Guidato, LH Tsai, J Woodgett, and CC Miller. Differential cellular phosphorylation of neurofilament heavy side-arms by glycogen synthase kinase-3 and cyclin-dependent kinase-5. *J Neurochem*, 66:1698–2306, 1996.

[137] MK Gupta, JN Whitaker, C Johnson, and H Goren. Measurement of immunoreactive myelin basic protein peptide (45-89) in cerebrospinal fluid. *Ann Neurol*, 23:274–280, 1988.

[138] D Gveric, R Hanemaaijert, J Newcombe, NA van Lent, CFM Stier, and MJ Cuzner. Plasminogen activators in multiple sclerosis lesions: implications fot the inflammatory response and axonal damage. *Brain*, 124:1978–1988, 2001.

[139] KG Haglid, Q Ynag, A Hamberger, S Bergman, A Widerberg, and N Danielsen. S100b stimulates neurite outgrowth in the rat sciatic nerve grafted with acellular muscle transplants. *Brain Res*, 69:196–201, 1997.

[140] R Hallgren, A Terent, L Wide, K Bergstrom, and G Birgegard. Cerebrospinal fluid ferritin in patients with cerebral infarction or bleeding. *Acta Neurol Scand*, 61:384–392, 1980.

[141] HP Hartung. Immune-mediated demyelination. *Ann Neurol*, 33:563–507, 1993.

[142] R Hashimoto, Y Nakamura, T Ichiro, et al. Quantitative analysis of neurofilament proteins in Alzheimer's brain by enzyme linked immunosorbent assay system. *Psychiat and Clin Neurosci*, 53:587–591, 1999.

[143] M Hattori, A Fujiyama, TD Taylor, et al. The DNA sequence of human chromosome 21. *Nature*, 405:311–309, 2000.

[144] MC Haugh, A Probst, J Ulrich, J Kahn, and BH Anderton. Alzheimer neurofibrillary tangles contain phosphorylated and hidden neurofilament epitopes. *J Neurol Neurosurg Psychiatry*, 49:1213–1220, 1986.

[145] JC Hedreen and VE Kolliatsos. Phosphorylated neurofilaments in neuronal perikarya and dendrites in human brain following axonal damage. *J Neuropath Exp Neurol*, 53:663, 1994.

[146] MW Hentze, S Keim, P Papadopoulos, S O'Brien, W Modi, J Drysdale, WJ Leonard, JB Harford, and RD Klausner. Cloning, characterization, expression, and chromosomal localization of a human ferritin heavy-chain gene. *Proc Natl Acad Sci USA*, 83:7226–7230, 1986.

[147] M Herrmann, N Curio, S Jost, MT Wunderlich, H Synowitz, and CW Wallesch. Protein s-100b and neuron specific enolase as early neurobiochemical markers of the severity of traumatic brain injury. *Restorative Neurology Neuroscience*, 14:109–114, 1999.

[148] M Herrmann, S Jost, S Kutz, AD Ebert, T Kratz, MT Wunderlich, and H Synowitz. Temporal profile of release of neurobiochemical markers of brain damage after traumatic brain injury is associated with intracranial pathology as demonstrated in cranial computerized tomography. *J Neurotrauma*, 17:113–122, 2000.

[149] H Hidaka, T Endo, S Kawamoto, E Yamada, H Umekawa, K Tanabe, and K Hara. Purification and characterization of adipose tissue S-100b protein. *J Biol Chem*, 258:2705–2709, 1983.

[150] S Hisanaga, Y Gonda, M Inagaki, A Ikai, and N Hirokawa. Effects of phosphorylation of the neurofilament l-protein on filamentous structures. *Cell Regulation*, 1:237–248, 1990.

[151] PR Hof, K Cox, and JH Morrison. Quantitative analysis of a vulnerable subset of pyramidal neurons in alzheimer's disease: I superior frontal and inferior temporal cortex. *J Comp Neurol*, 301:44–54, 1990.

[152] PR Hof, LG Ungerleider, MJ Webster, R Gattass, MM Adams, CA Sailstad, and JH Morrison. Neurofilament protein is differentially distributed in subpopulations of corticocortical projection neurons in the macaque monkey visual pathways. *J Comp Neurol*, 376:112–27, 1996.

[153] PN Hoffman, DW Cleveland, JW Griffin, et al. Neurofilament gene expression: a major determinant of axonal caliber. *Proc Natl Acad Sci USA*, 84:3472–3476, 1987.

[154] FM Hofman, DR Hinton, K Johnson, and JE Merrill. Tumor necrosis factor identified in multiple sclerosis brain. *J Exp Med*, 170:607–612, 1989.

[155] R Hohlfeld. Biotechnological agents for the immunotherapy of multiple sclerosis - principles, problems and perspectives. *Brain*, 120:865–916, 1997.

[156] R Hohlfeld, F Meinl, F Weber, et al. The role of autoimmun T lymphocytes in the pathogenesis of multiple sclerosis. *Neurology*, 45:s33–s38, 1995.

[157] B Holmberg, L Rosengren, JE Karlsson, and B Johnels. Increased cerebrospinal fluid levels of neurofilament protein in progressive supranuclear palsy and multiple–system atrophy compared with Parkinson's disease. *Movement Disorders*, 13:70–77, 1998.

[158] EL Hoogervorst, NF Kalkers, BM Uitdehaag, and CH Polman. A study validating changes in the multiple sclerosis functional composite. *Arch Neurol*, 59:113–106, 2002.

[159] SW Hulet, SO Heyliger, S Powers, and JR Connor. Oligodendrocyte progenitor cells internalize ferritin via clathrin-dependent receptor mediated endocytosis. *J Neurosci Res*, 61:52–60, 2000.

[160] SW Hulet, S Powers, and JR Connor. Distribution of transferrin and ferritin binding in normal and multiple sclerotic human brains. *J Neurological Sciences*, 165:48–55, 1999.

[161] PJ Hutchinson, MT O'Connell, PG Al-Rawi, et al. Increases in GABA concentrations during cerebral ischaemia: a microdialysis study of extracellular amino acids. *J Neurol Neurosurg Psychiatry*, 72:99–105, 2002.

[162] C Iarlori, M Reale, G De Luca, A Di Iorio, C Feliciani, A Tulli, P Conti, D Gambi, and A Lugaresi. Interferon beta-1b modulates MCP-1 expression and production in relapsing-remitting multiple sclerosis. *J Neuroimmunol*, 123:170–179, 2002.

[163] T Ingebrigtsen, B Romner, S Marup-Jensen, M Dons, C Lundqvist, J Bellner, C Alling, and SE Borgesen. The clinical value of serum S-100 protein measurements in minor head injury: a Scandinavian multicentre study. *Brain Inj*, 14:1047–1055, 2000.

[164] RG Jackson, KM Sales, GS Samra, and L Strunin. Extra cranial sources of S100B. *Br J Anaesth*, 86:601, 2001.

[165] RG Jackson and GS Samra. Differences in the release of S100 protein during cardiopulmonary bypass. *Anaesthesia*, 57:91–2, 2002.

[166] LD Jacobs, RA Cookfair, DL Rudick, et al. Intramuscular interferon beta-1a for disease progression in relapsing multiple sclerosis. *Ann Neurol*, 39:285–294, 1996.

[167] SG Jacobson, RA Eames, and WI McDonald. Optic nerve fibre lesions in adult cats: pattern of recovery of spatial vision. *Exp Brain Res*, 36:491–508, 1979.

[168] H Jacomy, QZ Zhu, S Couillard-Després, JM Beaulieu, and JP Julien. Disruption of type IV intermediate filament network in mice lacking the neurofilament medium and heavy subunits. *J Neurochem*, 73:972–984, 1999.

[169] H Jaffe, Veeranna, KT Shetty, and HC Pant. Characterization of the phosphorylation sites of human high molecular weight neurofilament protein by electrospray ionization tandem mass spectrometry and database searching. *Biochemistry*, 37:3931–3940, 1998.

[170] JO Jeppsson, CB Laurell, and B Franzen. Agarose gel electrophoresis. *Clin Chem*, 25:629–638, 1979.

[171] PJ Jongen, S Floris, WH Doesburg, WA Lemmens, OR Hommes, and KJ Lamers. Composite cerebrospinal fluid score in relapsing-remitting and secondary progressive multiple sclerosis. *Mult Scler*, 4:108–10, 1998.

[172] PJ Jongen, KJ Lamers, WH Doesburg, WA Lemmens, and OR Hommes. Cerebrospinal fluid analysis differentiates between relapsing-remitting and secondary progressive multiple sclerosis. *J Neurol Neurosurg Psychiatry*, 63:446–451, 1997.

[173] JP Julien. Neurofilament functions in health and disease. *Curr Opin Neurobiol*, 9:554–560, 1999.

[174] JP Julien. Amyotrophic lateral sclerosis: unfolding the toxicity of the misfolded. *Cell*, 104:581–591, 2001.

[175] CW Jung and TB Shea. Regulation of neurofilament axonal transport by phosphorylation in optic axons in situ. *Cell Motility Cytoskeleton*, 42:230–240, 1999.

[176] KG Kahl, N Kruse, KV Toyka, and P Rieckmann. Serial analysis of cytokine mrna profiles in whole blood samples from patients with early multiple sclerosis. *J Neurol Sci*, 200:53–5, 2002.

[177] NF Kalkers, E Bergers, JA Castelijns, et al. Optimizing the association between disability and biological markers in MS. *Neurology*, 57:1253–1258, 2001.

[178] JP Kapfhammer. Beeinflussung des nervenwachstums durch hemmende und stimulierende moleküle. *Freiburger Universitätsblätter*, 1996.

[179] JP Kapfhammer, F Christ, and ME Schwab. The growth-associated protein gap-43 is specifically expressed in tyrosine hydroxylase-positive cells of the rat retina. *Brain Res Dev Brain Res*, 101:257–264, 1997.

[180] JP Kapfhammer and ME Schwab. Modulators of neuronal migration and neurite growth. *Curr Opin Cell Biol*, 4:863–808, 1992.

[181] JP Kapfhammer and ME Schwab. Inverse Patterns of myelination and GAP-43 expression in the adult CNS: Neurite growth inhibitors as regulators of neuronal plasticity? *J Comp Neurol*, 340:194–206, 1994.

[182] R Kapoor, M Davies, and KJ Smith. Temporary axonal conduction block and axonal loss in inflammatory neurological disease. A potential role for nitric oxide? *Ann N Y Acad Sci*, 893:304–308, 1999.

[183] L Kappos, D Moeri, et al. Predictive value of gadolinium–enhanced magnetic resonance imaging for relapse rate and changes in disability or impairment in multiple sclerosis: a meta–analysis. *Lancet*, 353:964–969, 1999.

[184] O Kastrup, P Stude, and V Limmroth. Balo's concentric sclerosis Evolution of active demyelination demonstrated by serial contrast-enhanced MRI. *J Neurol*, 249:811–804, 2002.

[185] G Keir, N Tasdemir, and EJ Thompson. Cerebrospinal-fluid ferritin in brain necrosis - evidence for local synthesis. *Clin Chim Acta*, 216:153–166, 1993.

[186] M Kerschensteiner, E Gallmeier, L Behrens, et al. Activated human T cells, B cells, and monocytes produce brain–derived neurotrophic factor in vitro and in inflammatory brain lesions: a neuroprotective role of inflammation? *J Exp Med*, 189:865–870, 1999.

[187] J Kesselring, DH Miller, SA Robb, et al. Acute disseminated encephalomyelitis. *Brain*, 113:291–302, 1990.

[188] NE Khan, AC De Souza, and JR Pepper. S100 protein: its use as a marker of cerebral damage in cardiac operations. *Ann Thorac Surg*, 72:666–607, 2001.

[189] D Kidd, F Barkhof, R McConnell, PR Algra, IV Allen, and T Revesz. Cortical lesions in multiple sclerosis. *Brain*, 122:17–26, 1999.

[190] D Kidd, JW Thorpe, BE Kendall, et al. MRI dynamics of brain and spinal cord in progressive multiple sclerosis. *J Neurol Neurosurg Psychiatry*, 60:15–19, 1996.

[191] CE King, I Jacobs, TC Dickson, and JC Vickers. Physical damage to rat cortical axons mimics early alzheimer's neuronal pathology. *Neuroreport*, 8:1663–1605, 1997.

[192] P Kivisakk, N Teleshova, V Ozenci, Y Huang, D Matusevicius, S Fredrikson, M Soderstrom, and H Link. No evidence for elevated numbers of mononuclear cells expressing mcp-1 and rantes mrna in blood and csf in multiple sclerosis. *J Neuroimmunol*, 91:108–12, 1998.

[193] J Kong and Z Xu. Overexpression of neurofilament subunit nf-l and nf-h extends survival of a mouse model for amyotrophic lateral sclerosis. *Neurosci Lett*, 281:72–4, 2000.

[194] EH Koo, SS Sisodia, DR Archer, et al. Precursor of amyloid protein in Alzheimer disease undergoes fast anterograde axonal transport. *Proc Natl Acad Sci USA*, 87:1561–1565, 1990.

[195] B Kornek, MK Storch, R Weissert, E Wallstroem, A Stefferl, T Olsson, C Linington, M Schmidbauer, and H Lassmann. Multiple sclerosis and chronic autoimmune encephalomyelitis: a comparative quantitative study of axonal injury in active, inactive, and remyelinated lesions. *Am J Pathol*, 157:267–276, 2000.

[196] M Kotter, A Setzu, F Sim, N van Rooijen, and R Franklin. Macrophage depletion impairs oligodendrocyte remyelination following lysolecithin–induced demyelination. *Glia*, 35:204–212, 2001.

[197] J Kraus, BS Kuehne, J Tofighi, P Frielinghaus, E Stolz, F Blaes, C Laske, B Engelhardt, H Traupe, M Kaps, and P Oschmann. Serum cytokine levels do not correlate with disease activity and severity assessed by brain mri in multiple sclerosis. *Acta Neurol Scand*, 105:300–308, 2002.

[198] GW Kreutzberg. *The axon: structure, function and pathophysiology*, chapter Reaction of the neuronal cell body to axonal damage, pages 355–374. In Waxman et al.,[425] 1995.

[199] GW Kreutzberg. Microglia: A sensor for pathological events in the cns. *Trends Neurosci*, 19:312–318, 1996.

[200] LB Krupp, NG LaRocca, J Muir-Nash, and AD Steinberg. The fatigue severity scale application to patients with multiple sclerosis and systemic lupus erythematosus. *Arch Neurol*, 46:1121–1103, 1989.

[201] T Kuhlmann, G Lingfeld, A Bitsch, J Schuchardt, and W Bruck. Acute axonal damage in multiple sclerosis is most extensive in early disease stages and decreases over time. *Brain*, 125:2202–2212, 2002.

[202] P Kumar, K Dhital, M Hossein-Nia, S Patel, D Holt, and T Treasure. S-100 protein release in a range of cardiothoracic surgical procedures. *J Thorac Cardiovasc Surg*, 113:953–904, 1997.

[203] JF Kurtzke. A new scale for evaluating disability in multiple sclerosis. *Neurology*, 5:580–583, 1955.

[204] JF Kurtzke. On the evaluation of disability in multiple sclerosis. *Neurology*, 11:686–694, 1961.

[205] JF Kurtzke. Further notes on disability evaluation in multiple sclerosis. *Neurology*, 15:654–661, 1965.

[206] JF Kurtzke. Rating neurological impairment in multiple sclerosis: an expanded disability status scale (EDSS). *Neurology*, 33:1444–1452, 1983.

[207] JF Kurtzke. *Epidemiology of multiple sclerosis*, volume 47, pages 259–287. Elsevier, Amsterdam, 1985.

[208] JF Kurtzke. The disability Status Scale for multiple sclerosis: aplogia pro DSS sua. *Neurology*, 39:291–302, 1989.

[209] JF Kurtzke. Natural history and clinical outcome measures for multiple sclerosis studies. Why at the present time does EDSS scale remain a preferred outcome measure to evaluate disease evolution? *Neurol Sci*, 21:339–341, 2000.

[210] JF Kurtzke, K Hyllested, Arbuckle JD, et al. Multiple sclerosis in Faroe Islands: 7 Results of a case control questionnaire with multiple controls. *Acta Neurol Scand*, 96:149–157, 1997.

[211] KJ Lamers, BG van Engelen, FJ Gabreels, et al. Cerebrospinal neuron-specific enolase, S–100 and myelin basic protein in neurological disorders. *Acta Neurol Scand*, 92:247–251, 1995.

[212] KJ Lamers, BG van Engelen, FJ Gabreels, OR Hommes, GF Borm, and RA Wevers. Cerebrospinal neuron-specific enolase, S-100 and myelin basic protein in neurological disorders. *Acta Neurol Scand*, 92:247–251, 1995.

[213] JP Larsen, G Kvaale, T Riise, H Nyland, and JA Aarli. Multiple sclerosis–more than one disease? *Acta Neurol Scand*, 72:145–50, 1985.

[214] RJ Lasek and MM Black, editors. *Intrinsic determinants of neuronal form and function*, volume 37 of *Neurology and Neurobiology*, 41 East 11th Street, New York, NY 10003, 1988. Alan R Liss. Proceedings of a Meeting on Intrinsic Determinants of Neuronal Form and Function held at the Bio–architectonics Center, School of Medicine, Case Western Reserve University, Cleveland, Ohio, May 12–14, 1986.

[215] H Lassmann. The pathology of multiple sclerosis and its evolution. *Phil Trans R Soc Lond B*, 354:1635–1640, 1999.

[216] H Lassmann. Classification of demyelinating diseases at the interface between etiology and pathogenesis. *Curr Opin Neurol*, 14:253–258, 2001.

[217] MA Lee, S Smith, J Palace, S Narayanan, N Silver, L Minicucci, M Filippi, DH Miller, DL Arnold, and PM Matthews. Spatial mapping of T2 and gadolinium-enhancing T1 lesion volumes in multiple sclerosis: evidence for distinct mechanisms of lesion genesis? *Brain*, 122:1261–1270, 1999.

[218] MK Lee, JR Marszalek, and Cleveland DW. A mutant neurofilament subunit causes massive, selective motor neuron death: implications for the pathogenesis of human motor neuron disease. *Neuron*, 13:975–988, 1994.

[219] JF Lees, PS Shneidman, SF Skuntz, MJ Carden, and RA Lazzarini. The structure and organization of the human heavy neurofilament subunit (NF-H) and the gene encoding it. *EMBO1988*, 7:1947–1955, 1988.

[220] V Lejon, LE Rosengren, P Buscher, JE Karlsson, and HN Sema. Detection of light subunit neurofilament and glial fibrillary acidic protein in cerebrospinal fluid of trypanosoma brucei gambiense-infected patients. *Am J Trop Med Hyg*, 60:94–98, 1999.

[221] A Leonardi, S Penco, C Gramigni, C Bason, G Ribizzi, P Gazzola, GL Mancardi, G Bianchi-Scarra, M Abbruzzese, and C Garre. Granulocyte-macrophage colony-stimulating factor activity in cerebrospinal fluid. *Acta Neurol Scand*, 100:274–207, 1999.

[222] SM LeVine, SG Lynch, CN Ou, MJ Wulser, E Tam, and N Boo. Ferritin, transferrin and iron concentrations in the cerebrospinal fluid of multiple sclerosis patients. *Brain Res*, 821:511–505, 1999.

[223] J Lew and JH Wang. Neuronal cdc2–like kinase. *Trends Biochem Sci*, 20:33–37, 1995.

[224] J Lew, RJ Winkfein, HK Paudel, and JH Wang. Brain proline-directed protein-kinase is a neurofilament kinase which displays high sequence homology to P34(cdc2). *J Biol Chem*, 267:25922–25926, 1992.

[225] H Li, J Newcombe, NP Groome, and ML Cuzner. Characterization and distribution of phagocytic macrophages in multiple sclerosis plaques. *Neuropathol Appl Neurobiol*, 19:214–223, 1993.

[226] CF Lippa and TW Smith. Chromatolytic neurons in Werdnig-Hoffmann disease contain phosphorylated neurofilaments. *Acta Neuropathol*, 77:91–94, 1988.

[227] L Liu, JKE Persson, M Svensson, and H Aldskogius. Glial cell responses, complement, and clusterin in the central nervous system following dorsal root transection. *Glia*, 23:221–238, 1998.

[228] CT Lloyd, R Ascione, MJ Underwood, F Gardner, A Black, and GD Angelini. Serum S-100 protein release and neuropsychologic outcome during coronary revascularization on the beating heart: a prospective randomized study. *J Thorac Cardiovasc Surg*, 119:148–54, 2000.

[229] C Lock, G Hermans, R Pedotti, et al. Gene-microarray analysis of multiple sclerosis lesions yields new targets validated in autoimmune encephalomyelitis. *Nat Med*, 8:500–508, 2002.

[230] NA Losseff, L Wang, HM Lai, et al. Progressive cerebral atrophy in multiple sclerosis: a serial MRI study. *Brain*, 119:2009–2019, 1996.

[231] NA Losseff, SL Webb, JI O'Riordan, et al. Spinal cord atrophy and disability in multiple sclerosis A new reproducible and sensitive MRI method with potiential to monitor disease progression. *Brain*, 119:701–708, 1996.

[232] J Losy and G Michalowska-Wender. In vivo effect of interferon-beta 1a on interleukin-12 and TGF-beta(1) cytokines in patients with relapsing-remitting multiple sclerosis. *Acta Neurol Scand*, 106:44–46, 2002.

[233] J Losy and A Niezgoda. IL-18 in patients with multiple sclerosis. *Acta Neurol Scand*, 104:171–103, 2001.

[234] OH Lowry, NJ Rosebrough, AL Farr, and RJ Randall. Protein measurement with the folin phenol reagent. *J Biol Chem*, 193:265–275, 1951.

[235] L Lubinska. Early course of wallerian degeneration in myelinated fibres of the rat phrenic nerve. *Brain Res*, 130:47–63, 1977.

[236] FD Lublin and SC Reingold. Defining the clinical course of multiple sclerosis: results of an international survey National Multiple Sclerosis Society (USA) Advisory Committee on Clinical Trials of New Agents in Multiple Sclerosis. *Neurology*, 46:907–911, 1996.

[237] C Lucchinetti, W Bruck, J Parisi, B Scheithauer, M Rodriguez, and H Lassmann. Heterogeneity of multiple sclerosis lesions: implications for the pathogenesis of demyelination. *Ann Neurol*, 47:707–717, 2000.

[238] CF Lucchinetti, W Brück, M Rodriguez, and H Lassmann. Distinct patterns of multiple sclerosis pathology indicate heterogeneity in pathogenesis. *Brain Pathol*, 6:259–274, 1996.

[239] ER Lunn, VH Brown, and VH Perry. The pattern of axonal degeneration in the peripheral nervous system varies with different types of lesion. *Neuroscience*, 35:157–165, 1990.

[240] JR Lupski. Axonal charcot–marie–tooth disease and the neurofilaemtn light gene (NF-L). *Am J Hum Genet*, 67:8–10, 2000.

[241] J Lycke, O Andersen, and L Rosengren. Neurofilament in cerebrospinal fluid: a potential marker of activity in multiple sclerosis. *Eur J Neurol*, 3:100, 1996.

[242] JN Lycke, JE Karlsson, O Andersen, and LE Rosengren. Neurofilament protein in cerebrospinal fluid: a potential marker of activity in multiple sclerosis. *J Neurol Neurosurg Psychiatry*, 64:402–404, 1998.

[243] D Ma, L Descarries, JP Julien, and G Doucet. Abnormal perikaryal accumulation of neurofilament light protein in the brain of mice transgenic for the human protein: sequence of postnatal development. *Neuroscience*, 68:135–49, 1995.

[244] T Magnus, A Chan, O Grauer, et al. Microglial phagocytosis of apoptotic inflammatory T cells leads to downregulation of microglial immune activation. *J Immunol*, 167:5004–5010, 2001.

[245] DJ Mahad, SJ Howell, and MN Woodroofe. Expression of chemokines in the CSF and correlation with clinical disease activity in patients with multiple sclerosis. *J Neurol Neurosurg Psychiatry*, 72:498–502, 2002.

[246] V Manetto, NH Sternberger, G Perry, et al. Phosphorylation of neurofilaments is altered in amyotrophic lateral sclerosis. *J Neuropathol Exp Neurol*, 47:642–653, 1988.

[247] O Marburg. Die sogenannte "akute Multiple Sklerose". *J Psychiatric Neurol*, 27:211–312, 1906.

[248] JE Martin, KS Mather, M Swash, O Garofalo, GE Dale, PN Leigh, and BH Anderton. Spinal cord trauma in man: studies of phosphorylated neurofilament and ubiquitin expression. *Brain*, 113:1553–1562, 1990.

[249] G Martino, A Consiglio, DM Franciotta, A Corti, M Filippi, K Vandenbroeck, FL Sciacca, G Comi, and LM Grimaldi. Tumor necrosis factor alpha and its receptors in relapsing-remitting multiple sclerosis. *J Neurol Sci*, 152:51–61, 1997.

[250] AR Massaro, G Carbone, A Laudisio, and P Tonali. La patologia gliale nella sclerosi multipla evidenziata mediante l'analisi liquorale. *Riv Neurobiol*, 43:273–278, 1997.

[251] AR Massaro, F Michetti, A Laudisio, and P Bergonzi. Myelin basic protein and S-100 antigen in cerebrospinal fluid of patients with multiple sclerosis in the acute phase. *Ital J Neurol Sci*, 6:53–56, 1985.

[252] PM Matthews, E Pioro, S Narayanan, et al. Assessment of lesion pathology in multiple sclerosis using quantitative MRI morphometry and magnetic resonance spectroscopy. *Brain*, 119:715–722, 1996.

[253] WL Maxwell, JT Povlishock, and DL Graham. A mechanistic analysis of nondisruptive axonal injury: A review. *J Neurotrauma*, 14:419–440, 1997.

[254] KA McClintock and GS Shaw. A logical sequence search for S100B target proteins. *Protein Sci*, 9:2043–2006, 2000.

[255] WI McDonald. The pathological and clinical dynamics of multiple sclerosis. *J Neuropathol Exp Neurol*, 53:338–343, 1994.

[256] WI McDonald. Relapse, remission, and progression in multiple sclerosis. *N Engl J Med*, 343:1486–1487, 2000.

[257] WI McDonald, A Compston, G Edan, D Goodkin, HP Hartung, FD Lublin, HF McFarland, DW Paty, CH Polman, SC Reingold, M Sandberg-Wollheim, W Sibley, A Thompson, S van den Noort, BY Weinshenker, and Wolinsky JS. Recommended diagnostic criteria for multiple sclerosis: guidelines from the international panel on the diagnosis of multiple sclerosis. *Ann Neurol*, 50:121–127, 2001.

[258] WI McDonald, DH Miller, and D Barnes. The pathological evolution of multiple sclerosis. *Neuropathol Appl Neurobiol*, 18:319–334, 1992.

[259] WI McDonald and TA Sears. Effect of demyelination on conduction in the central nervous system. *Nature*, 221:182–183, 1969.

[260] HF McFarland, F Barkhof, J Antel, and DH Miller. The role of MRI as a surrogate outcome measure in multiple sclerosis. *Mult Scler*, 8:40–51, 2002.

[261] HF McFarland, JA Frank, PS Albert, et al. Using gadolinium–enhanced magnetic resonance imaging lesions to monitor disease activity in multiple sclerosis. *Ann Neurol*, 32:758–766, 1992.

[262] DE McFarlin and HF McFarland. Multiple-sclerosis 1. *New Eng J Med*, 307:1183–1188, 1982.

[263] DE McFarlin and HF McFarland. Multiple-sclerosis 2. *New Eng J Med*, 307:1246–1251, 1982.

[264] RE McLendon, PC Burger, CN Pegram, et al. The immunohistochemical application of three anti-GFAP monoclonal antibodies to formalin-fixed, paraffin-embedded, normal and neoplastic brain tissues. *J Neuropathol Exp Neurol*, 45:692–703, 1986.

[265] C McManus, JW Berman, FM Brett, H Staunton, M Farrell, and CF Brosnan. MCP-1, MCP-2 and MCP-3 expression in multiple sclerosis lesions: an immunohistochemical and in situ hybridization study. *J Neuroimmunol*, 86:20–29, 1998.

[266] E Meinl and R Hohlfeld. Immunopathogenesis of multiple sclerosis: MBP and beyond. *Clin Exp Immunol*, 128:395–307, 2002.

[267] IV Mersiyanova, AV Perepelov, et al. A new variant of Charcot–Marie–Tooth disease type 2 is probably the result of a mutation in the neurofilament–ligth gene. *Am J Hum Genet*, 67:37–46, 2000.

[268] F Michetti, L Lauriola, M Rende, VM Stolfi, F Battaglia, and D Cocchia. S-100 protein in the testis An immunochemical and immunohistochemical study. *Cell Tissue Res*, 240:137–42, 1985.

[269] F Michetti, A Massaro, and M Murazio. The nervous system-specific S-100 antigen in cerebrospinal fluid of multiple sclerosis patients. *Neurosci Lett*, 11:171–105, 1979.

[270] F Michetti, A Massaro, G Russo, and G Rigon. The S–100 antigen in cerebrospinal fluid as a possible index of cell injury in the nervous system. *Neurol Sci*, 44:259–263, 1980.

[271] Dj Miljkovic, J Drulovic, V Trajkovic, S Mesaros, I Dujmovic, D Maksimovic, T Samardzic, N Stojsavljevic, Z Levic, and M Mostarica Stojkovic. Nitric oxide metabolites and interleukin-6 in cerebrospinal fluid from multiple sclerosis patients. *Eur J Neurol*, 9:413–408, 2002.

[272] JHD Millar, CJ Vas, MJ Noronha, et al. Long term treatment of multiple sclerosis with corticotrophin. *Lancet*, 2:429–431, 1967.

[273] CC Miller, S Ackerley, J Brownlees, AJ Grierson, NJ Jacobsen, and P Thornhill. Axonal transport of neurofilaments in normal and disease states. *Cell Mol Life Sci*, 59:323–330, 2002.

[274] DH Miller, F Barkhof, JA Frank, GJ Parker, and AJ Thompson. Measurement of atrophy in multiple sclerosis: pathological basis, methodological aspects and clinical relevance. *Brain*, 125:1676–1695, 2002.

[275] M Mirabella, RB Alvarez, M Bilak, WK Engel, and V Askanas. Difference in expression of phosphorylated tau epitopes between sporadic inclusion-body myositis and hereditary inclusion-body myopathies. *J Neuropathol Exp Neurol*, 55:774–786, 1996.

[276] U Missler, M Wiesmann, et al. Measurement of glial fibrillary acidic protein in human blood: Analytical method and preliminary clinical results. *Clin Chem*, 45:138–141, 1999.

[277] G Moalem, R Leibowitz-Amit, E Yoles, et al. Autoimmune T cells protect neurons from secondary degeneration after central nervous system axotomy. *Nat Med*, 5:49–55, 1999.

[278] K Mokuno, K Kato, K Kawai, Y Matsuoka, T Yanagi, and I Sobue. Neuron-specific enolase and S-100 protein levels in cerebrospinal fluid of patients with various neurological diseases. *J Neurol Sci*, 60:443–451, 1983.

[279] BW Moore. A soluble protein characteristic of the nervous system. *Biochem Biophys Res Commun*, 19:739–744, 1965.

[280] JH Morrison, DA Lewis, MJ Campbell, GW Huntley, DL Benson, and C Bouras. A monoclonal antibody to non-phosphorylated neurofilament protein marks the vulnerable cortical neurons in Alzheimer's disease. *Brain Res*, 416:331–336, 1987.

[281] TH Moss and SJ Lewkowicz. The axon reaction in motor and sensory neurones of mice studied by a monoclonal antibody marker of neurofilament protein. *J Neurol Sci*, 60:267–280, 1983.

[282] DG Munoz, C Greene, DP Perl, and DJ Selkoe. Accumulation of phosphorylated neurofilaments in anterior horn motoneurons of amyotrophic lateral sclerosis patients. *J Neuropathol Exp Neurol*, 47:9–18, 1988.

[283] Y Nakamura, M Takeda, KJ Angelides, T Tanaka, K Tada, and T Nishimura. Effect of phosphorylation on 68 kda neurofilament subunit protein assembly by the cyclic-amp dependent protein-kinase in vitro. *Biochem Biophys Res Comm*, 169:744–750, 1990.

[284] Y Nakazato, J Hirato, Y Ishida, S Hoshi, M Hasegawa, and T Fukuda. Swollen cortical neurons in Creutzfeldt-Jakob disease contain a phosphorylated neurofilament epitope. *J Neuropathol Exp Neurol*, 49:197–205, 1990.

[285] Y Nakazato, A Sasaki, J Hirato, and Y Ishida. Monoclonal antibodies which recognize phosphorylated and nonphosphorylated epitopes of neurofilament protein. *Biomed REs*, 8:369–376, 1987.

[286] S Narayanan, L Fu, E Pioro, et al. Imaging of axonal damage in multiple sclerosis: spatial distribution of magnetic resonace imaging lesions. *Ann Neurol*, 41:385–391, 1997.

[287] HE Nelson, editor. *National Adult reading test: Manual*. Windsor: NFER-Nelson, 1982.

[288] J Newcombe. Distribution of glial fibrillary acidic protein in gliosed human white matter. *J Neurochem*, 47:1713–1719, 1986.

[289] J Newcombe and ML Cuzner. Microglia-derived macrophages in early multiple sclerosis plaques. *Neuropathol Appl Neurobiol*, 22:207–215, 1996.

[290] J Newcombe, N Naik, and ML Cuzner. Monoclonal antibody 14E recognizes an antigen common to human oligodendrocytes, Schwann cells, Bergmann glia, and a subpopulation of reactive glia. *Neurochem Res*, 17:933–938, 1992.

[291] MD Nguyen, JP Julien, and S Rivest. Innate immunity: the missing link in neuroprotection and neurodegeneration? *Nat Rev Neurosci*, 3:216–227, 2002.

[292] MD Nguyen, RC Lariviere, and JP Julien. Reduction of axonal caliber does not alleviate motor neuron disease caused by mutant superoxide dismutase 1. *Proc Natl Acad Sci USA*, 97:12306–12311, 2000.

[293] MD Nguyen, RC Lariviere, and JP Julien. Deregulation of Cdk5 in a mouse model of ALS: toxicity alleviated by perikaryal neurofilament inclusions. *Neuron*, 30:135–47, 2001.

[294] RA Nixon. The regulation of neurofilament protein dynamics by phosphorylation - clues to neurofibrillary pathobiology. *Brain Pathology*, 3:29–38, 1993.

[295] RA Nixon, PA Paskevich, RK Sihag, and CY Thayer. Phosphorylation on carboxyl-terminus domains of neurofilament proteins in retinal ganglion-cell neurons in- vivo - influences on regional neurofilament accumulation, interneurofilament spacing, and axon caliber. *J Cell Biology*, 126:1031–1046, 1994.

[296] M Noppe, R Crols, D Andries, and A Lowenthal. Determination in human cerebrospinal fluid of glial fibrillary acidic protein, S-100 and myelin basic protein as indices of non-specific or specific central nervous tissue pathology. *Clin Chim Acta*, 155:143–150, 1986.

[297] M Noppe, A Lowenthal, D Karcher, and J Gheuens. A two-site immunoradiometric assay for the determination of alpha-albumin. *J Immunol Methods*, 27:75–81, 1979.

[298] JH Noseworthy, C Lucchinetti, M Rodriguez, and BG Weinshenker. Multiple sclerosis. *N Engl J Med*, 343:938–952, 2000.

[299] H Openshaw, O Stuve, JP Antel, R Nash, BT Lund, LP Weiner, A Kashyap, P McSweeney, and S Forman. Multiple sclerosis flares associated with recombinant granulocyte colony-stimulating factor. *Neurology*, 54:2147–2150, 2000.

[300] World Health Oranization. International classification of impairments, disabilities and handicaps. *Geneva*, 1980.

[301] M Otto, J Wiltfang, E Schutz, et al. Diagnosis of Creutzfeldt-Jakob disease by measurement of s100 protein in serum: prospective case-control study. *BMJ*, 316:577–582, 1998.

[302] CN Pegram, LF Eng, CJ Wikstrand, et al. Monoclonal antibodies reactive with epitopes restricted to glial fibrillary acidic proteins of several species. *Neurochem Pathol*, 3:119–38, 1985.

[303] K Pennypacker, I Fischer, and P Levitt. Early in vitro genesis and differentiation of axons and dendrites by hippocampal neurons analyzed quantitatively with neurofilament-H and microtubule-associated protein 2 antibodies. *Exp Neurol*, 111:25–35, 1991.

[304] L Persson, HG Hardemark, J Gustafsson, G Rundstrom, I Mendel-Hartvig, T Esscher, and S Pahlman. S-100 protein and neuron-specific enolase in cerebrospinal fluid and serum: markers of cell damage in human central nervous system. *Stroke*, 18:911–908, 1987.

[305] JW Peterson, L Bo, S Mork, A Chang, and BD Trapp. Transected neurites, apoptotic neurons, and reduced inflammation in cortical multiple sclerosis lesions. *Ann Neurol*, 50:389–400, 2001.

[306] TV Petrova, J Hu, and LJ Van Eldik. Modulation of glial activation by astrocyte-derived protein S100B: differential responses of astrocyte and microglial cultures. *Brain Res*, 853:74–80, 2000.

[307] A Petzold, MJ Eikelenboom, D Gveric, G Keir, M Chapman, RHC Lazeron, ML Cuzner, Ch Polman, BMJ Uitdehaag, EJ Thompson, and G Giovannoni. Markers for different glial cell responses in multiple sclerosis: Clinical and pathological correlations. *Brain*, 125:1462–1473, 2002.

[308] A Petzold, AJE Green, G Keir, et al. Serum s100b in brain injury: An early predictor of high intracranial pressure and mortality in brain injury: A pilot study. *Crit Care Med*, 2002. in press.

[309] MJ Politis, RG Pellegrino, and PS Spencer. Ultrastructural studies of the dying-back process v axonal neurofilaments accumulate at sites of 2,5-hexanedione application: evidence for nerve fibre dysfunction in experimental hexacarbon neuropathy. *J Neurocytol*, 9:505–516, 1980.

[310] CM Poser. The epidepmiology of multiple sclerosis: a general overview. *Ann Neurol*, 36 Suppl 2:S180–193, 1994.

[311] CM Poser, WP Donald, L Scheinberg, WI McDonald, et al. New diagnostic criteria for multiple sclerosis: Guidelines for research protocols. *Annals of Neurology*, 13:227–231, 1983.

[312] JW Prineas and JS Graham. Multiple sclerosis: capping of surface immunoglobulin g on macrophages engaged in myelin breakdown. *Ann Neurol*, 10:149–158, 1981.

[313] TJ Putnam. Studies in multiple sclerosis vii similarities between some forms of "encephalomyelitis" and multiple sclerosis. *Arch Neurol Psychiatry*, pages 1289–1308, 1935. Read before the American College of Physicians, Philadelphia, April 29, 1935.

[314] A Raabe, C Grolms, M Keller, J Döhnert, O Sorge, and V Seifert. Correlation of computed tomography findings and serum brain damage markers following severe head injury. *Acta Neurochir*, 140:787–792, 1998.

[315] CS Raine. *Multiple Sclerosis*, chapter The neuropathology of multiple sclerosis, pages 151–170. Volume 1 of Raine et al.,[316] 1997.

[316] CS Raine, HF McFarland, and WW Tourtellotte, editors. *Multiple Sclerosis*, volume 1. Chapman & Hall Medical, 2-6 Boundary Row, London SE1 8HN, UK, 1997.

[317] N Ranish and S Ochs. Fast axoplasmic transport of acetylchoninesterase in mammalian nerve fibres. *J Neurochem*, 19:2641–2649, 1972.

[318] MV Rao, MK Houseweart, TL Williamson, TO Crawford, J Folmer, and DW Cleveland. Neurofilament-dependent radial growth of motor axons and axonal organization of neurofilaments does not require the neurofilament heavy subunit (NF-H) or its phosphorylation. *J Cell Biol*, 143:171–81, 1998.

[319] LS Rasmussen, M Christiansen, PB Hansen, and JT Moller. Do blood levels of neuron-specific enolase and S-100 protein reflect cognitive dysfunction after coronary artery bypass? *Acta Anaesthesiol Scand*, 43:495–500, 1999.

[320] EJ Redford, R Kapoor, and KJ Smith. Nitric oxide donors reversibly block axonal conduction: demyelinated axons are especially susceptible. *Brain*, 120:2149–2157, 1997.

[321] SA Reeves, LJ Helman, A Allison, and MA Israel. Molecular cloning and primary structure of human glial fibrillary acidic protein. *Proc Natl Acad Sci USA*, 86:5178–5182, 1989.

[322] I Reisert, G Wildemann, D Grab, and C Pilgrim. The glial reaction in the course of axon regeneration: a stereological study of the rat hypoglossal nucleus. *J Comp Neurol*, 10:121–128, 1984.

[323] P Rieckmann, M Albrecht, B Kitze, et al. Tumor necrosis factor α messenger RNA expression in patients with relapsing remitting multiple sclerosis is associated with disease activity. *Ann Neurol*, 37:82–88, 1995.

[324] P Rieckmann and M Maurer. Anti-inflammatory strategies to prevent axonal injury in multiple sclerosis. *Curr Opin Neurol*, 15:361–370, 2002.

[325] E Rindfleisch. Histologisches Detail zur grauen Degeneration von Gehirn und Rückenmark. *Arch Pathol Anat Physiol Klin Med (Virchow)*, 26:474–483, 1863.

[326] NP Robertson, D Clayton, M Fraser, J Deans, and DAS Compston. Clinical concordance in sibling pairs with multiple sclerosis. *Neurology*, 47:347–352, 1996.

[327] MJ Robson and RP Alston. Time course of neurone-specific enolase and S-100 protein release during and after coronary artery bypass grafting. *Br J Anaesth*, 83:531; discussion 532–500, 1999.

[328] HM Roder, FJ Hoffman, and W Schroder. Phosphatase resistance of erk2 brain kinase PK40(erk2). *J Neurochem*, 64:2203–2212, 1995.

[329] HM Roder and VM Ingram. 2 novel kinases phosphorylate-tau and the KSP site of heavy neurofilament subunits in high stoichiometric ratios. *J Neuroscience*, 11:3325–3343, 1991.

[330] M Rodriguez, A Siva, SA Cross, et al. Optic neuritis: a population based study in Olmsted County, Minnesota. *Neurology*, 45:244–250, 1995.

[331] I Roitt. *Essential Immunology*. Blackwell Science, 9th edition, 1999.

[332] LE Rosengren, G Ahlsen, M Belfrage, C Gillberg, KG Haglid, and A Hamberger. A sensitive ELISA for glial fibrillary acidic protein - application in CSF of children. *J Neurosci Meth*, 44:113–119, 1992.

[333] LE Rosengren, A Aurell, P Kjellstrand, and KG Haglid. Astrogliosis in the cerebral cortex of gerbils after long-term exposure to 1,1,1-trichloroethane. *Scand J Work Environ Health*, 11:447–455, 1985.

[334] LE Rosengren, JE Karlsson, et al. Neurofilaments protein levels in CSF are increased in dementia. *Neurology*, 52:1090–1093, 1999.

[335] LE Rosengren, JE Karlsson, JO Karlsson, LI Persson, and C Wikkelso. Patients with amyotrophic lateral sclerosis and other neurodegenerative diseases have increased levels of neurofilament protein in CSF. *J Neurochem*, 67:2013–2018, 1996.

[336] LE Rosengren, J Lycke, and O Andersen. Glial fibrillary acidic protein in CSF of multiple sclerosis patients — relation to neurological deficit. *J Neurol Sci*, 133:61–65, 1995.

[337] LE Rosengren, C Wikkelso, and L Hagberg. A sensitive ELISA for glial fibrillary acidic protein - application in CSF of adults. *J Neuroscience Methods*, 51:197–204, 1994.

[338] RD Rothoerl, C Woertgen, M Holzschuh, et al. Rapid evaluation of S-100 serum levels Case report and comparison to previous results. *Brain Injury*, 13:387–391, 1999.

[339] GA Rouleau, AW Clark, K Rooke, A Pramatarova, A Krizus, O Suchowersky, JP Julien, and D Figlewicz. SOD1 mutation is associated with accumulation of neurofilaments in amyotrophic lateral sclerosis. *Ann Neurol*, 39:128–131, 1996.

[340] S Roy, P Coffee, G Smith, et al. Neurofilaments are transported rapidly but intermittently in axons: implications for slow axonal transport. *J Neurosci*, 20:6849–6861, 2000.

[341] B Runmarker and O Andersen. Prognostic factors in a multiple sclerosis incidence cohort with twenty-five years of follow-up. *Brain*, 116:117–134, 1993.

[342] MHA Russell, IJ Murray, RA Metcalfe, et al. The visual defect in multiple sclerosis and optic neuritis. *Brain*, 114:2419–2435, 1991.

[343] BJ Sahakian and MA Owen. Computerized assessment in neuropsychiatry using CANTAB. In *discussion paper*, volume 85, pages 399–402. J R Soc Med, 1992.

[344] M Sanberg-Wollheim, H Bynke, S Cronqvist, et al. A longterm prospective study of optic neuritis: evaluation of risk factors. *Ann Neurol*, 27:386–393, 1990.

[345] E Scarpini, D Galimberti, P Baron, R Clerici, M Ronzoni, G Conti, and G Scarlato. IP-10 and MCP-1 levels in CSF and serum from multiple sclerosis patients with different clinical subtypes of the disease. *J Neurol Sci*, 195:41–46, 2002.

[346] HH Schaumburg and PS Spencer. Degeneration in central and peripheral nervous systems produced by pure n-hexane: an experimental study. *Brain*, 99:183–192, 1976.

[347] WW Schlaepfer and RP Bunge. The effects of calcium ion concentrations on the degradation of amputated axons in tissue culture. *J Cell Biol*, 59:456–470, 1973.

[348] WW Schlaepfer, C Ledd, JA Trojanowski, and VMY Lee. Persistence of immunoreactive neurofilament protein breackdown products in transected rat sciatic nerve. *J Neurochem*, 43:857–864, 1984.

[349] WW Schlaepfer, C Lee, VMY Lee, and UJP Zimmerman. An immunoblot study of neurofilament degradation in situ and during calcium–activated proteolysis. *J Neurochem*, 44:502–509, 1985.

[350] LM Schonrock, T Kuhlmann, S Adler, A Bitsch, and W Bruck. Identification of glial cell proliferation in early multiple sclerosis lesions. *Neuropathol Appl Neurobiol*, 24:320–330, 1998.

[351] E Schuller, N Delasnerie, G Deloghe, and M Loridan. Multiple sclerosis: a two–phase disease. *Acta Neurol Scand*, 49:453–460, 1973.

[352] K Selmaj, CS Raine, and AH Cross. Anti-tumor necrosis factor therapy abrogates autoimmune demyelination. *Ann Neurol*, 30:694–700, 1991.

[353] YK Semra, OA Seidi, and MK Sharief. Heightened intrathecal release of axonal cytoskeletal proteins in multiple sclerosis is associated with progressive disease and clinical disability. *J Neuroimmunol*, 122:132–109, 2002.

[354] M Shaaban-Ali, M Harmer, RS Vaughan, JA Dunne, IP Latto, R Haaverstad, EN Kulatilake, and EG Butchart. Changes in serum S100beta protein and mini-mental state examination after cold (28 degrees c) and warm (34 degrees c) cardiopulmonary bypass using different blood gas strategies (alpha-stat and ph-stat). *Acta Anaesthesiol Scand*, 46:10–6, 2002.

[355] MK Sharief and R Hentges. Association between tumor necrosis factor-alpha and disease progression in patients with multiple sclerosis. *N Engl J Med*, 325:467–472, 1991.

[356] MK Sharief, MA Noori, M Ciardi, A Cirelli, and EJ Thompson. Increased levels of circulating ICAM 1 in serum and cerebrospinal fluid of patients with active multiple sclerosis Correlation with TNF alpha and blood brain barrier damage. *J Neuroimmunol*, 43:15–22, 1993.

[357] TB Shea and ML Beerman. Evidence that the monoclonal antibodies SMI 31 and SMI 34 recognize different phosphorylation-dependent epitopes of the murine high molecular mass neurofilament subunit. *J Neuroimmunol*, 44:117, 1993.

[358] KT Shetty, WT Link, and HC Pant. Cdc2-like kinase from rat spinal-cord specifically phosphorylates kspxk motifs in neurofilament proteins - isolation and characterization. *Proceedings National Academy Sciences United States America*, 90:6844–6848, 1993.

[359] RK Sihag and RA Nixon. Invivo phosphorylation of distinct domains of the 70- kilodalton neurofilament subunit involves different protein- kinases. *J Biol Chem*, 264:457–464, 1989.

[360] RK Sihag and RA Nixon. Phosphorylation of the amino-terminal head domain of the middle molecular mass 145-kda subunit of neurofilaments - evidence for regulation by 2nd messenger-dependent protein- kinases. *J Biol Chem*, 265:4166–4171, 1990.

[361] RK Sihag and RA Nixon. Identification of ser-55 as a major protein kinase-a phosphorylation site on the 70-kda subunit of neurofilaments - early turnover during axonal-transport. *J Biol Chem*, 266:18861–18867, 1991.

[362] E Sindern, Y Niederkinkhaus, M Henschel, LM Ossege, T Patzold, and JP Malin. Differential release of beta-chemokines in serum and CSF of patients with relapsing-remitting multiple sclerosis. *Acta Neurol Scand*, 104:88–91, 2001.

[363] CJ Sindic, MP Chalon, CL Cambiaso, EC Laterre, and PL Masson. Assessment of damage to the central nervous system by determination of S-100 protein in the cerebrospinal fluid. *J Neurol Neurosurg Psychiatry*, 45:1130–1105, 1982.

[364] CJ Sindic, D Collet-Cassart, CL Cambiaso, PL Masson, and EC Laterre. The clinical relevance of ferritin concentration in the cerebrospinal fluid. *J Neurol Neurosurg Psychiatry*, 44:329–333, 1981.

[365] KJ Smith and SM Hall. Factors directly affecting impulse transmission in inflammatory demyelinating disease: recent advances in our understanding. *Curr Opin Neurol*, 14:289–298, 2001.

[366] KJ Smith, R Kapoor, SM Hall, and M Davies. Electrically active axons degenerate when exposed to nitric oxide. *Ann Neurol*, 49:470–406, 2001.

[367] KJ Smith and WI McDonald. The pathophysiology of multiple sclerosis: the mechanisms underlying the production of symptoms and the natural history of the disease. *Phil Trans R Soc Lond B Biol Sci*, 354:1649–1673, 1999.

[368] ME Smith and LF Somera, FP Eng. Immunocytochemicial staining for glial fibrillary acidic protein and the metabolism of cytoskeletal proteins in experimental autoimmune encephalomyelitis. *Brain Res*, 264:241–253, 1983.

[369] HE Solberg. *Tietz Textbook of Clinical Chemistry*, chapter Establishing and Use of Reference Values, pages 454–484. WB Saunders Company, Philadelphia, Pensylvania 19106, 2nd edition, 1994.

[370] G Sorci, AL Agneletti, R Bianchi, and R Donato. Association of S100B with intermediate filaments and microtubules in glial cells. *Biochim Biophys Acta*, 1448:277–289, 1998.

[371] PS Spencer and HH Schaumburg. Ultrastructural studies of the dying-back process IV Differential vulnerability of PNS and CNS fibers in experimental central-peripheral distal axonopathies. *J Neuropathol Exp Neurol*, 36:300–320, 1977.

[372] S Sriram and M Rodriguez. Indictment of the microglia as the villain in multiple sclerosis. *Neurology*, 48:464–470, 1997.

[373] BJ Steinhoff, H Tumani, M Otto, K Mursch, J Wiltfang, G Herrendorf, HJ Bittermann, K Felgenhauer, W Paulus, and E Markakis. Cisternal s100 protein and neuron-specific enolase are elevated and site-specific markers in intractable temporal lobe epilepsy. *Epilepsy Res*, 36:75–82, 1999.

[374] L Steinman. Multiple sclerosis: a coordinated immunological attack against myelin in the central nervous system. *Cell*, 85:299–302, 1996.

[375] L Steinman. Multiple sclerosis: a two-stage disease. *Nat Immunol*, 2:762–704, 2001.

[376] LA Sternberger, editor. *Immunocytochemistry.* John Wiley, New York, third edition, 1986.

[377] LA Sternberger, LW Harwell, and NH Sternberger. Neurotype: Regional individuality in rat brain detected by immunocytochemistry with monoclonal antibodies. *Proc Natl Acad Sci USA*, 79:1326–1330, 1982.

[378] LA Sternberger and NH Sternberger. Monoclonal antibodies distinguish phosphorylated and non phosphorylated forms of neurofilaments *in situ*. *Proc Natl Acad Sci USA*, 82:6126–6130, 1983.

[379] NH Sternberger, LA Sternberger, and J Ulrich. Aberrant neurofilament phosphorylation in alzheimer disease. *Proc Natl Acad Sci USA*, 82:4274–4276, 1985.

[380] G Stoll, JW Griffin, CY Li, and BD Trapp. Wallerian degeneration in the peripheral nervous system: participation of both Schwann cells and macrophages in myelin degradation. *J Neurocytol*, 18:671–683, 1989.

[381] G Stoll, BD Trapp, and JW Griffin. Macrophage function during Wallerian degeneration of rat optic nerve: clearance of degenerating myelin and Ia expression. *J Neurosci*, 9:2327–2335, 1989.

[382] MK Storch, S Piddlesden, M Haltia, M Iivanainen, P Morgan, and H Lassmann. Multiple sclerosis: in situ evidence for antibody- and complement-mediated demyelination. *Ann Neurol*, 43:465–471, 1998.

[383] WJ Streit, MH Graeber, and GW Kreutzberg. Functional plasticity of microglia: a review. *Glia*, 1:301–307, 1988.

[384] K Strle, JH Zhou, WH Shen, SR Broussard, RW Johnson, GG Freund, R Dantzer, and KW Kelley. Interleukin-10 in the brain. *Crit Rev Immunol*, 21:427–449, 2001.

[385] MJ Strong, WL Strong, H Jaffe, B Traggert, MM Sopper, and HC Pant. Phosphorylation state of the native high-molecular-weight neurofilament subunit protein from cervical spinal cord in sporadic amyotrophic lateral sclerosis. *J Neurochem*, 76:1315–1325, 2001.

[386] JH Su, BJ Cummings, and Cotman CW. Plaque biosynthesis in ageing brain and Alzheimer's disease II Progressive transformation and developmental sequence of dystrophic neurites. *Acta Neuropath*, 96:463, 1998.

[387] JS Su, BJ Cummings, and CW Cotman. Plaque biosynthesis in brain ageing and Alzheimer's disease: I Progressive changes in phosphorylation states of paired helical filaments and neurofilaments. *Brain Res*, 739:79, 1996.

[388] F Suzuki, K Kato, T Kato, and N Ogasawara. S-100 protein in clonal astroglioma cells is released by adrenocorticotropic hormone and corticotropin-like intermediate-lobe peptide. *J Neurochem*, 49:1557–1563, 1987.

[389] M Tabaton, G Perry, L Autilio-Gambetti, V Manetto, and P Gambetti. Influence of neuronal location on antigenic properties of neurofibrillary tangles. *Ann Neurol*, 23:604–610, 1988.

[390] K Takahashi, T Isobe, Y Ohtsuki, T Akagi, H Sonobe, and T Okuyama. Immunohistochemical study on the distribution of alpha and beta subunits of s-100 protein in human neoplasm and normal tissues. *Virchows Arch B Cell Pathol Incl Mol Pathol*, 45:385–396, 1984.

[391] M Takayasu, M Shibuya, M Kanamori, Y Suzuki, K Ogura, N Kageyama, H Umekawa, and H Hidaka. S-100 protein and calmodulin levels in cerebrospinal fluid after subarachnoid hemorrhage. *J Neurosurg*, 63:417–420, 1985.

[392] W Tetzlaff, MB Graeber, MA Bisby, and Kreutzberg GW. Increased glial fibrillary acidic protein synthesis in astrocytes during retrograde reaction of the rat facial nucleus. *Glia*, 1:90–95, 1988.

[393] AJ Thompson. Multiple sclerosis: Rehabilitation measures. *Seminars Neurology*, 18:397–403, 1998.

[394] AJ Thompson, J Brazil, C Feighery, et al. CSF myelin basic protein in multiple sclerosis. *Acta Neurol Scand*, pages 577–583, 1985.

[395] EJ Thompson and AJE Green. Protein markers of brain damage. *Mult Scler*, 4:5–6, 1998.

[396] TM Tikka and JE Koistinaho. Minocycline provides neuroprotection against N-methyl-D-aspartate neurotoxicity by inhibiting microglia. *J Immunol*, 166:7527–7533, 2001.

[397] TM Tikka, NE Vartiainen, G Goldsteins, SS Oja, PM Andersen, SL Marklund, and J Koistinaho. Minocycline prevents neurotoxicity induced by cerebrospinal fluid from patients with motor neurone disease. *Brain*, 125:722–731, 2002.

[398] BD Trapp, JP Peterson, et al. Axonal transection in the lesions of multiple sclerosis. *N Eng J Med*, 338:278–285, 1998.

[399] BD Trapp, R Ransohoff, and R Rudick. Axonal pathology in multiple sclerosis: relationship to neurologic disability. *Curr Opin Neurol*, 12:295–302, 1999.

[400] BD Trapp, RM Ransohoff, E Fisher, and RA Rudick. Neurodegeneration in multiple sclerosis, relationship to neurological disability. *Neuroscientist*, 5:48–57, 1999.

[401] JQ Trojanowski, VM Lee, and Schlaepfer WW. Neurofilament breakdown products in degenerating rat and human peripheral nerves. *Ann Neurol*, 16:349–355, 1984.

[402] L Truyen, JH van Waesberghe, MA van Waldervaan, et al. Accumulation of hypointense lesions ("black holes") on T1 spin echo MRI correlates with disease progression in multiple sclerosis. *Neurology*, 47:1496–1476, 1996.

[403] M Tsuda, T Tashiro, and Y Komiya. Increased solubility of high-molecular-mass neurofilament subunit by suppression of dephosphorylation: its relation to axonal transport. *J Neurochem*, 68:2558–2565, 1997.

[404] M Tsuda, T Tashiro, and Y Komiya. Selective solubilization of high-molecular-mass neurofilament subunit during nerve regeneration. *J Neurochem*, 74:860–808, 2000.

[405] N Ulfig, J Nickel, and J Bohl. Monoclonal antibodies smi 311 and smi 312 as tools to investigate the maturation of nerve cells and axonal patterns in human fetal brain. *Cell Tissue Research*, 291:433–443, 1998.

[406] N Ulfig, J Nickel, and Saretzki. Influence of reduced nutrition on the onset of myelination in the human fetal brain. *Clin Neuropath*, 14:291, 1995.

[407] E Ulvestad, K Williams, C Vedeler, J Antel, H Nyland, S Mork, and R Matre. Reactive microglia in multiple sclerosis lesions have an increased expression of receptors for the Fc part of IgG. *J Neurol Sci*, 121:125–31, 1994.

[408] P Van Der Voorn, J Tekstra, RH Beelen, CP Tensen, P Van Der Valk, and CJ De Groot. Expression of MCP-1 by reactive astrocytes in demyelinating multiple sclerosis lesions. *Am J Pathol*, 154:45–51, 1999.

[409] JH van Waesberghe, W Kamphorst, CJ De Groot, MA van Walderveen, JA Castelijns, R Ravid, GJ Lycklama a Nijeholt, P van der Valk, CH Polman, AJ Thompson, and Barkhof F. Axonal loss in multiple sclerosis lesions: magnetic resonance imaging insights into substrates of disability. *Ann Neurol*, pages 747–754, 1999.

[410] N Vartiainen, T Tikka, R Keinanen, PH Chan, and J Koistinaho. Glutamatergic receptors regulate expression, phosphorylation and accumulation of neurofilaments in spinal cord neurons. *Neuroscience*, 93:1123–1133, 1999.

[411] KT Veeranna Shetty, ND Amin, NG Ahn, H Jaffe, CA Winters, P Grant, and HC Pant. Mitogen-activated protein kinases (Erk1,2) phosphorylate Lys-Ser-Pro (KSP) repeats in neurofilament proteins NF-H and NF-M. *J Neurosci*, 18:4008–4021, 1998.

[412] B Veronesi, ER Peterson, MB Bornstein, and PS Spencer. Ultrastructural studies of the dying-back process VI Examination of nerve fibers undergoing giant axonal degeneration in organotypic culture. *J Neuropathol Exp Neurol*, 42:153–65, 1983.

[413] WW Vick, CJ Wikstrand, DE Bullard, et al. The use of a panel of monoclonal antibodies in the evaluation of cytologic specimens from the central nervous system. *Acta Cytol*, 31:815–824, 1987.

[414] JC Vickers and JH Morrison. Aberrant neurofilament protein immunoreactivity in hippocampal pyramidal neurons in Alzheimer's disease. *J Neuropath Exper Neurol*, 51:319, 1992.

[415] A Waller. Experiments on the section of glossopharyngeal and hypoglossal nerves of the frog and observations of the alternatives produced thereby in the structure of their primitive fibres. *Philos Trans R Soc London*, 140:423, 1850.

[416] A Wallin, K Blennow, and LE Rosengren. Glial fibrillary acidic protein in the cerebrospinal fluid of patients with dementia. *Dementia*, 7:267–272, 1996.

[417] W Wandschneider, M Thalmann, E Trampitsch, G Ziervogel, and G Kobinia. Off-pump coronary bypass operations significantly reduce S100 release: an indicator for less cerebral damage? *Ann Thorac Surg*, 70:1577–1509, 2000.

[418] S Wang, GJ Lees, LE Rosengren, JE Karlsson, A Hamberger, and KG Haglid. Proteolysis of filament proteins in glial and neuronal cells after in vivo stimulation of hippocampal NMDA receptors. *Neurochem Res*, 17:1005–1009, 1992.

[419] EK Warrington, editor. *Recognition memory tests*. NFER Nelson: Windsor, 1984.

[420] T Wataya, A Nunomura, MA Smith, et al. High molecular weight neurofilament proteins are physiological substrates of adduction by the lipid peroxidation product hydroxynonenal. *J Biol Chem*, 207:4644–4648, 2002.

[421] K Waterloo, T Ingebrigtsen, and B Romner. Neuropsychological function in patients with increased serum levels of protein S-100 after minor head injury. *Acta Neurochir*, 139:26–31; discussion 31–2, 1997.

[422] D Watson. Regional in the abundance of axonal cytoskeletal proteins. *J Neurosc Res*, 30:226, 1991.

[423] DF Watson, JD Glass, and JW Griffin. Redistribution of cytoskeletal proteins in mammalian axons disconnected from their cell bodies. *J Neurosci*, 13:4354–4360, 1993.

[424] SG Waxman. Demyelinating diseases — new pathological insights, new therapeutic targets. *N Eng J Med*, 338:323–325, 1998.

[425] SG Waxman, JD Kocsis, and PK Stys, editors. *The axon: structure, function and pathophysiology*. Oxford University Press, New York, Oxford, 1995.

[426] HJ Weinberg and PS Spencer. The fate of schwann cells isolated from axonal contact. *J Neurocytol*, 7:555–569, 1978.

[427] BG Weinshenker and D Miller. *Frontiers in multiple sclerosis*, chapter Multiple sclerosis: one disease or many?, pages 37–46. 1999.

[428] S Westaby, P Johnsson, AJ Parry, et al. Serum S100 protein: a potential marker for cerebral events during cardiopulmonary bypass. *Ann Thorac Surg*, 61:88–92, 1996.

[429] D Whitaker. S100 release as an indicator of cerebral damage. *Ann Thorac Surg*, 71:2085–2006, 2001.

[430] JN Whitaker and PK Herman. Human myelin basic protein peptide 69-89: immunochemical features and use in immunoassays of cerebrospinal fluid. *J Neuroimmunol*, 19:47–57, 1988.

[431] JN Whitaker, RD Kachelhofer, EL Bradley, et al. Urinary myelin basic protein–like material as a correlate of the progression of multiple sclerosis. *Ann Neurol*, 38:625–632, 1995.

[432] JN Whitaker, PH Williams, BA Layton, et al. Correlation of clinical features and findings on cranial magnetic resonance imaging with urinary myelin basic protein-like material in patients with multiple sclerosis. *Ann Neurol*, 35:577–585, 1994.

[433] M Wiesmann, U Missler, H Hagenstrom, and D Gottmann. S-100 protein plasma levels after aneurysmal subarachnoid haemorrhage. *Acta Neurochir*, 139:1155–1160, 1997.

[434] PT Wilder, RR Rustandi, AC Drohat, and DJ Weber. S100B(betabeta) inhibits the protein kinase C-dependent phosphorylation of a peptide derived from p53 in a Ca2+-dependent manner. *Protein Sci*, 7:794–708, 1998.

[435] M Willard and C Simon. Modulations of neurofilament axonal-transport during the development of rabbit retinal ganglion-cells. *Cell*, 35:551–559, 1983.

[436] TL Williamson, LI Bruijn, et al. Absence of neurofilaments reduces the selective vulnerability of motor neurons and slows disease caused by amyotrophic lateral sclerosis–linked superoxide dismutase 1 mutant. *Proc Natl Acad Sci USA*, 95:9631–9636, 1998.

[437] JR Willison, DJ Thomas, GH du Boulay, et al. Effect of high haematocrit on alertness. *Lancet*, 19:846–848, 1980.

[438] JR Wujek, C Bjartmar, E Richer, et al. Axon loss in the spinal cord determines permanent neurological disability in an animal model of multiple sclerosis. *J Neuropathol Exp Neurol*, 61:23–32, 2002.

[439] MR Wunderlich, AD Ebert, T Kratz, et al. Early neurobehavioral outcome after stroke is related to release of neurobiochemical markers of brain damage. *Stroke*, 30:1190–1195, 1999.

[440] DR Wynn, M Rodriguez, O'Fallon WM, and LT Kurland. Update on the epidemiology of multiple sclerosis. *Mayo Clin Proc*, 256:225–228, 1989.

[441] Z Xu, LC Cork, JW Griffin, and DW Cleveland. Increased expression of neurofilament subunit NF–L produces morphological alterations that resemble the pathology of human motor neuron disease. *Cell*, 73:23–33, 1993.

[442] Z Xu and VW Tung. Overexpression of neurofilament subunit M accelerates axonal transport of neurofilaments. *Brain Res*, 866:326–332, 2000.

[443] Z Xu and VW Tung. Temporal and spatial variations in slow axonal transport velocity along peripheral motoneuron axons. *Neuroscience*, 102:193–200, 2001.

[444] DL Yao, HD Webster, LD Hudson, M Brenner, DS Liu, AI Escobar, and S Komoly. Concentric sclerosis (Balo): morphometric and in situ hybridization study of lesions in six patients. *Ann Neurol*, 35:18–30, 1994.

[445] J Zelena, L Lubinska, and E Gutmann. Accumulation of organelles at the ends of interupted axons. *Z Zellforsch Mikrosk Anat*, 91:200–219, 1968.

[446] H Zhang, NH Sternberger, LJ Rubinstein, et al. Abnormal processing of multiple proteins in Alzheimer disease. *Proc Natl Acad Sci USA*, 86:8045–8049, 1989.

[447] Q Zhu, M Lindenbaum, F Levavasseur, H Jacomy, and JP Julien. Disruption of the NF-H gene increases axonal microtubule content and velocity of neurofilament transport: relief of axonopathy resulting from the toxin beta,beta'-iminodipropionitrile. *J Cell Biol*, 143:183–193, 1998.

[448] DR Ziegler, CE Innocente, RB Leal, R Rodnight, and CA Goncalves. The S100B protein inhibits phosphorylation of gfap and vimentin in a cytoskeletal fraction from immature rat hippocampus. *Neurochem Res*, 23:1259–1263, 1998.

[449] AS Zigmond and RP Snaith. The hospital anxiety and depression scale. *Acta Psych Scandi*, 67:361–370, 1983.

Index